Université catholique de Louvain

Faculté de Pharmacie et Sciences Biomédicales

Institut de Recherche Expérimentale et Clinique

Pôle de Pharmacologie et Thérapeutique (FATH)

MiR-199a family members: new actors of cardiovascular functions in health and disease

Virginie JORIS

Thesis submitted in fulfillment of the requirements for the PhD degree in Biomedical and Pharmaceutical Sciences

Thesis Supervisor : Pr. Chantal Dessy (IREC, FATH)

August 2020

“Une personne qui n’a jamais commis d’erreur n’a jamais tenté d’innover”

-Albert Einstein-

“Happiness can be found even in the darkest of times if one only remembers to turn on the light”

-A.D.-

Jury members

Thesis promotor

Professor Chantal Dessy

Pôle de Pharmacologie et Thérapeutique (FATH), Institut de Recherche Expérimentale et Clinique (IREC), Université catholique de Louvain (UCLouvain), Brussels, Belgium

President of the jury

Professor Luc Bertrand

Pôle de Recherche Cardiovasculaire (CARD), Institut de Recherche Expérimentale et Clinique (IREC), Université catholique de Louvain (UCLouvain), Brussels, Belgium

UCLouvain jury members

Professor Marie-Christine Many

Pôle de Morphologie (MORF), Institut de Recherche Expérimentale et Clinique (IREC), Université catholique de Louvain (UCLouvain), Brussels, Belgium

Professor Nathalie Delzenne

Louvain Drug Research Insitute (LDRI) Université catholique de Louvain (UCLouvain), Brussels, Belgium

Professor Jean-Luc Balligand

Pôle de Pharmacologie et Thérapeutique (FATH), Institut de Recherche Expérimentale et Clinique (IREC), Université catholique de Louvain (UCLouvain), Brussels, Belgium

External jury members

Professor Daniel Henrion

MITOVASC Institute and CARFI Facility, INSERM U1083, , CNRS, UMR 6015, Angers University, Angers, France

Doctor Daniele Catalucci

Humanitas Clinical and Research Center, IRCCS, Rozzano, Italy and National Research Council, Institute of Genetic and Biomedical Research - UOS Milan, Milan, Italy

Remerciements

Voici que j'arrive à la fin de cette thèse après de longues années de labeur. Je réalise que ce travail n'aurait pas été ce qu'il est sans la présence de certains collègues, amis et famille et je réalise que la liste va être longue.

Les premières personnes que je souhaite remercier sont mes parents car sans eux je n'aurais pas été bien loin dans cette aventure.

Je remercie ma promotrice Chantal Dessy. Merci de m'avoir permis de réaliser ma thèse au sein de votre groupe de recherche. Je vous suis reconnaissante du temps que vous avez pris pour encadrer mon travail et relire les papiers ainsi que cette thèse. Merci de m'avoir laissée m'épanouir dans le laboratoire et ce même si nous n'étions pas toujours en accord. Vos conseils m'ont permis de fournir le meilleur de moi-même ainsi qu'un travail de qualité. Merci également de m'avoir permis de voyager et de partager les connaissances lors des congrès scientifiques.

Je souhaiterais ensuite adresser mes remerciements au Professeur Marie-Christine Many du laboratoire de Morphologie (MORF) pour m'avoir permis d'enseigner l'histologie et la biologie dans son équipe d'assistants. Merci de m'avoir soutenue et encouragée tout au long de ces 7 années de travail. Merci pour votre écoute, pour votre gentillesse et votre compréhension. J'ai réellement eu l'impression d'avoir une deuxième maman au laboratoire et cela m'a vraiment aidée à tenir le coup. Je vous remercie de m'avoir soutenue quand je pleurais de fatigue et d'avoir toujours eu la patience de chercher des solutions avec moi malgré votre emploi du temps chargé. Aucun mot ne peut vraiment traduire ma reconnaissance : MERCI.

J'adresse également mes sincères remerciements aux Professeurs Jean-Luc Balligand, Pierre Sonveaux et Olivier Feron du laboratoire de Pharmacologie et Thérapeutique (FATH) pour leurs commentaires constructifs ainsi que leurs conseils avisés tout au long de mon travail.

Je remercie les membres de mon jury les Professeurs Jean-Luc Balligand, Nathalie Delzenne, Marie-Christine Many et Luc Bertrand pour le temps consacré au suivi de ma thèse. Merci au Professeur Daniel Henrion et au Docteur Daniele Catalucci qui ont amené leurs points de vue externes sur ce travail afin de l'améliorer.

Je remercie Elvira, Gaëtane, Irina, Delphine, Hrag, Laurent, Estelle et Thomas du laboratoire de FATH pour leur aide technique, leur participation et leurs conseils tout au long de ce travail. Merci également à Evangelos et Sandrine Horman du pôle de recherche cardiovasculaire pour leur expertise sur la deuxième partie de cette thèse.

Je tiens à remercier tous les gens que j'ai rencontrés au laboratoire FATH pour la bonne ambiance et les bons moments passés dans le laboratoire. Merci de m'avoir supportée moi et mes sautes d'humeur. Merci également à Marie-Pierre, Cyril, Steve et Déborah pour leur aide administrative.

Je souhaite particulièrement remercier Julie Craps du laboratoire MORF. Merci pour ton encadrement lors de mon mémoire, c'est toi qui m'as redonné goût à la recherche et qui m'a donné l'envie de faire un doctorat. Merci d'avoir partagé tes connaissances avec moi. Merci pour nos fous rires et pour les moments où tu m'as soutenue et écoutée quand c'était difficile. Merci de t'être toujours assurée que j'allais bien et d'avoir su remarquer quand ce n'était pas le cas. J'ai trouvé en toi une amie formidable et une marraine de qualité pour Daphné.

Merci également à Selena Toma. Tu as su voir les compétences que je pouvais avoir et tu m'as toujours encouragée à les exploiter. Je te remercie également pour les bons moments passés ensemble, je suis heureuse de t'avoir rencontrée et je me remémorerai toujours nos fous rires. Merci pour tes conseils et ton amitié, sache qu'elle est chère à mes yeux.

Je souhaite également remercier Sébastien Lafont. Tu as été là dans des moments qui ont été difficiles. Tu as toujours su trouver les mots pour m'encourager sans jamais te plaindre toi. Tu as été témoin de mes pleurs, de mes colères et de mes joies sans doute plus que certains autres. Je te remercie du fond du cœur pour ta gentillesse et ton oreille attentive. Merci également d'être un parrain en or pour Clément.

Je remercie également Dorothée Marchand et Lisa Menchi. Sachez que ce fut un plaisir de vous encadrer dans le laboratoire. Merci pour l'aide que vous m'avez apportée, vous ne réalisez pas à quel point elle a été précieuse. J'ai également trouvé en vous des amies. Je vous remercie pour votre investissement dans ce travail.

Merci à Marco Macri, Michael Hepp et Gaëlle de Jesus Silva qui sont sans doute tous les trois passés maîtres pour mettre de l'ambiance au laboratoire. Merci pour votre confiance et votre bonne humeur. Sachez que vous aurez toujours des hauts et des bas dans la vie mais grâce à votre personnalité vous en en sortirez toujours. Merci pour les fous rires et pour tous ces moments qui resteront gravés dans ma mémoire.

I would particularly thank Ruben Martherus to believe in me during this work. You were a real support for me, a teacher, a friend and forever my evil big brother. Thank you from the bottom of my heart for your time, your expertise and your kindness.

Merci à toutes les personnes du laboratoire de Morphologie pour tous les bons moments passés ensemble. Thomas, Mickaël, Véronique et Adeline, merci pour la bonne ambiance dans le bureau. Merci à Michelle et Walter pour leur gentillesse et leur disponibilité.

Je remercie également tous les étudiants que j'ai encadrés ou rencontrés en laboratoire. Mattéo, Marie, Alexis, Axel, Elliott, Sabina et An-Catherine. Vous avez réalisé un travail formidable et m'avez permis de m'épanouir dans l'encadrement pédagogique. Merci à vous pour votre contribution et votre implication dans votre recherche.

Merci également aux chercheurs avec lesquels j'ai collaboré, Tom Darius, Louis Maistriaux et Jérôme Duisit. Merci pour ce partage de connaissances.

Merci à toute l'équipe d'assistants de biologie, d'histologie et d'histologie spéciale, Clara, Antonia, Marie, Sophie, Catherine, Charlotte, Adrien et Nadia pour les moments passés en TP et le temps investi dans la préparation des TP et les corrections. Non je n'oublie pas certains autres assistants.

Merci à Laurent Wallemme pour le temps passé à m'apprendre l'histologie dans ses moindres détails. Merci pour les fous rires, les sarcasmes et autres blagues que nous avons pu avoir en TP. Merci pour ta gentillesse et ton ouverture d'esprit, elles auront été un bol d'air dans les moments difficiles.

Merci à Emilie André pour les bons moments passés au labo ou en TP. Merci de m'avoir écoutée quand j'en avais besoin sans me juger. Les séances de corrections

au labo resteront des moments difficiles mais qui resteront gravés dans ma mémoire grâce à ta bonne humeur et ton sourire.

Je souhaite également remercier Inês Belo. Merci d'avoir cru en moi quand je t'ai proposée mon aide. Merci pour tous les fous rires au laboratoire ou en TP, les moments au quick ou en attendant nos sushis le dimanche au labo. Merci de m'avoir soutenue et d'être passée régulièrement me voir pour prendre des nouvelles. Je ne te l'ai sans doute pas dit mais je suis très fière de toi quoiqu'il arrive. Reste une battante. Merci pour tout.

Merci également à Sabrina Contino et Maxime Vergouts pour les moments hilarants que nous avons passés lors des TP de biologie. Ils resteront gravés dans ma mémoire grâce à vous.

Je souhaite évidemment remercier ma famille. Merci Papa et Maman pour le soutien que m'avez toujours apporté. Merci d'avoir subi mes sautes d'humeur et mon caractère difficile. Merci de m'avoir poussée à continuer mes études quand j'étais dans le doute. Merci d'avoir fait de moi ce que je suis aujourd'hui. Bref… Merci pour votre amour et votre patience. Merci à mon frère, Jérémy, pour m'avoir écoutée dans les moments difficiles et de m'avoir soutenue et aidée tout aux longs de ces années. Sache que je suis fière d'avoir un frère comme toi. Je ne vous le dis pas suffisamment mais je vous aime.

Merci également à mes amis Eugénie, Bertrand, Marie-Hélène, Leslie et Thibault pour m'avoir écouté débattre pendant des heures sur ma thèse sans forcément comprendre. Merci pour votre soutien et votre présence durant ce long parcours.

Finalement je souhaite remercier mon compagnon dans la vie de tous les jours, Thomas. Merci de m'avoir soutenue sur les dernières années de ma thèse. Désolée pour toutes les colères et les larmes que tu as dû voir. Car si je ne montrais pas beaucoup mes sentiments au labo c'est bien parce que tu étais là pour m'écouter pleurer, m'énerver et rire à la maison. Tu m'as été d'un réel réconfort durant ces périodes difficiles. Je te remercie de ne jamais m'avoir jugée et de m'avoir toujours encouragée. Merci d'avoir cru et de toujours croire en moi et en mes compétences. Merci de m'avoir rappelé en permanence que j'étais plus qu'une doctorante. Merci pour ton amour et tout ce que tu fais au quotidien pour mon bien-être même si je ne le remarque pas forcément. Enfin un grand merci

d’être un papa si attentionné et merveilleux pour Clément et Daphné, tu m’as vraiment fait le plus beau des cadeaux.

Summary

The vascular endothelium participates to cardiovascular homeostasis by controlling inflammation, thrombogenesis, angiogenesis and by adapting vascular tone and perfusion to tissue needs. To meet these critical functions, endothelial cells combine very sophisticated sensory properties, signal processing and a balanced production of autocrine/paracrine effectors among which NO is the more prominent. Endothelial dysfunction, often defined as a reduced NO bioavailability, is a recognized early key marker of most cardiovascular diseases, it reflects the integrated effects of risk factors on the vasculature. Members of microRNA-199a family, first described in cancers, have been identified as potential regulators of cardiac homeostasis and are described as modified during cardiac remodeling, diabetes or liver diseases. Moreover, an upregulation of miR-199a expression in cardiomyocytes was reported to influence endothelial cell function.

In this work, we first demonstrated that both mature forms of miR-199a, namely, miR-199a-3p and miR-199a-5p, are also expressed by endothelial cells where they participate in a redundant network of regulation of the NO-synthase/nitric oxide pathway. By combining in silico, in vitro and ex vivo analysis, we have identified direct and indirect targets of these miRs that modulate nitric oxide production and degradation thereby supporting angiogenesis and modulation of vascular tone.

Our work also highlighted that miR-199a family members are differentially regulated in health and disease. Indeed, we documented in two different murine models of pathologic cardiac hypertrophy, an up-regulation of both strands in the heart and vessels of the mice. Interestingly, we found that vascular and cardiac tissue of mice submitted to voluntary exercise, exhibit a blunted expression of miR-199a family members, correlated with improved cardiac and endothelial functions. MiR-profiling in plasma revealed that circulating levels of the -5p arm reflect cardiac and endothelial levels in the pathologic and physiologic experimental models (and therefore cardiac and vascular health), which might support a diagnostic or prognostic value.

In summary, our results demonstrated that miR-199a family members are key players of cardiac and endothelial functions at the crossroad of health and disease.

Table of Contents

Table of Contents

Table of Contents

Abbreviations

ADMA	Asymmetrical Dimethylarginine
Ago	Argonaute
Akt	Protein Kinase B
AMP	Adenosine Monophosphate
AMPK	AMP-activated Protein Kinase
Ang	Angiotensin
ANP	Atrial natriuretic peptide
AP	Activator Protein
ApoE	Apolipoprotein E
AR	Adrenergic receptor
BAEC	Bovine Aortic Endothelial Cells
BH_2	Dihydrobiopterin
BH_4	Tetrahydrobiopterin
BMSC	Bone-marrow derived Mesenchymal Stem Cells
BNP	Brain Natriuretic Peptide
Ca^{++}	Calcium
CaM	Calmodulin
CaMK	Calmodulin Kinase
Cav	Caveolin
cGMP	cyclic Guanosine Monophosphate
COX	Cyclooxygenase
Cx	Connexin
DDAH	Dimethylarginine Dimethylaminohydrolase
DGCR	DiGeorge syndrome Critical Region
DMD	Duchenne Muscular Dystrophy
DNA	Desoxyribonucleic Acid
EC	Endothelial Cells
EDHF	Endothelial-Derived Hyperpolarizing Factor
EGR	Early Growth Response
eNOS	Endothelial nitric oxide synthase
ERK	Extracellular signal-regulated Kinase
ET1	Endothelin
FAD	Flavin Adenine Dinucleotide
FMN	Flavin Mononucleotide
FOXO	Forkhead box protein O
GLP	Glucagon Like Peptide
GLUT	Glucose Transporter

Abbreviations

GSK	Glycogen Synthase Kinase
GTP	Guanosine Triphosphate
H/R	Hypoxia/Reoxygenation
H_2O_2	Hydrogen Peroxide
HAEC	Human Aortic Endothelial Cells
HDL	High-density lipoprotein
HIF	Hypoxia Inducible Factor
HMEC	Human Microvascular Endothelial Cells
Hsp	Heat Shock Protein
HUVEC	Human Umbilical Vein Endothelial Cells
ICAM	Intracellular Adhesion Molecule
IL	Interleukin
iNOS	Inducible nitric oxide synthase
JAK	Janus Kinase
KLF	Krüppel-like factor
LDL	Low-density lipoprotein
LNA	Lock nucleic acid
L-NAME	L-Nω-Nitro arginine methyl ester
LPS	Lipopolysaccharide
MAPK	Mitogen-Activated Protein Kinase
MEK	Mitogen-activated Protein Kinase kinase
MHC	Myosin Heavy Chain
MI	Myocardial Infarction
miR	microRNA
MMP	Matrix Metalloproteinase
mRNA	messenger RNA
mTOR	mechanistic Target of Rapamycin
NADPH	Nicotinamide Adenine Dinucleotide Phosphate (reduced)
NAFLD	Non-Alcoholic Fatty Liver Disease
NF	Nuclear Factor
NFκB	Nuclear Factor kappa-light-chain-enhancer of activated B cells
nNOS	Neuronal nitric oxide synthase
NO	Nitric Oxide
$NO_2^{\cdot}$	Nitrite
Nox	NADPH oxidase
Nrf	Nuclear factor erythroid 2-related factor 2
Nt	Nucleotide
O_2	Oxygen
$O_2^{-\cdot}$	Superoxide anion

$ONOO^-$	Peroxynitrite
oxLDL	oxidized Low-density lipoprotein
PECAM	Platelet Endothelial Cell Adhesion Molecule
PGC	Peroxisome proliferator-activated receptor gamma coactivator
PI3K	Phosphatidylinositol-3-kinase
PKA	Protein Kinase A
PKC	Protein Kinase C
PKG	Protein Kinase G
PPAR	Peroxisome Proliferator-Activated Receptor
PRD	Positive Regulatory Domain
PRDX	Peroxiredoxin
PRMT	Protein arginine N-methyltransferase
PTEN	Phosphatase and tensin homolog
RAA	Renin-Angiotensin-Aldosterone
RISC	RNA-induced silencing complex
RNA	Ribonucleic Acid
ROS	Reactive Oxygen Species
Ser	Serine
SERCA	Sarcoendoplasmic Reticulum Calcium transport ATPase
Sirt	Sirtuin
SOD	Superoxide Dismutase
STAT3	Signal Transducer and Activator of Transcription
TAC	Transaortic Constriction
TGF	Transforming Growth Factor
Thr	Threonine
TNF	Tumor Necrosis Factor
TSC	Tuberous Sclerosis Complex
TWIST	Twist Family BHLH Transcription Factor 1
TXA2	Thromboxane A2
UTR	Untranslated Region
VCAM	Vascular Adhesion Molecule
VEGF	Vascular Endothelial Growth Factor
VEGFR	Vascular Endothelial Growth Factor Receptor
VSMC	Vascular Smooth Muscle Cells

Introduction

Cardiovascular system: a general introduction

The cardiovascular (CV) system functions as a closed circuit that ensures blood transport from the heart to the whole organism, allowing gas exchanges (oxygen versus carbon dioxide), and supplying nutrients to organs. The CV system constantly adapts to meet organism needs in response to neurologic and humoral signals ensuring, at the short and the long term, an optimal perfusion of the whole body. Pollution, smoking, sedentarity and an unhealthy diet constitute major insults to the CV functions via a direct impact on the endothelium (see Figure 1).

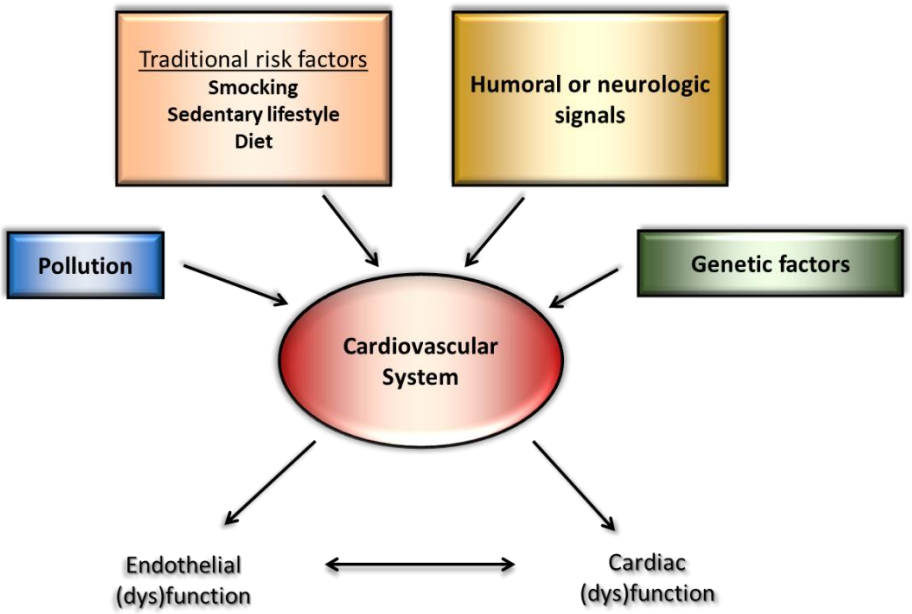

Figure 1: Regulation of the cardiovascular system. CV system is influenced by environmental, physiologic and genetic factors. Pollution, life style and diet can impact positively or negatively the CV system leading to modulation of endothelial and cardiac functions.

Endothelium

Endothelial Physiology

The endothelium is the innermost layer of blood vessels that forms an interface between circulating blood and the media. It is an essential part of the vessel wall as it fulfils critical functions to guarantee vascular homeostasis. The endothelium is composed of a single layer of highly specialized endothelial cells; it is closely associated with a basal membrane to form the intima of the vessel.

Endothelial function and dysfunction

Homeostasis of cardiovascular system is a fine-tuned phenomenon. The vascular endothelium participates to this well-regulated process by controlling inflammation and leucocyte adhesion, thrombogenesis and platelets aggregation, or angiogenesis. The endothelium is also the main actor that adapts vascular tone to tissue needs and controls blood/tissue exchanges. To meet these critical functions, endothelial cells combine very sophisticated sensory properties, signal processing and a balanced production of autocrine/paracrine effectors (see Figure 2) with antagonistic properties. Any disruption of this tight equilibrium is called endothelial dysfunction and can promote the development of pathogenesis. A dysfunctional endothelium phenotype is associated with impaired vasodilation, a pro-inflammatory and pro-thrombotic status, contributing to local and systemic manifestations of cardio-metabolic diseases such as atherosclerosis, hypertension or diabetes (1).

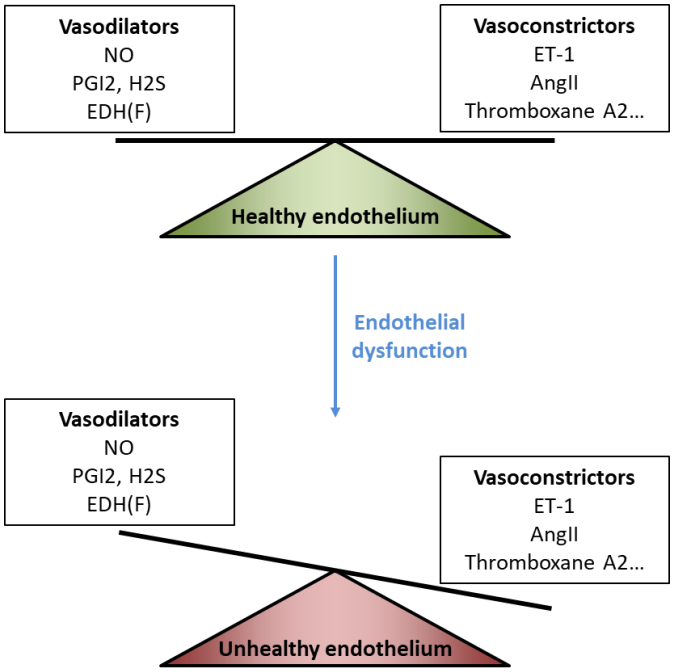

Figure 2: Endothelial-derived vasorelaxing and vasoconstricting factors. Vasodilation and vasoconstriction factors production are finely regulated to maintain a balance assuring vascular homeostasis. The disruption of the equilibrium leads to the so-called endothelial dysfunction. NO: nitric oxide, PGI2: prostacyclin, H2S: hydrogen sulphide, EDHF: Endothelial-derived hyperpolarization/ (hyperpolarizing factor), ET-1: endothelin 1 and AngII: Angiotensin II.

Endothelium-derived vasodilating factor is a generic term that includes a wide range of substances/modes of activation, the importance of which varies from a vascular bed to another and varies also depending on the physio/pathological status. It includes prostacyclins (PGI2) being the products of arachidonic acid metabolism by cyclooxygenases/prostacyclin synthase; Endothelial-derived hyperpolarizing factor (EDH(F)) which is not a factor *per se* but corresponds to the transmission of an hyperpolarizing stimulus to the media by the endothelium, and the gasotransmitters hydrogen sulfide (H_2S), carbon monoxide (CO) and nitric oxide (NO). If EDH(F) is mainly associated with the

control of vascular tone in resistance arteries due to increased potassium conductance (2), the other endothelium-dependent factors display multiple properties that often overlap. PGI2 is indeed a potent vasodilator but also a potent inhibitor of platelet aggregation (3). H_2S shares with NO anti-inflammatory, anti-apoptotic, and anti-oxidant properties in addition to being strong vasodilators. H_2S as NO may prime endothelial cells toward angiogenesis and inhibit vascular smooth muscle cells (VSMC) proliferation (4). Similarly, CO was shown to prevent vascular dysfunction, regulate blood pressure, inhibit blood platelet aggregation or have anti-inflammatory effects (5).

Additionally, endothelial cells are the site of production of constricting factors. Although an integrant part of the tight balance needed to insure a proper perfusion, they are more than often considered as harmful and associated with pathogenesis. The major « deleterious » factors include endothelin-1 (ET-1), the mature product of a preproET-1 precursor; thromboxane A2, the result of arachidonic acid metabolism by the cyclooxygenase (COX)/thromboxane synthase pathway, and Angiotensin II (AngII) produced from angiotensinogen via the renin-angiotensin-aldosterone (RAA) system. All these molecules globally counteract the beneficial properties of gasotransmitters and PGI2; they are reinforced in pathological states linked with endothelial dysfunction where they induce vasocontraction in addition to proliferation or pro-oxidant properties (6-8). Endothelial ET-1 and thromboxane enhanced inflammation, platelets aggregation and free radical formation while AngII promotes NADPH oxidase activity to produce superoxide anion ($O_2^{-\cdot}$) (9) leading to an inhibition of endothelial nitric oxide synthase (eNOS) and NO bioavailability (10).

Although a little restrictive, endothelium dysfunction is often considered as the result of a reduced NO bioavailability, nitric oxide being the more abundant

and multi-tasking protective factor. Down-regulation of eNOS expression or pharmacological inhibition of NOS and subsequent decreased NO production in experimental animal models (11) or even in human (12) have been undoubtedly associated with the development of hypertension for instance.

In the work presented here, we therefore focused on the NOS/NO pathways.

Nitric Oxide production

NO is a versatile compound that is active as mediator of numerous biological processes in the nervous, immune, and cardiovascular systems. It is a radical in nature which should be put in link with its relatively high reactivity and short half-life. It maintains cardiovascular health mainly by activation of soluble guanylate cyclase, an ensuing cyclic guanosine monophosphate (cGMP) production and Protein Kinase G (PKG) activation (13). A significant part of its activity also results from protein (cysteine) nitrosylation; this aspect has been inconsiderate for a long time, but it could tremendously impact protein conformation, localization and/or function (14). Depending of its concentration and the redox environment, NO acts as a signaling molecule or cytotoxic agent. In the presence of oxygen, autoxidation of NO to form nitrite (NO_2^-), a strong oxidizing and nitrating agent is favored in hydrophobic environment such as lipoproteins or membranes (15). NO_2^- is for instance a major actor in environmental toxicology. Nitrite and nitrate are the end-products of NO metabolism but may also serve as a reservoir of NO. Indeed, several enzymes are able to transform nitrite and nitrate in NO (16). Additionally, acidic conditions favor the formation of NO from nitrite in tumor microenvironment (17). The reaction of NO with superoxide anion ($O_2^{\cdot-}$) leads to the formation of peroxynitrite ($ONOO^-$) which can stimulate cysteine nitrosylation and tyrosine nitration leading

to potential alterations of DNA, lipids or protein structure and function (18). Protein nitration participates in the pathogenesis of diabetes, cancers, hepatic diseases or cardiovascular disorders (18;19).

NO synthases

NO is formed in equimolar amounts with L-citrulline by nitric oxide synthases (NOS) in the presence of L-arginine and molecular oxygen. Structurally, the NOS protein is a homodimeric multidomain enzyme; it catalyzes the oxidation of L-arginine using nicotinamide adenine dinucleotide phosphate (NADPH), flavin adenine dinucleotide (FAD), flavin mononucleotide (FMN), heme prosthetic group, tetrahydrobiopterin (BH_4) and O_2 as cofactors. At the dimer interface, NOS contains a zinc ion that coordinates a tetrahedral conformation with cysteine (C94 and C99 from two adjacent subunits). This site is essential for the binding of BH_4 and L-arginine (13;20).

Three NO-synthases have been formerly identified: NOS1 or neuronal NO-synthase (nNOS), NOS2 or inducible NO-synthase (iNOS) and NOS3 or endothelial NO-synthase (eNOS). The nNOS is constitutively expressed in approximately 2% of the body neurons, its enzymatic activity is primarily regulated by Calcium/Calmodulin (Ca^{++}/CaM) (21). Neuronal NO is implicated in synaptic transmission modulation, learning, memory or neurogenesis (22). The macrophagic NOS is inducible in an inflammatory context in response to lipopolysaccharides (LPS), cytokines or other inflammatory agents (22). iNOS is mostly expressed in immune cells but it can be virtually expressed in all cell types; its constitutive activation promotes the production of unregulated amounts of NO. iNOS-derived NO is an anti-viral and anti-bacteria effector that could be considered as potentially harmful for any cells due to its radical nature and its close association with $ONOO^-$ production (23;24). iNOS has been implicated in

septic shock where it promotes increased arteriolar vasodilation, hypotension and microvascular damages (25;26).

Endothelial NO synthase: eNOS, different levels of regulation

Despite the presence of nNOS in blood vessels and the inducible aspect of iNOS, in endothelial cells, the main recognized producer of NO is eNOS. Endothelial NOS as nNOS is considered as a constitutive, Ca^{++}/CaM dependent enzyme; the activity of which is triggered by the binding of endogenous or pharmacological activator on endothelial receptors and in response to mechanical stimulation by the shear forces exerted by blood flow (13). eNOS-derived NO production is a tightly regulated process that results from a combination of transcriptional, posttranscriptional and post-translational effects that we will briefly illustrate (13;22).

Marsden et al. have found that transfection of human eNOS promoter/reporter in non-endothelial cells, where steady state levels of eNOS mRNA were not appreciably expressed, lead to a high eNOS promoter activities suggesting that the methylation status of eNOS DNA is essential to regulate eNOS expression (27;28). Hence, they found that eNOS promoter is heavily methylated in non-endothelial cells limiting the availability of binding sites for transcription factors (28). In another context, Krause et al. found reduced eNOS expression in human umbilical vein endothelial cells (HUVECs) from intrauterine growth-restricted fetuses compared to HUVECs from normal fetuses, correlated with diminished DNA methyltransferase 1 expression and an increased methylation at CpG-352 in the hypoxia response element of eNOS promoter (29). Similarly, synthetic methylated eNOS construct presented a decreased response of well-known transcription factors Sp1, Sp3 and Ets1 (28) arguing again for eNOS promotor methylation as the primary level of regulation of the NOS/NO pathway.

The physiological regulation of eNOS depends also on a range of regulatory elements binding to eNOS promoter. The detailed study of eNOS promoter revealed that basal eNOS transcription results from two regulatory regions. Positive regulatory domain (PRD I) presents a high affinity for Sp1 and Sp3 while PRD II binds transcriptions factors Ets-1, Elf-1, YY-1, Sp1 and MYC-associated zinc finger protein (30). More than this *cis*-regulation, there is evidence that basal eNOS promoter activity also depends on *trans*-regulation as *trans*-acting factors can bind both PRD sites. In addition to the *cis*-elements present near the transcription start, other *cis*-regulatory DNA sequences exist as Sp1, AP-1 and AP-2 or NF-1 binding sites as well as sterol regulatory element and shear stress response element (27;31). These zones allow modulation of eNOS expression under certain conditions. For instance, in bovine aortic endothelial cells (BAEC), NF-1 transcription factor mediate the up-regulation of eNOS expression by transforming growth factor (TGF) β1 (32;33) while tumor necrosis factor (TNF) α diminishes the binding of Sp1 and Sp3 to eNOS promoter to decrease eNOS transcription (34). Such modulations can be observed at the onset of pathologies such as atherosclerosis. Reactive oxygen species (ROS) synthesis as hydrogen peroxide (H_2O_2) also modulates eNOS expression in endothelial cells by activating the Calmodulin Kinase (CaMK) II/ Janus Kinase (JAK) 2 pathway leading to a higher binding of Sp1 on eNOS promoter (35). Additionally, hypoxia regulates eNOS expression via redox sensitive AP-1 mediated transcriptional control (36). This regulation is location dependent as aortic tissues present a down-regulation of eNOS under hypoxia while lungs vessels show an up-regulation (37;38). Moreover, transcription factors up-regulated under laminar shear stress such as Krüppel like factor (KLF) 2 and 4 (KLF4) can positively impact eNOS expression. This point will be described in more details below (see Shear stress and NO).

The protein expression of eNOS is also the result of epigenetic mechanisms modulating the transcription or the translation of eNOS. For instance, as described in more details below, microRNAs (miR) can interact with the 3'untranslated (UTR) region of messenger RNA (mRNA) and induce their degradation or the repression of translation. Interestingly, a limited number of miRs have been identified as directly binding the 3'UTR region of eNOS. In HUVECs, miR-24 direct binding to eNOS mRNA induced down-regulation of its subsequent protein level (39). In human endothelium, miR-155 binds eNOS mRNA and leads to a decreased of protein expression. Accordingly, the repression of eNOS and eNOS-dependent relaxation has been described in a mouse model of endothelial dysfunction and attributed to the direct binding of miR-155 to eNOS transcript (40). In endothelial cells kept under normoxic conditions, a silencing of miR-214 increased eNOS expression and El Azzouzi et al. confirmed a direct interaction of this miR with eNOS mRNA (41). They also shown that miR-214 is up-regulated in myocardium during hypoxia. The last identified miR able to target eNOS mRNA is miR-765. Interestingly, this miR does not affect eNOS transcript in normoxia due to a stabilization of 3'UTR of eNOS mRNA by heterogeneous nuclear ribonucleoprotein (hnRNP). Under hypoxic conditions, a detachment of hnRNP induces a sensitization to miR-765 (42). Eventually, miRs also indirectly modulate NO levels through a regulation of the upstream or downstream pathways of eNOS, this is precisely the subject of this thesis.

Mechanisms and post-translational regulations of eNOS

Many studies have emphasized the importance of L-arginine and the co-factor BH_4 in NO production (see Figure 3). As such, substrate (L-arginine) or cofactor deficiency (BH4) would convert eNOS from a NO-producing enzyme to an enzyme that produce deleterious superoxide anions. This condition called eNOS

uncoupling has been largely associated with cardiovascular diseases. Among many others, Landmesser et al. have highlighted that endothelium of hypertensive mice present a higher oxidation of BH_4 into BH_2 (as a result of NADPH-derived ROS production), that led to uncoupling of eNOS and an impairment of endothelial function (43). In the context of smoking as a major cardiovascular risk factor, depletion of BH_4 was pointed out in aortic endothelial cells exposed to cigarette smoke extracts as leading to uncoupling of eNOS and decreased levels of NO. Moreover, de novo synthesis of BH_4 is limited in these cells as cigarette smoke extracts exposure leads to decreased expression of guanosine triphosphate cyclohydrolase (44). Functional eNOS uncoupling is a prominent feature of aging and CV diseases (45), structural uncoupling might not be as prevailing as technical pitfalls may have tainted earlier observations (46).

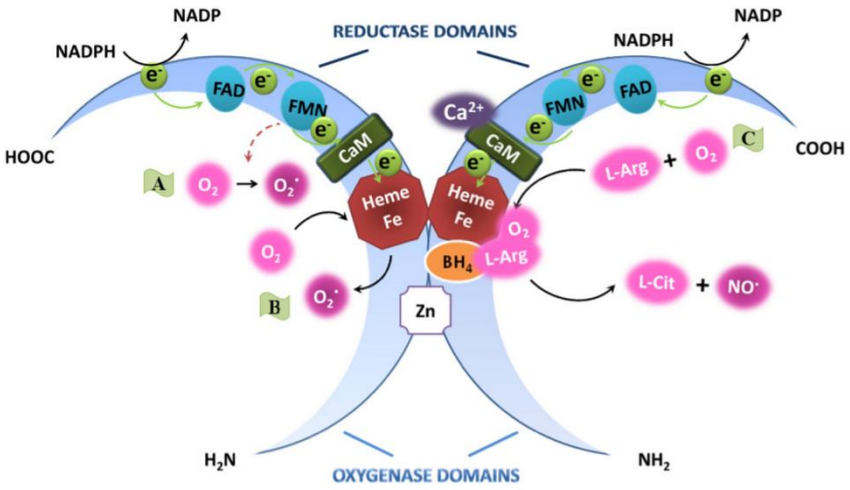

Figure 3: Representation of eNOS dimeric protein. Production of NO requires L-arginine (L-Arg) but also the presence of several co-factors as tetrahydrobiopterin (BH4), Flavin adenine dinucleotide (FAD), Flavin mononucleotide (FMN), calmodulin (CaM) and heme. eNOS is produced as monomer but must form a homodimer to produce NO. During NO synthesis, NADPH-derived electrons are transferred to flavins in the reductase domain and then to the heme. At this point, electrons are used to reduce and activate O_2. From Vanhoutte et al. (13)

NO pathway: postranscriptional regulation

In endothelial cells, palmytoylation and myristoylations promote eNOS trafficking from the Golgi to the plasma membrane and its localization in caveolae. In caveolae, eNOS is compartmentalized in close proximity to other actors of its activating cascade and held inactive (but ready to be activated) via a direct binding with Caveolin-1 (Cav-1). Any stimulus associated with a cytosolic increase in calcium and formation of the Ca^{++}/Calmodulin complex (following neurohormonal stimulation or increase in shear stress) would reverse the tonic inhibition by cav-1 and promote NO production. This has been largely documented in our lab; Cav-1 genetically deficient mice have allowed the characterization of this functional interaction *in vitro*, *ex vivo* and *in vivo* (47;48). Hyperlipidemia and cholesterol drives Cav-1 expression and promotes eNOS repression in rodent models (49-51).

If NO production is triggered by Ca^{++}/CAM binding, it is also further regulated by phosphorylation. eNOS protein sequence contains many potential sites for posttranslational modification (see Figure 4) among which Ser^{114}, Thr^{495}, Ser^{615}, Ser^{633} and Ser^{1177} have been described to be phosphorylated. Functional consequences are diverse and the best-known example (and more pertinent) is the fact that Ser1177 phosphorylation increases NO production while Thr495 phosphorylation hinders eNOS activation. Ser1177 phosphorylation of eNOS evokes conformation changes and increases electron flux transfer, promoting eNOS heme reduction (the limiting step in NO production) (52). Additionally, Chen et al. have recently highlighted that Ser1177 phosphorylation also enhances the enzyme affinity for its substrate and other co-factors (53). Classically, phosphorylation of eNOS on Ser1177 site has been attributed to Protein kinase B

(Akt) activity (54;55). The relation between phosphatidylinositol-3-kinase (PI3K)/Akt pathway and eNOS is indeed well documented in many physio/pathological models. Intravenous administration of insulin increases phosphorylation of Akt and eNOS as well as NO production in myocardial tissue of male rats. The effect on both Akt and eNOS is totally abrogated by pre-treatment with wortmannin, a PI3K inhibitor (56). Similar results were observed by Wang et al. demonstrating the exercise improved insulin sensitivity in aorta of rats and increases PI3K/Akt activity and phosphorylation of eNOS on Ser1177 (57). On the contrary, high-fat diet or apolipoprotein E (ApoE) genetic deficiency repress NOS activity through diminished phosphorylation on Ser1177, leading to a reduced NO production (58-60). Other modulators, such as vascular endothelial growth factor (VEGF), could also regulate the activity of the PI3K/Akt pathway and lead to modifications of NO production (61), Interestingly, knockout studies have demonstrated that the basal level of active eNOS is decreased in endothelial cells with suppressed expression of Akt1 (the main Akt isoform in endothelial cells) while suppression of Akt2 and Akt3 do not affect NO production (62).

In addition, in human endothelial cells, cyclic adenosine monophosphate (cAMP) effector Protein Kinase A (PKA) could also trigger Ser1177 eNOS phosphorylation (directly and indirectly via the PI3K pathway) explaining the cAMP dependent endothelial relaxation (63). For instance, proliferation of human coronary artery endothelial cells stimulated by Exendin 4 appears to be a PKA and PI3K/Akt/eNOS process (64). Yet, PKA and Akt also act independently to activate eNOS in the endothelium of rats during early ischemia preconditioning (65). Another kinase able to phosphorylate eNOS on Ser1177 site is AMP-activated protein kinase (AMPK) as observed by Morrow and coll. with 5-Aminoimidazole-4-carboxamide ribonucleotide (AICAR) in human aortic endothelial cells (66). In the same line, fenofibrate, a peroxisome proliferator-activated receptor (PPAR) α

agonist, increase eNOS activity via AMPK in HUVECs improving endothelial function (67). However, a recent study from Zippel et al. revealed that endothelial-specific deletion of AMPKα1 slightly improved acetylcholine-induced relaxation contradicting earlier assumption. They, in fact, demonstrated that AMPKα1 is more prone to phosphorylate eNOS Thr495 residue thereby reducing NO generation (68). Nevertheless, protein kinase C (PKC) and Rho kinase are considered as the main kinases responsible for eNOS phosphorylation on the Thr495 site. A variety of agonists activate eNOS through the Ser1177 phosphorylation concomitantly with Thr495 dephosphorylation, resulting in increased NO production with a basal level of calcium. Thr495 is indeed localized in the Ca^{++}/CAM binding domain, hence phosphorylation impedes Ca^{++}/CAM binding and eNOS activation. This site appears to be phosphorylated at basal state in endothelial cell meaning that an increase of NO production requires a fast dephosphorylation of this residue. If there is evidence of a correlation between dephosphorylation of Thr495 and phosphorylation on Ser1177, Schmitt et al. found that dephosphorylation of Thr495 site of eNOS without concomitant increase of Ser1177 phosphorylation is sufficient to enhance eNOS activity in human endothelial cells (69). The Ca^{++}/calmodulin-activated serine/threonine protein phosphatase calcineurin is recognized as the main protein in charge of thr495 (and Ser116) dephosphorylation.

Earlier work in our lab has illustrated that Hsp90 acts as an adaptor for both Akt and calcineurin leading to an increase of NO production through phosphorylation of Ser1177 (70) and dephosphorylation of Thr495 residues. *In vivo* Hsp90 over-expression indeed promoted NO production and reduced infarct size in pigs (70). More recently, Desjardin et al. highlighted that modulation of Hsp90 activity by activator of Hsp90 ATPase 1 promoted Hsp90/eNOS association as well as eNOS phosphorylation and NO production (71).

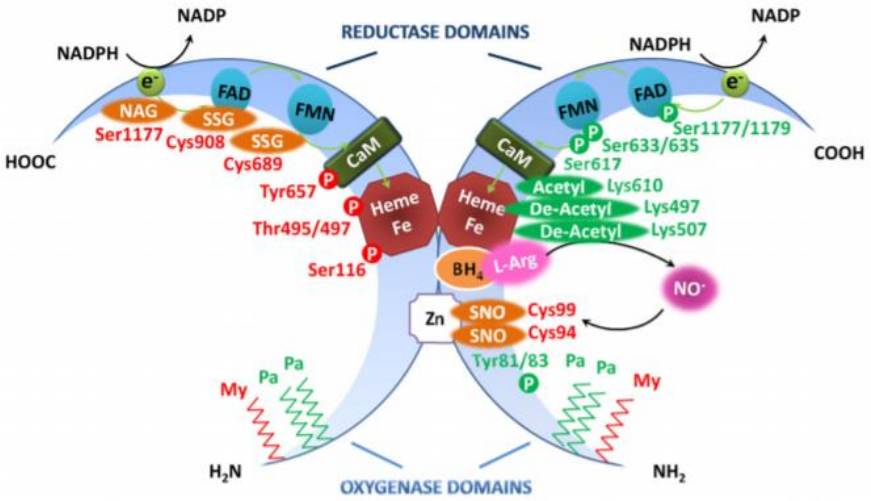

Figure 4: Post-translational modulations of eNOS. eNOS intracellular localization and activity can be modulated by thio-palmitoylation (Pa), N-myristoylation (My), S-nitrosylation (SNO), S-glutathionylation (SSG), N-acetylglucosamine (NAG) or phosphorylation (P). Modifications that enhance or reduce enzymatic activity are in green or red respectively. Cyst: cysteine, Ser: serine, Thr: threonine and Tyr: tyrosine. From Vanhoutte et al. (13)

Oxidative stress

In cardiovascular diseases, endothelial function and NO bioavailability are also determined by the oxidative environment. Indeed, vascular oxidative stress can modulate NO levels by interfering with both production and post-production fate of NO. Oxidative stress is generally defined as a discrepancy between the synthesis of ROS and the capacity of the cell to detoxify reactive intermediates or repair the consequential damages. Guzik et al. found that veins and arteries from diabetic patients present higher NADPH activity and expression and a dysfunctional eNOS protein compared to healthy patients, leading to an increased $O_2^{-\cdot}$ generation (72). In the same line, db/db mice present increased oxidative stress. Moreover, the authors demonstrated that incubation of aorta of C57Bl/6J

mice in a high glucose medium increases ROS production and decreases endothelium-dependent relaxation (73). Oelze and colleagues highlighted that AngII treatment caused endothelial dysfunction and increased $O_2^{-\cdot}$ production in Wistar rat. Oxidative stress is due to increased expression and activity of NADPH oxidase as well as enhanced eNOS uncoupling (74). Similar effects of AngII were observed in our lab by Lobysheva in endothelial cells. They demonstrated that inhibition of Cav-1 inhibited AngII-mediated NADPH activity and reversed eNOS uncoupling (10). HUVECs treatment with glucagon-like peptide (GLP)-1 diminishes oxidative stress-induced endothelial dysfunction and autophagy by decreasing ROS production (75). Pharmacological treatment of $ApoE^{-/-}$ mice with canagliflozin improved their aortic endothelial function through a decrease of NADPH oxidase subunits such as Nox2 and p22phox (76). This is consistent with a previous study showing that $ApoE^{-/-}$ mice present an impaired endothelial function with decreased NO level and increased oxidative stress. The use of an inhibitor of Thromboxane (TxA2) biosynthesis and biological activities, improves endothelial function through an increased phosphorylation of both Akt and eNOS and reduced oxidative stress (60). All these studies lay the emphasis on the detrimental role of ROS on NO bioavailability and endothelial function and fortunately point to the efficiency of various therapeutic strategies to prevent these deleterious effects. On a more mechanistic point of view, a high NADPH oxidases activity leads to oxidative degradation of BH_4 which promotes eNOS uncoupling leading to a production of $O_2^{-\cdot}$ by the enzyme as detailed earlier. $O_2^{-\cdot}$ can rapidly interact with NO and produced $ONOO^-$. This highly toxic component promotes DNA fragmentation and lipid peroxidation in addition to eNOS uncoupling (through oxidation of BH_4 to BH_2) (77) or worse structural dissociation of eNOS dimer (i.e. through oxidation of the Zn cluster). Interestingly, Zou et al. found that ONOO- increases eNOS phosphorylation on Ser1177 but nevertheless

blunts NO production; $ONOO^-$ could increases AMPK-mediated phosphorylation of eNOS at the expense of Akt-mediated phosphorylation, leading to uncoupling of the enzyme (78).

The superoxide anion, when produced without excess, could be processed by anti-oxidant enzymes as superoxide dismutase (SOD) to form H_2O_2 which is more stable and can cross the plasmatic membranes. H_2O_2 can be further transformed into water by catalase or peroxiredoxin (PRDX) to detoxify cell environment. Hu et al. demonstrated that mice expressing an endothelium-specific PPARγ dominant negative are more sensitive to AngII treatment than WT mice as they present higher Nox2 expression and lower SOD and catalase expressions (79). In the same line, L-N^{ω}-Nitro arginine methyl ester (L-NAME)-induced hypertension is characterized by reduced levels of glutathione (GSH), SOD and catalase (80).

Other modulators

More than the phosphorylation status, other post-translational modifications can act on eNOS activity. NO-dependent nitrosylation of cysteines 94 and 99 (active part of the Zn cluster), leads to eNOS inhibition as part of an auto-inhibitory loop. Another way to modify eNOS activity is by modulating its acetylation state. Indeed, Mattagajasingh et al. found that Sirtuin 1 (SIRT1) promotes endothelium-dependent vasodilation while inhibition of arterial SIRT1 blunts vasorelaxation and NO production. They demonstrated that SIRT1 and eNOS colocalize in HUVEC where SIRT1 deacetylates eNOS on lysines 496 and 506 increasing eNOS activity (81). The lysines deacetylated by Sirt1 lie in the calmodulin-binding domain of eNOS protein and their deacetylation leads to a more efficient binding of the Ca^{++}/CaM complex. Inhibition of SIRT1 in HUVECs also induces a decreased eNOS expression (82). This is however not the only role

of SIRT-1 on the regulation of the NOS/NO pathway as, SIRT1-mediates eNOS transcriptional expression (in response to resveratrol) via Forkhead box protein O (FOXO)1 and FOXO3a (83). Moreover, SIRT1 overexpression in heart of diabetic rats improved cardiac function through increased eNOS phosphorylation and reduced eNOS acetylation. The authors also found that superoxide anion production is decreased correlated with an increase of SOD expression (84).

In pathologic states such as acute coronary events, hypercholesterolemia or atherosclerosis, an increased expression of asymmetrical dimethylarginine (ADMA) is measurable (85;86). This molecule is a natural occurring competitive inhibitor of eNOS for the L-arginine binding site, its association with eNOS would prevent NO production. Protein arginine N-methyltransferase (PRMT) and Dimethylarginine Dimethylaminohydrolase (DDAH), the enzymes responsible for ADMA generation or degradation are dysregulated in pathological conditions (87;88). Plasma levels of ADMA correlates with vascular dysfunction severity and impaired vasodilation (89-91). Recently, Trittman and colleagues found that, similarly to ADMA treatment, down-regulation of DDAH1 in human fetal pulmonary microvascular endothelial cells induces a reduction of tube formation and NO production without modification of eNOS protein (92).

Shear stress and NO

Physiologically, the most important trigger of eNOS activity and NO generation in the endothelium is fluid shear stress in response to blood flow (93).

Shear stress could be defined as the tangential forces exerted by blood flow on the vascular wall (expressed in dyn/cm2); in linear arteries, the flow is considered as laminar, ordered in parallel layers and pulsatile (93) (see Figure 5). Shear stress regulates acute changes in vascular diameter and when sustained induce slow, adaptive, structural-wall remodeling, it is considered a critical

process to limit the development of atherosclerosis (94). In this line, Dumont and colleagues demonstrated that high flow (corresponding to laminar shear) induces outward hypertrophic remodeling in mesenteric arteries of rats correlated with an overexpression of eNOS with subsequent activation of matrix metalloproteinase (MMP) 9. Inversely, low flow is characterized by reduction of arteries diameter and decreased eNOS expression (95). The conversion of mechanical stresses to biochemical responses, known as mechanotransduction is initiated on the cell surface and transmitted to the cytoskeleton, in the direction of intercellular junction sites and cell-matrix adhesion sites, as well as toward the nucleus for transcription regulation. It promotes the (transient or sustained) up-regulation of specific genes among which 15% are under the control of KLF2 (96;97) and the downregulation of ET-1 and vascular cell adhesion molecule (VCAM) 1 for instance (98). A synergy between KLF2 and nuclear factor erythroid 2-related factor (Nrf) 2 allows the development of a quiescent endothelial phenotype and decreases inflammation. At branches, bifurcations and curved segments of the arterial tree, flow disturbance and transient vortices occur resulting in oscillating shear forces of lower amplitude (99;100) (see Figure 5). These arterial segments are considered as more atheroprone (101); a reduced activation of the NOS/NO pathway, inflammation, endothelial cell apoptosis and activation of vascular repair would be observed (102-104). In the next chapter, we will focus our interest on how mechanical forces could translate in activation of the NOS/NO pathway.

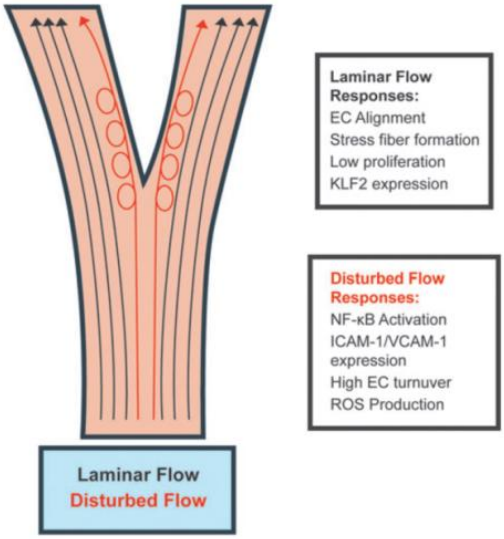

Figure 5: Laminar and disturbed flow both present in the vasculature. Straight and uniform zones of vasculature present a laminar flow whereas disturbed flow occurs at bifurcations or highly curved segments. In response to laminar shear stress, cells aligned in the direction of the flow and expressed higher KLF2. Disturbed flow response, considered as "atheroprone", comprises NFkB activation, EC proliferation and ROS production. EC: endothelial cells, KLF2: Kruppel like Factor 2, ROS: reactive oxygen species. From Givens et al. (105)

Flow meditated vasodilation in human arteries is indeed at least partly NO-dependent and its pharmacological inhibition blunts the effects of shear stress on angiogenesis. The early endothelial response to laminar shear stress includes ion channels and enzymes activity (mitogen-activated protein kinase (MAPK), eNOS and Akt among others) leading to the production of NO and ROS. Ando et al. demonstrated that flow induces the opening of potassium channels (106) and Ca^{++} channels with a subsequent increase in cytosolic calcium and eNOS activation (107;108). Also, a calcium influx through the mechanosensitive Transient Receptor Potential Cation Channel Subfamily V Member 4 (TRPV4) promotes NO-dependent relaxation (109;110). Another major trigger of NOS activity is the flow-sensitive cationic channel, Piezo-type mechanosensitive ion channel component

(PIEZO) 1 which mediates activation of PKA and eNOS through phosphorylation of Ser632 (111). This mechanism acts synergistically with Gq/11-mediated activation of the cell-cell complex platelet endothelial cell adhesion molecule (PECAM)-1, VE-cadherin and vascular endothelial growth factor receptor 2 (VEGFR2) which, through an activation of PI3K/Akt pathway, the phosphorylation of eNOS on Ser1177 increasing NO formation (112;112). Other kinase as AMP-activated protein Kinase (AMPK) phosphorylates the Ser1177 site of eNOS after induction of laminar shear stress (113). When discussing mechanosensing, we should not forget to mention the glycocalix which is the first cellular component in contact with blood flow. Although it is not fully understood how modulation of the glycocalix by flow transduces in NOS activation, there is ample proof that enzymatic degradation of the endothelial glycocalix by neuraminidase, heparinase, or hyaluronidase decreases flow-induced NO production (114). In this context, elements of the cytoskeleton, vimentin and dystrophin appears critical partners to promote Akt-dependent phosphorylation of eNOS (115). Also glypican appears to be a major regulator of flow-induced eNOS phosphorylation, its co-localization with caveolin-1 in the membrane raft fraction takes probably part in the explanation.

It should also be noted that activation of integrins also promotes activation of Ras homolog family member A (RhoA) GTPase. RhoA and Rac, these specific pathways participate in the typical alignment of endothelial cells with flow and the establishment of a cell polarity. This intermediate response to shear stress involves target genes of nuclear factor kappa-light-chain-enhancer of activated B cells (NFκB) such as intercellular Adhesion Molecule 1 (ICAM-1) (105) (see Figure 6).

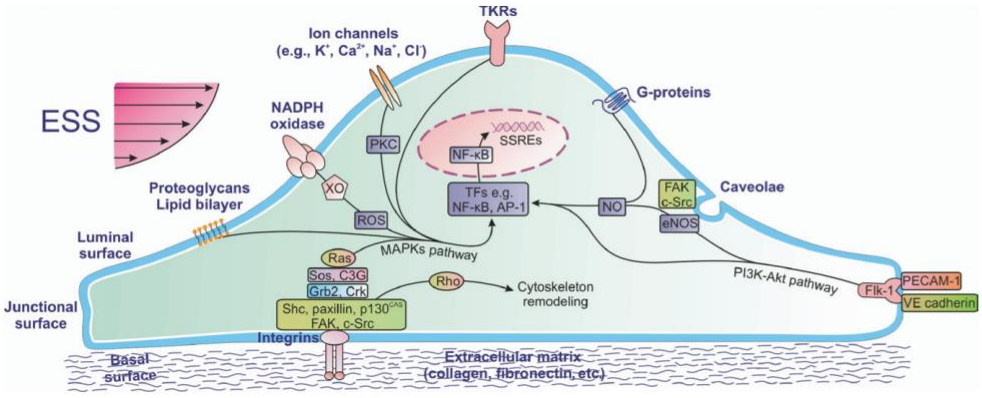

Figure 6: Mechanotransduction of laminar shear stress in endothelial cell. Luminal mechanosensors comprise Ionic channels, G proteins, caveolae, tyrosine kinase receptor or plasma membrane lipid bilayer. Shear stress signal is also transmitted through integrins or mechansensory complex (PECAM-1, VE-cadherin, Flk1). Subsequently, activation of several pathways including PI3k/Akt, eNOS or MAPK ensures the transmission of shear signal. From Chatzizisis et al. (116)

Laminar shear stress also upregulates eNOS mRNA both *in vitro* and *in vivo*. Several pathways have been described to explain the effect of laminar shear stress on eNOS transcription. Some have demonstrated that cSrc is responsible of an increased eNOS transcription and stabilization under laminar shear condition. As mentioned before, shear flow activates the MAPK pathway Ras/Raf/Mitogen-activated protein kinase kinase (MEK) 1/2 and ERK1/2 inducing the transcription of eNOS. Also, NFκB subunits p50 and p65 can bind to the shear-responsive element of eNOS promoter and increases its transcription and NO production. Finally, the shear stress-induced transcription factors KLF2 and KLF4 that bind the KLF site of eNOS promotor and stimulates its expression. Also, under basal condition the 3' poly(A) tail of eNOS mRNA is short (117). Shear stress promotes the transcription of eNOS mRNA with long 3' poly(A) tail which increases the half-life of the transcript and helps the rate of translation (118).

The specific role of miR in shear stress will be discussed below.

Exercise-mediated shear stress improves endothelial function

Changes in shear stress provide the principal physiological stimulus to adaptation in flow-mediated endothelial function (and vascular remodeling) in response to exercise. Clinical evidence highlights that patients performing physical exercise under CV rehabilitation present benefits regarding hospitalization rate and mortality due to CV disease (119). However, there is a large variability of vascular modulation in response to various kind of training. Indeed, Goto et al. found that aerobic exercise of moderate intensity stimulates NO synthesis and bioavailability leading to improved endothelial-dependent vasorelaxation, while high-intensity exercise induces an increase of ROS production (120;121). Also, repetitive exposure to exercise enhanced NO bioavailability and angiogenesis in animals (122;123) and humans (124). Patients presenting stable coronary disease and performing daily training 4 weeks before surgery developed an increased flow mediated vasodilation. Moreover, eNOS and Akt expression and activation are higher in cells isolated from these patients compared to untrained people. Yet, during exercise, functional adaptation precedes structural one (125;126). Tinken et al. demonstrated that a physical exercise of 2-6 weeks enhances NO bioavailability due to increased shear stress but after 6 weeks, there is a normalization of shear associated with vascular remodeling and NO level returns to baseline (127;128).

Cardiac tissue

Cardiac hypertrophy

Even more than the vasculature, the heart itself adapts to its environment to provide the required O_2 and nutrients supplies to organs. In

chronic hypertension, the heart facing pressure overload will adapt with left ventricular hypertrophy, increase in contractility and diminish physical stress on the ventricular wall to maintain cardiac efficiency. Similarly, in case of increased needs in the course of exercise or pregnancy, the heart would adapt to answer the demand. Depending on the type, strength and duration of upstream stimuli, cardiac hypertrophy will differ. The cardiac remodeling that happen in response to hypertensive is qualified of pathologic, it irremediably evolves to a maladaptive process and reduced cardiac function, while the cardiac alterations in response to exercise can be called physiologic, being adaptive, reversible and devoid of deleterious consequences on (or even improve) cardiac function (129;130). Experimentally, models based on AngII (131) or catecholamine receptor (either α or β) stimulation (132) of isolated cardiomyocytes could recapitulate most feature of pressure-overload-induced hypertrophy while physiological hypertrophy can be mimicked by thyroid hormones (133) or NO (induced by exercise for example) (134).

Cardiac adaptions comprise both structural and functional modifications of the left ventricle; It is accepted that adult cardiomyocytes have a very limited potential to proliferate, nevertheless , cardiac tissue displays significant plasticity, cardiomyocytes can grow, shrink or die in response to physiological of pathological stress (130).

Structurally, the development of pathological and physiological hypertrophies clearly differs (see Figure 7). Pathological hypertrophy is characterized by a reduction of left ventricular dimension and an increase of ventricular wall thickness. This deformation, called concentric hypertrophy and might evolve into eccentric hypertrophy with a strong dilatation of ventricular cavity due to a preferential lengthening of cardiomyocytes, this would progressively lead to heart failure (135). On the opposite, in the course of

physiological remodeling, cardiomyocytes grow both in length and width, that promotes the development of a milder increase of cardiac mass with a normal architecture as reviewed in athletes' heart by Weeks and McMullen. Interestingly, capillarity density increases with cardiomyocytes growth in training heart which would allow an adequate supply in both nutrients and oxygen (136). Conversely, several works on rodents demonstrated a mismatch between vascular density and cardiomyocytes growth following pressure-overload leading to hypoxia in the cardiac tissue (137-139). This is explained by a disrupted angiogenesis due to inhibition of the VEGF pathway.

As reviewed by Shimizu et al., cardiac dysfunction is characterized (and at least partly explained) by a spectrum of pathophysiological modifications including, sarcomere disorganization, metabolic changes, altered calcium handling, cell death, inflammation and fibrosis. Early work of Contard and colleagues and many others have highlighted that components of the extracellular matrix (ex. fibronectin and collagen) accumulate in cardiac tissue, in response to pressure overload inducing cardiac hypertrophy (140). These pathological fibrotic scars contain resident myofibroblasts which secrete high amounts of collagens (*Col1a1, Col1a2, Col3a1*) leading, *in fine*, to a loss a ventricular function (141;142). This particular feature is not encountered in the process of a physiological hypertrophy.

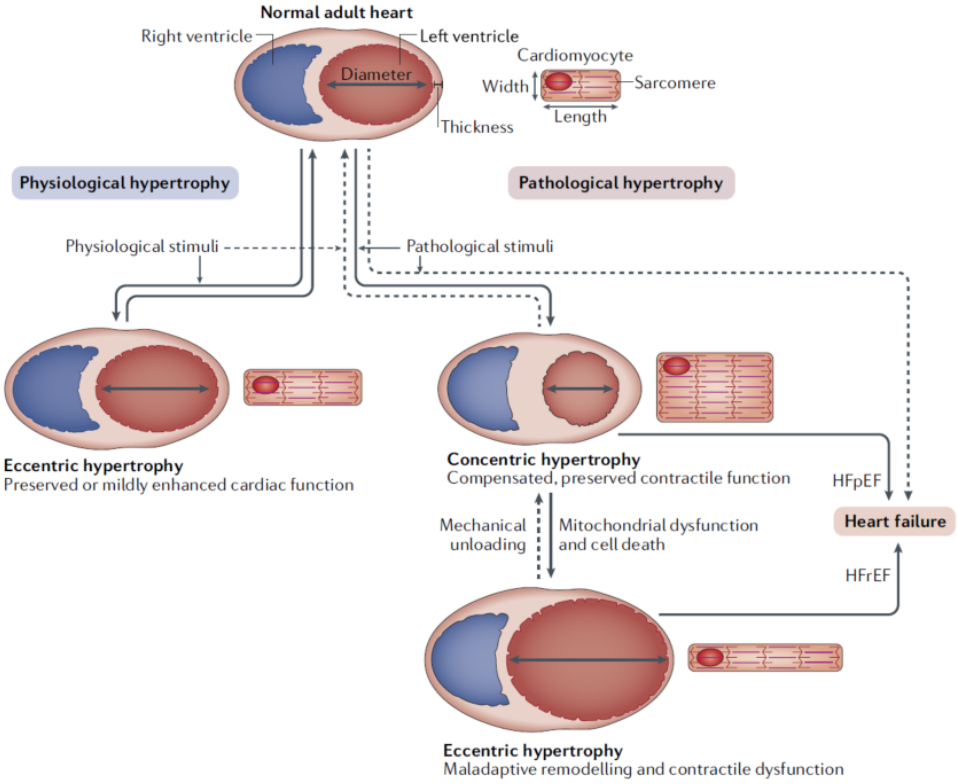

Figure 7: Comparison between pathological and physiological cardiac hypertrophy. Pathological hypertrophy is characterized by a reduction of ventricle dimension accompanied with an increase a wall thickness. This concentric hypertrophy presents a preserved contractile function but can evolve into eccentric hypertrophy with a strong dilation of ventricle cavity and a slimming of ventricular wall leading to a loss of cardiac function. Physiological hypertrophy presents a slight increase of ventricle cavity and a preserved or improved cardiac function. From Nakamura (129)

As already stated, the short-term phase of pathological hypertrophy is considered as adaptive and allows the maintenance of a correct contractile function. Among the initial adaptations, in response to the increased load of the ventricle and myocardial stretch, cardiac cells respond by promoting the synthesis and secretion of diuretic, natriuretic, anti-hypertrophic, anti-fibrotic and vasodilating peptides (atrial natriuretic peptide (ANP) and brain natriuretic

peptide (BNP)), these molecules are often not modulated in a more physiological hypertrophy although this is still under discussion. Also, alterations in the composition of contractile proteins can be observed very early in the remodeling process, with among others, a switch in myosin heavy chain (MHC) isoform contain. αMHC is the major isoform expressed in healthy adult human heart (143;144). In hypertrophic and failing heart, a shift towards the βMHC isoform occurs, it results from a reduced expression of αMHC and an increased in βMHC, allowing an increase in cross-bridge force with reduced energy expenditure. Measurement of βMHC transcription is actually considered as an early and sensitive marker of pathological cardiac hypertrophy. This takes part in a larger reprogramming of fetal gene which is not observed during physiological hypertrophy (see Figure 8).

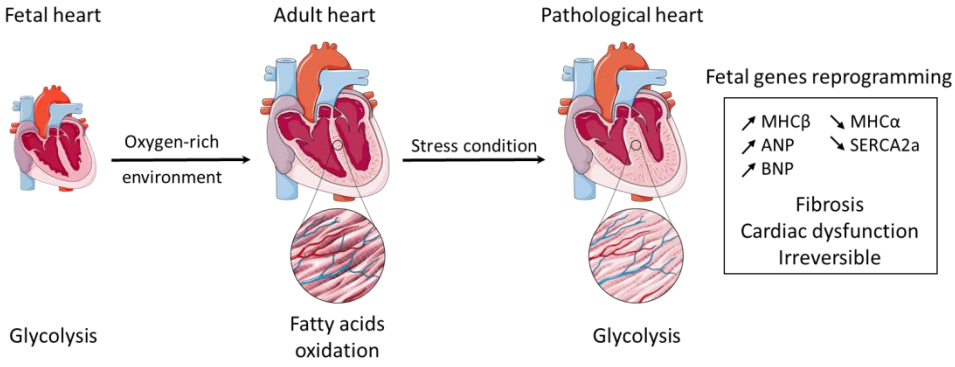

Figure 8: Fetal genes reprogramming. Fetal heart uses glycolysis (glucose and lactate) as main source of energy while adult heart uses preferentially fatty acids oxidation. Stress conditions inducing a pathological hypertrophy leads to a switch from fatty acid oxidation to glycolysis and the re-expression of fetal genes to maintain a correct cardiac function. MHC: Myosin heavy chain, ANP: atrial natriuretic peptide, BNP: brain natriuretic peptide, SERCA: sarcoendoplasmic reticulum calcium transport ATPase.

Acting synergistically with the alterations of the contractile apparatus, increased Ca^{++} influx and mobilization also occur during the initial stages of pressure overload-induced hypertrophy (145;146). However, as the heart develops in mass, protein implicated in calcium handling, as sarco/endoplasmic reticulum Ca^{++}-ATPase (SERCA) 2a, are decreased, translating the adverse effect of later stages of hypertrophy on cardiac function (147;148).

Gene reprograming in the remodeling heart is also referred as fetal gene reprograming as many alterations promote a fetal-like phenotype. This is particularly the case when considering the energy supply/consumption. In the fetal heart, glycolysis is the major pathway to produce energy. After birth, lactate and glucose oxidation is replaced by a predominance of fatty acid oxidation correlated with an increase of mitochondrial oxidative capacity. Lehman and colleagues demonstrated that passage from a relatively hypoxic environment to an oxygen-rich is characterized by an upregulation of several transcriptional regulatory circuits. This is the case for PPARα and its coactivator peroxisome proliferator-activated receptor gamma coactivator (PGC1α) which are upregulated after birth. They control fatty acid uptake and oxidation and boosts mitochondrial biogenesis (149). When submitted to a stress as hypertrophy, the heart returns to a more glycolytic state at cost of fatty acid oxidation. This metabolic reprogramming is accompanied with a downregulation of gene involved in mitochondrial biogenesis. Activation of cell-survival pathways (i.e. PI3K/Akt and mTOR), also participates in the metabolic switch as Akt activation increases glycogen synthesis in myocardial cells (150). Moreover, Akt is also known to phosphorylate GLUT4 to increase the glucose supply in adipocytes reinforcing its implication in metabolism (151). Interestingly in this context, there is some overlap between pathological and physiological activated pathways of hypertrophy as short-term Akt activation also plays a key role in the development

of physiological hypertrophy (152) probably through phosphorylation of glycogen synthase kinase (GSK)-3 (153) and tuberous sclerosis complex (TSC) 2 (154) leading to a regulation of heart size. The kinetic of the events is probably the key determinant of whether it would drive to a pathologic versus physiologic phenotype. Indeed, overexpression studies have highlighted that short-term overexpression of Akt leads to development of physiological hypertrophy while long-term overexpression tends to promote a pathological one (152). Moreover, DeBosch et al. found that training mice lacking Akt1 isoform do not develop cardiac hypertrophy while pressure-overload induces a hypertrophy suggesting that Akt1 isoform is critical for exercise-induced heart growth (155). In neonatal rat cardiomyocytes exposed to phenylephrine (a common model of cardiac hypertrophy *in vitro*) a reduced PPARα gene expression and altered activity are observed, this leads to a blunted capacity for lipid and energy homeostasis (156). Interestingly in physiologic cardiac hypertrophy promoted by exercise, PPAR genes are overexpressed (157). Also In the specific context of exercise, Narkar et al. showed increased AMP levels in the cell, promoting AMPK activation and increase of PGC1α to control mitochondrial biogenesis and energy metabolism. Activation of AMPK by gavage of mice with AICAR, enhanced training adaptation (157). Actually, in physiological hypertrophy both fatty acids oxidation and glycolysis might be up-regulated (158).

MicroRNAs: generalities

MicroRNAs production

Description and Synthesis

MicroRNAs (miR) are small (21-25 nucleotides) endogenous non-coding RNAs that are highly conserved in mammalians and form a novel class of

regulators. They are involved in post-transcriptional gene silencing meaning that they negatively regulate gene expression by targeting the 3' untranslated (UTR) region of messenger RNAs (mRNA). Inhibition of translation or a degradation of targeted mRNA will follow depending on the complementarity between miR and mRNA sequences.

Briefly, the synthesis of miR is initiated in the nucleus where RNA-polymerase II or III induces formation of a long transcript from genomic DNA, the primary microRNA transcript or pri-miR, which is 5'-capped and 3'-polyadenylated and forms an imperfect hairpin structure. Pri-miRs are either monocistronic or polycistronic leading respectively to the formation of a sole miR duplex or clustered miRs. The pri-miR is processed within the nucleus, by RNAse III endonuclease Drosha and double strand RNA binding protein DiGeorge syndrome Critical Region 8 (DGCR8), leading to a cleavage and the production of a shorter sequence of around ~70 nucleotides (nt) organized in a stem-loop structure called microRNA precursor or pre-miR. This pre-miR is then exported into the cytoplasm by GTP-binding nuclear protein Ran (RanGTP)/Exportin 5 complex and where it could be further processed by another RNAse III enzyme, Dicer, which excises the precursor loop to generate a mature miRNA duplex (~20nt). The selection of sense/antisense strand occurs when miR duplex is loaded onto Argonaute protein (Ago), an effector of the RNA-induced silencing complex (RISC) (159). The antisense miR binds the 3' untranslated region (UTR) of target mRNA promoting mRNA destabilization, degradation or translational inhibition, depending on the complementarity between miR and target sequences (159;160) (see Figure 9). More than 60% of genes coding for protein are regulated by microRNAs (161;162). This positions microRNAs as essential regulators in cellular biology.

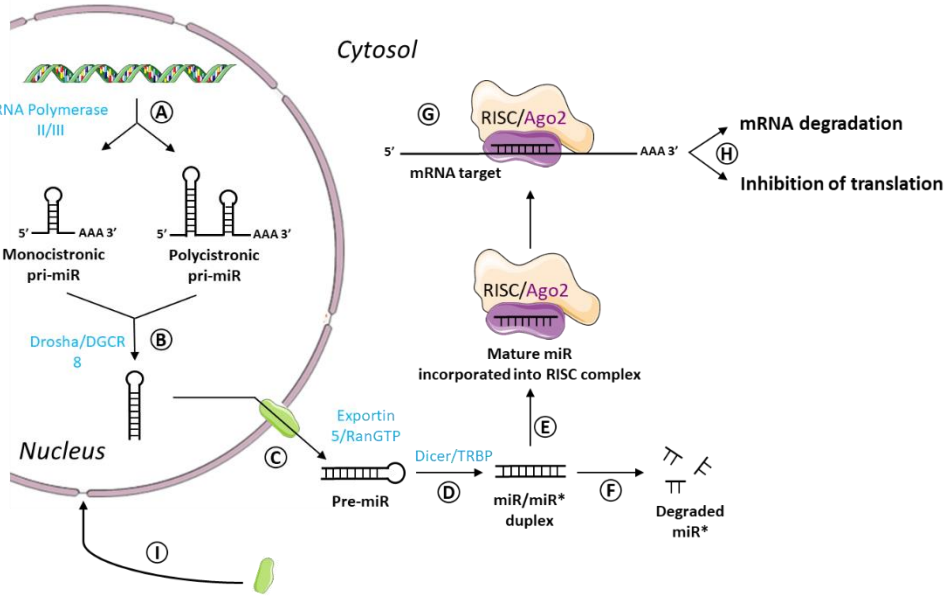

Figure 9: miR biogenesis. A. Primary miR is transcribed from DNA by RNA polymerase II or III. B. The endonuclease Drosha and DGCR8 cleave pri-miR to form a shorter sequence, the miR precursor or pre-miR. C. Pre-miR is exported from the nucleus to the cytoplasm thanks to Exportin5 protein. D. In the cytoplasm, pre-miR is cleaved by Dicer to form a miR duplex containing a major strand (miR) and a passenger strand (miR*). Usually, the major strand is incorporated into the RISC complex to form the mature miR and F. passenger strand is degraded. G. The RISC complex allows the alignment between mature miR and targeted mRNA. H. Depending on the complementarity, mRNA is degraded or translation is inhibited. I. Exportin returns to the nucleus after the release of pre-miR.

Nomenclature

The miRBase published in 2011, contained more than 20 000 mature miR products listed in 168 species and this number continues to increase. Among these miRs more than 2000 are described in humans (163). MicroRNAs denomination follows a strict nomenclature. Conventionally, they are identified as illustrated in Figure 10. The first three letters refer to the species of origin, with hsa- for human or mmu- for mouse. The abbreviation “miR” indicates a mature

microRNA in opposition to mir which refers to the precursor. A lettered suffix indicates very similar sequences; for instance, miR-199a and miR-199b display very close sequences (1-2 nt out of 21-25 nt) but originate from distinct precursors (encoded from DNM3 and DNM2 for miR-199a and from DNM1 for miR-199b). Thanks to cloning studies, it was also highlighted that two ~20nt miR can originate from a same predicted precursor. Depending of the arm of origin in the hairpin they are named -3p and -5p originating from the 3' and 5' arm respectively. An older convention mentioned miRs as miR and miR* depending on the abundance of sequences in the cell, highly present for miR (antisense) and poorly or not present for miR* (passenger strand, sense) (164-166).

Figure 10: Conventional nomenclature for microRNA. First three letters described the species. Suffix letter indicate a certain precursor sequence and 3p or 5p gives information about the arm of origin in the hairpin.

miR* and miR: both useful for the cell

Although both strands of a duplex are produced in equal quantity, their accumulation is asymmetric at steady state probably due to a greater degradation of miR passenger strand (167). It has been accepted for a long time that one strand of the miR duplex (passenger strand or miR*) is degraded while the major strand (biologically active miR, antisense) is incorporated into the RISC complex to induce gene silencing (168). Once associated to Ago, selected miRNA is highly stable with a half-life estimated to ~ 14 hours (169). More recent work has

revealed that both strands of the miR duplex could be fully functional in a specific cell type, be highly expressed and associated with Ago. The miR/miR* ratio can vary during the development or according pathological states (167;170;171). For instance, miR-152 is described as a tumor suppressor regulating migration and invasion in gastric epithelial cells. However, all these effects are attributed to the miR-152-3p. The passenger strand miR-152-5p has been just ignored as it was considered to be degraded. Yet, You et al. demonstrated that gastric cancer tissues and cells present an abnormal proportion of miR-152-3p/miR-152-5p ratio. Indeed, mir-152-5p appears strongly down-regulated in gastric cancer compared to normal cells while miR-152-3p is nearly not impacted. Interestingly, in normal cells miR-152-5p regulates the same target than its major strand miR-152-3p (172). In the same line, the oncomiR miR-21 is known to be up-regulated in different types of cancer and is a marker of low survival. Pink et al. have highlighted that miR-21-3p, the miR* of miR-21 duplex is able to target tumor suppressor genes and enhances resistance of ovarian cell lines to cisplatin while miR-21-5p has exactly the opposite effect (173). In addition to demonstrating functionality of miR passenger strands, these studies pointed out that miR and miR* can have antagonistic or synergetic effects.

A large role of regulation

As one miR can target several mRNAs and one mRNA can be targeted by several miRs, this produces a very dense and complex regulation network. Indeed, due to their short length and a high efficiency despite a partial complementarity with mRNA sequence, one miR can have dozens of targets. Prediction algorithms have been developed to help researchers in their quest for potential targets, among them TargetScan, Pictar and microRNA.org. The broad potential impact of miRs adds to the fact that a sole mRNA presents multiple potential binding sites

for (different) miRs and explains why translation regulation by one miR may vary in different cell types. However, tissue-specific patterns of miR also provide insights into more specific functions. Indeed, many miRNAs display marked organ specific expression patterns. In some cases, miR expression can even be restricted to a single tissue layer within an organ as illustrated in embryonic hearts by Zhao et al. (174).

To illustrate the importance of redundancy in cardiovascular development, mice presenting a deletion for individual miRs might show an altered cardiac phenotype, but this does not lead to 100% lethality. In opposition, experiments aimed to delete protein implicated in miR biogenesis (Dicer, Drosha or Argonaute) in the heart, resulted in lethality during the early gestation period (175). This also points to miRs as subtle protein regulators or fine-tuners instead of on/off switches.

Circulating microRNAs

In 2007, it was highlighted that miR are able to circulate from one cell type to another with the corollary that miR can be easily measured in body fluids as plasma, urine, saliva. The existence of extracellular miR suggested also that they could play a role as signaling molecules. These circulating miR or c-miR are highly stable and can resist to freezing, RNase or different pH environments (176;177). Their stability results at least partly from their association with different carriers going from vesicles to simple chaperone. Several types of c-miR-carrier vesicles have been described: microvesicles (100nM-1µm), exosomes (40-100nm) and apoptotic bodies (1-4µm) (178;179). In all these vesicles, miRs are associated with Ago2 (180). Moreover, miRs can also be found simply complexed with Ago proteins (181) or associated with high-density lipoproteins (HDL) (182) (see Figure 11). Repartition of miR with different carriers is variable, some are

predominant in vesicles and others are mostly found “free” in complex with Ago (183). In 2014, Kopper-Lalic et al. revealed that miRs can undergo post-transcriptional modifications. These non-templated nucleotide additions can define intra- or extracellular localization of miRs. For example, miRs presenting 3’-terminal adenosine are retained in the cell while miRs with 3’-terminal uridine are included in exosomes (184).

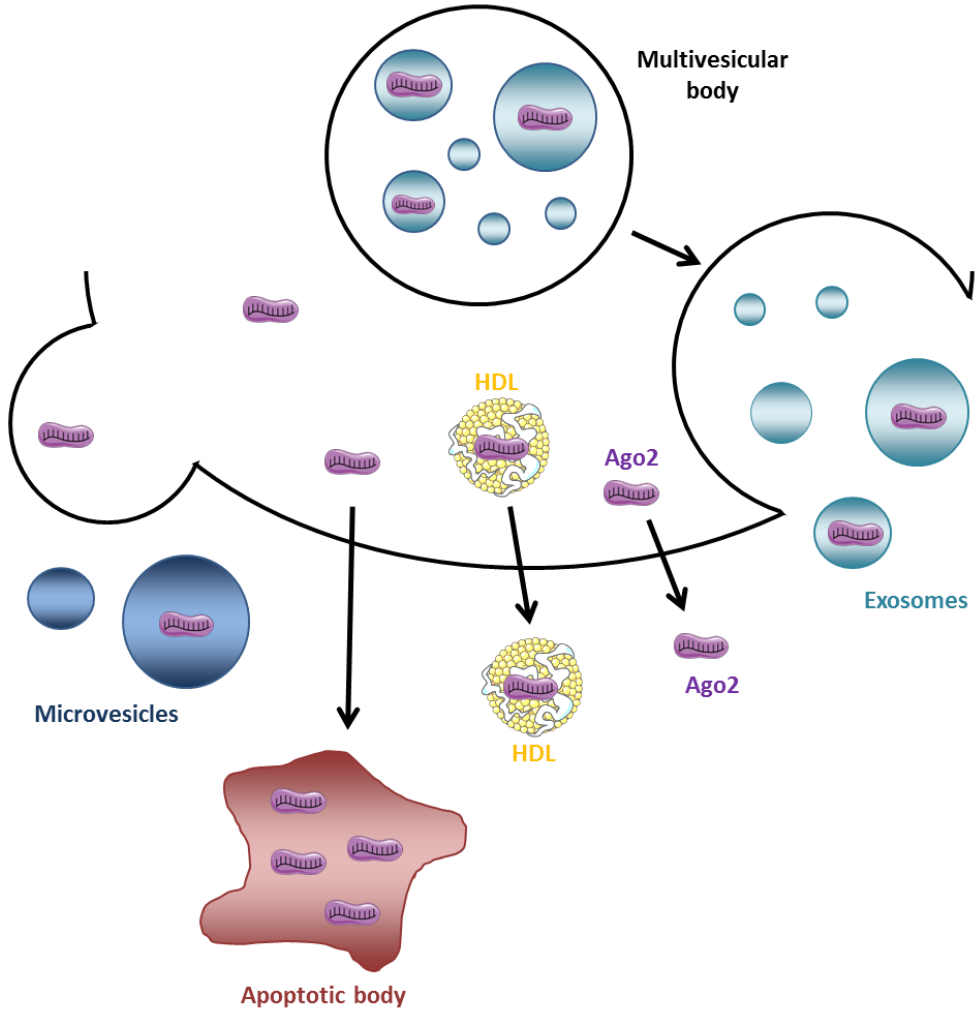

Figure 11: Schematic representation of miR secretion pathways. MiR can be excreted in extracellular medium in microvesicles, exosomes and apoptotic bodies or coupled to Ago2 or HDL. Ago2: Argonaute 2, HDL: High-density lipoprotein.

Different studies have shown that miRs contained in exosomes are able to transfer biological information *in vivo*. At the vascular level, it was highlighted that exosomes excreted by cultured endothelial cells and containing high level of miR-

143/miR-145 induce a decrease of atherosclerotic lesions in *ApoE*$^{-/-}$ mice (185). Interestingly, alteration of miR carriers was observed in human diabetes or diabetic nephropathy. MiR-21 and miR-126 are increased in extracellular vesicles while miR-660 is increased simply complexed with Ago2 and miR-132 decreased in HDL fraction (186). This demonstrated that c-miRs can be considered as a new type of signaling molecules and act as cellular modulators.

miR can also convey from cell to cell through gap junctions as previously demonstrated for short interfering RNA. Peng and colleagues demonstrated that gap junctions composed of Connexin (Cx) 43 allow the trafficking of miR between cancerous cells. However, all gap junctions do not possess the ability to transfer miR as reported by the same authors for gap junctions containing Cx32 or Cx37 (187). This type of transfer also exists between different types of cells and this is particularly important for endothelial cells as it allows the transfer of miR from the endothelium to surrounding tissues. For instance, Thuringer and colleagues revealed that a functional inhibition of gap junction abrogates the transfer of miR-145-5p from human microvascular endothelial cells (HMEC) to U87 human glioblastoma cells or between HMEC and colon cancer cells (188;189). In a co-culture of Bone-marrow derived mesenchymal stem cells (BMSC) and HUVEC, formation of gap junctions composed of Cx43 between the two cell types allows transfer of miR-200b from BMSC to HUVEC to decreases angiogenesis (190) showing the importance of this kind of transfer on cell physiologic functions.

MicroRNAs and therapeutics

As miRs are detectable in plasma of patients, they can act as non-invasive biomarkers for several diseases. The most striking example is in cancerous pathologies where circulating miR levels of patients are often dysregulated. The use of miRs as biomarkers in cancers is a very attractive diagnosis option but one

problematic is that a same miR can be modulated in different types of tumor. Yet, Lin et al. have demonstrated that the study of a panel of 7 miRs (miR-29a, miR29c, miR-143, miR-145, miR-133a, miR-192 and miR-507) containing tissue-specific miRs presents a superior diagnosis sensitivity to detect hepatocellular carcinoma than the clinical biomarker α-fetoprotein (191). Other diseases as nonalcoholic fatty liver disease (192), hepatitis C or even cardiovascular diseases present specific signature of miRs dysregulated in plasma of patients. For instance, Wang et al. highlighted 3 circulating miRs (miR-3135b, miR-3908 and miR-5571-5p) as signature in patients with dilated cardiomyopathy (193). In the same line, miR-124 and miR-150 have been identified as markers of vascular inflammation in obese patients, they are modulated by exercise and the associated improvement of endothelial-dependent response (194).

Early marsh 2020, a search for the simple term “miR” on the website “ClinicalTrials.gov” retrieve 342 studies, mostly related to the search for a miR profile associated with a pathology, aggravation, efficiency or resistance to treatment. Indeed, at this time miRs are not (yet) used as therapeutic targets in humans. The relative specificity is a limiting factor. Yet, phase I and II studies were already performed using miR-122 as a target to treat hepatitis C. MiR-122 acts positively on Hepatitis C virus (HCV) enhancing its viral replication, viral translation and genome stabilization. As miR-122 is considered as liver-specific, a therapy based on miR-122 inhibition was launched. First experiments on animals demonstrated that Miravirsen, a specific miR-122 inhibitor, reduced RNA levels of HCV. The same effect was observed in human patients during the phase 2a of the clinical trial, proving that miR-based therapies are also possible in humans (195).

Miravirsen development is based on a technology largely used in fundamental and preclinical research to repress targeted miRs, the use of short

modified oligonucleotide sequences designed to associate with the miR of interest in a Watson-Crick recognition pattern and repress its expression/activity. Sequences similar to a specific miR (or premiR) are also tools that are frequently used to enhance or replace miR expression (see Figure 12). Modulation of miR expression in cell/tissue remains challenging, in addition to the problematic potential off-targets, two major issues should be overcome: stability and delivery. Hence, many strategies have been developed to stabilize these molecules. The more effective involve the use of a phosphorothioate backbone that protects the oligo sequence from a rapid degradation by plasma and intracellular nucleases (often only part of the bonds is "phosphorothioated"). 2'-O-methoxyethyl modification or the presence of a bridge between 2'- oxygen and 4'-carbon (LNA or locked-nucleic acid) in ribonucleotides are also frequently proposed to enhance stability. Addition of a cholesterol motif at the 3' end through a hydroxyprolinol modified linkage should enhance distribution and cell permeation of antagomiRs. A non-perfect complementarity between the miR and the inhibitory sequence such as introduction of a mispairing at the cleavage site of Ago2 (or other base modification) inhibits Ago2 cleavage. Although antimiRs (antagomiRs, LNA) or mimics have been shown to be effective in many studies following a simple intravenous injection in animal; the use of viral or liposome delivery system are also possible. Injection of the coding sequence would promote a long-standing effect, while the use of miR sponges with multiple binding sites would enhance miR repression efficiency. For these, viral or liposome delivery is mandatory (196).

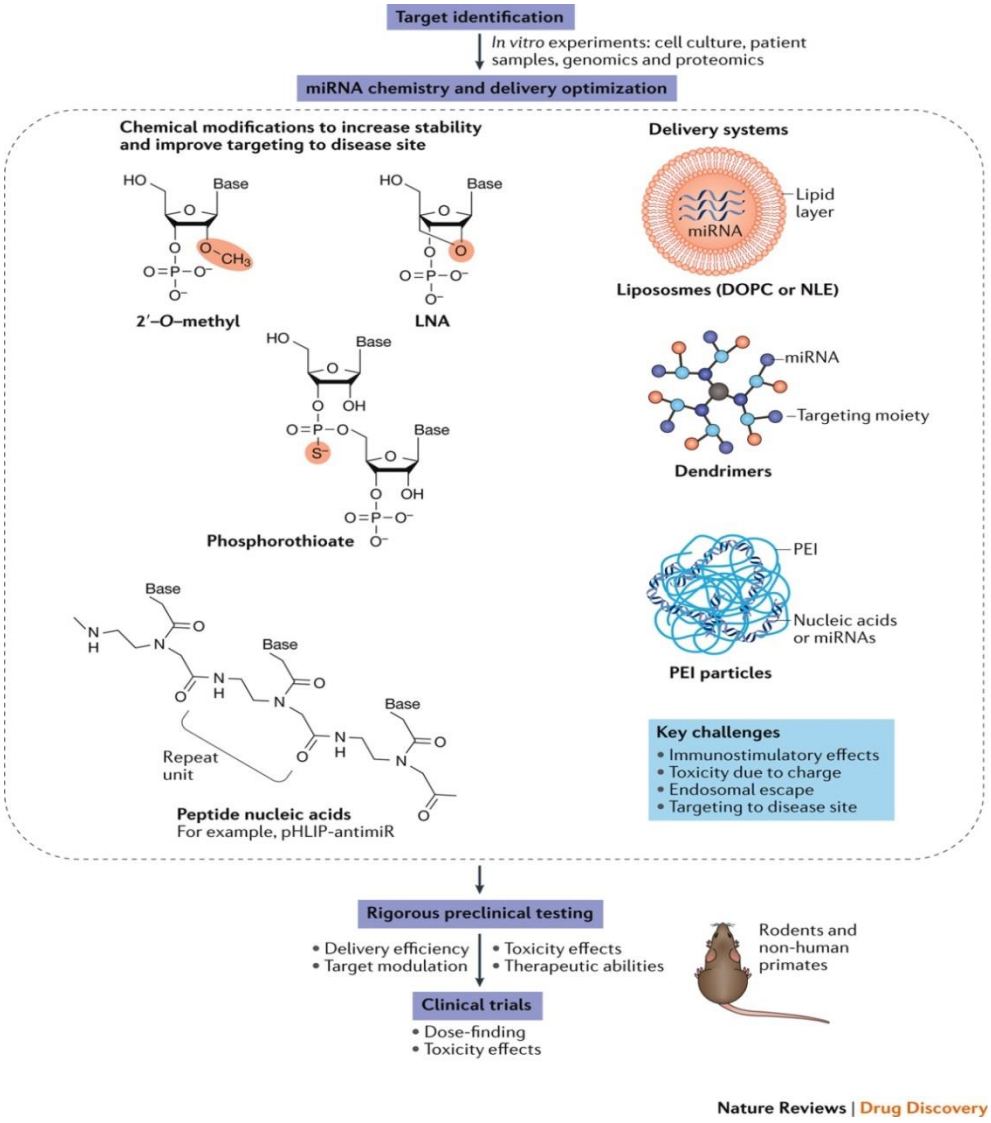

Figure 12: miR therapeutic approach. Target identification is done based on patient blood samples and studying the biology and relevance of miR candidate through *in vitro* and *in vivo* models. miR therapeutic requires the use of chemical molecules. Their stability can be increased by chemical modification as for LNA or by encapsulation methods as lipid nanoparticle or dendrimer complex. DOPC: 1,2-dioleoyl-sn-glycero-3-phosphotydylcholine; PEI: polyethylenimine; pHLIP: pH low insertion peptide. From Rupaimoole et al. (196)

Among many other studies aiming to modulate miR expression in preclinical experiments, Thum et al. efficiently induced silencing of miR-21 in the heart of mice through simple intravenous injection of antagomiR. They demonstrated that in pressure-overload model of mice, the inhibition of miR-21 reduced ERK/MAPK activity as well as fibrosis and cardiac dysfunction (197). In the same line, intravenous injection of LNA antimiR-208 in a model of hypertensive rats improved cardiac function and survival and prevents pathological switch of myosin and cardiac remodeling (198). In obese mice, miR-103/107 is increased. Trajkovski and colleagues found that silencing miR-103/107 improves glucose homeostasis and insulin sensitivity. They used liver-targeting lipid nanoparticles to deliver the anti-miR to the liver (199). Ai and colleagues found that injection of cholesterol-conjugated miR-411 mimic in rat model of deep venous thrombosis induces an inhibition of vein wall fibrosis through a decrease of Hif1α and MMP-2 (200). PremiR are also used to mimic miR physiology. For instance, the transfection of synthetic precursor, premiR-455, in cultured cardiac myocytes down-regulates calreticulin levels. This study suggests that activating transcription factor 6 decreases miR-455 and thus up-regulates calreticulin leading to a cardioprotective effect (201).

MicroRNAs in cardiovascular system

MicroRNAs in endothelial homeostasis and diseases

Importance of miRs in vascular development has been first highlighted through the silencing of Dicer, the major regulator of miR biogenesis. At embryonic level, mice presenting a hypomorphic Dicer allele developed vascular abnormalities. In adult, specific deletion of Dicer in endothelial cells does not lead to overt adverse phenotype. However, Dicer KO impairs angiogenesis as well as

proliferation and migration (202;203). In the same line, Suarez et al. assured that *in vitro* deletion of Dicer in HUVECs leads to an increase of endothelial cells-specific genes expression as eNOS, Tie-2 and KDR (202).

Hundreds of miRs have already been associated with all aspects of endothelial function. Some of them such miR-155, miR-222, miR-320 and miR-126 were shown to impact junction assembly or cell morphology, both factors related to vascular permeability while other inhibit or promote angiogenesis (204). As another example, the metalloproteinase ADAM15 which promotes hyperpermeability is a direct target of miR-147b. LPS-induced endothelial barrier dysfunction, evidenced by a reduction in transendothelial electric resistance and increase in albumin flux across endothelial monolayers, could be attenuated in cells treated with miR-147b mimics (205). In another context, miR-25-3p has been shown to regulate indirectly VEGFR2, Zonula occludens-1, occludin and Claudin5 in endothelial cells by targeting KLF2 and KLF4, consequently favoring vascular permeability and angiogenesis and promoting colon cancer metastasis (206). Further, miR-125b is transiently stimulated by VEGF or ischemia and can directly target VE-cadherin. Injection of miR-125b into the tumor represses VE-cadherin expression in endothelial cells and leads to formation of non-functional blood vessels (207). On the opposite, down-regulation of miR-125b is observed in human retina microvascular endothelial cells treated with high glucose. This is correlated to an increased expression of VE-cadherin and increased proliferation and tube formation (208).

Interestingly, vascular diameter can also be modulated by miRs, through the control of ion channel or receptor expression as with miR-155 or miR210 (209;210). The endothelial NOS/COX-dependent pathways are also strategic targets. Dicer deletion in endothelial cells has been shown to upregulate eNOS

expression, a process counteracted by miR-222 upregulation. However, miR-222 does not target the 3'UTR region of eNOS suggesting an indirect modulation of eNOS expression by these miRs via regulation of gene expression or translational efficiency (202).

In aortic endothelial cells, TNF-induced dysfunction down-regulates miR-145 expression while the use of Baicalin, an anti-inflammatory product, induces an increase of miR. Moreover, the specific down-regulation of miR-145 in human aortic endothelial cells (HAECs) counteracts the beneficial effect of Baicalin through the JNK and p38 pathway (211).

AngiomiRs

AngiomiRs is a generic term used to qualify miRNAs able to regulate angiogenesis. They are produced by the endothelial cell itself or by other cells to impact the endothelial function, proliferation and migration.

The bad guys

miR-17/92 cluster was first described in cancerous cells where it is able to modulate tumor angiogenesis by inhibiting the angiogenic repressor connective tissue growth factor (212). On the contrary, Bonauer et al. showed that miR-92a is an endogenous repressor of angiogenesis in endothelial cells and decreases integrin subunit alpha 5 and eNOS protein expression. Moreover, this study revealed that *in vivo* inhibition of miR-92a enhances recovery of ischemic tissue (213).

In human microvascular endothelial cells, miR-21 is up-regulated after angiotensin II (AngII) treatment. Accordingly, a specific inhibition of miR-21 blocks the effect of AngII treatment in these cells. This observation relates to the fact that, *in vitro*, AngII induces an increase of signal transducers and activators of

transcription (STAT) 3 followed by an up-regulation of miR-21 and a down-regulation of Phosphatase and tensin homolog (PTEN) expression. *In vivo*, the STAT3/miR-21 pathway is implicated in the development of AngII-induced angiogenesis (214). In the same line, retinal tissues from a rat model of diabetic retinopathy presented an up-regulation of miR-21 as well as PI3K/Akt/VEGF pathway while PTEN expression is decreased. The use of a specific miR-21 inhibitor inhibits apoptosis and angiogenesis and promotes viability (215) confirming miR-21 as a potential target in angiogenic diseases.

Fiedler et al. proposed miR-24 as a negative regulator of angiogenesis. Moreover, miR-24 expression also induced endothelial cells apoptosis and inhibits cell sprouting. MiR-24 targets GATA2 and PAK4 leading to modulation of Sirt1 signaling pathways. Endothelial inhibition of miR-24 increases vascularization and limits infarct size by decreasing endothelial apoptosis (216;217).

The good guys

miR-126 is one of the most expressed miRs in endothelial cells that plays a role in vascular integrity and inflammation. Indeed, deletion of miR126 *in vivo* leads to leaky vessels, hemorrhaging as well as defect in angiogenesis and endothelial cells proliferation (218). Moreover, this miR targets VCAM-1 and regulates leucocytes adhesion to the endothelium (219). Also, miR-126 has been implicated in neovascularization of the heart after myocardial infarction (218). Interestingly, miR-126 is highly expressed in endothelial cells-derived apoptotic bodies. Injection of these bodies intravenously leads to mobilization of progenitor cells and to their incorporation into atherosclerotic plaques to, finally, limits the progression of the disease (220).

In HUVECs, hypoxia induced miR-210 expression which up-regulates endothelial cells survival and angiogenesis. Fasanaro et al. found that in normoxia, an overexpression of miR-210 increases angiogenesis and migration while a down-regulation of miR-210, during hypoxia, decreases angiogenesis. Moreover, miR-210 inhibition induces apoptosis in both normoxic and hypoxic cells (221;222). In the same vein, blunted expression of miR-210 in human microvascular endothelial cells decreases tube formation through enhancing Ephrin-A3 expression (221;223).

A more recent study also identifies miR-193-5p as a new angiomiR produced in endothelial cells. Actually, miR-193-5p is overexpressed in diabetic myocardial microvascular endothelial cells (MMEC) compared to physiological condition. A forced down-regulation of this miR in diabetic MMEC induces an increase of proliferation and angiogenesis due to an up-regulation of IGF2, a direct target of miR-193-5p (224).

The list of so called angiomiR is clearly not exhaustive, in addition non-endothelial cells also produce angiomiRs, table1 summarizes the most studied angiomiRs from endothelial and non-endothelial cells (212;225-228).

Cell type	miRs	Targets	Angiogenic function	ref
Non-endothelial cells	miR-17/92	CTGF, TSP1	Pro-angiogenic	208
	miR-378	Sufu, Fus-1	Pro-angiogenic	221
	miR-15b/miR-16	VEGF	Anti-angiogenic	222
	miR-328	CD44	Anti-angiogenic	224
Endothelial Cells	miR-21	PTEN	Pro-angiogenic	211
	miR-126	VCAM-1, SPRED-1, PIK3R2	Pro-angiogenic	215
	miR-210	Ephrin A3	Pro-angiogenic	217,219
	miR-17/92	ITGA	Anti-angiogenic	209
	miR-24	GATA2, PAK4	Anti-angiogenic	212, 213
	miR-221/222	C-kit	Anti-angiogenic	223

Table1: AngiomiRs produced by non-endothelial or endothelial cells.

If angiomiRs refer to miR presenting angiogenic capacity, they should not be confused with hypoxamiR described as hypoxia-induced miRs. Indeed, hypoxia can modulate miR biogenesis through several positive or negative regulations. For instance, Dicer expression can be impaired under hypoxic conditions leading to a decrease of miR production (229). The RISC component Ago2 presents an increased hydroxylation due to hypoxia and accumulates in the cell leading to an increase of miR levels (230). Additionally, the hypoxia-inducible factor Hif1α regulates the expression of several miRs as miR-155 or miR-210 which in turn directly target Hif-1α to form a positive or negative feedback loop (222;231). Interestingly, several angiomiRs are also hypoxamiR as demonstrated in endothelial cells for miR-210, miR-21 and miR-24 (232).

In the context of specialized miR we can also mentioned the fibromiRs. The concept of fibromiRs largely extends beyond the cardiovascular system , with miRs involved in renal, lung or hepatic fibrotic diseases (233). Some like miR-21 are pro-fibrotic by promoting ERK activation and ECM deposition while others modulate the TGFβ pathway. MyomiRs is another miR family that has a particular

interest in the cardiovascular system (but not only). They are enriched in smooth, skeletal or cardiac muscle. In the heart, the best known myomiRs are miR-1, miR-133, miR-208 and miR-499, they are involved in cardiac development, cell differentiation, proliferation or apoptosis. They also are implicated in cardiac hypertrophy, MI, arrhythmia and heart failure (234). Again the nomenclature should remain permeable as some myomiRs, as miR-133, are also implicated in fibrosis development. Several myomiR will be described below (see miR in cardiac tissue).

Shear stress: an key modulator of endothelial microRNA expression

miRs activated in response to shear forces are referred as “mechanomiRs” or with the more restricted appellation “flow-responsive” miR. Laminar and disturbed flows are indeed clearly associated with different panels of miRs.

Laminar shear stimulates the production of miR-10a while disturbed flow down-regulates it. MiR-10a regulates the NFκB pathway playing a role in increasing inflammation at site of bifurcation. Moreover, anti-inflammatory effects that were associated to vesicles from endothelial origin have been also attributed to miR-10a (235). In the same line, laminar shear stress-induced KLF2 leads to an increase of miR-30-5p known to diminish cell-cell adhesion molecules like VCAM1 and decrease inflammation. Shear stress also promotes cell cycle arrest (236). This phenomenon could be related to miRs 23b and 19a, induced by laminar shear and known to modulate cell cycle by directly targeting cyclin H and cyclin D1, respectively (237;238). Schober et al. demonstrated that “passenger” strand of the miR duplex, miR-126-5p is downregulated by disturbed flow (239). In the same line, laminar flow increases pre-miR-126 and miR-126-5p expression but not miR126-3p. Laminar flow also induces release of miR-126 coupled to Ago2 in

microvesicles which modulates vascular smooth muscle cells turnover. Furthermore, a decrease expression of miR-126-5p was highlighted at the predilection sites of plaques development in $ApoE^{-/-}$ mice aorta. MiR-143/145 is induced by KLF2 or AMPKα2 under laminar shear stress and is transfer to smooth muscle cells by secretion in microvesicles.

Oscillatory or disturbed flow also modulates the expression profile of specific miRs in endothelial cells. For instance, oscillatory shear increases miR-21 expression. The role of miR-21 in this condition is dual. It directly targets PPARα and stimulates, *in fine*, inflammation by increasing VCAM1 expression. But, interestingly, miR-21 also directly inhibits PTEN which antagonize the PI3K/Akt pathway, leading to an increased NO production (240). *In vitro* and *in vivo* studies have highlighted that miR-92a is regulated by shear stress. Actually, this miR is overexpressed in atheroprone areas and represses flow-responsive transcription factors, KLF2 and KLF4 expression. Wu et al. also showed that flow-dependent regulation of KLF2 is mediated by miR-92a (241). Furthermore, a downregulation of miR-92a prevents atherosclerosis as well as endothelial dysfunction in mice (242). *In vitro*, turbulent flow combined to oxidized low density lipoprotein (oxLDLs) increases miR-92a expression in HUVEC in a STAT3-dependent manner. The pro-atherogenic miR-712 is overexpressed in athero-susceptible sites and promotes endothelial permeability (243). Some miRs can also be preventive as miR-663 which is up-regulated by oscillatory shear stress, but targets genes implicated in inflammation and adhesion (244). Endothelial cells senescence due to p53/p21 activation appears under disturbed flow. Interestingly, both p53 and oscillatory shear induce an overexpression of miR-34. This miR increases ICAM and VCAM expression and indirectly diminishes Sirt1 expression and activation of NFκB (245;246).

As for miR-21, the role of miR-155 is dual. In HUVECs, laminar shear stress promotes miR-155 expression. This miR decreases myeloid inflammatory cell recruitment at plaque site during atherosclerosis. But studies also revealed a pro-atherogenic effect of miR-155. Indeed, a direct target of this miR is eNOS leading to an impairment of vasodilation (40). It is also shown that deficiency of miR-155 diminishes inflammatory aspect of atherosclerosis by reducing the immune response of macrophages.

These differences in miRs expression between laminar and disturbed shear stress suggest different pathways of regulation following laminar or turbulent flow, intensity of flow might also be an important variable.

MicroRNAs in cardiac tissue

The importance of miRs in cardiac development and homeostasis has been highlighted by a specific cardiac deletion of Dicer. This deletion increases the occurrence of pericardial edema and dysfunctional ventricular myocardium during the early heart development. On the contrary, deletion of one specific miR does not lead to impaired cardiac phenotype highlighting a redundancy in miR functions.

miR-17-92 cluster, already described as an angiomiR, also plays key roles in cardiac development. Indeed, it was highlighted that a down-regulation of this cluster induces ventricular walls thickness and ventricular septal defects. Wang et al. also showed an implication in myocardial differentiation of cardiac progenitors. Also, the bicistronic miR-1/133 is implicated during heart development. Indeed, miR-1 is able to promote differentiation and negatively regulates cardiac growth. On the contrary, miR-133 inhibits differentiation of cardiomyocytes. In adult heart, a specific deletion of miR-133a induced cardiomyopathy and heart failure

while its forced overexpression inhibits cardiac proliferation (247;248). Overexpression of miR-133 in cardiomyocytes under β1 adrenergic receptor (AR) stimulation leads to reduced cAMP accumulation and downstream pathways. Mice overexpressing miR-133 and presenting a transaortic constriction maintain their cardiac function and present an attenuated apoptosis and fibrosis (249). Recently, Di Mauro and colleagues found that miR-133 also has a role in other cellular compartments than the cytoplasm. Indeed, under Wnt inhibition, miR-133 translocates into the nucleus and forms a complex with Ago2 to repress Dnmt3b expression (250). The miRs-208a, 208b and 499 are encoded by αMHC, βMHC and Myh7b genes, respectively. As their host genes their expression is variable over time. MiR-208b is expressed in embryonic heart, miR-208a in postnatal heart and miR-499 in both. Interestingly, they participate in the regulation of their host genes. Particularly the miR-208a is important in response to cardiac stress. Indeed, suppression of this miR induces a resistance to aortic constriction while its overexpression leads to cardiac hypertrophy (247;248).

In adult heart, alteration of the miR expression profile has been often link to cardiac pathology (see Figure 13). van Rooij and colleagues have highlighted that after myocardial infarction (MI), cardiac tissue adjacent to infarcted area is depleted in miR-29. Their work showed that miR-29 family members regulate collagen, fibrillin and elastin genes leading to a regulation of fibrosis in the heart. Down-regulation of miR-29 induces expression of collagens, as well as development of fibrosis, and over-expression reduces it (251). In line with this study, berberine induces increase of miR-29b in cardiac tissue after MI. This up-regulation improves heart function and reduces infarct size but also promotes proliferation and migration of endothelial cells and thus angiogenesis (252). Overexpression of miR-210 increases cardiomyocytes proliferation, rescues heart function, improves angiogenesis and reduces cell death after MI. This miR targets

APC and induces cardiomyocytes cell cycle re-entry (253). Another angiomiR, miR-21 appears to contribute to cardiac remodeling. It circulates at a higher level in patients with hypertensive heart disease; its suppression prevents hypertrophic cardiac remodeling by the TGF-β1 signaling pathway (254). Cardiac remodeling and fibrosis are also under the control of miR-217, through a regulation of its direct target PTEN (255).

Exercise as well modulates miR in cardiac tissue (see Figure 13). Indeed, it was highlighted that miR-29c is upregulated in female rats undergoing intensive swimming training and is correlated with a decrease of collagen gene expression (256). Moreover, intermitted aerobic exercise induces an upregulation of miR-29a and miR-101a which finally lead to a reduced fibrosis and scar formation after myocardial infarction (257). MiR-222 is also proposed as a key factor for exercise-induced cardiomyocytes growth and acts as protector against pathological cardiac remodeling (258). Also, voluntary exercise increases Akt and ERK1/2 expression after 8 weeks and is linked to an enhancement of miR-126 and miR-210 leading to an improvement of heart angiogenesis (259).

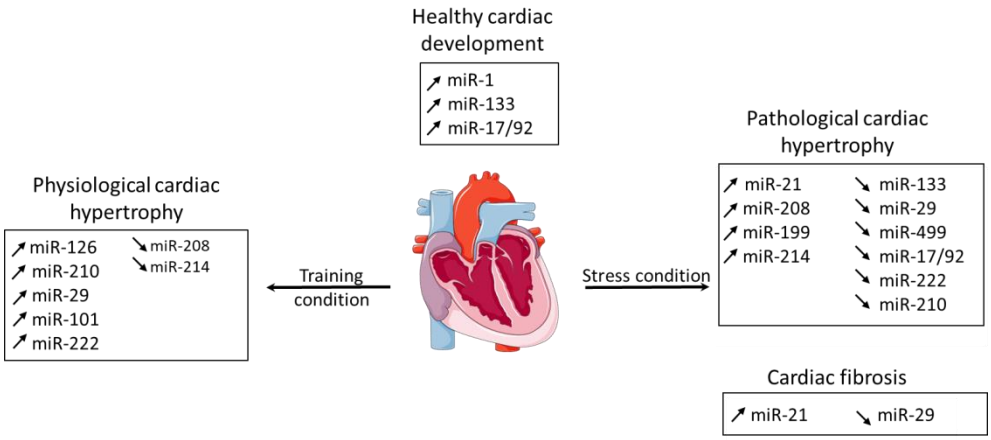

Figure 13: Modulation of miRs following pathological or physiological hypertrophy. A panel of miRs is deregulated during pathological hypertrophy and participates in the development of fibrosis or impairment of cardiac function. In contrast, miRs regulated during physiological hypertrophy generally improved cardiac function. The miR profile can be measured in plasma and used as biomarkers of cardiac function.

As the list of miRs playing key roles in endothelial and cardiac functions keep growing, the Long non-coding and circular RNA should also be mentioned, by their capacity to binds multiple miRs, they add again another layer of regulation.

MiRs profiling in cardiovascular diseases

As mentioned earlier, many cardiovascular diseases have been associated with a specific signature in circulating miRs. Patient with dilated cardiomyopathy show a signature a three circulating miRs (193) while obese patients present an upregulation of two specific miRs (194). In the same line, Faccini and colleagues identified three miRs (miR-145, miR-155 and miR-let-7c) as powerful markers of coronary artery disease (260). Additionally, patients with aortic stenosis present a specific miR profile with 6 miRs overexpressed (miR-193a-3p, miR-29b-1-5p, miR-505-5p, miR-194-5p, miR-99b-3p, and miR-200b-3p) and 14 miRs down-regulated (miR-3663-3p, miR-513a-5p, miR-146b-5p, miR-1972, miR-718, miR-3138, miR-21-

5p, miR-630, miR-575, miR-301a-3p, miR-636, miR-34a-3p, miR-21-3p, and miR-516a-5p) compared to healthy patients (261). More recently, Gigante and colleagues identified a miR signature predicting the risk of major adverse coronary events revealing a complex functional network with a central role of miR-320b (262).

miR199a family members

Production and regulation

In human, miR-199a family members comprise two mature strands derived from the same precursor, miR-199a-5p from the 5' arm of the hairpin and miR-199a-3p from the 3', and. This miR sequence is highly conserved between all mammals, with 99% of homology between human and mouse miR-199a-2 sequences. In the human genome, two loci have been identified as encoding the precursor of miR-199a family members: on Chromosome 1 and on Chromosome 19. Actually, Chromosome 19 contains miR-199a-1 which is inserted in the anti-sense strand of intron 15 of Dynamin 2 and Chromosome 1 contains miR-199a-2 which is inserted in the anti-sense strand of intron 14 of Dynamin 3. miR-199a-2 is produced in cluster with miR-214. These two miRs have been repeatedly described as produced together as in skin morphogenesis (263), primary central nervous system lymphoma (264) or in response to cardiac stress or hypertrophy (265).

A number of works have focused on the regulation of miR-199a expression. In this line, hypermethylation of miR-199a promoter has been described in ovarian cancers where it is correlated with a decreased miR-199a expression. Same was observed in testicular, lung, colorectal or breast cancers. On the opposite, a high expression of miR-199a is observed in glioblastoma due to a hypomethylation of the promotor. These observations support the existence of an

inversed correlation between methylation status of the promotor and miR-199a production. In addition to this, Lee et al. proposed the nuclear transcription factor Twist1 as a regulator of the miR-199a/214 cluster. They found that an overexpression of Twist1 leads to an increased expression of Dynamin 3 gene (DNM3) which encoded for miR-199a/214 cluster (266). This kind of regulation was also highlighted in the context of cardiac pathologies. Indeed, Twist-1 controls the miR-199a/214 production in human end-stage dilated cardiomyopathy leading to a down-regulation of the ubiquitin proteasome activity (267). Interestingly while Twist1 and EGR1 promote the production of mir-199a-2 on chromosome 1, methylation status can impact both mir-199a-1 and mir-199a-2.

Generalities

The particularity of miR-199a members is that in many contexts they do not modulate the same targets leading to a high regulation potential (see Figure 14).

MiR 199a-3p has been first associated with cancer prognosis, progression or resistance to treatment. As early as 2008, Migliore and colleagues showed that inhibition of miR-199a-3p in lung and colon carcinoma increases the invasion potential of the tumor by modulating expression of its oncogene target Met (268). Actually miR-199a-3p is downregulated in many cancers as, for instance, papillary thyroid carcinoma (269), ovarian cancer (270), hepatocellular carcinoma (271;272) or glioma (273) where it is associated with invasion and metastasis. The specific roles of miR-199a-3p have been largely documented thanks to the use of mimics and anti-miR approaches *in vitro* (274;275). In hepatocellular carcinoma, miR-199a-3p overexpression represses VEGFA, VEGFR1, VEGFR2, hepatocyte growth factor (HGF) and MMP2 but also mechanistic target of Rapamycin (mTOR) and

PAK4 and, consequently inhibits tumor growth, migration, invasion and angiogenesis (271;272). Overexpression of miR-199a-3p was also showed to inhibit ovarian cancer progression via downregulation of c-MET, phospho-ERK and phospho-Akt (270). In glioma, decreased expression of miR-199a-3p modulates mTOR expression as well as Akt, p70S6 kinase (p70S6K) and 4eIF4E-binding protein (4EBP1) phosphorylation (273). Interestingly, Shatseva et al. have described miR-199a-3p as able to increase proliferation and survival of endothelial cells and breast cancer cells by targeting Cav2 (276). miR-199a-3p implication extends way beyond the field of cancer. Indeed, mice with alcoholic or non-alcoholic fatty livers presented difference in miR-199a-3p expression (277). Also related to the liver, *in vitro* studies about hepatitis C virus highlighted that miR-199a-3p possess antiviral capacity in link with the control of ERK, oxidative stress or PI3K/Akt pathways (278). MiR-199a-3p is also dysregulated in type 2 Diabetes Mellitus (279) and is increased in mature adipocytes compared to pre-adipocytes. In mature adipocytes, miR expression appears to be stimulated by free fatty acids, TNFα, interleukin (IL)-6 and leptin and is higher in visceral adipose tissue of obese patients (280). In line, suppression of miR-199a-3p increases differentiation and thermogenesis in human brown adipose tissue by relieving its suppressive effect on the mTOR signaling pathway (281). In osteoarthritis chondrocytes cyclooxygenase (COX)-2 is described as a direct target of miR-199a-3p (282).

miR-199a-5p, plays also key roles in cancerous diseases. For instance, miR-199a-5p is downregulated in serous ovarian cancer and is correlated with tumor progression (283). This down-regulation is similarly observed in cutaneous squamous cell carcinoma or glioma (284;285). More surprisingly, miR-199a-5p is up-regulated in gastric cancer, melanoma or esophageal adenocarcinoma (286). Moreover, modulation of miR-199a-5p expression points also to very pertinent targets. For instance, Dai et al. demonstrated that, in endometrial stromal cells

undergoing hypoxia, forced overexpression of miR-199a-5p attenuates angiogenesis by targeting Hypoxia inducible factor (Hif) 1α/VEGF pathway (287;288). Proliferation of non-small cell lung cancer cells under hypoxia is abrogated by overexpression of miR-199a-5p through a direct repression of Hif1α/VEGF pathway and blockage of downstream Pyruvate Dehydrogenase Kinase 1 (289;290). Liu et al. speculated that miR-199a-5p prevents proliferation and invasion of human ovarian cancer cells by targeting NFκB (291). In glioma, miR-199a-5p acts as a tumor suppressor and directly target k-RAS suppressing the subsequent activation of Akt and ERK as well as Hif-1α expression (285). In cutaneous squamous cell carcinoma, miR-199a-5p targets the SIRT1/CD44 pathway and impacts migration and tumorigenicity (284).

Similarly to its opposite strand, miR-199a-5p extends outside the field of cancer. For instance, in hippocampus of rat undergoing intrauterine growth restriction, miR-199a-5p directly targets SIRT1 and PI3K (292). This miR promotes osteoblasts differentiation targeting Ten-Eleven Translocation 2 (293). Furthermore, miR-199a-5p boosts hepatocytes proliferation and liver regeneration through targeting TNFα/caspase pathway (294). Also, during differentiation onto brown or beige adipose tissue or in response to cold, miR199a/214 cluster is diminished. On the contrary this cluster is augmented in white adipose tissue in obese subjects. This study also proved that the cluster suppresses PRDM16 and PGC1α (295). miR-199a-5p (and to a lesser extend the -3p) is part of the fibromiRs; it has been associated with liver fibrosis progression for instance (296) where it down-regulates Cav-1, repressing the internalization of TGFβ receptors; Cav-1 inhibition also promotes Smad phosphorylation (297). More recently, it has been shown to affect the same cascade in the lung and the kidney (298). The role of miR-199a in fibrosis does not appear univocal. Indeed anti-fibrotic effect has also been reported by cellular or exosomal miR-199a-5p

targeting connective tissue growth factor (CCN2) in hepatic stellate cells. The list of physiological and pathological effects of miR-199a family members described above although already large is clearly not exhaustive. Tables of miR-199a-3p and -5p targets of interest in human and mouse are presented in Annexes.

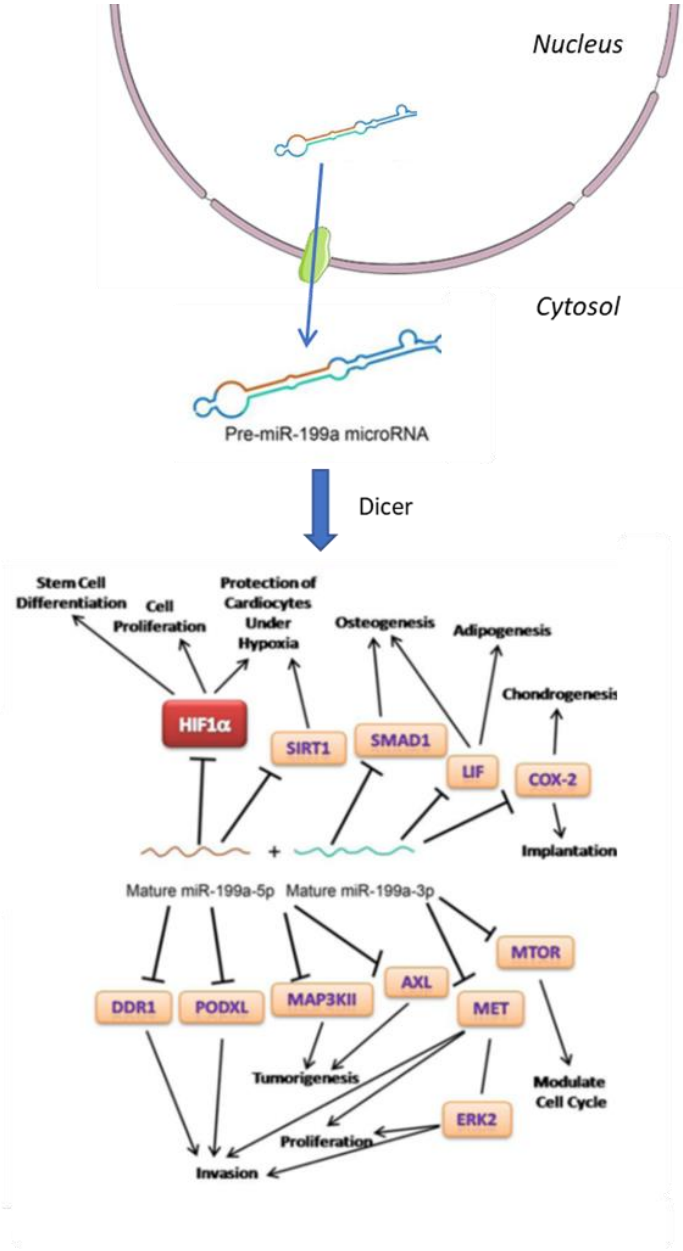

Figure 14: Representation of miR-199a family targets. Both miR-199a-3p and -5p are able to target cancerous and cardiovascular pathways. Hypoxic and angiogenic pathways are well-described targets of miR-199a family members Modified from Gu et al. (286)

miR199a: a circulating microRNA

Several studies have highlighted that miR-199a is excreted by cells and circulates in blood or cell medium. In 2014, Jansen et al proposed that miR-199a is modulated during coronary artery disease and detectable in plasma of patients. They described miR-199a as circulating in microvesicles mainly produced by platelets (299). However, more recent work has highlighted that miR-199a could also circulates in blood in exosomes. Indeed, fibroblasts from Duchenne muscular dystrophy (DMD) produced exosomes enriched in miR-199a-5p compared to exosomes from control fibroblasts. Moreover, DMD-derived exosomes promoted a myofibroblastic phenotype when administrated to normal fibroblasts. This includes an increase of collagen and fibronectin expression, cell proliferation and Akt and ERK activation. *In vivo*, injection of these DMD-derived exosomes in muscle produced more fibrosis after cardiotoxin-induced necrosis than control exosomes due to the direct targeting of Cav-1 by miR199a-5p (300). Wang et al. demonstrated that exosomes allow the transfer of miR-199a-5p from bone marrow-derived mesenchymal stem cells to renal tubular epithelial cells and decreases ischemia/reperfusion-induced ER stress via the targeting binding immunoglobulin protein (301). In the vascular field, it is known that HUVECs that undergo Hypoxia/reoxygenation (H/R) present an increase of intracellular and exosomal miR-199a-5p expression. H/R-treated neural cells incubated in presence of HUVEC-derived exosomes exhibit an increase of intracellular miR-199a-5p, a decrease of cell apoptosis and inflammation, and a decrease of ER stress. All these effects are abrogated using a specific miR-199a-5p inhibitor, showing the importance of miR transfer between different cell types (302). All these studies point toward exosome as a preferential carrier for miR-199a-5p. Nevertheless, both processes (microvesicle versus exosomes) are not mutually exclusive as the cell origin and the physio/pathological processes involved might account for the

differences, we should also mention the difficulty to correctly characterize the vesicle type.

miR199a in cardiovascular system

miR-199a family members are also described in the development of cardiovascular system and diseases. For instance, Rane et al. highlighted that miR-199a-5p is sensible to decreasing level of O_2, bringing to a downregulation of miR expression. This leads to the release of Hif1α and Sirt1 and plays a role during hypoxia and hypoxia preconditioning. Moreover, they suggested that this regulation occurs due to post-transcriptional mechanisms as no modulation of miR precursors was observed. This study also showed that specific downregulation of miR-199a-5p during hypoxia induces apoptosis of cardiomyocytes while a downregulation of miR expression before hypoxia mimics preconditioning and protects cardiac tissue against hypoxic damages (303). It is also known that STAT3 transcription factor is able to regulate mir-199a-2 expression in cardiomyocytes. Indeed, a downregulation of STAT3 expression induces an increase of miR-199a-5p expression and a decrease of the targets ubiquitin conjugating enzyme E2G1 and ubiquitin conjugating enzyme E2I leading to an impairment in sarcomere structure and function (304). Moreover, STAT3 also regulates cardiac miR-199a-5p production during chronic hypoxia. This could be an important pathway in the protective adaption of myocardium during hypoxia (305). Recent studies highlighted a role of miR-199a-3p in cardiac tissue. Tao et al. described miR-199a-3p as an enhancer of cardiac proliferation through targeting CD151/p38 pathway (306). The inhibition of miR-199a-3p induces cardiac differentiation by increasing cardiac-specific markers (GATA4, cardiac troponin T, MHCα) in embryonic stem cells (307).

In addition to a role in cardiomyocyte survival in hypoxic states by targeting Hif-1α and Sirt1, many studies showed that miR-199a is also upregulated in the specific context of pathological cardiac hypertrophy. One of the earliest works to expose the impact of miR199a- in cardiac remodeling was the work of van Rooij and colleagues who described an up-regulation of miR-199a in mice hypertrophic heart and human failing heart. Their work also supported the hypothesis that cardiac-specific overexpression of miR-195 is sufficient to drive cardiomyopathy (265). In the same line, Song and colleague showed a 10 fold increase in miR -199a in the heart of rats that underwent abdominal aortic constriction. In this work, they also highlighted that an increase of miR-199a-5p expression results in an increase of cell size which let them to suggest that this miR is essential for maintenance of cardiomyocytes cell size. In agreement with their early data, they also showed that a downregulation of miR-199a alleviates phenylephrine-induced cardiac hypertrophy (308). Thanks to the hearts of β1 and β2 adrenergic receptor (AR) transgenic mice and culture neonatal cardiomyocytes stimulated with isoproterenol, Rane et al. further described the potential regulation of miR-199a-5p expression in cardiomyocytes by suggesting a functional antagonism between adrenergic and Akt pathways. Similarly, aberrant expression of miR-199a-5p observed in a mice model of pathological cardiac hypertrophy was normalized with enhanced PI3Kα (309)**.** Hou and colleagues confirmed miR-199a-5p has one of the 18 miRs upregulated by β-adrenoceptor stimulation in the rat heart, together with miR-214, its cluster sibling (310). In the same line, mice with trans-aortic constriction present an increase of miR-199a together with miR-214 expressions (311) and indeed repressing the cluster 214/199a in a model of pressure-overloaded induces less fibrosis and improves cardiac function (41). Control of autophagy in cardiac cells is among the critical role of miR-199a-5p in cardiomyocytes. This comes from observations that miR-

199a-5p could suppress starvation-induced autophagy by inhibiting heat shock protein family A member 5 and that overexpression of autophagy related gene 5 attenuated the hypertrophic effects of miR-199a overexpression on cardiomyocytes (312).

miR-199a-3p is not as widely described in the context of cardiac hypertrophy. Yet, Reddy and colleagues found that mice with right ventricle hypertrophy and failure induced by pulmonary artery constriction present an increased miR-199a-3p expression modulating cardiac survival and growth during hypertrophy (313).

Interestingly, Li et al. have developed a miR-sponge targeting miR-199 family members. With this technology, they induced a cardiac specific down-regulation of miR-199 and they observed the development of a physiological hypertrophy, this hypertrophic effect was correlated with a mild increase of PGC1α expression leading to an improvement of cardiac functions (314).

On the vascular side, in human dermal microvascular endothelial cells, suppression of miR-199a supports angiogenesis and on the contrary, its overexpression blunted angiogenesis (315). Also, hypoxic stress leads to an increase of Hif1α and adrenomedullin which is correlated with a decrease of miR-199a expression. Under this hypoxic condition, Hif1α knockdown leads to an increase of TNFα and IL-8 as well as a decrease of proliferation and migration and increased permeability while miR-199a-5p inhibition has the opposite effect (316). Tian et al. demonstrated that miR-199a-5p expression is up-regulated in blood of hypertensive patients and is correlated with the progression of hypertension. They also showed that overexpression of miR-199a-5p in HUVECs induces apoptosis, impairs proliferation and decreases numbers of autophagosomes leading to an aggravation of vascular endothelial injury (317). Interestingly, in

arteries, the regulator of miR-199a/miR-214 cluster, Twist1, is more expressed at atherosusceptible sites, where EC proliferation and inflammation occur (266;318).

Heuslein et al. highlighted that miR-199a is decreased under shear stress condition and it improves arteriogenesis. Forced overexpression of miR-199a in endothelial cells undergoing shear stress modifies inhibitor of nuclear factor kappa-B kinase subunit beta (IKKβ) and Cav1 expressions. Furthermore, this study revealed that miR-199a is able to regulate monocyte recruitment and adhesion to endothelial cells. Diminished miR-199a-5p expression stimulates arteriogenesis, perfusion recovery and macrophages recruitment (319).

From the cell to the clinic

Several studies suggest that miR-199a family members can be used as biomarkers in clinic. Specifically, in the cardiovascular field, a recent study highlighted that miR-199a-1 is up-regulated in blood of patient during acute myocardial infarction. They showed that miR-199a-1 together with others has a high diagnostic efficiency for the prediction of acute MI (320). Pre-clinical study on mice demonstrated that intra-cardiac injection of miR-199a-3p improves cardiac function after myocardial injection (321). However, the targeting of miR-199a as a therapeutic approach is still not described in clinical studies.

Objectives

Part1: Identification of endothelial targets of miR-199a family members

Previous studies about the roles of miR-199a family members in the cardiovascular system described altered miR levels in pathologies as cardiac hypertrophy or non-alcoholic fatty liver disease (NAFLD). Interestingly, these pathologies are linked to an endothelial dysfunction. Given the impact of miR-199a on cav-1 expression in microvascular endothelial cells, as well as previous studies pointing out Hif1 or Sirt1 as targets of these miR in heart, we speculated that these miRs could also take part to the complex mechanistic regulation of endothelial function and more particularly NO production in endothelial cells or in murine aortic vessels. Our investigations were supported by studies highlighting that an overexpression of miR-199a in HUVECs leads to endothelial injuries. Our main research objectives were:

1. To evaluate the implication of miR-199a family members in the control of endothelial function and NO production by down-regulating their expression both *in vitro* and *ex vivo*
2. To identify key endothelial targets of miR-199a family members through *in silico*, *in vitro* and *ex vivo* studies

Results are described in a manuscript published in Atherosclerosis, Thrombosis and Vascular Biology. An editorial related to our paper has been published in Arteriosclerosis, Thrombosis, and Vascular Biology. 2018;38:2278–2280.

Part2: Implication of miR-199a family members in a context of improved endothelial function, physical training

We and others have described an up-regulation of miR-199a in hypertrophic heart from animal models of pathological hypertrophy. Specifically, in our hands, miR-199a-3p and -5p were upregulated in the heart of mice submitted to AngII infusion for 14 days or following thoracic aorta banding. At the beginning of this work, nothing was virtually known on the regulation of the miR-199a family members in a context of physiological hypertrophy. We therefore generate a mouse model of physiological hypertrophy by subjecting mice to voluntary exercise. Considering our first discoveries on the implication of miR-199a on endothelial function, we extended our study to the vascular phenotype associated with exercise and shear stress. The specific aims of this part of the study were:

1. To evaluate miR-199a family members expression in cardiovascular tissues of voluntary running mice
2. To analyze the expression of well-described targets of our miRs of interest in heart and vessels in order to evaluate their potential impact on cardiac and vascular function
3. To study how miR-199a are regulated in tissues of running mice through the study of transcription factor and premiR.

Results are described in a manuscript submitted in American Journal of Physiology-Heart and Circulatory Physiology.

Part3: AMPKα1 participates in the regulation of miR199a during cardiac hypertrophy

The third part of this thesis comprises preliminary data analyzing the regulation of miR-199a in a context of pathologic cardiac hypertrophy. An up-regulation of miR-199a-5p is recognized for a long time in the context of pathologic cardiac hypertrophy. We have used different murine models to evaluate together the fate of the -5p and -3p of miR-199a in cardiovascular samples. In the course of our experiments, we have uncovered a potential role of the kinase AMPK. We have verified how the kinase affects miR-199a3p/5p production and stability in *ex vivo* and *in vitro* models. The specific objectives of this part are:

1. To evaluate miR-199a family members expression in cardiovascular tissues of hypertrophic mice (pressure overload)
2. To evaluate the role of AMPK in miR production or stabilization through the use of genetic approach

These results are preliminary and require further investigation.

Results PART I

MicroRNA-199a-3p and MicroRNA-199a-5p Take Part to a Redundant Network of Regulation of the NOS (NO Synthase)/NO Pathway in the Endothelium

Virginie Joris[1], Elvira Leon Gomez[1], Lisa Menchi[1], Irina Lobysheva[1], Vittoria Di Mauro[2,3,4], Hrag Esfahani[1], Gianluigi Condorelli[2,3,4], Jean-Luc Balligand[1], Daniele Catalucci[3,4] and Chantal Dessy[1]

1 Pole of Pharmacology and Therapeutics, Experimental and Clinical Research Institute (IREC), Université catholique de Louvain, Brussels, Belgium

2 Humanitas University, Rozzano (Milan), Italy

3 Humanitas Clinical and Research Center, Rozzano (Milan), Italy.

4 Institute of Genetics and Biomedical Research, Milan Unit, National Research Council, Milan Italy.

Manuscript published in Arteriosclerosis, Thrombosis, and Vascular Biology. 2018;38:2345–2357. An editorial related to our paper has been published in Arteriosclerosis, Thrombosis, and Vascular Biology. 2018;38:2278–2280.

Results PART I

Abstract

Objective—Members of the microRNA (miR)-199a family, namely miR-199a-5p and miR-199a-3p, have been recently identified as potential regulators of cardiac homeostasis. Also, upregulation of miR-199a expression in cardiomyocytes was reported to influence endothelial cells. Whether miR-199a is expressed by endothelial cells and, if so, whether it directly regulates endothelial function remains unknown. We investigate the implication of miR-199a products on endothelial function by focusing on the NOS (nitric oxide synthase)/NO pathway.

Approach and Results—Bovine aortic endothelial cells were transfected with specific miRNA inhibitors (locked-nucleic acids), and potential molecular targets identified with prediction algorithms were evaluated by Western blot or immunofluorescence. *Ex vivo* experiments were performed with mice treated with antagomiRs targeting miR-199a-3p or -5p. Isolated vessels and blood were used for electron paramagnetic resonance or myograph experiments. eNOS (endothelial NO synthase) activity (through phosphorylations Ser1177/Thr495) is increased by miR-199a-3p/-5p inhibition through an upregulation of the PI3K (phosphoinositide 3-kinase)/Akt (protein kinase B) and calcineurin pathways. SOD1 (superoxide dismutase 1) and PRDX1 (peroxiredoxin 1) upregulation was also observed in locked-nucleic acid–treated cells. Moreover, miR-199a-5p controls angiogenesis and VEGFA (vascular endothelial growth factor A) production and upregulation of NO-dependent relaxation were observed in vessels from antagomiR-treated mice. This was correlated with increased circulated hemoglobin-NO levels and decreased superoxide production. Angiotensin infusion for 2 weeks also revealed an upregulation of miR-199a-3p/-5p in vascular tissues.

Conclusions—Our study reveals that miR-199a-3p and miR-199a-5p participate in a redundant network of regulation of the NOS/NO pathway in the endothelium. We highlighted that inhibition of miR-199a-3p and -5p independently increases NO bioavailability by promoting eNOS activity and reducing its degradation, thereby supporting VEGF-induced endothelial tubulogenesis and modulating vessel contractile tone.

Introduction

Endothelial dysfunction characterized by reduced NO (nitric oxide) bioavailability is commonly recognized as a cause and consequence of most cardiovascular diseases (322). In the endothelium, NO production mostly arises from the conversion of L-arginine to equimolar amounts of citrulline and NO, catalyzed by eNOS (endothelial NO synthase). In response to agonists or fluid shear stress, eNOS activation requires a cascade of events that start with changes in cytosolic Ca^{2+}, translocation of the enzyme from caveolar microdomains to the oxygen-rich cytosol, followed by substrate and cofactors interactions (48;55;323;324). An additional layer of regulation results from post-translational modifications of eNOS, including activating/inactivating phosphorylation, glycosylation, glutathionylation, nitrosylation, and acetylation (48;325).

Decreased availability of the substrate L-arginine contributes to NO deficiency and endothelial dysfunction. This is observed when the breakdown of L-arginine by arginase is accelerated as reported in the context of aging, diabetes mellitus, and hypertension. In these conditions, elevated serum levels of asymmetric dimethyl arginine (ADMA), the endogenous negative competitor of arginine, also participate in the reduction of NO production (89). Oxidative stress is another common denominator to many cardiovascular diseases characterized by endothelial dysfunction. In diabetes mellitus, atherosclerosis, or hypertension, generation of superoxide anions (also produced by uncoupled NOS) leads to the formation of (deleterious) peroxynitrite thereby reducing the abundance of bioactive NO (326;327). Although eNOS expression is only subject to modest degrees of regulation in physiological conditions, transcriptional and post-transcriptional modes of eNOS regulation are frequently described in pathological states (328), including heart failure (329), atherosclerosis (328;330), diabetes mellitus, and hypercholesterolemia (331;332). Among post-transcriptional

regulations, epigenetic mechanisms are less well studied. MicroRNAs (miRNAs/miRs) are highly conserved, small noncoding RNAs which negatively regulate gene expression. The miRNA-199a gene, comprising miR-199a-3p and -199a-5p, was originally described in cancer cells because of its capacity to regulate proliferation (333) and angiogenesis (334). In the past years, interest arose in the cardiovascular field when van Rooij et al reported that miR-199a takes part in a miRNA signature associated with cardiac hypertrophy and heart failure (265;335;336). Other investigators showed that cardiomyocyte-specific overexpression of miR-199a was sufficient to impair cardiomyocyte autophagy and thereby induce cardiac hypertrophy through mTOR (mammalian target of rapamycin) activation (312). Paradoxically, another study using myocyte-specific miR-199a-sponge documented that a 20% to 30% decrease in endogenous miR-199a-5p levels leads to physiological cardiac hypertrophy through the upregulation of metabolism-related gene expression (314). Interestingly, tissue profiling analysis has revealed that miR-199a is highly expressed in rat lung and cardiac tissues (308). In the heart, miR-199a was predominantly, but not exclusively, expressed in cardiomyocytes. Also, changes in miR-199a expression in cardiomyocytes were reported to influence neighboring cells. In particular, an increase in ADMA levels in the culture supernatant of pre-miR-199a-exposed cardiomyocytes actually lowered NO bioavailability in rat cardiac endothelial cells (304). Although the above studies suggested that miR-199a may play critical roles in various tissues, including blood vessels, whether they are expressed by endothelial cells and if so, whether they regulate endothelial function are largely unexplored. Here, we have used bioinformatic algorithms to predict potential targets of miR-199a in endothelial cells and validated several of them through the dissection of the *in vitro* and *in vivo* effects of miRNAs 199a-targeting locked-nucleic acid (LNA) and antagomiR, respectively, on eNOS activity.

Materials and Methods

Cell Culture and LNA Transfection

Bovine aortic endothelial cells (BAEC) were cultured on 0.2% gelatin-coated 12-well plates using DMEM (Gibco) supplemented with 10% FBS and 100U penicillin/100 µg streptomycin. Endothelial cells were plated into 12-well culture plates and transfected with 40nM LNA targeting miR 199a-3p (Exiqon 4100888-001), -5p (Exiqon 4101096-001), mimics (Qiagen YM00472279 and YM00471589), or scramble sequence (Exiqon 199006-001) overnight using DNA Transfection Reagent (Biotool) in Opti-Mem diluted in DMEM supplemented with 10% FBS without antibiotics. Transfection was stopped by replacing transfection medium with complete culture medium (DMEM+FBS 10%+antibiotics). For the immunoblotting, cells were collected 48 or 72 hours after transfection in lysis buffer (Tris HCl 50 mmol/L, NaCl 150 mmol/L, EDTA 1 mmol/L, 0.1% SDS, 0.5% sodium deoxycholate, Triton-100× 10%) containing a protease inhibitor cocktail (Sigma) and a phosphatase inhibitor (Roche). Transfection efficiency was characterized by studying the modulation of direct targets of miR-199a-3p, -5p in endothelial cells after inhibition of these miRNAs.

Pharmacological Treatments

For the PI3K (phosphoinositide 3-kinase)/Akt (protein kinase B) inhibition experiments, LY294002 treatment (LY, 20 µM; Millipore) was initiated 1 day before LNA transfection and maintained up to the harvesting of the cells. For inhibition of VEGFA (vascular endothelial growth factor A), Bevacizumab (2 µM; Roche) was used during LNA transfection and maintained up to harvesting. Forty-eight hours after transfection, cells were collected in RIPA lysis buffer to perform immunoblotting.

LNA and Akt1 siRNA Cotransfection

To study the implication of Akt1 in the pathway modulated by miRNA inhibition, we have proceeded in 2 steps. Endothelial cells were plated into 12-well culture plates and transfected during 5 hours with 50 nM of siRNA (small-interfering RNA) directed against Akt1 (Riboxx) using Lipofectamine RNAimax (Invitrogen) in Opti-Mem diluted in DMEM

supplemented with 10% FBS. Transfection was stopped by adding complete culture medium (DMEM+FBS 10%+antibiotics). After overnight recovery, cells were transfected with 40 nM of each LNA or control sequence using Lipofectamine RNAimax in Opti-Mem diluted in DMEM supplemented with 10% FBS. Once again, transfection was stopped by adding complete culture medium (DMEM+FBS 10%+antibiotics). Cells were collected 48 hours after the second transfection in RIPA lysis buffer.

miRNA Extraction

Endothelial cells were suspended in homogenisation buffer provided by Promega in the Maxwell RSC miRNA Tissue Kit (ref AS1460) and added with thioglycerol (20 µl/1 mL). Heart and vessel tissues were crushed in homogenisation buffer added with thioglycerol, and plasmas were just added with thioglycerol. Samples were processed following the manufacturer's instructions. In brief, lysis buffer and proteinase K were added to the samples and mixed by vortexing. Samples were incubated at room temperature (RT) during 10 minutes and loaded in cartridges provided in the kit. Cartridge was previously prepared by adding 10 µl of DNAse 1, excepted for samples where miR inhibition by LNA was measured. Samples were processed using Maxwell RSC Instrument (Promega) for miRNA extraction and eluted in nuclease-free water.

miRNA Reverse Transcription and Quantitative PCR

Reverse transcription and quantitative polymerase chain reaction (PCR) for miR were performed following the protocol A for individual assays provided with miRCURY LNA Universal RT microRNA PCR kits (Exiqon 203301–203351). First-strand cDNA synthesis was performed with 2 µl of RNA sample adjusted to a concentration of 5 ng/µL. RT mix containing reaction buffer and enzyme mix was added to the samples and incubated at 42°C during 1 hour followed by a step of heat-inactivation at 95°C for 5 minutes. Regarding the quantitative PCR, samples were diluted following manufacturer's recommendations, and 4 µl were loaded in 96-well PCR plates. PCR master mix and PCR primers set were added, and PCR was performed in iQ5 cycler Biorad machine following the kit protocol. Primers used were the following miR-199a-3p (Exiqon 204536), miR-199a-

5p (Exiqon 204494), U6 (Exiqon 203907), and miR-let-7i-5p (Exiqon 204394), the latter was used for plasma and vessels following the recommendations of the manufacturer.

Western Blot

Endothelial cells and tissues were suspended in RIPA lysis buffer. A Bicinchoninic Acid Protein Assay Kit (Pierce) was used to determine the protein concentration of each sample according to the manufacturer's protocol. Ten µg of proteins were loaded per Western blot well, and the migration was performed in migration buffer (Tris-EDTA, SDS, glycine) under a voltage of 120 V. After migration, proteins were transferred on a nitrocellulose membrane with constant amperage of 350 mA for 1 hour 30 minutes (transfer buffer: Tris-base, glycine, SDS, methanol). The membranes were then incubated in a blockage solution consisting in TBS (Tris buffer saline)-Tween 0.1% BSA 5% for 1 hour at RT. For the immuno-detection of the targeted proteins, primary antibodies were incubated overnight at 4°C in TBS-Tween/BSA 5%. Primary antibodies are the following: anti-phosphoSer1177eNOS (1 µl/mL; Cell Signaling, 9571), anti-phosphoThr308Akt (1 µl/ mL; Cell Signaling, 2965), anti-Akt (1µl/mL; Cell Signaling, 9272) anti-Akt1 (1 µl/mL; Cell Signaling, 2938), anti-phosphoTh495eNOS (0.5 µg/mL; BD transduction, 612706), anti-calcineurin (1 µg/mL; Millipore, 07–1491), anti-SOD1 (superoxide dismutase 1; 1 µg/mL; Abcam, ab13498), anti-Cav1 (caveolin-1; 0.05 µg/mL; BD transduction, 610407), anti-Hsp90 (heat shock protein 90; 0.25 µg/mL; BD transduction, 610419), anti-DDAH1 (dimethylarginine dimethylaminohydrolase; 0.5 µg/mL; Abcam, ab2231), anti-PRMT1 (protein arginine N-methyltransferase; 2.5 µg/mL; Abcam, ab12189), anti-PDK1 (pyruvate dehydrogenase kinase; 2 µg/mL; Gentaur, KAP-PK112), anti-βactin (0.02 µl/mL; Sigma, A5441), and anti-VEGFA (1 µg/mL; Abcam, ab46154); this last antibody recognizes all the splicing forms of VEGFA. Membranes were washed in TBS-Tween and incubated with the peroxidase-conjugated secondary antibody for 1 hour at RT and developed by enhanced chemiluminescence (ECL, Amersham) on CL-Xposure film (Thermo Scientific). Films were scanned, and protein bands were quantified by densitometry using ImageJ software (National Institutes of Health). Levels of all proteins of interest were normalized to β-actin level. The levels of phosphorylated proteins were normalized to the level of total proteins.

NO Measurement on Cells

Electron paramagnetic resonance (EPR) spectroscopy was used to detect NO production in BAECs after formation of the paramagnetic adduct Fe(II)NO (diethyldithiocarbamate)$_2$ in reaction of NO with the spin trap [Fe(II)(diethyldithiocarbamate)$_2$] as previously described (337). In brief, cells transfected with LNA were treated with or without L-nitroarginine methyl ester (2.5 mmol/L) for 1 hour and incubated for 30 minutes at 37°C with KREBS buffer (NaCl 99 mmol/L, KCl 4.69 mmol/L, KH2PO4 1.03 mmol/L, MgSO4 1.2 mmol/L, NaHCO3 25 mmol/L, glucose 5 mmol/L, HEPES 20 mmol/L, and CaCl2 2 mmol/L) containing 0.2% BSA. Cells were then treated for 45 minutes at 37°C with 0.5 mmol/L of [diethyldithiocarbamate]2-Fe(II) colloid complex, scrubbed, and frozen in calibrated tubes. The EPR signals were recorded with following EPR parameters: microwave power, 20 mW; modulation amplitude 5G; time constant, 80 ms; 7 scans; 77 K, and normalized per µg of proteins.

Immunofluorescence

BAEC cells were fixed in paraformaldehyde 4% for 10 minutes at RT, washed in PBS, and blocked for 1 hour at RT in PBS containing 0.1% saponin and 5% BSA. PRDX1 (peroxiredoxin 1) was detected by incubating the fixed cells with anti-PRDX1 rabbit primary polyclonal antibody (5 µg/mL; Abcam, ab15571) in PBS/saponin 0.1%/BSA 1% at 4°C overnight, followed by incubation with Alexa Fluor 488-conjugated goat anti-rabbit (6 µg/mL; Life's technologies) for 1 hour at 37°C. Cells were incubated with Dapi nuclear stainer (1:10 000 in PBS) for 5 minutes at RT and mounted with Dako fluorescent Medium (Dako). Negative controls were performed by incubation with the secondary antibody only.

Dihydroethidium Staining

Dihydroethidium is able to permeate cells. In the presence of superoxide anion, it is oxidized to 2-hydroxyethidium and ethidium, which are trapped by intercalation with DNA resulting in bright red fluorescence. In brief, cells were cultured in 12-well vessels on gelatin-coated cover glasses and transfected with LNA, as described above. After 48 hours,

cells were washed with PBS and incubated in the presence of dihydro-ethidium (10 µM) for 1 hour at 37°C. Cells were incubated with Hoechst nuclear stainer (1:10 000 in PBS) for 5 minutes at RT and mounted with Dako fluorescent Medium (Dako). Nuclear staining of dihydroethidium is directly analyzed using Axioskop 40 microscopy system.

ADMA Measurement

To assess ADMA level in culture media, ADMA high sensitive ELISA kit from DLD diagnostika GMBH (EA209/96) was used following the manufacturer recommendations. In brief, ADMA in the samples is acylated and competes with ADMA bound in the microtiter plate for a fixed number of rabbit anti-ADMA antiserum binding sites. The absorbance is read at 450 nM with spectrophotometer and is inversely proportional to the ADMA concentration of the sample.

Angiogenesis Test

BAEC were transfected overnight with LNA or scramble sequence on 0.2% gelatin-coated plates. After transfection, cells were trypsinized, counted, and mixed in equal volume with growth factor–reduced Matrigel (≈10 mg/mL proteins). Each mixture was put in culture in 12-well plate. After polymerization of the Matrigel for 1 hour at 37°C, each well containing mixture with cells was covered with 500 µl of complete medium. Each condition was performed in duplicate. After 48 and 72 hours, cells underwent migration and alignment to form tubes.

Luciferase Assay

A 3’ UTR (untranslated region) fragment of the VEGFA, calcineurin, and SOD1 mRNAs were subcloned by using In-Fusion HD Cloning Kits (Clonotech) according to manufacturer’s instruction, into the pmiRGlo Dual-Luciferase vector (Promega) immediately downstream of 3´ of the firefly luciferase gene (luc2). The miR-199a/a* mature sequence was cloned into the pcDNA6.2-GW/EmGFP-miR vector according to the manufacturer’s protocol (Thermo Fisher Scientific). HEK (human embryonic kidney)-293T cells were transfected with pmiRGlo-3’UTR and pcDNA6.2-GW/ EmGFP-miR-199a/a* (miR-199a-5p/-3p) plasmids. Forty-eight hours post-transfection, cells were lysed, and luciferase activity was

measured using the Nano-Glo Dual-Luciferase Reporter (NanoDLR) Assay System as described by the manufacturer (Promega). To confirm specific targeting of the 3'UTR of target genes by miR-199a/a*, site-specific mutagenesis at the predicted sites were obtained by using the QuikChange Site-Directed Mutagenesis Kit according to the manufacturer's instructions (Agilent technologies). Mutated constructs were then tested in luciferase assays, and the rescue of chemiluminescent signal in the presence of miR-199a/a* identified real targeting sites. Moreover, alignments between human and bovine sequences were performed using clustalW and assessed that within the calcineurin gene, the putative binding sites for both miR-199a family members are conserved between Homo Sapiens and Bos Taurus. VEGFA gene has only the region containing the putative binding site for miR-199a-5p, which is conserved between the 2 species. Concerning SOD1 gene, conservation of miR-199a-3p and -5p sites is almost identical except for few nucleotides between Homo Sapiens and Bos Taurus.

Animals and Treatments

All experimental procedures and protocols were approved by the local Ethics Committee (Comité d'Ethique pour l'Expérimentation animale), Secteur des Sciences de la Santé, Université Catholique de Louvain, according to National Care Regulation and Directive 2010/63/EU of European Parliament and of the Council. Only male mice were used in this study to avoid confounding effects. Indeed, estrogens are well-characterized modulators of endothelial function through regulation of the NOS/NO pathway.

Seven-week-old C57Bl6 male mice (30 animals) were injected in caudal vein 3 days in a row with a specific antagomiR (Fidelity systems, 75 mg/kg per day) directed against miR-199a-3p and -5p specifically, a scramble sequence or saline solution (197;338;339). These injections were performed each day by the same experimented technician. Mice were then housed 1 per cage in a 12/12-hour night and day cycle for 30 days, and their behavior was checked every day. At the day of the euthanization, blood and vessels were collected; the arteries were mounted on a wire myograph to evaluate the endothelium-dependent response, some vessels samples were frozen for further analysis (Western blotting as

described above). Blood samples were used for assessment of NO and superoxide anion rates by EPR or plasma isolated for miR profiling.

Twelve-week-old C57Bl6/J male mice (12 animals) were treated with continuous infusion of angiotensin II (2 mg/kg per day) or saline solution during 14 days using osmotic minipumps (Alzet 2002) subcutaneously implanted between the scapulae in anesthetized mice with Isoflurane, as described in the literature (340). Mice were housed 1 per cage after the implantation of the minipumps, and their wellbeing was checked every day. After 14 days, terminal anesthesia was performed by intraperitoneal injection of ketamine (100 mg/ mL) and xylazine (20 mg/mL), mice were weighed, blood, heart, and vessels were collected and frozen in liquid nitrogen for further miR profiling.

Bias and Randomization

All mice were cared for equally in an unbiased fashion by animal technicians and investigators. Mice were randomly allocated into 4 groups (Figure 28) or 2 groups (Figure 29). Although the mouse groups were not blinded, the people involved in functional studies on vessel relaxation, in hemoglobin-NO (HbNO) dosage, osmotic pump surgical implantation, and quantitative PCR were different, and data were never shared between them up to article writing. In addition, HbNO dosage and osmotic pump-related surgery were performed by platform logisticians and quantitative PCR by Masters students who were not aware of the nature of the study. Finally, we took care of adding a saline solution condition besides the antagomiR scramble control to exclude any bias related to the mouse injection, including the stress associated with mouse handling. For the same reasons, minipumps loaded with saline solution were implanted to be used as the most appropriate control of angiotensin-loaded pumps.

NO Measurement in Venous Blood

NO bioavailability was assayed as the concentration of circulating hemoglobin nitrosylated at heme-FeII (HbNO) *in vivo*. Whole venous blood of male C57Bl6 mice treated or not with antagomiRs against miR-199a-3p, -5p or scrambled antagomiR was collected and frozen immediately in calibrated tubes as previously described (47). The EPR spectra were

recorded by a Bruker spectrometer (AMXmicro, X-band; microwave frequency 9.35 GHz, modulation frequency 100 kHz) with following setting: microwave power, 20 mW; modulation amplitude, 0.7 mT; 5 scans, at 77 K using a finger dewar. The level of HbNO was quantified from hyperfine structure (gz=2.011; Az=16.8G) of the EPR signal after digital subtraction of a signal of protein-centered free radicals (g=2.005; linewidth≈19G) using Bruker software, Xenon. Samples were normalized by volume.

Anion Superoxide Measurement in Aortic Rings

Superoxide anion production was assayed quantitatively by EPR in isolated aortic rings using reactive oxygen species (ROS)–sensitive spin probe at 1 mmol/L (1-hydroxy-3-methoxycarbonyl-2,2,5,5-tetramethylpyrrolidine, CM-H; Alexis Biochemichal, Inc) in situ, as previously described (341). In brief, aortic rings were preincubated in KREBS-DTPA (diethylenetriaminepentaacetic acid)-Hepes buffer (0.1 mmol/L DTPA, 20 mmol/L HEPES, pH 7.5) in presence or not of SOD (100U/mL). Then the aortic rings were inserted in capillaries and the kinetics of the CM-H EPR signal formation was recorded on-line in capillary interposed into the cavity of the EPR spectrometer during 10 to 15 minutes at 37°C (10 scans) using the X-band EPR spectrometer MS400, Magnettech (microwave frequency, 100 kHz; microwave power, 20 mW; modulation amplitude, 0.1 mT). The rate of the CM. radical formation was calculated as a slope of linearized kinetic curve. Results were normalized by the length of aortic ring. SOD-sensitive signal was accepted as superoxide anion formation.

Myograph Experiments

Thoracic aortic arteries were mounted in a wire myo-graph. NO-mediated relaxation was measured as previously described (342;343). In brief, 2 40 µm wires were threaded into the lumen of the vessel segments and incubated in a bath continuously perfused with physiological solution, gassed, and maintained at 37°C. Aorta from antagomiR-treated or control mice was contracted with a high-KCl solution (to prevent implication of endothelium-derived hyperpolarization) in the presence of indomethacin (10 µmol/L), a Cox2 (cyclooxygenase-2) inhibitor, and exposed to an increased concentration of acetylcholine.

Statistical Analyses

All experiments were reproduced at least 3×. All data are expressed as the mean±SEM. Shapiro-Wilk normality test and Bartlett or Levene equal variance tests were performed, and statistically significant differences were determined using a 2-way ANOVA or 1-way ANOVA followed by Tukey-Kramer post hoc ANOVA test or by using a Kruskal-Wallis test for nonparametric data. $P<0.05$ was considered statistically significant.

Results

miR-199a-3p and miR-199a-5p Are Expressed in Endothelial Cells

As a preamble to this study, we first evaluated the expression of the mature miR-199a arising from both arms of the precursor miR-199a, respectively miR-199a-3p (3'arm) and miR- 199a-5p (5' arm) in human and BAEC. Of note, sequences of human and bovine miR-199a are strictly identical. Both mature miRNAs were detected in significant and similar amounts in endothelial cells (PCR threshold cycle values for miR-199a-5p and -3p in BAEC: Ct 27.4 and 27.5 and in human aortic endothelial cells: Ct 26.3 and Ct 26.4, respectively). We used bioinformatic algorithms (target scan, Pictar, miRNA.org) to predict potential targets of miR-199a-3p and -5p in endothelial cells, in particular in the eNOS/NO pathway (Table 2). Although eNOS gene per se was not identified as a theoretical target for either miR-199a, matching sequences were identified in a series of genes coding for proteins related to the NO pathway (see below).

	miR	miRSVR	TargetScan	Pictar	miRSVR Mouse
eNOS	miR-199a-3p	n.i.	n.i.	n.i.	n.i.
	miR-199a-5p	n.i.	n.i.	n.i.	n.i.
Akt1	miR-199a-3p	n.i.	n.i.	n.i.	−0.0011
	miR-199a-5p	n.i.	n.i.	n.i.	n.i.
Calcineurin	miR-199a-3p	−0.03	−0.24	1.78	−0.0305
	miR-199a-5p	n.i.	n.i.	3	−0.0366
PDK1	miR-199a-3p	n.i.	n.i.	n.i.	−0.1428
	miR-199a-5p	n.i.	n.i.	n.i.	−0.1813
CAV1	miR-199a-3p	n.i.	n.i.	n.i.	−0.0497
	miR-199a-5p	−0.8069	−0.68	3.88	−0.47
HSP90	miR-199a-3p	n.i.	n.i.	n.i.	−0.0273
	miR-199a-5p	n.i.	n.i.	n.i.	n.i.
SOD1	miR-199a-3p	n.i.	n.i.	n.i.	n.i.
	miR-199a-5p	−0.4026	n.i.	n.i.	n.i.
PRDX1	miR-199a-3p	−0.0142	n.i.	n.i.	n.i.
	miR-199a-5p	n.i.	n.i.	n.i.	−0.0196
DDAH1	miR-199a-3p	−0.0076	n.i.	n.i.	−0.0428
	miR-199a-5p	n.i.	n.i.	n.i.	n.i.
PRMT1	miR-199a-3p	n.i.	n.i.	n.i.	n.i.
	miR-199a-5p	n.i.	n.i.	n.i.	n.i.
VEGFA	miR-199a-3p	−0.20	n.i.	n.i.	−0.24
	miR-199a-5p	−0.1218	−0.71	n.i.	−0.1441

Table 2. miRSVR, TargetScan, and Pictar Scores for Indicated Target mRNA. These scores are representative of an alignment of the seed sequence of the miRNA of interest with mRNA in humans; last column is miRSVR score in mouse. Akt indicates protein kinase B; CAV, caveolin; DDAH, dimethylarginine dimethylaminohydrolase; eNOS, endothelial NO synthase; HSP, heat shock protein; miR/ miRNA, microRNA; miRSVR, miR scoring by vector regression; n.i., nonidentified matching sequences; NO, nitric oxide; PDK, pyruvate dehydrogenase kinase; PRDX, peroxiredoxin 1; PRMT, protein arginine N-methyltransferase; SOD, superoxide dismutase; and VEGFA, vascular endothelial growth factor A.

Matching between miR- 199a-3p or miR-199a-5p and some of the predicted targets were verified using luciferase-based reporter assays. As highlighted in Figure 15, both miR-199a-3p and miR-199a-5p target the 3'UTR region of *VEGFA, Calcineurin,* and *SOD1* mRNA.

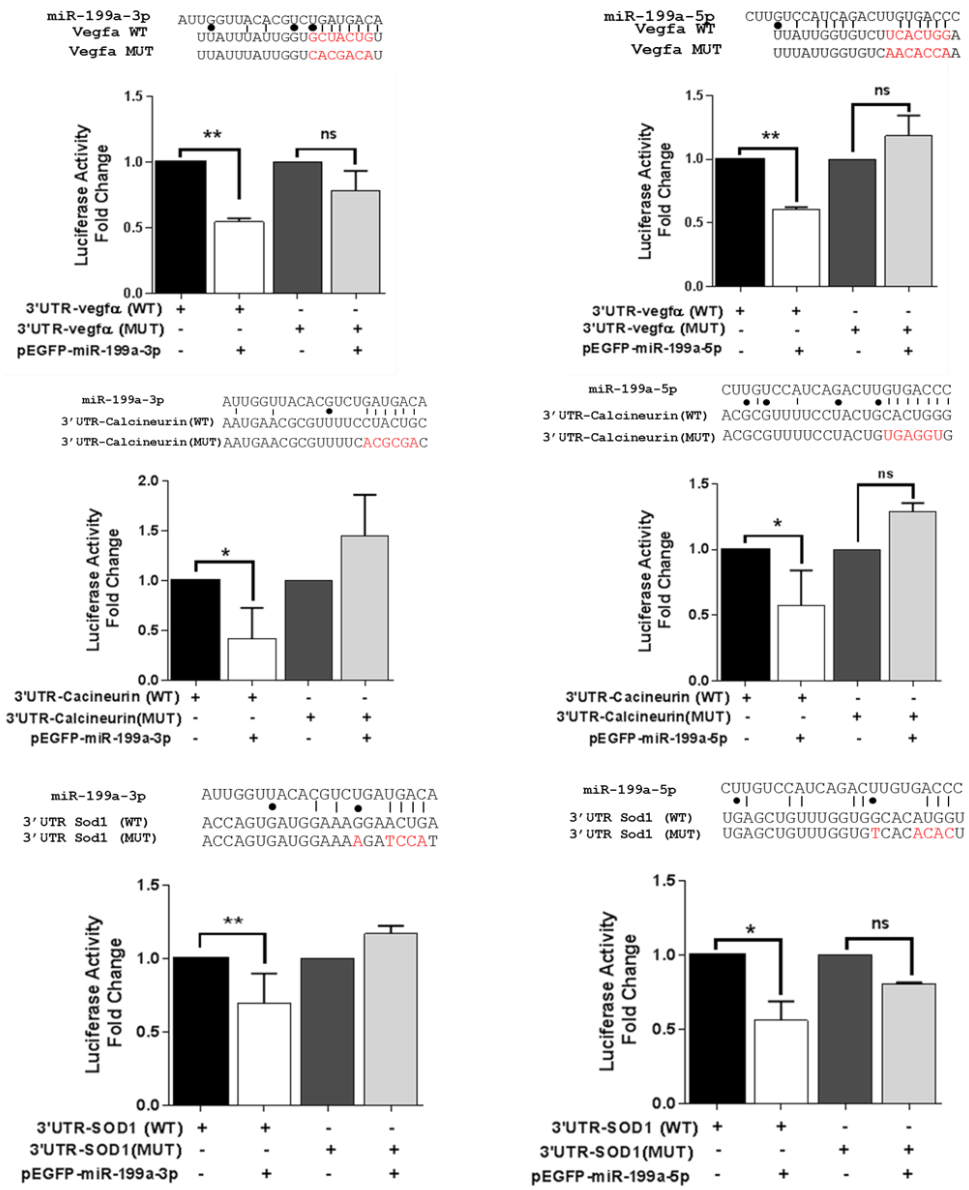

Figure 15: Luciferase-based reporter assays highlight matching sequence between miR-199a-3p or miR-199a-5p and predicted mRNAs targets including VEGFA, Calcineurin and SOD1. HeK-293T cells were transfected with pmiRGlo-3'UTR and pcDNA6.2-GW/EmGFP-miR-199a/a* plasmids. 48h post transfection, cells were lysed and luciferase activity was

NO Production Is Increased After Repression of miR-199a-3p or miR-199a-5p in Endothelial Cells

Transfection of LNA directed against either arm of miR-199a was effective in reducing the expression of the targeted miR as measured 48 or 72 hours after transfection (Figure 16A and 16B).

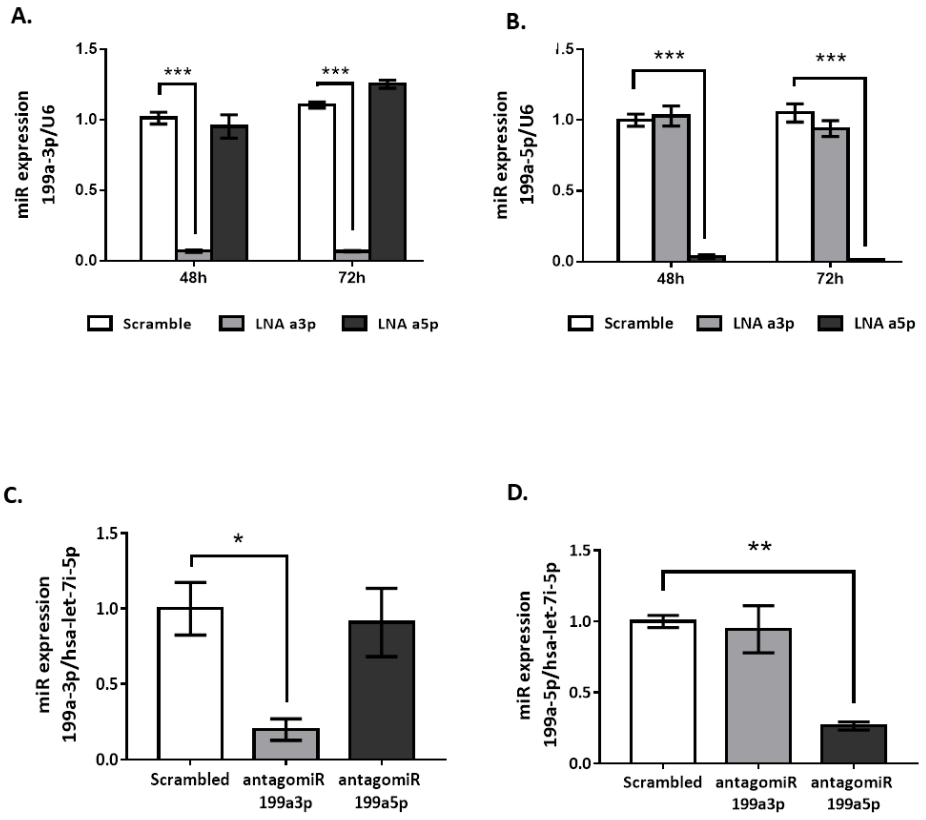

Figure 16: Locked-Nucleic Acid and antagomiRs induced a decrease of targeted microRNAs. BAEC cells were transfected ON with LNA directed against miR199a-3p or 199a-5p specifically (A and B). Mice were treated on three consecutive days with antagomiRs (75mg/kg/day) against miR 199a-3p/-5p and sacrificed 30 days after treatment (C and D). Results are expressed as mean ± SEM of 5 individual experiments for cells and 4 mice for *in vivo* study. *, *P.*<0.05; **, *P.*<0.01 and ***, P<0.001 *vs.* control.

LNA-based repression of miR-199a-3p or miR-199a-5p practically doubled basal NO production in BAECs (Figure 17).

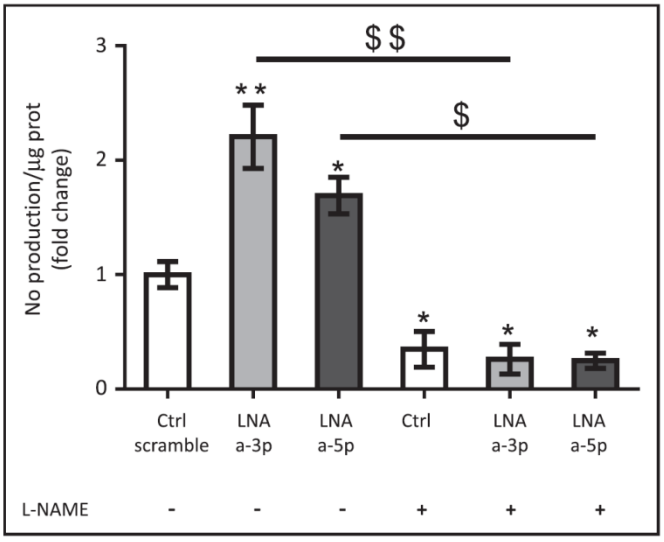

Figure 17. MicroRNA (miR) 199a-3p or -5p inhibition induces changes in nitric oxide (NO) production in endothelial cells. Bovine aortic endothelial cells were transfected with locked-nucleic acid (LNA) directed against miR-199a-3p or -199a-5p, and NO production was measured by electron paramagnetic resonance spin trapping after exposure to the spin trap colloid complex [(diethyldithiocarbamate)2Fe(II)] for 45 min. Results are expressed as mean±SEM. Numbers of individual experiments are the following: Scramble,n=6; LNA a-3p, n=6; LNA a-5p, n=4; Scramble+ L-nitroarginine methyl ester (L-NAME), n=3; LNA a-3p+L-NAME, n=3 and LNA a-5p+L-NAME, n=3. *P<0.05 and **P<0.01 vs control (ctrl); $P<0.05 and $$P<0.01 vs L-NAME treatment.

Treatment of BAECs with the nonselective NOS inhibitor L-nitroarginine methyl ester reduced NO levels to baseline amounts, indicating that miR-199a-3p or -5p blockade somehow led to an increase in NOS synthase(s) activity or in bioavailable NO. The expression of eNOS (the predominant NOS isoform expressed in endothelial cells) was not significantly altered by repression of miR-199a-3p or -5p (see total eNOS in Figure 20A). Similarly, expression of Cav1 and Hsp90, 2 critical

eNOS regulators in endothelial cells, remained unaltered after LNA treatments (Figure 18).

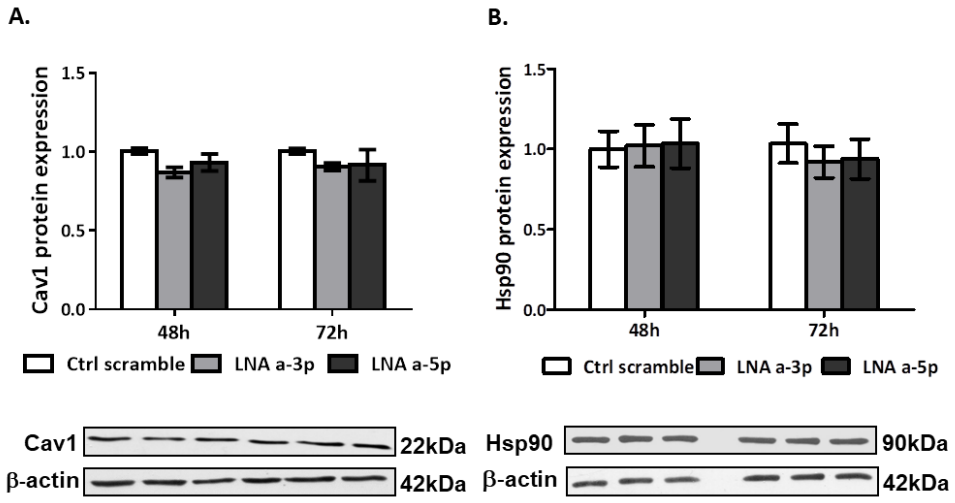

Figure 18: MicroRNA 199a-3p or -5p inhibition did not induce any modification of Caveolin-1 (Cav1) and Hsp90 expression in BAEC cells. BAEC cells were transfected ON with LNA directed against miR199a-3p or 199a-5p specifically. Expression of Cav1 (A) and Hsp90 (B) were detected by Western Blotting and quantified.

Also, neither the presence (in culture media) of ADMA, the endogenous competitive substrate for eNOS, nor the expression of its production/degradation enzymes in endothelial cells, namely DDAH1 and PRMT1 (the latter being a theoretical potential miR-199a target [Table 2]), were affected by either LNA treatments (Figure 19A–19C).

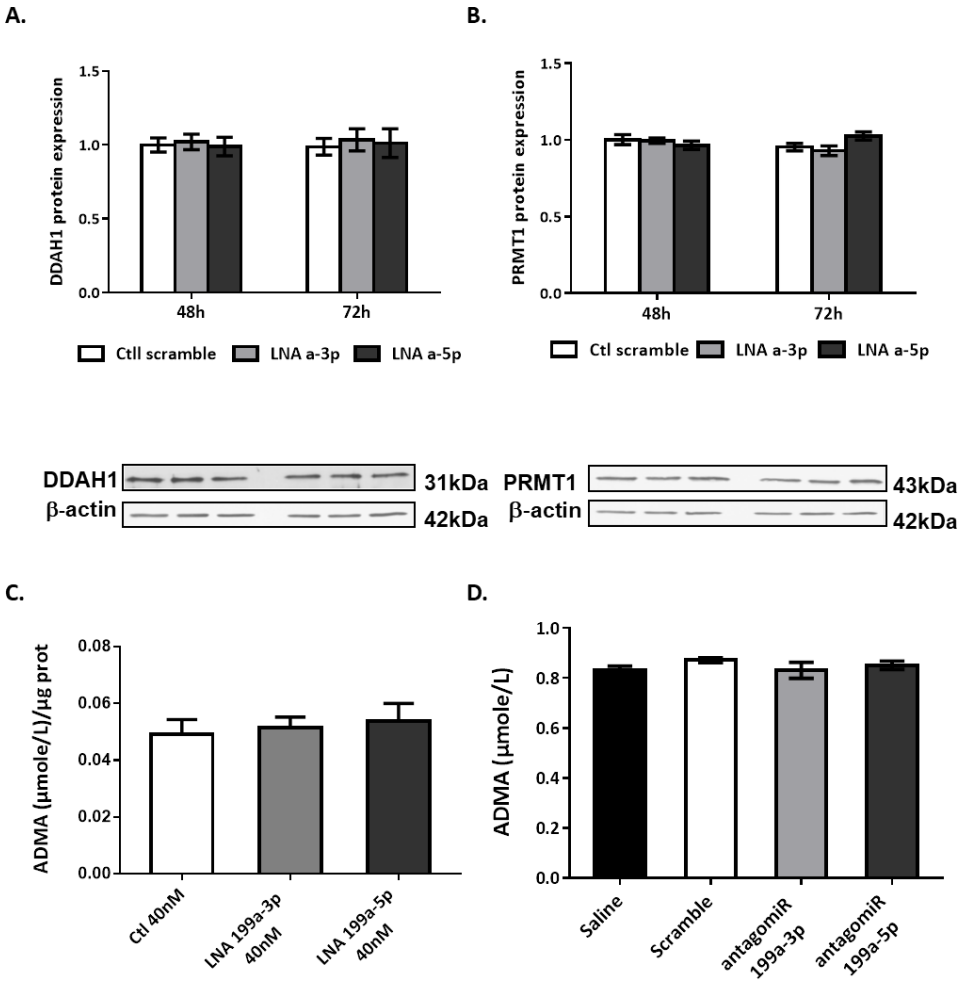

Figure 19: MicroRNA 199a-3p or -5p inhibition did not induce any modification of ADMA pathway in BAEC cells or in mice. BAEC cells were transfected ON with LNA directed against miR199a-3p or 199a-5p specifically. ADMA level was measured by ELISA quantification kit (C) and expression of PRMT1 and DDAH1 were detected by Western Blotting and quantified (A and B). Mice were treated with antagomiRs against miR 199a-3p/5p specifically, three days in a raw and sacrificed 30 days after treatment. ADMA level was measured in plasma using ELISA quantification kit (D).

eNOS Phosphorylation on Ser1177 is Modulated by miR-199a-3p and miR-199a-5p Repression Through the PI3K/Akt Pathway

Post-translational modifications of eNOS include changes in its phosphorylation state. We found that miR-199a-3p and -5p repression independently induced a prolonged increase in eNOS phosphorylation on Ser1177 (Figure 20A) after transfection of BAECs with either LNAs. These results correlated with a significant increase in Thr308 Akt phosphorylation 48 and 72 hours after the initiation of miRNA repression (Figure 20B). Similar results were observed in human aortic endothelial cells (data not shown). To prove a role of Akt in the LNA- supported increase in Ser1177 eNOS phosphorylation, we repeated the above experiments after silencing of Akt1 (62;344), the sole Akt isoform associated with eNOS (344) phosphorylation, and after treatment with the PI3K inhibitor LY294002. Akt1 siRNA treatment blunted the LNA-induced eNOS activation (Figure 20C), whereas LY294002 prevented both the phosphorylation of Akt on Thr308 and the increase in Ser1177 eNOS phosphorylation resulting from miR-199a-3p or -5p blockade (Figure 20D).

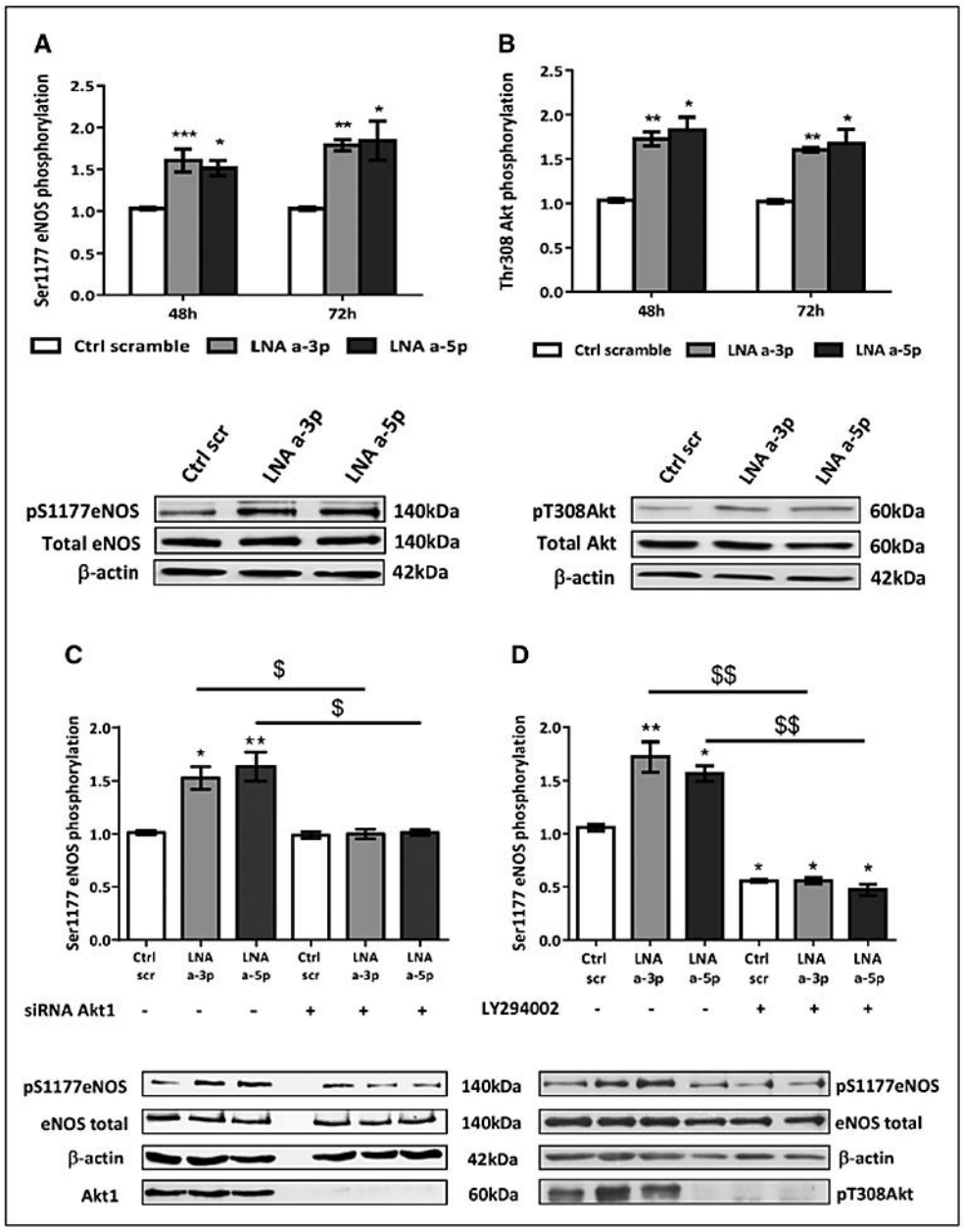

Figure 20. MicroRNA (miR) 199a-3p or -5p inhibition induces changes in Ser1177 eNOS (endothelial nitric oxide synthase) phosphorylation through modulation of the PI3K (phosphoinositide 3-kinase)/Akt (protein kinase B) pathway in endothelial cells. Bovine aortic endothelial cells (BAECs) were transfected with locked-nucleic acid (LNA) directed against

miR-199a-3p or -199a-5p. Levels of Ser1177 phosphorylated eNOS and Thr308 phosphorylated Akt were detected by Western blotting and quantified (A and B, respectively). In some experiments, LNA-treated BAECs were also treated with Akt1 siRNA (small interfering RNA; C) or LY294002 (D), and level of Ser1177 phosphorylated eNOS was detected by Western blotting and quantified. Results are expressed as mean±SEM. Numbers of individual experiments are the following: n=10 for each condition for graphs A and B and n=4 (without Akt inhibitor) or 3 (with Akt inhibitor) for graphs C and D. *P<0.05, **P<0.01 and ***P<0.001 vs scramble control (ctrl scr); $P<0.05 and $$P<0.01 vs Akt inhibition treatment.

Of note, we did not identify any effects of either LNA on the expression of PDK1 (Figure 21), the master kinase responsible for the activation of Akt (downstream of PI3K) identified as a potential miR-199a target (Table 2).

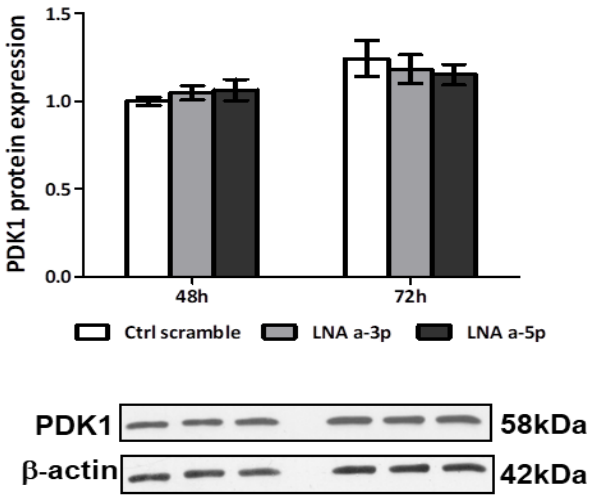

Figure 21: PDK1 is not modulated by microRNAs 199a-3p/5p modulation. BAEC cells were transfected ON with LNA directed against miR199a-3p or 199a-5p specifically. Expression of PDK1 was detected by Western Blotting and quantified.

In agreement with these results, transfection of miR-199a-3p or miR-199a-5p mimics evoked a decrease of eNOS activation through its phosphorylation on Ser1177 (Figure 22A).

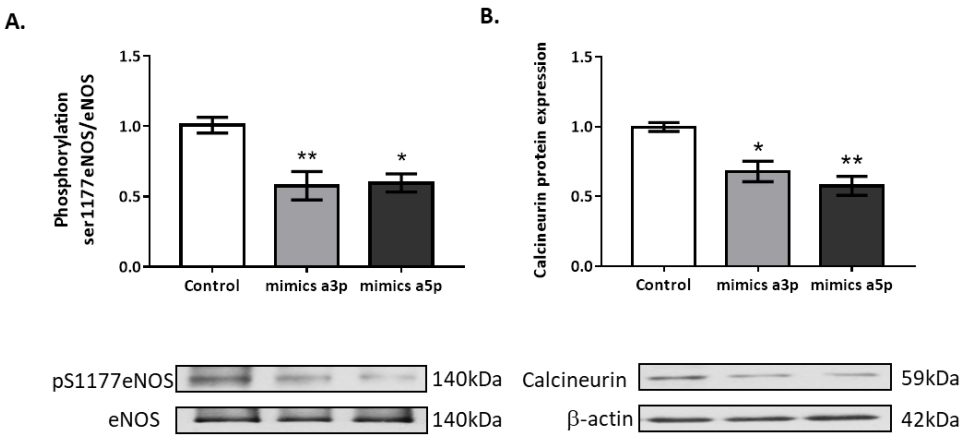

Figure 22: MicroRNA 199a-3p or -5p mimicking induces changes in serine 1177 eNOS phosphorylation and calcineurin expression. BAEC cells were transfected ON with mimics of miR199a-3p or 199a-5p specifically. eNOS phosphorylation and Calcineurin expression were detected by Western Blotting and quantified. Results are expressed as mean ± SEM of 3 individual experiments. *, *P.*<0.05 and **, *P.*<0.01 *vs.* control.

eNOS Phosphorylation on Thr495 is Modulated by miR-199a-3p and miR-199a-5p Repression Through the Calcineurin Pathway

Another well-known regulatory phosphorylation site within the eNOS sequence is the inactivating site, Thr495. We observed that LNA-based repression of miR-199a-3p and miR-199a-5p independently induced a decrease in the extent of Thr495 eNOS phosphorylation (Figure 23A). Importantly, we found that expression of calcineurin, the well-described phosphatase for Thr495 phosphorylated eNOS, was increased by >50% when miR-199a-3p or -5p were repressed (Figure 23B) in agreement with the identification of the calcineurin mRNA as a potential molecular target of miR-199a (Table 2). Accordingly, miR-

199a-3p or -5p mimics transfection significantly reduced the phosphatase expression (Figure 22B).

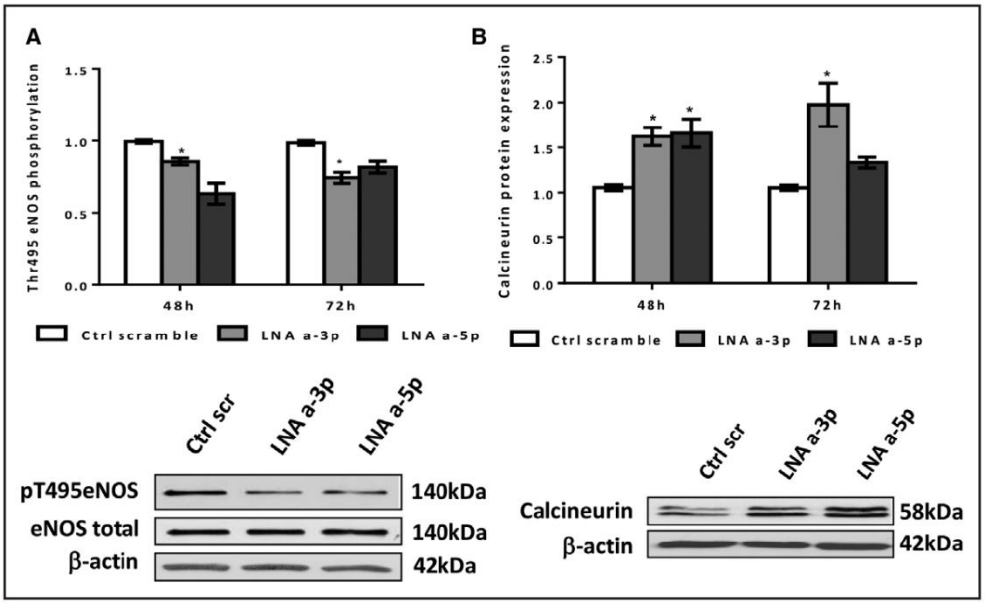

Figure 23. MicroRNA (miR) 199a-3p or -5p inhibition induces changes in Thr495 eNOS (endothelial nitric oxide synthase) phosphorylation through calcineurin phosphatase modulation in endothelial cells. Bovine aortic endothelial cells were transfected with locked-nucleic acid (LNA) directed against miR-199a-3p or -199a-5p. Levels of Thr495 phosphorylated eNOS and calcineurin were detected by Western blotting and quantified (A and B, respectively). Results are expressed as mean±SEM. Numbers of individual experiments are the following: Scramble, n=5; LNA a-3p, n= 4; LNA a-5p, n=4. Lower, Representative phosphoblot of endothelial extracts at 48 h *P<0.05 vs scramble control (ctrl scr).

Repression of miR-199a-3p and miR-199a-5p Modulates the NO Bioavailability by Modulating SOD1 Expression

The above experiments indicated that miR-199a repression was associated with an increase in eNOS activity. We next evaluated whether the increase in NO abundance (Figure 17) could also arise from a decreased NO degradation because of a lesser reaction with superoxide anion ($O_2^{\cdot-}$). We first documented that

repression of both miR-199a-3p and miR-199a-5p induced a marked reduction of $O_2^{\cdot-}$ levels in endothelial cells, as measured by dihydroethidium staining (Figure 24A).

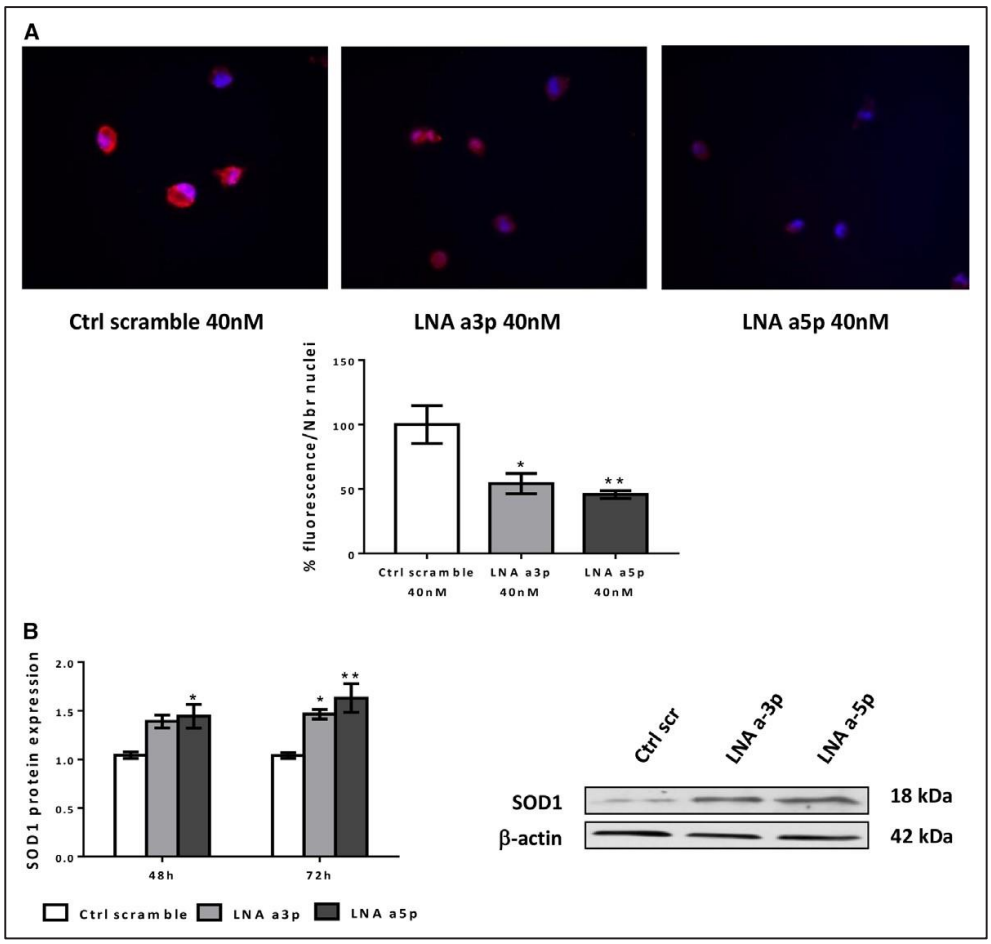

Figure 24. MicroRNA (miR) 199a-3p or -5p inhibition induces a reduction in superoxide anion production in endothelial cells through an increase in SOD1 (superoxide dismutase 1) expression. Bovine aortic endothelial cells were transfected with locked-nucleic acid (LNA) directed against miR-199a-3p or -199a- 5p, and superoxide anion levels were assessed by dihydroethidium (DHE) staining (A, red) and quantified (see bar graph); nucleus was counterstained using Hoechst dye (A, blue). Expression of SOD1 was detected by Western blotting and quantified (B). Results are expressed as mean±SEM. Numbers of individual

experiments are the following: n=3 for each condition for DHE staining and n=4 for each condition for SOD1 quantification. *P<0.05 and **P<0.01 vs control (ctrl). Scr indicates scramble.

We also examined the expression of 2 ROS-regulating enzymes that we identified among the theoretical targets of miR-199a (Table 2), namely SOD1 and PRDX1, which catalyze the dismutation of $O_2^{-\cdot}$ Into hydrogen peroxide (H_2O_2) and transform H_2O_2 in oxygen and water, respectively. We found that both miR-199a-targeting LNAs led to a net increase in SOD1 (Figure 24B), whereas PRDX1 expression was only increased on transfection with miR-199a-5p-targeting LNA (Supplemental Figure 25).

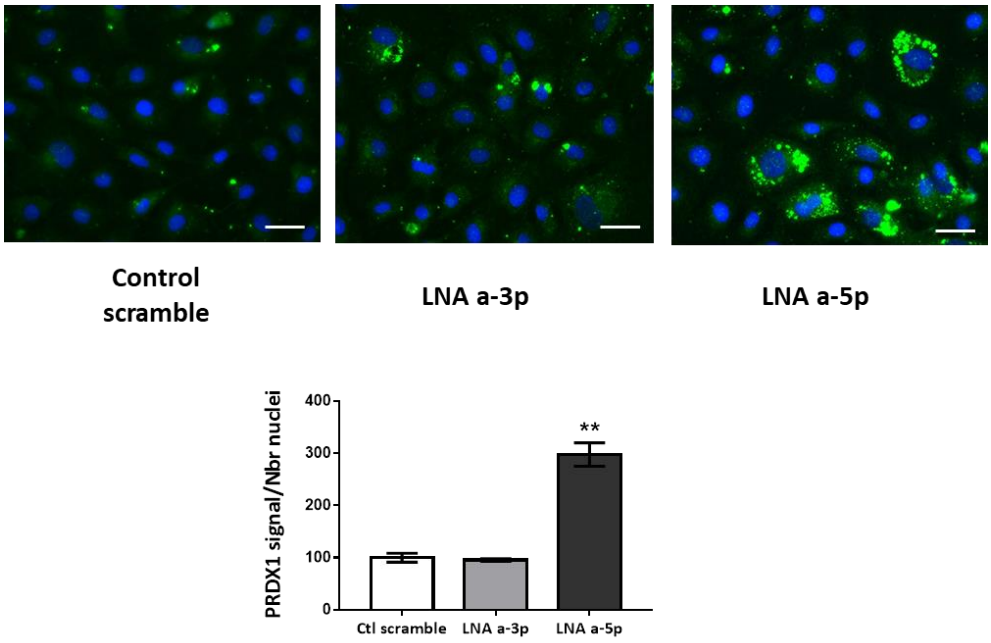

Figure 25: MicroRNA 199a-5p inhibition induced an increase of PRDX1 expression in BAEC cells. BAEC cells were cultured on glass coverslip and transfected ON with LNA directed against miR199a-3p or 199a-5p specifically. Cells were fixed with PFA 4% and incubated ON with anti-PRDX1 antibody (in green, Abcam). Nucleus were labeled using Dapi dye (blue). The signal was quantified with Image J software. Results are expressed as mean ± SEM of at least 3 individual experiments. **, *P.*<0.01 compared with control, Scale bar equals 10µm.

Inhibition of miR-199a-5p Induces an Increase in VEGFA Protein Expression and Tube Formation

We next aimed to evaluate the effects of dedicated LNA on endothelial tube formation, a process known to be NO-mediated. This experiment was further guided by previous reports and our luciferase-based reporter assay identifying VEGFA (comprising all splicing variants) as a putative direct target of miR-199a-5p (288) (Table 2). Note that the absence of pairing between bovine VEGFA and miR-199a-3p is likely to account for the lack of regulation by LNA3p in BAECs. We confirmed an increase in VEGFA expression in cells transfected with miR-199a-5p inhibitor (but not miR-199a-3p; Figure 26A). Bevacizumab treatment of endothelial cells partially inhibited eNOS phosphorylation on Ser1177 observed following LNA5p transfection (Figure 27). In addition, the extent of precapillary tube formation, as assessed by plating endothelial cells on Matrigel and quantified with Image J software, was increased in response to miR-199a-targeting LNA, in particular when miR-199a-5p was repressed (Figure 26B and 26C).

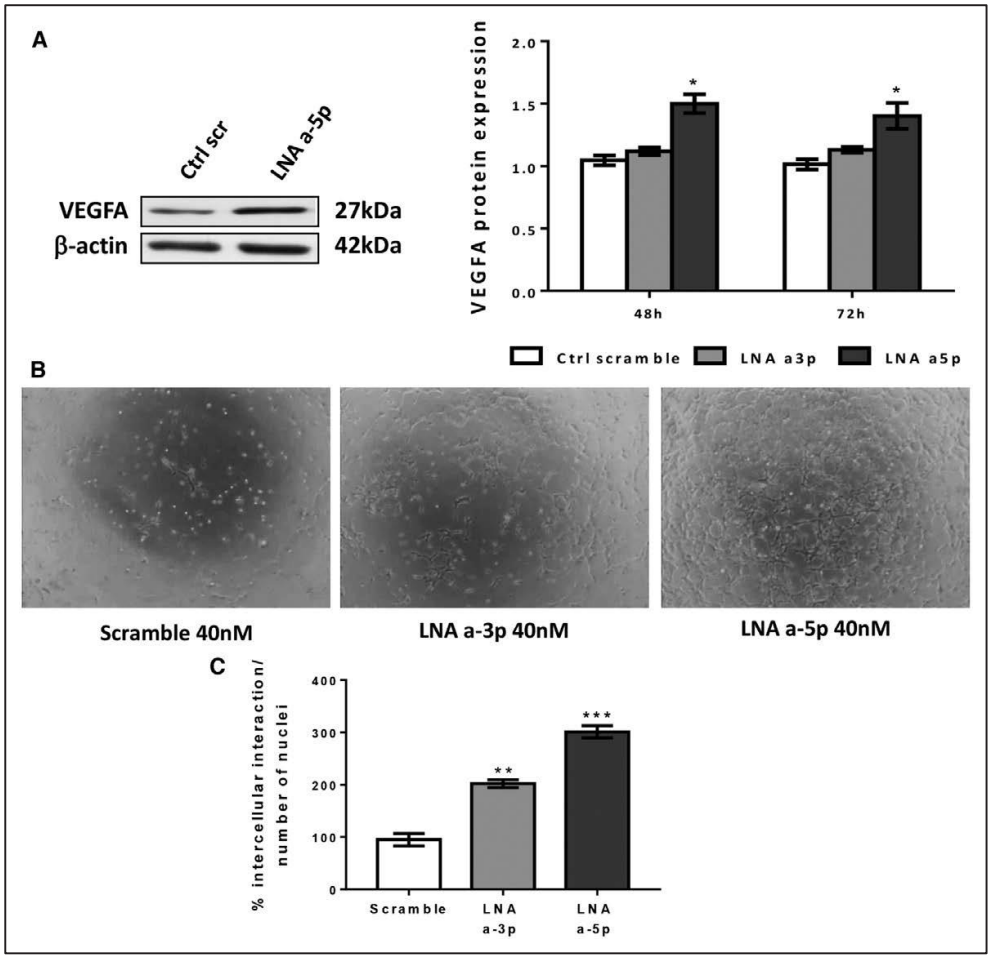

Figure 26. MicroRNA (miR) 199a-3p or -5p inhibition induces an increase of VEGFA (vascular endothelial growth factor A) expression and endothelial tube formation. Bovine aortic endothelial cells (BAECs) were transfected with locked-nucleic acid (LNA) directed against miR-199a-3p or -199a-5p, and expression of VEGFA was detected by Western blotting and quantified (**A**). In some experiments, LNA-treated BAECs were collected and mixed with equal volume of Matrigel to assess tube formation (**B**). Results are expressed as mean±SEM. Numbers of dual experiments are the following: n=4 for each condition for VEGF quantification and Matrigel assay. **P*<0.05, ***P*<0.01, and ****P*<0.001 vs scramble control (ctrl scr).

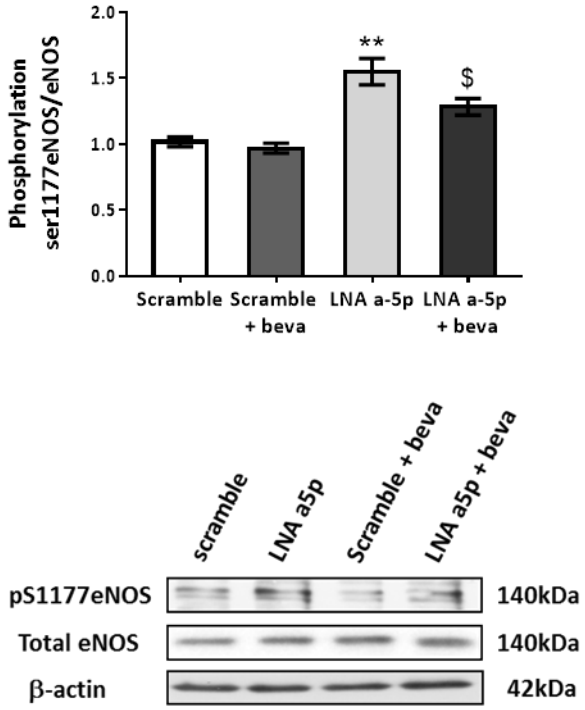

Figure 27: Bevacizumab treatment does not induce a significant reduction of eNOS phosphorylation on serine 1177 induced by LNAa-5p. BAEC cells were transfected ON with LNA directed against miR199a-5p specifically and treated or not with bevacizumab. Phosphorylation of eNOS was detected by Western Blotting and quantified. Results are expressed as mean ± SEM of at least 3 individual experiments. **, *P.*<0.01 compared with scramble and $, P<0.05 compared with scramble + beva

Mice Treated With AntagomiRs Directed Against miR-199a-3p and miR-199a-5p Present an Improvement of Their Endothelial Function

To prove that miR-199a repression influences the amounts of bioactive NO *in vivo*, C57Bl6 male mice were treated with antagomiRs directed against miR-199a-3p or miR- 199a-5p. At the time of euthanization (30 days after the initiation of *in vivo* antagomiR administration), plasma was collected to verify the expression of circulating miRs. A specific decrease of the targeted miR was observed without significant alterations in the expression of the opposite

strand (Figure 16C and 16D). Isolated aorta presented a significantly larger NO-dependent relaxation as measured in KCl precontracted vessels (versus vessels from mice treated with saline or scramble sequence; Figure 28A). These results were further validated by the detection of increased levels of circulating hemoglobin-NO (HbNO) in the venous blood of antagomiR-treated mice (Figure 28B). Also, EPR measurements of $O^{-\cdot}$ production in aortic rings obtained from mice treated with antagomiRs against miR-199a-3p or -5p revealed a net reduction in $O^{-\cdot}$ levels (versus control conditions; Figure 28C). In agreement with the data obtained in cultured endothelial cells, an increase of eNOS phosphorylation on Ser1177 (Figure 28D) was observed in the aorta of antagomiR-treated mice (versus control mice). Moreover, an increase of calcineurin and SOD1 expression (Figure 28E and 28F) was also identified in isolated vessels further supporting our *in vitro* data. Finally, as observed in cultured endothelial cells, antagomiR-treated and control mice presented the same levels of ADMA in their plasma (Figure 19D).

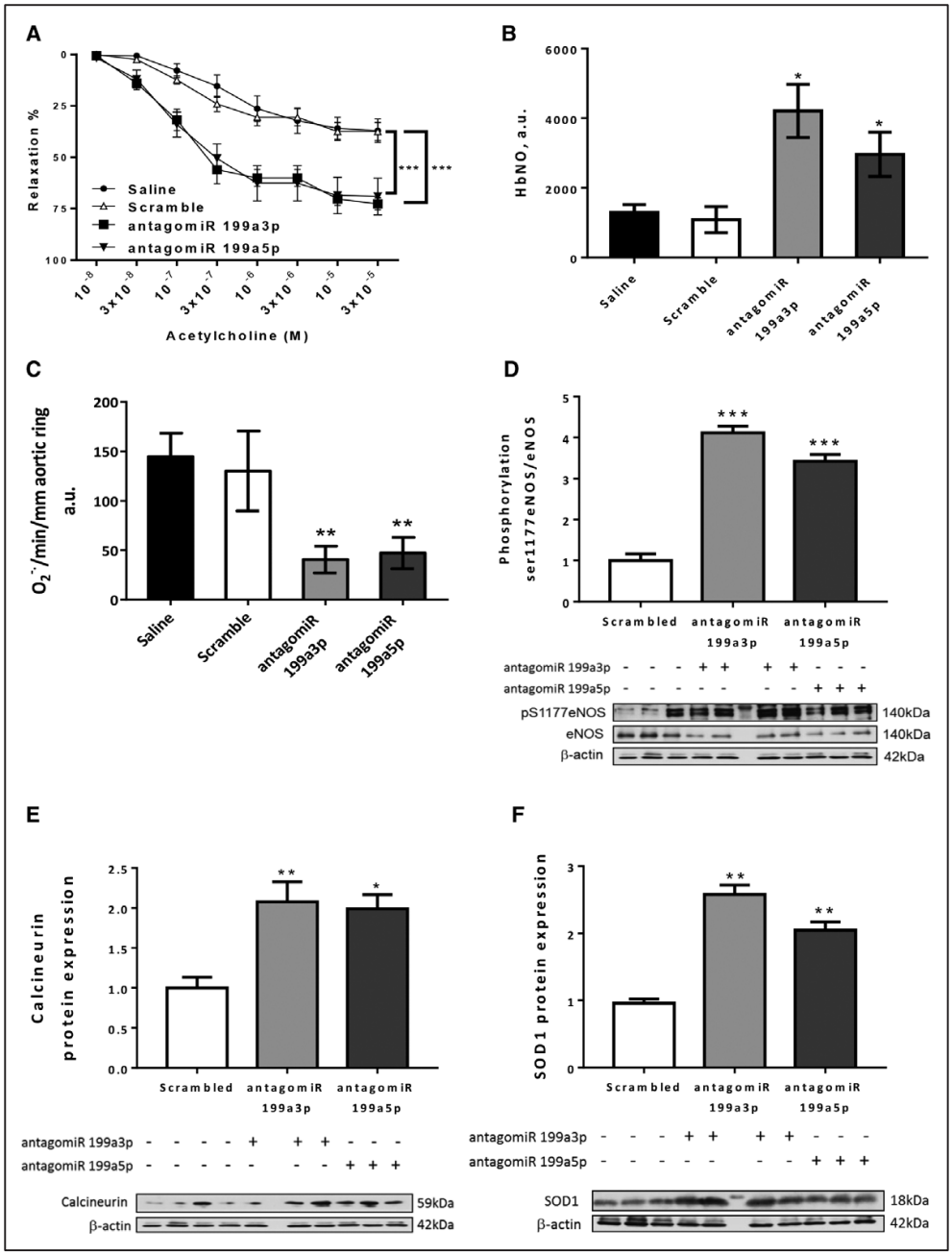

Figure 28. Vessels isolated from mice treated with microRNA (miR)-199a-3p or -199a-5p inhibitors exhibit an increased endothelium-dependent nitric oxide (NO)-dependent relaxation. Mice were treated on 3 consecutive days with antagomiRs (75 mg/kg per day)

against miR 199a-3p/-5p and euthanized 30 d after treatment. Dose-dependent effects of acetylcholine on mouse aorta relaxation determined on a wire myograph (A). Venous blood from these mice (B) and aortic rings (C) were also collected to assess hemoglobin-NO (HbNO) and superoxide anion levels, respectively, by electron paramagnetic resonance. Level of Ser1177 phosphorylated eNOS (endothelial NO synthase), calcineurin, and SOD1 (superoxide dismutase 1) was detected by Western blotting and quantified (D–F). Results are expressed as mean±SEM of at least 5 animals for physiological experiments and 6 (D–E) or 4 (F) animals for Western blot experiments *P<0.05, **P<0.01 and ***P<0.001 vs indicated controls (saline or scramble).

miR-199a-3p and miR-199a-5p are Increased in Mice Model of Hypertension

To verify the implication of miR-199a in pathological conditions, mice were implanted with angiotensin infusing minipump (2 mg/kg per day) for 14 days, a well-described model of hypertension and cardiac hypertrophy (47). Heart and aorta isolated from these mice exhibited a larger expression of both mature miR-199a. Interestingly, a dysregulation of miR expression was only observed for miR-199a-5p in the plasma of hypertensive mice (Figure 29).

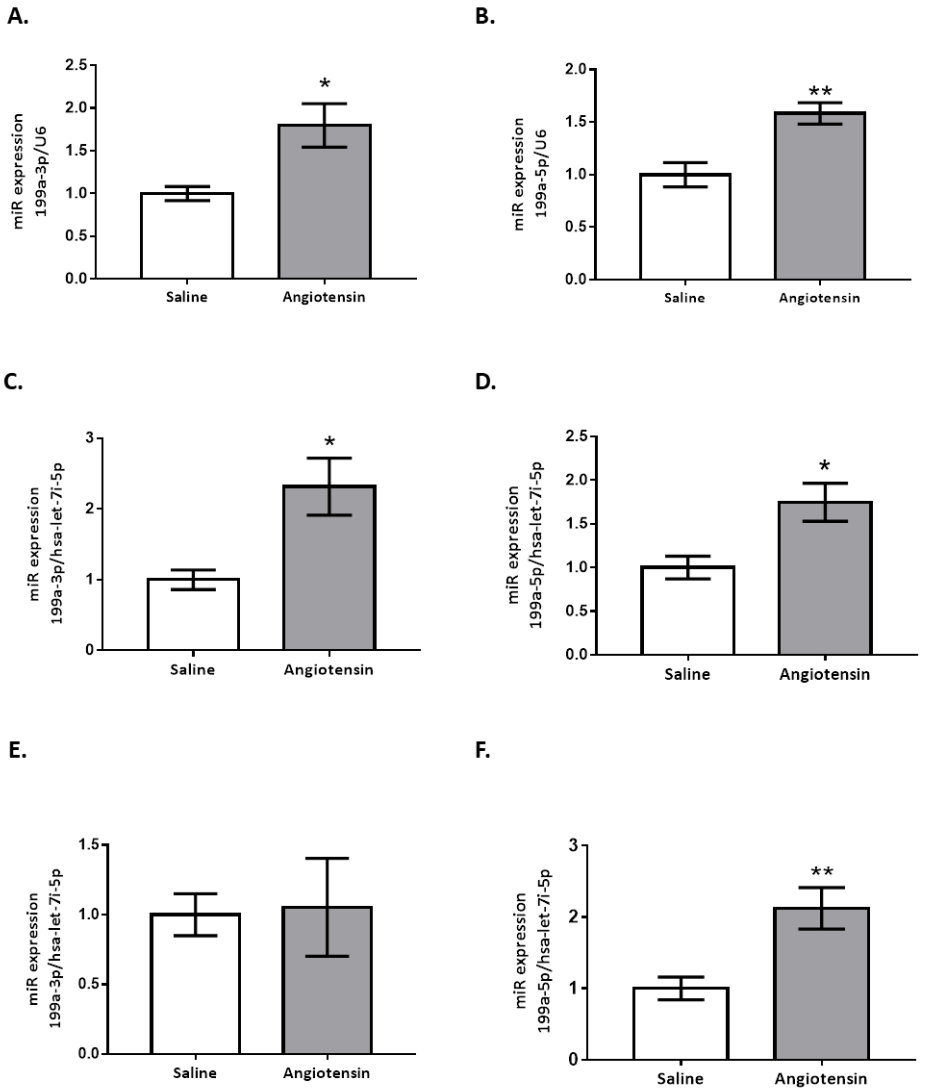

Figure 29: Hearts, vessels and plasmas isolated from mice treated with angiotensin exhibit an increased microRNAs 199a expression. Mice were treated with angiotensin or saline solution during 14 days. MiR-199a-3p and miR-199a-5p were measured in hearts (A-B), aorta (C-D) and plasmas (E-F). Results are expressed as mean ± SEM of 5 animals. *, *P.*<0.05 and **, *P.*<0.01 vs. saline.

Discussion

miRNAs derived from the precursor miR-199a are known to play critical roles in the maintenance of cardiac homeostasis (142;336). Our study reveals that both mature miRNAs (namely miR-199a-3p and miR-199a-5p) also participate in a redundant network of eNOS regulation in the endothelium (see Graphic Abstract). In particular, we highlighted how inhibition of miR-199a-3p and miR-199a-5p independently increases NO bioavailability by promoting eNOS enzymatic activity and reducing NO degradation, thereby, supporting VEGFA-induced endothelial tubulogenesis and modulating vessel contractile tone.

miR-199a is well conserved in different species (286) and in the human genome, it is encoded by 2 loci within introns of the *DNM* (dynamin 2 and 3), miR-199a-1 in chromosome 19 and mir-199a-2 in chromosome 1. Classically, 1 of the 2 strands derived from the precursor is considered as mature (miR) and the other one (miR*) is degraded, the ratio miR/miR* varying according to the rate of degradation of the immature strand. There is, however, growing evidence that both strands might exhibit regulatory activities (170). Accordingly, both strands (-5p and -3p) from pre-miR-199a can form mature miRNAs that may behave differently depending on the pathological contexts (286). In this study, we found that both miRNAs, miR- 199a-3p and miR-199a-5p were significantly expressed in endothelial cells and independently regulated NO production. Based on various *in vitro* and *ex vivo* assays, we found that NO availability was increased through an increased eNOS enzymatic activity, an effect further reinforced by reduced superoxide production.

Strikingly, we identified that the eNOS phosphorylation status was altered not only on the stimulatory Ser1177 site but also on the inactivating Thr495 site. We identified the stimulatory effects of miR-199a-3p and -5p-targeting LNAs on the

PI3K/Akt pathway and on the calcineurin phosphatase as the respective triggers of this mode of eNOS activation. The upregulation of calcineurin on miR-199a blockade was in agreement with the *in silico* identification of calcineurin-encoding gene as a theoretical target of this miRNA (see Table) and further validated by a dedicated luciferase- based reporter assay. By contrast, although pharmacological inhibition of PI3K and Akt genetic silencing proved the role of this pathway on Ser1177 phosphorylation, we did not observe changes in the abundance of Akt (or PDK1) on LNA treatment (despite favorable matching scores between miRNAs sequences and Akt mRNA [Table]). Further studies are warranted to identify possible targets involved in the regulation of the PI3K/AKT pathway. Interestingly, the miR- 199a-mediated regulation of Akt was recently highlighted in mouse heart as supportive of physiological cardiac hypertrophy (314), myoblast differentiation (345) and cardiomyocyte proliferation (346), and survival under ischemic stress (347). Interestingly, besides increased eNOS activity resulting from increased Ser1177 phosphorylation and Thr495 dephosphorylation, our study also provides evidence that miR-199 blockade can increase NO bioavailability by preventing its inactivation. We actually found that SOD was increased on repression of miR-199a-3p or -5p, thereby, supporting a reduced oxidative stress and thus promoting an increase in NO availability. It is also worth noting that although similar effects (ie, changes in eNOS phosphorylation and SOD activity) were obtained with LNA targeting either miR-199a form, repression of miR-199a-5p exhibited a significantly stronger effect on the upregulation of PRDX1 (another ROS detoxifying enzyme) than on miR-199-3p blockade. A large effect of miR-199a-5p-targeting LNA was observed on VEGFA expression and endothelial tube formation. However, we cannot exclude that in human endothelial cells, miR-199a-3p could also regulate VEGFA to some extent. The respective contribution of VEGFA overexpression to eNOS activation in our experimental setup is actually

difficult to delineate because Akt phosphorylation itself (a main driver of eNOS phosphorylation) is independently increased in response to LNA treatment. Nevertheless, altogether, these data reinforce the redundant aspect of miR-199a regulation on the endothelial NOS/NO pathway.

Importantly, in our study, the effects of chronic mouse exposure to anti-miR-199a antagomiRs further provided several sets of evidence supporting a relevant role of miR-199a in *in vivo* settings. We have indeed observed a dramatic increase in the relaxation of vessels isolated from antagomiR-treated mice together with a reduced superoxide production and an increased circulating HbNO reflecting a global increase in NO availability. Modifications of eNOS phosphorylation, calcineurin, and SOD expression also argue in favor of a role of miR-199a-3p and 5p *in vivo*. It should be noted that previous publications have reported effects of either miR-199a-5p or -3p on eNOS activity through changes in Cav expression (348). In our hands, such regulation could not be observed, possibly suggesting differential miRNA regulation processes in different cell types or physio-pathological contexts. Also, we failed to document a link between the expression of miR-199a and the abundance of the endogenous eNOS inhibitor ADMA (and of the related producing/metabolizing enzymes), as previously reported in cardiomyocytes (304). However, the latter observation could result from differential targeting according to the cellular context (ie, cardiac myocytes versus endothelial cells) or nonspecific effects resulting from the overexpression of pre-miR-199a.

Taken together, our results indicate that miRNAs matured from miR-199a, working potentially in cluster, take part in a redundant network of regulation of the NOS/NO pathway in the endothelium and modulate key endothelial functions, including angiogenesis and vascular tone. miR-199a has, therefore, to be added to the short list of miRNAs reported to modulate eNOS expression or activity, such

as miR-155 and miR-21 (349). Our observations are in agreement with studies documenting that miRNAs often fine-tune cellular homeostasis through intercrossed regulatory networks controlled by multiple miRNAs (350). More specifically, the dysregulation of both mature arms of miR-199a initially reported in heart may now be extended to the vascular tissues, thereby opening new perspectives of treatment. Our study actually provides evidence that new therapeutic opportunities may stem from altering these subtle modes of regulation in blood vessels, for instance through the use of endothelial-directed aptamer inhibitors or miRNA-sponges.

Results PART II

Chronic exercise modifies the expression of the cardiac and endothelial regulators miR-199a-3p and miR-199a-5p

Virginie Joris[1]*, Thomas Metzinger[1]*, Laurent Dumas[1], Dorothée Marchand[1], Hrag Esfahani[1], Sabina Kurbanova[1], Louis Maistriaux[3], Estelle Bastien[1], Evangelos P. Daskalopoulos[2], Sandrine Horman[2], and Chantal Dessy[1]

1 Pole of Pharmacology and Therapeutics (FATH), Experimental and Clinical Research Institute (IREC), Université catholique de Louvain, Brussels, Belgium

2 Pole of Cardiovascular Research (CARD), Experimental and Clinical Research Institute (IREC), Université catholique de Louvain, Brussels, Belgium

3 Pole of Morphology, Experimental and Clinical Research Institute (IREC), Université catholique de Louvain, Brussels, Belgium

*Contributed equally

Manuscript submitted in American Journal of Physiology-Heart and Circulatory Physiology

Results PART II

Abstract

Aims: Among potential molecular mechanisms supporting exercise-driven regulation of cardiovascular homeostasis, miRNAs (miRs) represent interesting candidates. Recently, miR-199a family members were highlighted as key players regulating endothelial and cardiac functions. Our working hypothesis is that alterations in ECs and/or cardiac myocyte phenotypes driven by changes in miR-199a abundance account for cardiac and vascular adaptation to exercise.

Methods and Results: five weeks old C57Bl6/J mice were given access to voluntary wheel running. After 22 weeks, contractile profile and endothelial function were evaluated *ex vivo*. Heart, vessels and plasma were processed for miR profiling and/or protein expression analyses. Impact of chronic exercise on endothelium was mimicked by applying increased shear stress on bovine endothelial cells plated in Ibidi chambers. Chronic exercise induced a significant cardiac remodeling correlated with an improvement of basal endothelial function attested by a NO-dependent repression of contractile tone in mesenteric arteries of active mice. A downregulation of miR-199a-3p and miR-199a-5p expression was observed in heart of running mice, correlated with increased expression of direct targets, namely Sirt1, PGC1α and mTOR. Mir-199a-5p was also down-regulated in vessels of active mice and this correlated with an up-regulation of endothelial function measured through eNOS and Akt activation. This concurs with miR-199a profile and NOS activation in endothelial cells exposed to laminar shear stress.

Conclusion: Our results demonstrate that chronic mild exercise positively regulates cardiac and endothelial functions potentially through a modulation of miR-199a expression. miR-199a family should be added to the list of miR modulated by exercise in the cardiovascular system.

Introduction

Sedentary lifestyle and Western diet undoubtedly account for the spreading epidemic of obesity, diabetes and cardiovascular diseases (CVD) (351). Intervention trials demonstrated that lifestyle changes that include exercise prevent the incidence of premature cardiovascular (CV) events (352). In this context, during the last decades, physical training has become a cornerstone of (primary and) secondary prevention strategies.

A systematic review and meta-analysis of 33 cohort studies has reported that physical activity is associated with 35% risk reduction in CVD mortality and 33% risk reduction in all-cause mortality (353). Although an inverse relationship has not been clearly described, it appears from numerous studies that a certain level of physical exercise is already beneficial (354). Alterations in the myocardium, skeletal muscles and vasculature coordinate in order to respond to the increased physical demands generated by exercise and hence contribute to the beneficial effects on the CV system (355). Accordingly, long-term exercise training elicits integrated physiological and morphological adaptations, in particular an adaptive cardiac remodeling, associated with unchanged or improved ventricular function in stark contrast with pathological cardiac hypertrophy. Similarly, functional and/or structural adaptations in conduit, resistance, and micro-vessels account for a rise in vascular conductance (24).

Animal model use has largely contributed to decipher molecular mechanisms implicated in the beneficial impact of exercise on the CV system. One of the most important biological consequences of chronic moderate exercise training is the rise in nitric oxide (NO) bioavailability. NO not only modulates platelet aggregation and leucocytes adhesion (thereby preventing thrombogenesis and atherosclerosis), but also supports vasodilation which results in the lowering of peripheral resistance and improvements in perfusion. Flow-mediated shear stress

associated with physical exercise increases NO bioavailability through transcriptional, post-transcriptional and post-translational regulation of endothelial nitric oxide synthase (eNOS) (48). In addition, exercise-dependent increase in shear stress also limits oxidative stress, preventing eNOS uncoupling and NO degradation (48). In line with an improved endothelial function, exercise training increases arteriogenesis in the myocardium through the recruitment of progenitor cells and the production of growth factors such as Vascular Endothelial Growth Factor (VEGF) (356). In addition and besides modulation of the neurohormonal system, aerobic exercise also impacts the catabolic/anabolic systems and alters calcium handling (355). Profound cardiac transcriptomic changes elicited by exercise training illustrate the significant gene reprogramming driven by the increased workload demand. Among the most important changes are genes related to the maintenance of fatty acid oxidation, ATP production and mitochondrial biogenesis (129). Accordingly, many studies have identified the peroxisome proliferator-activated receptor gamma coactivator 1-alpha (PGC1-α) as a key regulator of cardiac exercise training adaptation. In line with that, PGC1 knock-out mice exhibit reduced rates of post-exercise muscle glycogen repletion, which translates into poor exercise performance (357).

Among the possible molecular mechanisms associated with the exercise-driven regulation of CV homeostasis is the modulation of microRNA (miRNA, miR) expression profile. These small non-coding RNAs regulated virtually all biological processes involved in homeostasis via a post-transcriptional control of gene expression (265;358). The corollary is that a dysregulation of specific miRNAs profile has been associated with many pathological states. For instance, circulatory miRs-26b, -29b and -30d were shown to be differentially regulated in CVD (obesity, type 2 diabetes and hypertension respectively) and following exercise training, suggesting that miRs may not only serve as biomarkers of CVD

but also directly participate in the protective counter-balancing effects offered by exercise (359;360). Several pieces of evidence suggest that alterations in miR-199a expression could also tip the balance toward either CVD or exercise-mediated vasculo-protective effects. We and others have indeed identified miR-199a mature products as negative regulators of CV function (308;319;361;362). Although originally identified as an actor of carcinogenesis, miR-199a has been involved as a master regulator of cardiac preconditioning and associated protection against ischemia-perfusion, in part through its action on Hypoxia inducible factor (HIF)-1α (286;303;309). A dysregulation of miR-199a has also been proposed in several CV pathologies, both in humans and animal models (361). For instance, miR-199a up-regulation has been associated with hypertension and/or pathological myocardial hypertrophy evoked by trans-aortic abdominal constriction (308) or angiotensin infusion (362). We have documented how conversely, a reduction in miR-199a is associated with an increase in eNOS activity/NO availability, thereby pointing to miR-199a as a key regulator of endothelial function (362). This finding was further supported by the work of Heuslein et al. reporting up-regulated miR-199a in the blood of peripheral arterial disease patients with intermittent claudication (319). Furthermore, the use of miR-199-sponge transgenic murine model to generate a cardiomyocyte-specific disruption of miR-199a, was shown to promote the development of physiological cardiac hypertrophy (314).

In this study, we developed a murine model of mild chronic exercise to test the hypothesis that alterations in endothelial cells (ECs) and/or cardiac myocyte phenotypes driven by changes in miR-199a abundance, account for cardiac and vascular adaptation to exercise.

Materials and methods

Animal housing and exercise protocol

Four-weeks-old C57BL6/J male mice (25 animals) were purchased from Janvier Labs (France) and housed 1 per cage in our local animal facility with a 12/12-hour night and day cycle with free access to both food and water. Their behavior and wellbeing were checked every day. At five weeks of age, animals were randomly assigned to a cage (Tecniplast, France) equipped or not with an activity wheel (Kit mini wheel and activity wheel with revolution counter, Intellibio, Nancy, France). Animals' body weight was measured every two weeks, while run distance covered was recorded every two days. After 22 weeks, terminal anesthesia was performed by intraperitoneal injection of ketamine (100 mg/ml) and xylazine (20 mg/ml), blood heart and vessels were collected and frozen in liquid nitrogen for miR profiling and Western Blotting analyses.

It is noteworthy that since miR-199a-3p appears to take part in the oestrogen regulatory network and male and female react differently to running exercise, this study was performed on male mice only (363;364).

All experimental procedures and protocols were approved by the local Ethics Committee (Comité d'Ethique pour l'Expérimentation animale; 2016/UCL/MD/017), Secteur des Sciences de la Santé, Université catholique de Louvain, according to National Care Regulation and Directive 2010/63/EU of European Parliament and of the Council.

Echocardiography

Cardiac adaptation to exercise was followed throughout the protocol by echocardiography. The baseline measurement (t=0) was performed prior to wheel installation; a second measurement was performed at week 14 and a third one prior to sacrifice, after 22 weeks of running. Two-dimensional (2D) B-mode and

M-mode transthoracic echocardiography was performed using a Vevo 2100 Imaging System (FUJIFILM-VisualSonics, Toronto, ON, Canada), equipped with a 40MHz transducer. Animals were anesthetized using isoflurane 2-3% for induction and 1-2% for maintenance. Left ventricular (LV) volumes were measured at end-systole and end-diastole (B-mode parasternal long-axis view), from which ejection fraction (EF %) was deduced. LV mass was calculated from LV long-axis measurements. Fractional shortening (FS %) was calculated using internal LV dimension measurements at end-systole and end-diastole (M-mode). All parameters were normalized by body weight (BW) and all measurements and analysis were performed by an experienced user, blinded to the experimental groups.

Tissue preparation

After 22 weeks, whole heart and vessels were excised and blood was collected for plasma isolation. All samples were stored at 4°C for physiological measurement or at -80°C until further processing for proteomics or RNA measurements. Vessels were cleaned from all fat and surrounding tissue. Samples were either snap frozen or directly used according to the desired experiment.

Histological staining

Samples of LV were fixed in 4% neutral formaldehyde diluted in phosphate-buffered saline and were paraffin embedded. LV samples were then cut into 5µm sections, deparaffined and processed for routine haematoxylin/eosin staining and Sirius red staining.

Briefly, the slides were incubated with a 0.1% Sirius Red solution dissolved in aqueous saturated picric acid for 1 hour, washed in acidified water (0.5% hydrogen chloride), dehydrated and mounted with DPX Mounting. Collagen content was red-stained.

Vascular function evaluation with wire and pressure myographs

Mesenteric arteries rings were mounted on wire (DMT 610M / 620M, Aarhus, Denmark) or pressure myographs. Vessel tension was normalized using standard procedure: arterial segments were stretched progressively to an internal circumference equivalent to 90% of the circumference that vessels would have reached if exposed to 100 mmHg transmural pressure (365).

For pressure myography, mice second branch mesenteric arteries were mounted onto two glass cannulae in the vessel chamber (5mL) of a Living Systems Instruments pressure myograph (Burlington, VT, USA) by knotting nylon strand. Bath was filled with Physiological Saline Solution (PSS) oxygenated with 95% O2 and 5% CO2 maintained at 37°C. The chamber was placed on the stage of an inverted microscope, connected to a pressure column. Vessels were stretched until they appear straight at 125mmHg. Pressure was lowered to 30mmHg and arteries allowed to recover for 25 min. Vessel integrity was assessed with KCl 50mM and rinsed with PSS. All measurements were realized in no flow condition.

For wire myograph, arteries were allowed to equilibrate for 45 min at 37 °C, contracted with KCl 50mM to assess vessel integrity and rinsed with PSS. Total endothelial relaxation was determined by cumulative addition of carbachol (CCh, 1.10^{-8}M to 1.10^{-4}M, 2min per concentration) on vessel pre-contracted with phenylephrine (Phe) (10^{-6}M). NO + prostacyclin (PGI2) relaxation, NO-mediated relaxation or PGI2-mediated relaxation were measured following cumulative addition of CCh on vessel pre-contracted with KCl 50mM alone and/or Nω-nitro-L-arginine methyl ester (L-NAME, 10^{-4}M). The Phe dose-response curve was obtained by cumulative addition of Phe (1.10^{-8}M to 1.10^{-4}M, 2min per dose). After each concentration-response session, vessels were washed with PSS until the tension returned to basal value.

MiRNA Extraction

MiRNA extraction from tissues was performed as previously described (362). Briefly, hearts and aortas of mice were suspended in homogenisation buffer, supplemented with thioglycerol as recommended by the manufacturer. Thioglycerol was also added to plasma samples. Lysis buffer and proteinase K were added to the samples and, after incubation for 10min at room temperature, loaded in the cartridges provided with the kit (AS1460 Promega). Cartridges were previously prepared by adding 10µl of DNase 1. Samples were eluted in nuclease-free water after a processing using the Maxwell RSC Instrument (Promega) for miRNA extraction.

MiRNA reverse transcription and quantitative PCR

Reverse transcription and quantitative polymerase chain reaction (PCR) for miRNAs were performed following the miRCURY® LNA® miRNA PCR Handbook for individual PCR Assay provided by Qiagen. To synthesize first-strand cDNA, RT mix (containing reaction buffer and enzyme mix) was added to 2 µl of RNA sample adjusted to a concentration of 20ng/µL and incubated at 42°C during 1 hour followed by a heat-inactivation of the enzyme at 95°C for 5 min and a cooling at 4°C. Regarding the quantitative PCR, samples were diluted following the manufacturer's recommendations, and 3µl of cDNA were loaded in duplicate into 96-well PCR plates. PCR master mix and PCR primers were added, and temperature cycling was performed in a iQ5 cycler Bio-Rad system following the kit protocol (Qiagen) consisting of a cycle at 95°C during 2min, followed by 40 cycles at 95°C during 10s and 56°C during 1min. Primers used were the following: miR-199a-3p (Qiagen YP00204536), miR-199a-5p (Qiagen YP00204494), U6 (Qiagen YP00203907), and miR-let-7i-5p (Qiagen YP00204394). The latter was used as housekeeping gene for plasma and vessels, following the manufacturer's

recommendations. Neither the U6 nor the miR-let-7i is modulated due to exercise.

MiRNA precursor reverse transcription and quantitative PCR

Reverse transcription and quantitative polymerase chain reaction (PCR) for pre-miRNAs were performed following the miRScript PCR System Handbook for precursor detection provided by Qiagen. To synthesize first-strand cDNA, 1µg of RNA sample was added with RT mix (containing Hiflex reaction buffer and enzyme mix) and incubated at 37°C during 1 hour followed by a heat-inactivation of the enzyme at 95°C for 5 min and a cooling at 4°C. The quantitative PCR, samples were diluted following the manufacturer's recommendations, and 1µl of cDNA were loaded in duplicate into 96-well PCR plates. PCR master mix and PCR primers were added, and temperature cycling was performed in a iQ5 cycler Bio-Rad system following the kit protocol (Qiagen) consisting of a cycle at 95°C during 15min, followed by 45 cycles at 94°C during 15s, 55°C during 30s and 70° during 30sec. Primers used for pre-miR were the following: mir-199a-1 (Qiagen MP00001365), mir-199a-2 (Qiagen MP00001372), and miR-let-7i-5p (Qiagen YP00204394). The latter was used as housekeeping gene for vessels, following the manufacturer's recommendations and was not modified in each condition.

RNA reverse transcription and quantitative PCR

Isolation of total RNAs was performed as described for microRNAs using the same method with Maxwell technology. One microgram of extracted RNA was engaged for first-strand cDNA synthesis. Briefly, a reverse transcription mix containing oligodT, DNTP mix (2,5mM), RNAsin, M-MLV buffer 5X and M-MLV enzyme, was added to the samples. Reaction was performed by heating samples at 42°C during 3 hours, followed by a heat inactivation step at 95°C during 5 min and a cooling step at 4°C. Quantitative PCR was performed on 2µl of cDNA

samples loaded in duplicate into a 96-well PCR plate. A PCR mix containing SYBR Green and primers was added to samples. PCR cycling was performed in an iQ5 cycler Bio-Rad system and consisted of one step at 95°C during 3min, followed by 40 cycles at 95°C during 15sec and 60°C during 30 sec.

Western Blot

Tissues were suspended in RIPA lysis buffer. Protein concentration of each sample was determined by using a Bicinchoninic Acid Protein Assay Kit (Pierce) according to the manufacturer's protocol. Western blot was realized as previously described (362). Briefly, 10µg of protein were loaded per well and underwent migration in migration buffer (Tris-EDTA, SDS, glycine), under a voltage of 120V. Proteins were then transferred on a nitrocellulose membrane with a constant amperage of 350mA during 1h30 in transfer buffer (Tris-base, glycine, SDS, methanol). Membranes were then blocked in TBS (Tris-buffered saline)-Tween 0,1%-BSA 5% for 1 hour at room temperature and incubated overnight at 4°C with primary antibodies diluted in TBS-Tween/BSA 5%. The primary antibodies that were used were the following: anti-phosphoSer1177eNOS (1µl/ml; Millipore, 07-428), anti-phosphoThr308Akt (1µl/ml; Cell Signaling, 2965), anti-eNOS (0,25µg/ml, BD transduction, 610297), anti-Akt (1µl/ml; Cell Signaling, 9272), anti-Twist1 (2µl/ml, Abcam, ab50581), anti-Sirtuin1 (1µl/ml, Cell Signaling, 9475), anti-PGC1α (1µ/ml, Abcam, ab54481), anti-mTOR (1µl/ml, Cell Signaling, 2983) anti-phosphoSer473 Akt (1µl/ml, Cell Signaling, 4060) anti-GAPDH (0,1µl/ml; Cell Signaling, 2118) and anti-βactin (0.02µl/ml, Sigma-Aldrich, A5441). After washing in TBS-Tween, peroxidase-conjugated secondary antibody was incubated during 1 hour at room temperature and developed by enhanced chemiluminescence (ECL, Amersham) on CL-Xposure film (Thermo Fisher Scientific). Films were scanned and protein bands were quantified by densitometry using the ImageJ software (National Institutes of Health [NIH]). Levels of all proteins of interest were

normalized to the housekeeping proteins β-actin for vessels or GAPDH for heart tissue. The levels of phosphorylated proteins were normalized to the level of total proteins.

Cell culture

Bovine aortic endothelial cells (BAEC) were purchased by Cell Applications Inc and cultured on 0.2% gelatin-coated dishes with Dulbecco's Modified Medium Eagle Medium (DMEM) (Thermo Fisher Scientific) containing glucose, sodium pyruvate and GutaMAX supplemented with 10% FBS and 1% penicillin/streptomycin. Cells were used between passage 4 and 8 for the experiments, in order to avoid dedifferentiation.

Laminar shear stress

BAEC were seeded at 3.0 x105 on µ-Slides I0.4 luer (Ibidi GmbH) and allowed to adhere for 2 hours. Cells were exposed either to no shear stress (static condition), or to a high laminar shear stress (HSS) started at 5 dynes/cm² and increased every 30 min by 5 dyne/cm² until reaching 20 dynes/cm². Media flow rate was maintained by a peristaltic pump for 48h in a humidified atmosphere at 37°C containing 5% CO2. Luer µ-slides were connected in series with a maximum of 3 at the same time. Immunofluorescence or microRNA extractions were performed on the slides.

Immunofluorescence

Following shear stress, BAECs were washed with PBS and fixed with PFA 4% for 10 min at room temperature (RT). Primary antibodies for eNOS (5µg/ml, BD Biosciences, 610297) and phosphoS1177 eNOS (10µl/ml, Abcam, 184154) were incubated overnight at 4°C. Cells were then incubated for 1 hour at RT with secondary antibodies including an Alexa Fluor 488-conjugated goat anti-mouse (8µg/ml, InVitrogen, A11029), an Alexa Fluor 568-conjugated goat anti-rabbit

(8µg/ml, InVitrogen, A11036) and phalloidin (3,3µl/ml, Far-Red Phalloidin, Thermo Fisher Scientific, A22287). Nuclear staining was performed with DAPI (1/1000) for 5 min at RT. Ibidi mounting media (50001, Ibidi) was dropped into channels for confocal microscopy. Pictures were captured with a confocal fluorescent microscope LSM510-Meta Multiphoton Zeiss using a 25x zoom lens.

MiRNA reverse transcription and quantitative PCR on cells

MiRNA extraction for shear stress studies was performed following the manufacturer's guidelines. Briefly, cells were washed twice with PBS, and 100µl of homogenization buffer (added with thioglycerol) from Maxwell RSC miRNA tissue kit (AS1460 Promega) were dropped into the channels. Cells were detached from the channels by repeatedly moving the plunger up and down in a 1ml syringe. End of miR extraction, reverse transcription and quantitative polymerase chain reaction (PCR) for miR were performed as described above.

Statistics

All experiments were reproduced at least three times. All data are expressed as the Mean±SEM. Shapiro-Wilk normality test was performed, and statistically significant differences were determined using a 2-way ANOVA with subsequent Bonferroni's post-hoc analysis test. For two groups' comparison, t-test student was used for parametric data or Mann-Whitney test for nonparametric data. $P<0.05$ was considered statistically significant.

Results

Voluntary wheel running engages mice to perform chronic exercise and modulates body weight gain

Five-week-old male C57BL6/J mice were placed in cages with free access to a running wheel for a period of 22 weeks. Daily average running distance increased during the first weeks reaching a peak at week 4 (7.17 ± 0.66 km) followed by a gradual decline until week 10 as previously described for male mice (366). From this time point, the mean covered distance did not show any significant variations until the end of the protocol, amounting 3.30 ± 0.21 km per 24 hours (Figure 30A).

From week 10 and at all time points until the end of the protocol (week 22), running mice gained significantly less body weight than their sedentary counterparts (Sed: 33.44 ± 0.40 g [n=10] vs. Run: 29.19 ± 0.64 g [n=8], $P<0.001$) (Figure 30B).

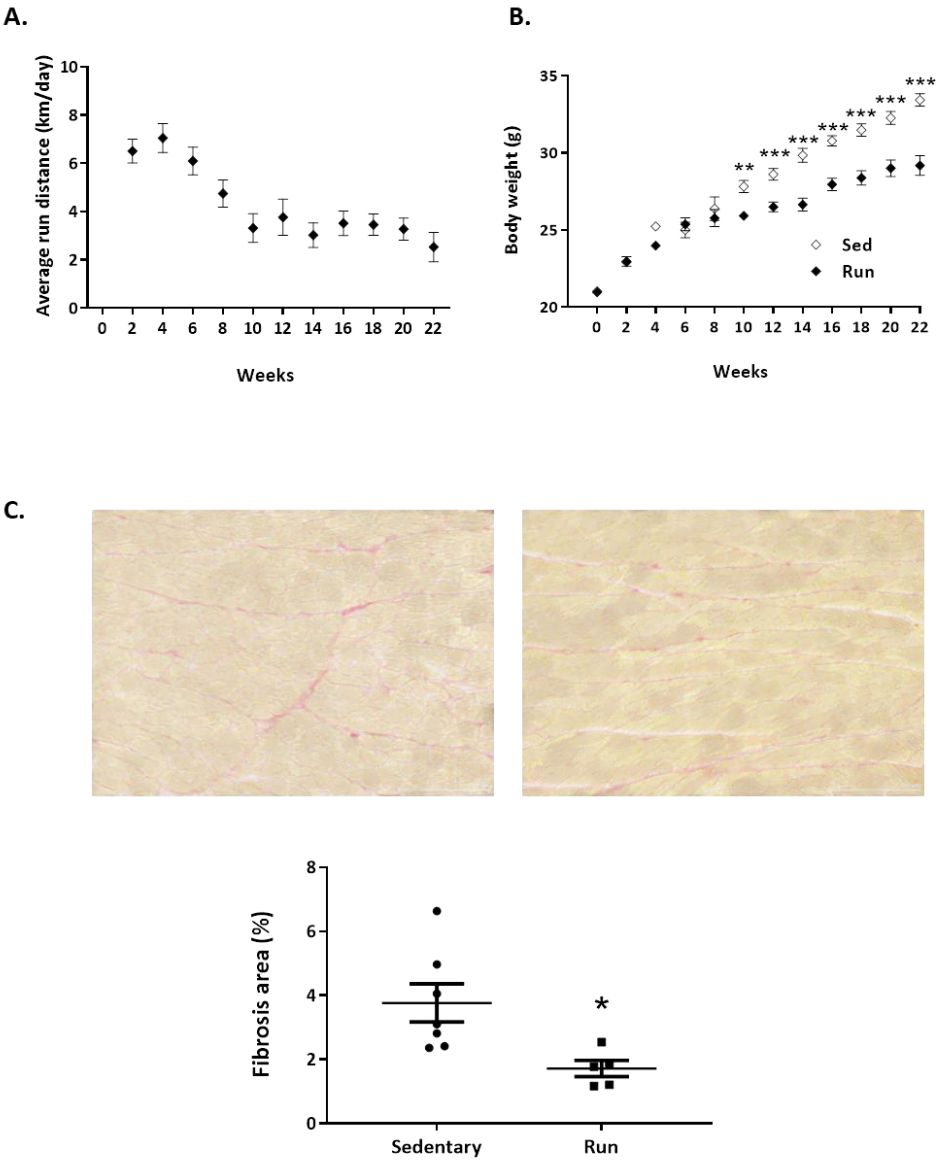

Figure 30: Mice were allowed to voluntary exercise in running wheels during 22 weeks Mechanical counters were attached to the wheels to measure distance covered (A). Evolution of body weight of animals during the exercise period (B). Results are expressed as mean ± SEM of 13 animals per group. Heart isolated from running mice develops less fibrosis. Fibrosis was evaluated by Sirius red staining on histological slides and quantified (C). Results are expressed as mean ± SEM of at least 5 animals. *, P.<0.05 , **P.<0,01 and ***, P.<0,001 vs. sedentary mice

Chronic exercise by voluntary wheel running promotes physiological cardiac hypertrophy and reduces cardiac fibrosis

Adaptation of the cardiac muscle to chronic exercise was evaluated by echocardiography throughout the training period. As BW differed substantially between active and sedentary mice ($p<0.001$), cardiac morphometric parameters were normalized to BW of corresponding animals (Table 3). The normalized myocardial thickness of the intraventricular septum (IVS) in systole ($p<0.01$ and $p<0.001$) and diastole ($p<0.001$ and $p<0.01$), as well as myocardial thickness of LV posterior wall (LVPW) in systole ($p<0.05$ and $p<0.01$) were significantly increased in running mice both at 14 and 22 weeks, compared to controls, while the normalized LVPW in diastole was found to be increased only at 14 weeks ($p<0.01$) in the running group. This result is consistent with a robustly increased LV mass/BW ratio at 14 weeks ($p<0.05$), however there is only a trend for increased ratio at 22 weeks. No differences were detected relating to the BW-normalized end diastolic (LVvol d) and end systolic volumes (LVvol s) between the sedentary and running groups, although at 14 weeks there was a strong trend for the BW-normalized diastolic LVvol in the Run group. In line with this, the BW-normalized LV internal dimension in diastole (LVID d) was moderately increased in the running mice at week 14 and week 22 ($p<0.05$), compared to sedentary mice. On the other hand, the normalized ejection fraction (EF/BW) and the normalized fractional shortening (FS/BW) were significantly different between the sedentary and running mice only at 14 weeks ($p<0.01$), but they were restored at 22 weeks, suggesting a reversibility of the beneficial effects of exercise between the 14 and 22 week time-points (Table 3).

		Baseline (week 0)			Week 14			Week 22		
Parameter	Units	Sed	Run	p-value	Sed	Run	p-value	Sed	Run	p-value
B-mode (2D)										
LVvol d / BW	ul/g	2,641 ± 0,262	2,559 ± 0,110	0,745	1,979 ± 0,115	2,201 ± 0,157	0,297	1,785 ± 0,069	1,761 ± 0,195	0,882
LVvol s / BW	ul/g	1,129 ± 0,232	1,387 ± 0,058	0,216	1,079 ± 0,073	1,078 ± 0,053	0,995	0,927 ± 0,063	0,971 ± 0,184	0,776
EF / BW	%/g	2,766 ± 0,334	2,605 ± 0,146	0,624	1,509 ± 0,066	1,962 ± 0,072	0,006**	1,412 ± 0,106	1,856 ± 0,215	0,059
LV mass / BW	mg/g	4,538 ± 0,094	4,388 ± 0,213	0,627	3,832 ± 0,159	4,577 ± 0,175	0,019*	3,462 ± 0,142	3,748 ± 0,240	0,303
HR	bpm	426,233 ± 7,719	422,244 ± 3,871	0,621	439,258 ± 7,424	466,630 ± 10,046	0,052	446,960 ± 15,028	475,178 ± 20,452	0,286
M-mode										
IVSd / BW	mm/g	0,037 ± 0,001	0,033 ± 0,001	0,051	0,027 ± 0,001	0,032 ± 0,0005	0,001***	0,025 ± 0,001	0,030 ± 0,001	0,004**
IVSs / BW	mm/g	0,049 ± 0,002	0,040 ± 0,002	0,027*	0,033 ± 0,001	0,040 ± 0,002	0,006**	0,032 ± 0,001	0,040 ± 0,001	0,0001***
LVIDd / BW	mm/g	0,174 ± 0,008	0,184 ± 0,003	0,201	0,131 ± 0,004	0,148 ± 0,004	0,02*	0,114 ± 0,002	0,127 ± 0,005	0,0125*
LVIDs / BW	mm/g	0,120 ± 0,012	0,132 ± 0,005	0,326	0,102 ± 0,004	0,109 ± 0,005	0,257	0,087 ± 0,003	0,092 ± 0,007	0,367
LVPWd / BW	mm/g	0,034 ± 0,001	0,033 ± 0,001	0,346	0,026 ± 0,001	0,031 ± 0,0005	0,002**	0,025 ± 0,001	0,027 ± 0,001	0,115
LVPWs / BW	mm/g	0,046 ± 0,002	0,045 ± 0,001	0,827	0,033 ± 0,001	0,037 ± 0,001	0,033*	0,031 ± 0,001	0,036 ± 0,002	0,01**
FS/BW	%/g	1,459 ± 0,221	1,339 ± 0,208	0,579	0,743 ± 0,038	0,993 ± 0,044	0,009**	0,707 ± 0,072	0,952 ± 0,140	0,109

Table 3: Cardiac echocardiographic parameters from sedentary and exercised mice normalized to body weight. Values are mean ± SEM. Sed n=8, Run n=7. EF, ejection fraction; FS, fractional shortening; LVvol d, left ventricular end-diastolic volume; LVvol s, left ventricular end-systolic volume; IVS d, interventricular septal thickness in diastole; IVS s, interventricular septal thickness in systole; LVID d, left ventricular internal dimension in diastole; LVID s, left ventricular internal dimension in systole; LVPW d, left ventricular posterior wall thickness in diastole; LVPW s, left ventricular posterior wall thickness in systole; BW, bodyweight. Presented data related to mice for which the heart rate was strictly within the 400 to 600 bpm range, although the same trends were observed taking into account the whole population. *p<0.05, **p<0.01 and ***p<0.001, compared with age-matched controls, t-test student.

Cardiac adaptation to increased workload may also implicate gene reprogramming. Voluntary wheel running for 22 weeks led to substantially increased messenger RNA (mRNA) levels of natriuretic peptides, ANP and BNP (Figure 31A and 31B, respectively). Neither the mRNA the ratio between adult (myh6) vs. fetal (myh7) myosin heavy chain mRNA levels, nor the mRNA expression for the calcium handling protein sarco/endoplasmic reticulum Ca2+-ATPase (SERCA2), were modulated by our protocol of chronic mild exercise (Figure 31C-D).

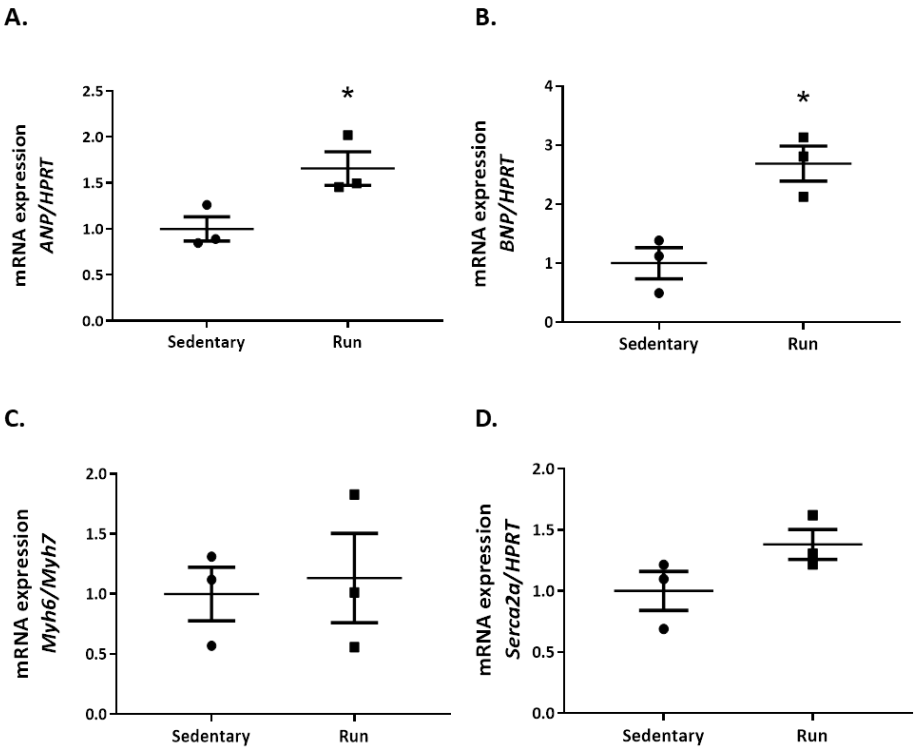

Figure 31: Cardiac tissues isolated from running mice present no fetal genes reprogramming. *ANP* (A), *BNP* (B)*, Myh6, Myh7* (C) and *Serca2a* (D). mRNAs levels were measured by using RT-qPCR and normalized by *HPRT* expression. Results are expressed as mean ± SEM of 3 animals. *, *P.*<0.05 vs. sedentary mice

Sirius red staining of collagen fibres in LV sections revealed a slight but significant fibrosis development in control mice, probably associated with aging in a context of sedentarity as it was prevented in running mice (Figure 30C).

Chronic exercise by voluntary wheel running improves endothelial function

At the time of sacrifice, mesenteric arteries were collected from animals, cleaned and mounted on pressure and wire myographs for vascular function evaluation. External vessel diameter, wall thickness, media/lumen ratio, cross sectional area and vessel distensibility (Figure 32A-E respectively) were comparable in vessels from trained and sedentary animals, attesting the absence of significant vascular remodeling in the course of our training protocol.

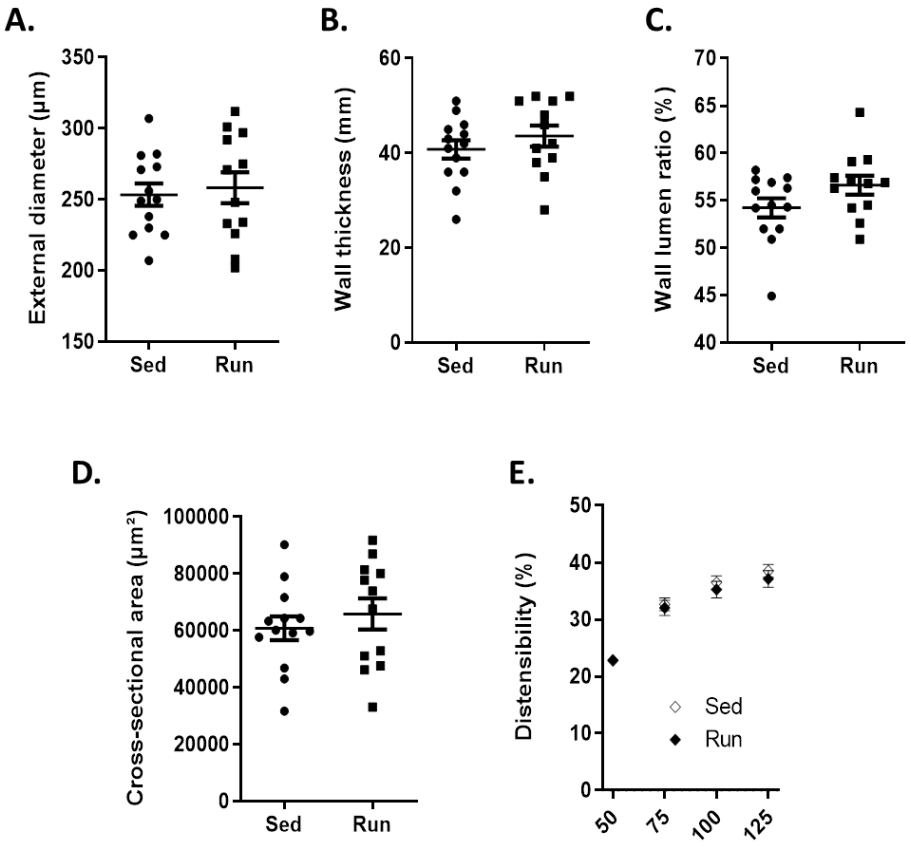

Figure 32: Running mice do not present vascular remodeling compared to sedentary mice. Measures were realized at constant internal pressure of 30mmHg, with no flow. (A) External diameter of arteries in µm. (B) Wall thickness of arteries measured in µm. (C) Wall lumen ratio expressed as %. (D) Vessel cross-sectional area given in µm². (E) Distensibility of arteries measured as %. Sed N=13, Run N=11.

Second order mesenteric arteries where challenged with high KCl 50mM solution. At the contraction plateau, relaxation to CCh was measured. Note that the smooth muscle cell depolarization evoked by this mode of contraction prevented any manifestation of endothelium-dependent hyperpolarization. Surprisingly, the total relaxation (NO- and PGI2-dependent) did not differ between vessels from sedentary and active mice (Figure 33A).

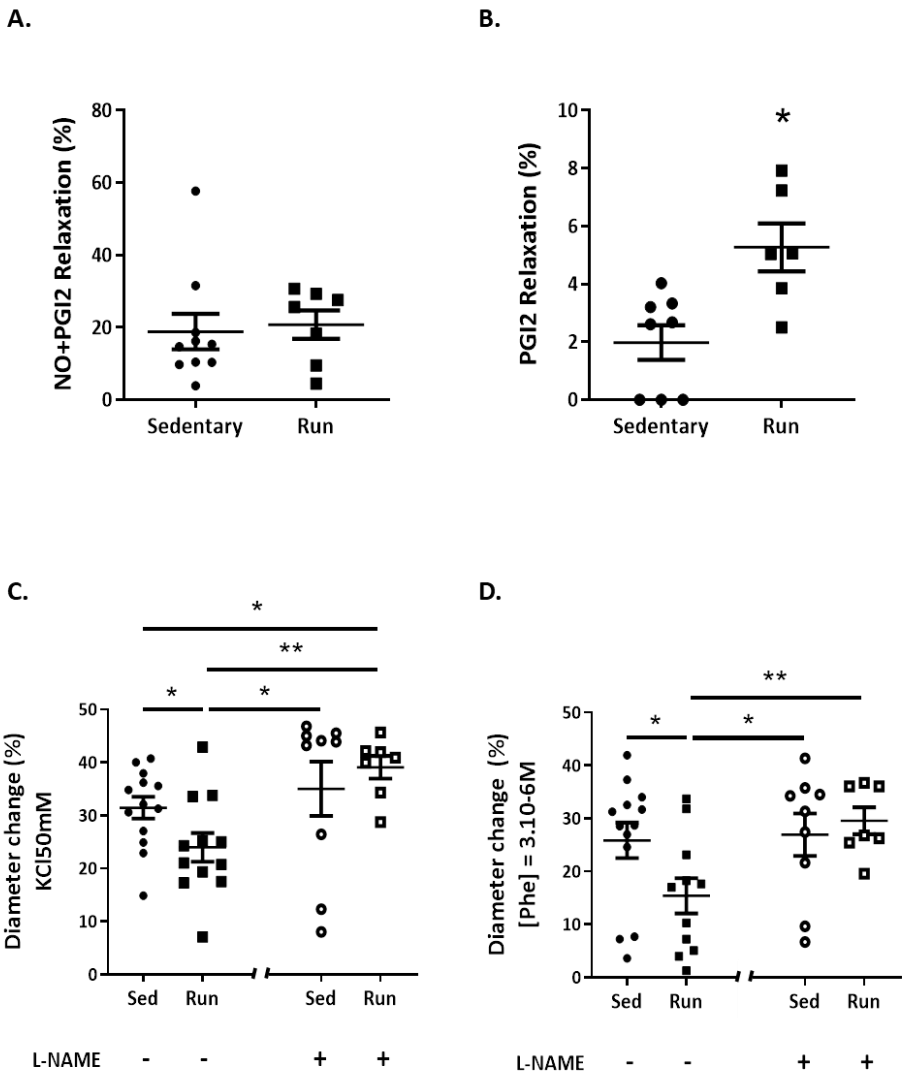

Figure 33: Exercise improves endothelial function. NO and PGI2 mediated relaxation evoked by carbachol was measured on mesenteric arteries using wire myograph (A). PGI2 mediated relaxation evoked by carbachol was measured on mesenteric arteries in presence of 0.1mmol/L L-NAME (B). Contraction of mesenteric vessels in response to depolarization with KCl 50mM (C) or in response to 3µmol/L phenylephrine (D) was measured in presence or absence of L-NAME (0.1mmol/L) using a pressure myograph. Results are expressed as mean ± SEM *, P.<0.05, **, P. <0.01.

Interestingly, the contraction to KCl (Figure 33C) (but also to Phe as illustrated in Figure 33D) was significantly reduced in mesenteric arteries from running animals. Pre-treatment of vessels with L-NAME increased the contractile response and completely abrogated the difference between vessels from running and sedentary animals (Figure 33C-D). This finding demonstrates that chronic exercise is associated with improved basal endothelial function and NO production, promoted by increased shear stress. Also, when the challenge with CCh was repeated in the presence of L-NAME, a statistically increased PGI2-dependent relaxation was also revealed (Figure 33B). Exercise has been previously shown to enhance myogenic constriction in rat soleus muscle arterioles (367). Contrary to the blunted contraction observed with Phe (3µmol/L) or KCl (50mM) in exercised animals, no difference emerged out of our murine model for myogenic response at physiologically relevant internal pressures (Figure 34).

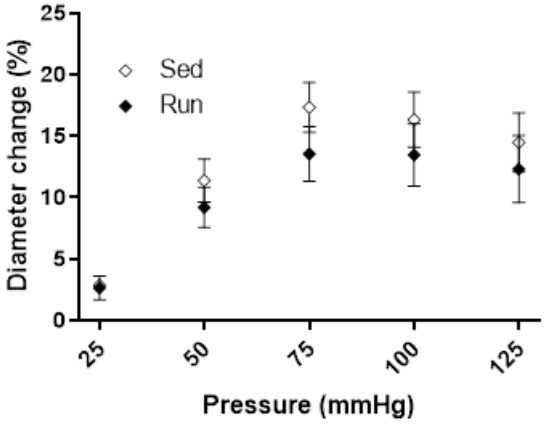

Figure 34: Myogenic response of vessels from running mice do not present any difference compared to sedentary condition at physiologically relevant internal pressure. Measures were realized using a pressure myograph at constant internal pressure of 30mmHg, with no flow. Myogenic tone was induced by increasing intraluminal pressure for the development of myogenic response. Sed N=13, Run N=11

Chronic exercise by voluntary wheel running decreases microRNAs 199a-3p and 199a-5p expression in cardiovascular tissue

We and others have described that pathological LV hypertrophy is associated with an up-regulation of miR-199a expression, i.e. in response to abdominal aortic constriction (308) or angiotensin infusion, in the heart and isolated aorta (362). We thought therefore to evaluate the regulation of both mature strands of miR-199a in the context of a more physiological cardiac hypertrophy. The expression of the mature forms of miR-199a, miR-199a-3p and miR-199a-5p was measured in LV samples from active and sedentary mice. Interestingly, a significant down-regulation of both miRs was observed in cardiac tissue of running mice, compared to extracts from sedentary animals (Figure 35A-B), suggesting a differential regulation in physiological vs. pathological cardiac hypertrophy.

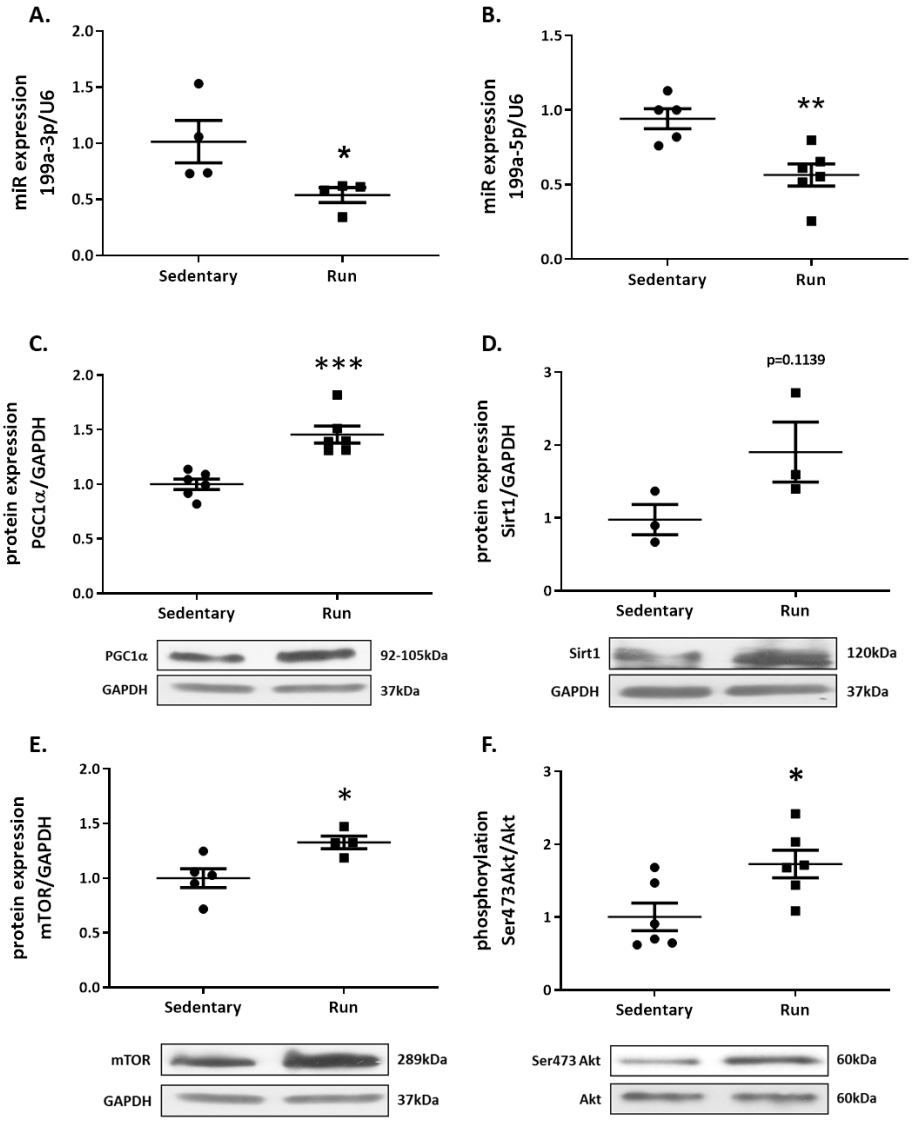

Figure 35: Hearts isolated from running mice exhibit decreased microRNAs 199a expression. MiR-199a-3p and miR-199a-5p levels were measured in hearts using RT-qPCR (A-B). Protein expression levels of PGC1a, Sirt1 and mTOR (C-E) and phosphorylation of Akt (F) were detected by Western Blotting and quantified. Results are expressed as mean ± SEM of 3-6 animals. *, P.<0.05,**; P.<0.01 and ***, P.< 0,001 vs. sedentary mice.

Similarly, a significant decline of miR-199a-3p and -5p expression was observed when mesenteric (Figure 36A-B) and aortic samples were processed (Figure 37A-B).

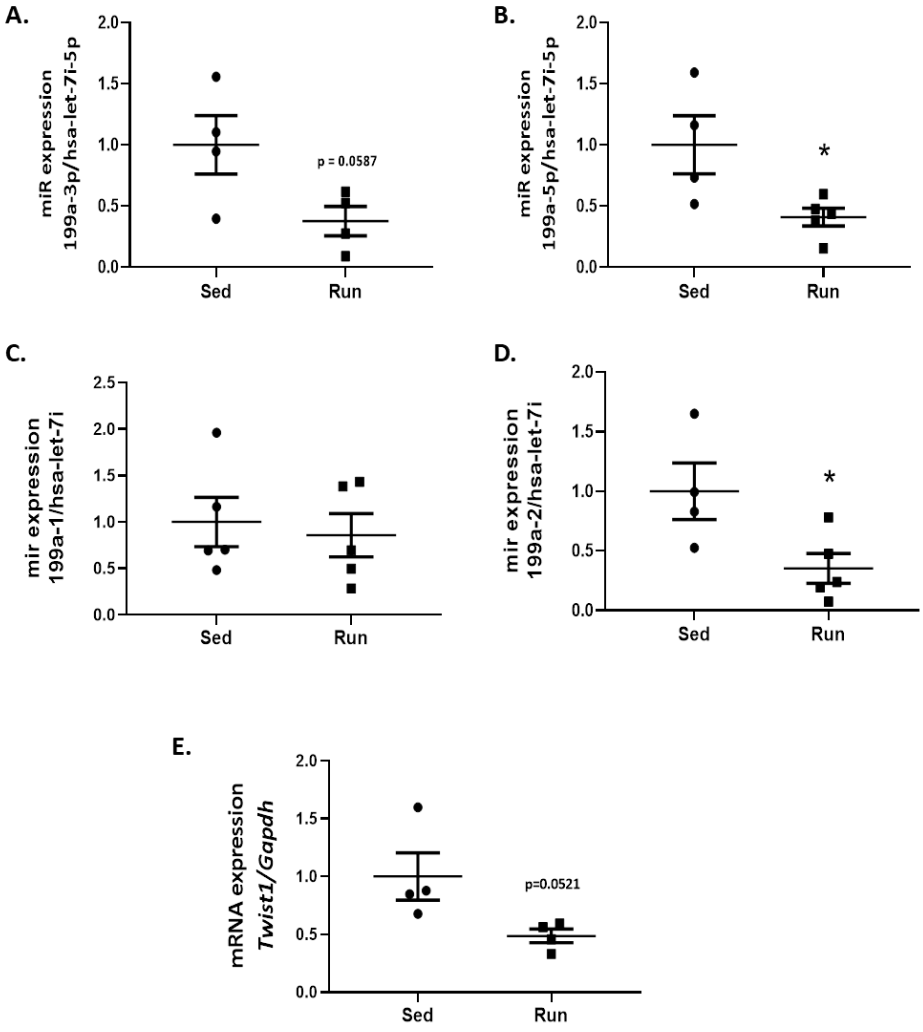

Figure 36: Mesenteric arteries isolated from running mice exhibit decreased microRNAs 199a expression and miR deregulation is induced by Twist1. MiR-199a-3p, miR-199a-5p, (A-B), premiR-199a (C-D) and Twist1 expression (E) were measured in vessels using RT-qPCR. Results are expressed as mean ± SEM of 4-5 animals. *, *P.*<0.05 vs. sedentary mice.

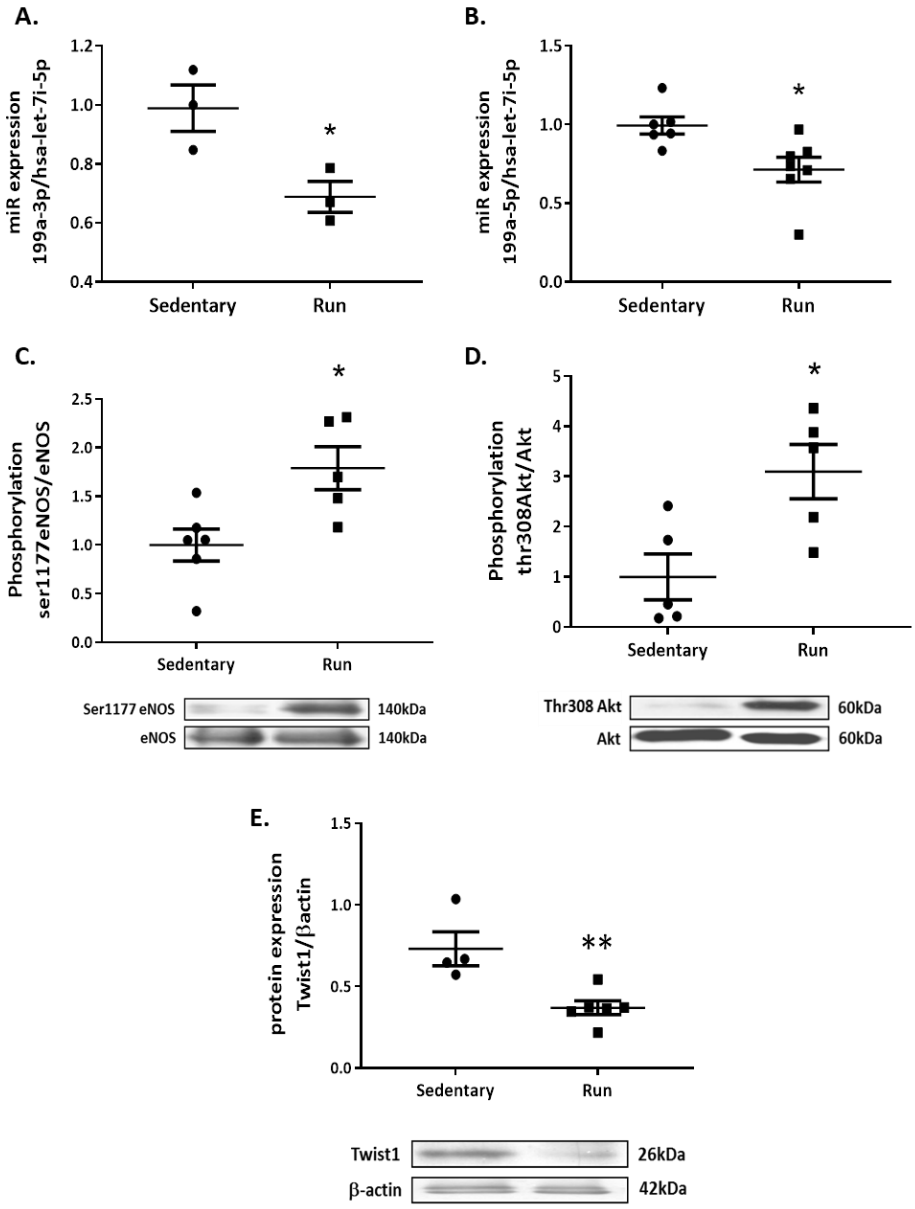

Figure 37: Aorta isolated from running mice exhibit decreased microRNAs 199a expression and an increased endothelial function. MiR-199a-3p, miR-199a-5p were measured in vessels using RT-qPCR (A-B and F). Phosphorylation of eNOS and Akt (C-D) and expression of Twist1 (E) were detected by Western Blotting and quantified. Results are expressed as mean ± SEM of 3-6 animals. *, *P.*<0.05 and **, *P.*<0.01 vs. sedentary mice.

In mesenteric arteries, a reduced expression of pre-miR 199a-2 but not 199a-1 (Figure 36C-D) was also pointed out. These results are in line with a context of improved endothelial function. Interestingly, miR-199a-5p was the sole form to appear dysregulated by exercise in plasma samples (Figure 38B).

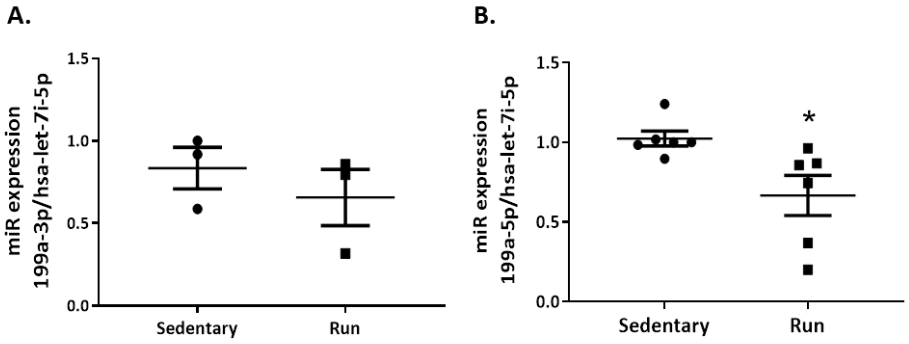

Figure 38: Plasma isolated from running mice exhibits decreased microRNAs 199a-5p expression compared to sedentary mice. Mice were allowed or not to voluntary wheel running during 22 weeks. MiR-199a-3p and miR-199a-5p were measured in plasma using RT-qPCR (A-B). Results are expressed as mean ± SEM of 5 animals. *, P.<0.05 vs. sedentary mice.

Chronic exercise by voluntary wheel running increases the expression of known miR-199a targets in cardiac and vascular tissues

From the list of signaling proteins described as actors of cardiac adaptation to exercise, we know from *in silico* analysis and other studies (292;303;345;368) that PGC1α, Sirt-1, and mammalian Target of Rapamycin (mTOR) are direct targets of miR-199a. Figures 35C-E show that accordingly our model of chronic exercise is associated with a significant up-regulation of PGC1α and mTOR expression and a non-significant trend for Sirt-1 expression. Interestingly in cardiac tissues, Akt expression is not modulated by exercise but its mTOR-dependent phosphorylation on serine473 is enhanced in running mice, compared to their sedentary counterparts, as observed in Figure 35F.

We next evaluated direct and indirect targets of miR-199a in vascular samples among them Ser1177 phosphorylated eNOS and Akt. As shown in Figure 37C, eNOS phosphorylation was robustly enhanced in aortas of running mice, compared to sedentary mice aortas. This is correlated with an increased activity of the PI3K/Akt pathway measured through the phosphorylation of Akt on its Thr308 site (Figure 37D).

Chronic exercise by voluntary wheel running represses the transcription factor TWIST-1 in vascular tissues

The transcription factor Twist-1 has been acknowledged as a driver for the expression of a 7.9-kb noncoding RNA transcript (from the Dynamin-3 gene intron) that encodes miR-199a and miR-214 cluster (266). Our results showed that Twist-1 mRNA (as measured in mesenteric extracts, see Figure 36E) and Twist-1 protein expression (as measured in aorta see Figure 37E) was reduced when samples originated from running mice in comparison to sedentary controls. Accordingly, miR-214 showed a decreased expression in mesenteric and aortas extracts (Figure 39A-B).

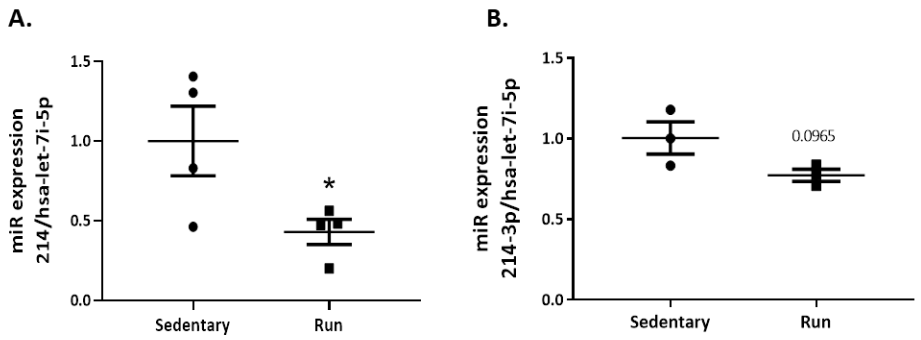

Figure 39: Vessels isolated from running mice exhibit a decrease of miR-214. Mice were allowed or not to voluntary wheel running during 22 weeks. MiR-214-3p was measured in mesenteric arteries (A) and aortas (B) using RT-qPCR. Results are expressed as mean ± SEM of 3 animals.

Shear stress down-regulates miR-199a expression in cultured endothelial cells

Exercise is known to exert major effects on the vasculature through the impact of repetitive exposure to hemodynamic stimuli, such as transmural pressure and shear stress. In order to evaluate whether shear forces modulation is the drive for miR-199a regulation in the endothelium, we mimicked exercise associated shear stress *in vitro* by exposing endothelial cells cultured on µ-Slides I0.4 luer (IBIDI GmbH to increased shear stress *in vitro*). When exposed to laminar shear stress, cultured bovine ECs aligned with the flow, as illustrated in Figure 40A. As expected, expression of proteins reflecting improved endothelial function, as eNOS and S1177eNOS, was up-regulated. Interestingly, as observed *in vivo*, expression of miR-199a-3p and -5p and Twist1 was significantly reduced in BAECs exposed to 20 dynes compared to static condition (Figure 40B-D).

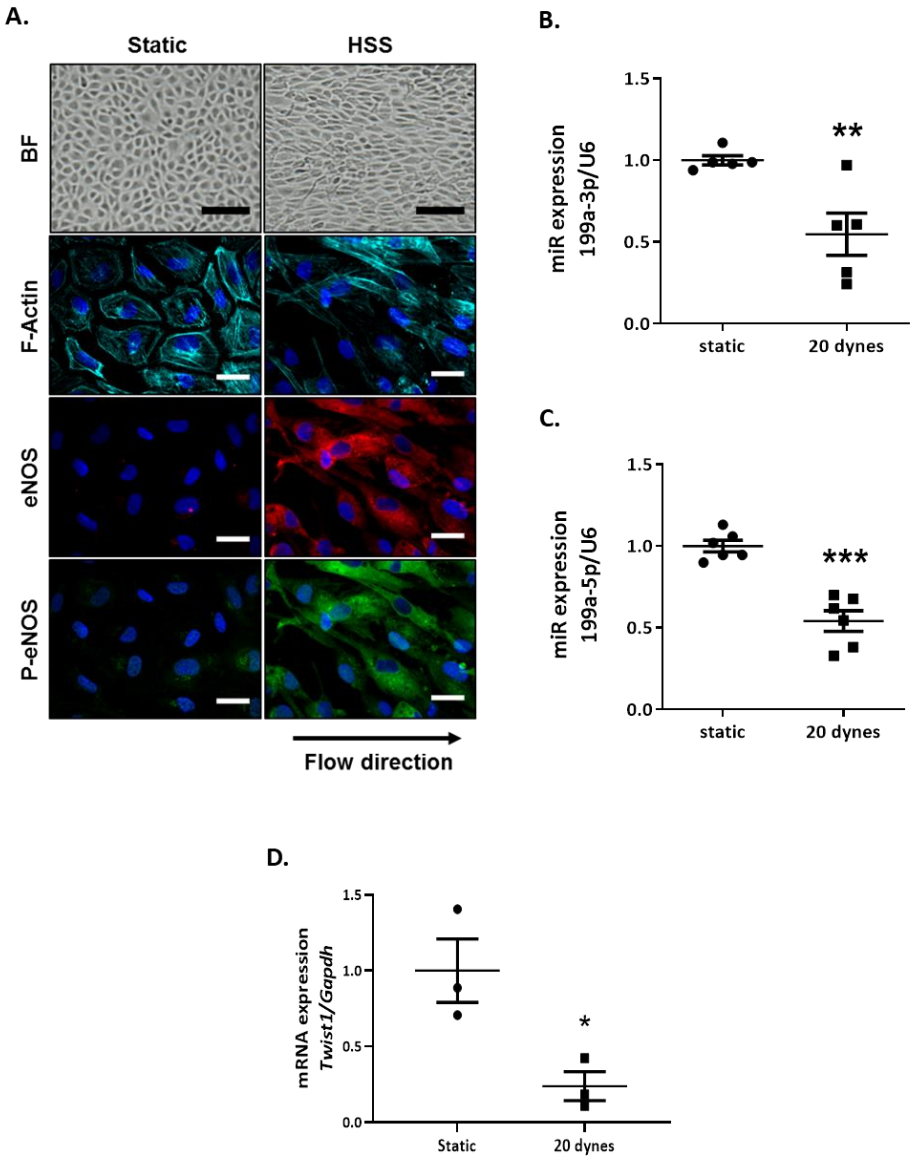

Figure 40: Endothelial cells undergoing shear stress exhibit a decreased miR-199a-3p and miR-199a-5p expression compared to static condition. Bovine aortic endothelial cells (BAEC) were grown on Ibidy® cell plates and submitted or not to shear stress (20 dynes/cm^2). MiR-199a-3p, miR-199a-5p and Twist1 expressions were measured in BAEC using RT-qPCR (B-D). Results are expressed as mean ± SEM of 5 individual experiments. *, *P.*<0,05; **, *P.*<0.01 and ***, *P.*<0,001 vs. static condition. Scales are 25µm for IF and 100 µm for bright field (BF)

Discussion

The Ancient Greek physician Hippocrates (460-377 BC) already recognized exercise as a factor of balance "between the force that one spends and that which one absorbs". Since a few decades, molecular justifications to this seminal observation accumulate. In this study, we developed a murine model of chronic mild exercise and evaluated whether changes in miR-199a abundance could account for cardiac and vascular adaptation to exercise. Our previous work has revealed miR-199a as a key regulator of endothelial function (362), and with this study we position miR-199a at the crossroad between CV health and diseases.

Our study shows that voluntary wheel running for up to 22 weeks evoked positive adaptations of both cardiac and vascular tissues which correlated with a modulation of miR-199a family members' expression. The first observation that this protocol of mild exercise was associated with a beneficial modulation of the CV system reinforces the message physicians hammer to their patients that in terms of physical activity, less is already better than none. Numerous studies have shown that the aging heart undergoes fibrotic remodeling with accumulation of collagen, leading to progressive increase in ventricular stiffness and impaired diastolic function. Similarly, intense exercise was shown to promote cardiac deterioration and myocardial fibrosis. Our program of voluntary physical activity induces a slight cardiac hypertrophy compared to sedentary mice and prevents fibrosis development in the heart of running mice, both characteristics commonly observed in the context of the so called "physiological cardiac hypertrophy" (369). Although the picture is clear in humans (370), the literature is quite inconsistent as regards to exercise-induced hypertrophic growth effects in rodents. While some groups demonstrated significant adaptations of the cardiac architecture (371), others reported that exercise training promoted very moderate or even no structural changes (372), correlated with an absence of adaptation of cardiac

function as assessed by echography (372). Types, duration and intensity of exercise training (373), species and genetic background (374) could pertain for these discordant observations.

In agreement with Kemi et al. we demonstrate that the systolic parameters of LVPW and IVS are significantly augmented following long-term exercise (371). This finding also agrees with the study of Bellafiore et al. where IVS and LVPW are shown to be substantially augmented following 15, 30 and 45 days of endurance exercise (high intensity), although the study failed to demonstrate an associated myocyte hypertrophy (change on number or size) to explain such differences (375). Interestingly, while we observed a clear beneficial effect on the normalized EF, FS and LV internal dimension in diastole at 14 weeks in the Run group, this effect is reduced in the end of the protocol at 22 weeks concurring more with previous findings about exercise training (short-term and more long-term as in our protocol) (372;376;377). We should however keep in mind that relief of physiological stimuli, like reduced exercise, promotes a reversibility of CV beneficial effects (129) and points to the substantial drop in physical effort demonstrated by our running mice after the first 3 weeks of intense activity. The change of running pattern with time was already described in C57bl6 mice (364;366), it probably accounts for the attenuated benefits on cardiac function.

The absence of a shift from α- (the adult form) to β-MHC isoform (the fetal form) and the absence of modulation of SERCA2a expression, confirmed that the contractile properties of the hearts are not negatively altered as classically observed in the heart of animal models and humans showing pathological cardiac hypertrophy (378). More ambiguously, the natriuretic peptides ANP and BNP have been often reported as unchanged or up-regulated in the heart of running mice (129). However, a transient up-regulation of ANP and BNP directly following exercise has already been described (379;380), which is consistent with the short

delay between nocturnal mice activity periods and the time of sacrifice in our setting.

To our knowledge, this is the first time that a down-regulation of miR-199a-3p and -5p is highlighted in cardiac (and vascular) tissue of mice submitted to a protocol of chronic exercise and exhibiting physiological hypertrophy. This observation is in dramatic contrast with what is observed in pathological cardiac hypertrophy. Indeed, miR-199a has been repeatedly shown to be up-regulated in pressure-overloaded hypertrophic hearts (309) following aortic banding (308) or angiotensin infusion (362). Molecular targets and signaling consequences of increased miR-199a expression in the heart are manifold. The miR-199a/214 cluster represses cardiac PPARδ expression, facilitating a metabolic shift from predominant reliance on fatty acid utilization in the healthy myocardium toward increased reliance on glucose metabolism at the onset of heart failure (41). Cardiomyocyte-specific miR-199a overexpression was likewise proposed to induce cardiac hypertrophy and heart failure by inhibiting autophagy, through an activation of mTOR complex signaling. In line with these results, our model of chronic mild exercise exhibits a down-regulation of miR-199a and a promotion of mTOR expression and Akt activation, both well-known targets of miR-199a. Together with the observed modulation of PGC-1α, our results agree with the previous work of Li et al. that used a cardiomyocyte-specific miR-sponge to repress miR-199a and showed that a 20-30% down-regulation of miR-199a in cardiomyocytes promotes a physiological cardiac hypertrophy linked with increased Akt and PGC-1α expression (314). The up-regulation of PGC1α is critical as it is recognized as a major regulator of cardiomyocyte metabolism, with a particularly dramatic impact on mitochondrial biogenesis (381). Consistently with a differential regulation of miR-199a in pathological versus physiological

hypertrophy, exercise activates PGC1α in the heart, whereas its activity is downregulated in pathological conditions (156).

Our previous work has identified miR-199a-3p and 5p at the center of a redundant network of regulation in the endothelium repressing eNOS activity and NO availability (362). Our current results are in total agreement with what we observed previously when blocking miR-199a-3p/5p in cultured endothelial cells, or by *in vivo* modulation of each mature strands of the miR-199a family by an antagomiR strategy. miR-199a-3p/5p repression promotes NO bioavailability, NO-dependent relaxation and increased NO circulation in the blood of treated mice (362). Here, we show that a physiological down-regulation of miR-199a-3p/-5p by chronic wheel running also promotes endothelial function in form of NO-dependent buffering of the contractile response. In agreement with our work (362), previously identified molecular targets of miR-199a-3p and/or -5p were upregulated following exercise, improving eNOS activity. Our results also agree with numerous studies showing that vessels contraction of exercising mice is blunted in a NO-dependent manner (382). Interestingly, the miR-199a down-regulation in vascular tissues correlates with a larger prostacyclin dependent relaxation. Although this could not be quantified in our study due to a lack of samples, this agrees with Cyclooxygenase 2 (COX2) being a direct target of miR-199a-5p and points towards a multiplicity of mechanisms that cooperate to enhance the ability of the circulation to deliver the required supply of oxygen to heart and muscles during exercise. Our previous work has also identified VEGF-A as a direct and indirect target of miR-199a-5p in the endothelium (362). VEGF-A is critical in the adaptive processes to balance capillary density with oxygen needs, a mechanism also deficient in pathological cardiac hypertrophy. In this study, we could however not demonstrate a significant increase in capillary density (not shown).

Vessels from running mice exhibited a repressed expression of the transcription factor Twist1, a well-known regulator of miR-199a expression (286). Mahmoud et al. have highlighted that Twist1 expression is increased at low shear stress region and can promote atherosclerosis (318), pointing out shear forces as a potential driver of miR-199a expression regulation. In agreement, exposure of BAECs to laminar shear stress is sufficient to reduce expression of both mature forms of miR-199a to less than a third of their expression in no-flow conditions. Our data reinforce an earlier demonstration from Heuslein et al. showing that miR-199a-5p was down-regulated by biomimetic flow waveform. We found that both strands of the miR were co-regulated following shear stress in ECs and chronic mild exercise in mouse vessels. Together with the observation that miR-214 expression, produced in cluster with miR-199a (286) and their precursor mir-199a-2 were also repressed in the vascular wall, this confirms a transcriptional regulation versus a modulation of miR-199a-3p/5p stability in response to shear forces. Both mature forms of miRs-199a were also significantly expressed and regulated in mouse heart extracts following our protocol of exercise training. Our unpublished work and work from others have clearly identified a significant expression of miR-199a in isolated cardiomyocytes (304;308). However, at this point, it is still not clear if the exercise-driven regulation of miR-199a production is restricted to endothelial cells or whether cardiomyocyte-specific miR production is also altered during physical training. This would warrant further investigation. At this stage, the mode of regulation of miR-199a in cardiomyocytes remains speculative following physical training. In the context of pathological hypertrophy, up-regulation of the miR cluster 199a/214 has been attributed to HIF-1α (41). This hypothesis is irreconcilable with our results. An up-regulation of HiF-1α has been constantly associated with intense exercise, while a down-regulation of miR-199a was constantly observed in our model of exercise. Incidentally, HIF-1α is one of

the first targets of miR-199a identified in cardiac tissues (303). Also, in skeletal muscle, exercise training upregulates PGC1α and stimulates VEGF expression, independently of the HIF1α pathway (383).

Taken together, our results indicate that chronic mild exercise positive regulation of cardiac and endothelial functions is associated with a modulation of miR-199a expression. MiR-199a family members have to be added to the list of miRs modulated by exercise in the CV system along with miR-126 or mR-29 (359;360). Interestingly, circulating miR-199a-5p expression mirrored the cardiac and vascular profile as previously observed in a context of pathological cardiac hypertrophy. Defining the miR expression signature associated with a protective CV response and identifying their molecular targets would provide potential therapeutic preventive or curative strategies.

Results PART III

AMPKα1 participates in the regulation of miR199a during cardiac hypertrophy

Introduction

Prolonged untreated hypertension is a major cause of pathological cardiac hypertrophy. This thickening of the heart muscle, initiated to overcome the cardiac overload naturally evolve in absence of treatment, toward a decrease in the size of the chambers of the heart, and a reduced capacity of the heart to pump blood to the tissues and organs. In the remodeling process, neurohormonal mechanisms are activated in order to maintain cardiac output, the most important being the sympathetic nervous system overdrive characterized by elevated circulating catecholamines and Renin–Angiotensin–Aldosterone System hyperactivity (384;385). Catecholamines signal via their interaction with α- and/or β-adrenergic receptors (ARs), a family of G protein-coupled receptors (GPCRs). Cardiomyocytes express three subtypes of β-AR (β_{1-3}) and three subtypes of the α_1-AR (386;387) although β1 largely predominates in most species (4 to 1 in the human heart). Both β_1-AR and β_2-AR physiological activation leads to increased inotropy, lusitropy, and chronotropy, through a coupling to the stimulatory G protein (Gαs) (388). This coupling leads to the activation of adenylyl cyclase, production of cAMP, and protein kinase A (PKA) activation which will phosphorylate numerous targets associated with Ca^{++} signaling and contractile protein regulation (310). Prolonged stimulation is associated with reduced cardiac β-ARs responsiveness, cardiomyocyte apoptosis and decreased cardiac function, all in agreement with the efficiency β_1-AR -antagonist treatments (389).

α_1-adrenergic receptors (α_1-ARs) as angiotensin receptors, share a similar coupling to Gαq to activate phospholipase Cβ1 (PLCβ1), which cleaves phosphatidylinositol 4,5-bisphosphate (PIP_2) to produce inositol 1,4,5-trisphosphate (IP_3) and diacylglycerol. Although probably differentially

compartmentalized (at least) in adult cardiac myocytes, ligand binding has been consistently associated with CaMKII/HDAC dependent transcriptional responses and cardiomyocytes hypertrophy (390;391).

AMP-activated protein kinase (AMPK), is a well characterized Ser/Thr kinase, that is ubiquitously expressed, and mainly acts as an energy sensor in the cell. In cardiomyocytes, two catalytic isoforms can be found, while AMPKα2 is predominant, lower but significant amounts of AMPKα1 can be observed. In the last 15 years, AMPK has evolved from a homeostatic protein to a major actor (and potential therapeutic target) in the context of cardiac hypertrophy (392). This is based on the ability of AMPK to hinder cardiac hypertrophy (393;394). There are indeed ample demonstrations that by inhibiting protein synthesis, prohypertrophic gene expression or O-GlcNAcylation of protein, AMPK prevents the hypertrophic response of cardiomyocytes to stress (340;392).

We and other have reported that pathologic cardiac hypertrophy that develops in response to increased pressure overload, catecholamine or angiotensin II infusion is associated with an upregulation of miR-199a-5p in cardiac tissue (308). Potential roles in the maintenance of cardiomyocyte size, apoptosis or metabolism have been proposed for the miR (308;309)(Song, Rane). Despite the description of AMPKα1 as a direct target of miR-199a-3p by miR databases, nothing is known about potential interactions between AMPK and miR-199a signaling.

Here, the expression of miR-199a family members has been assessed in *in vitro* or *in vivo* models of cardiac hypertrophy.

Results

Pathological cardiac hypertrophy induces an increase of miR-199a family members *in vivo* and *in vitro*

In vivo, transaortic constriction (TAC) was performed to induce pathological cardiac hypertrophy. A significant increase of left ventricle (LV) size is observed after 8 weeks of TAC correlated with a modulation of fetal genes (Figure 41), confirming the pathological aspect of the hypertrophy.

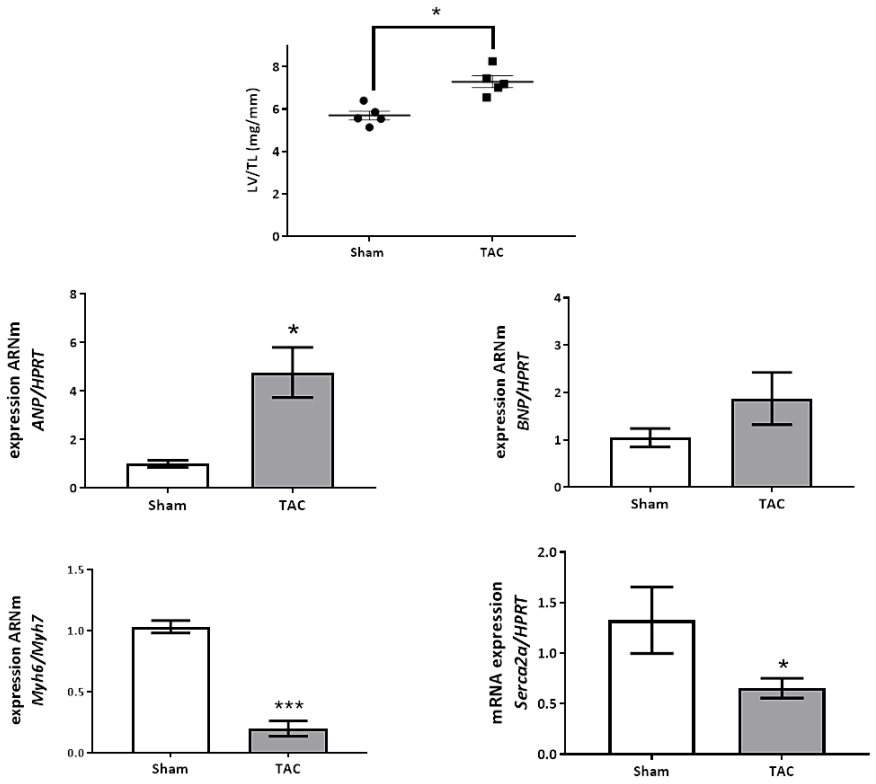

Figure 41: TAC induces a pathological cardiac hypertrophy with a fetal genes reprogramming. TAC were performed on C57bl6J male mice at 4 weeks of age. After 8 weeks, mice were sacrificed, blood and organs removed. LV were weighted and normalized on tibial length. Expression of fetal genes was assessed by RT-qPCR and normalized by *HPRT.* Results are expressed as mean ± SEM of 3 animals. *, P.<0.05 vs. Sham.

As already described, an augmented miR-199a-5p expression was observed in both heart and plasma in the hypertrophic mice (Figure 42B and D). Interestingly, an up-regulation of miR-199a-3p is also detected after aortic banding but in the heart only. A similar expression profile has been observed previously in angiotensin II hypertrophy model (362) (Figure 42A).

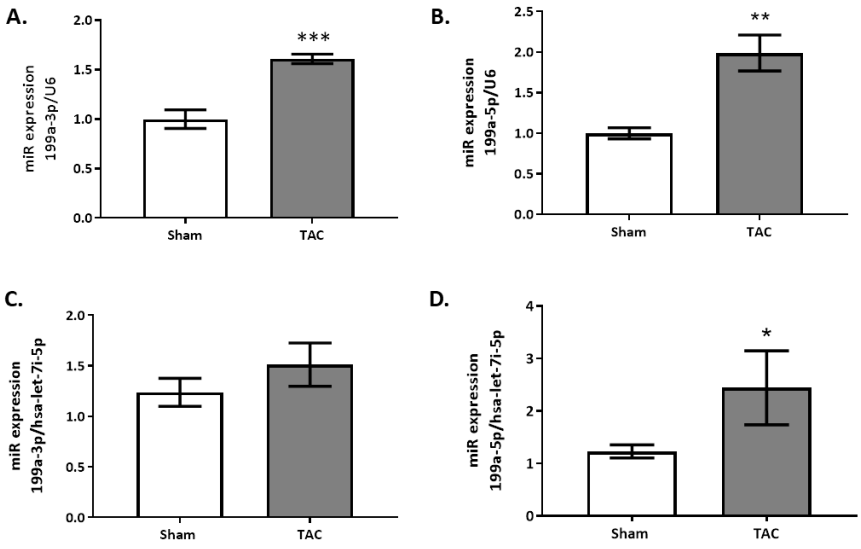

Figure 42: Hearts isolated from TAC mice exhibited an up-regulation of miR-199a-3p and miR-199a-5p. miR-199a-3p and miR-199a-5p levels were measured in hearts (A-B) and plasmas (C-D) of sham and TAC mice using RT-qPCR. Results are expressed as mean ± SEM of 5 animals. *, P.<0.05; **, P.<0.01; ***,P.<0.001 vs. Sham.

In order to mimic cardiac hypertrophy *in vitro*, primary neonatal rat cardiomyocytes were treated with phenylephrine (50µM). Figure 43A illustrates the increase in cardiomyocyte size compared to the control (Figure 43A). In agreement with our *in vivo* data, cardiomyocyte hypertrophy in response to PE was correlated with an up-regulation of both miR-199a-5p and miR-199a-3p (Figure 43B and C).

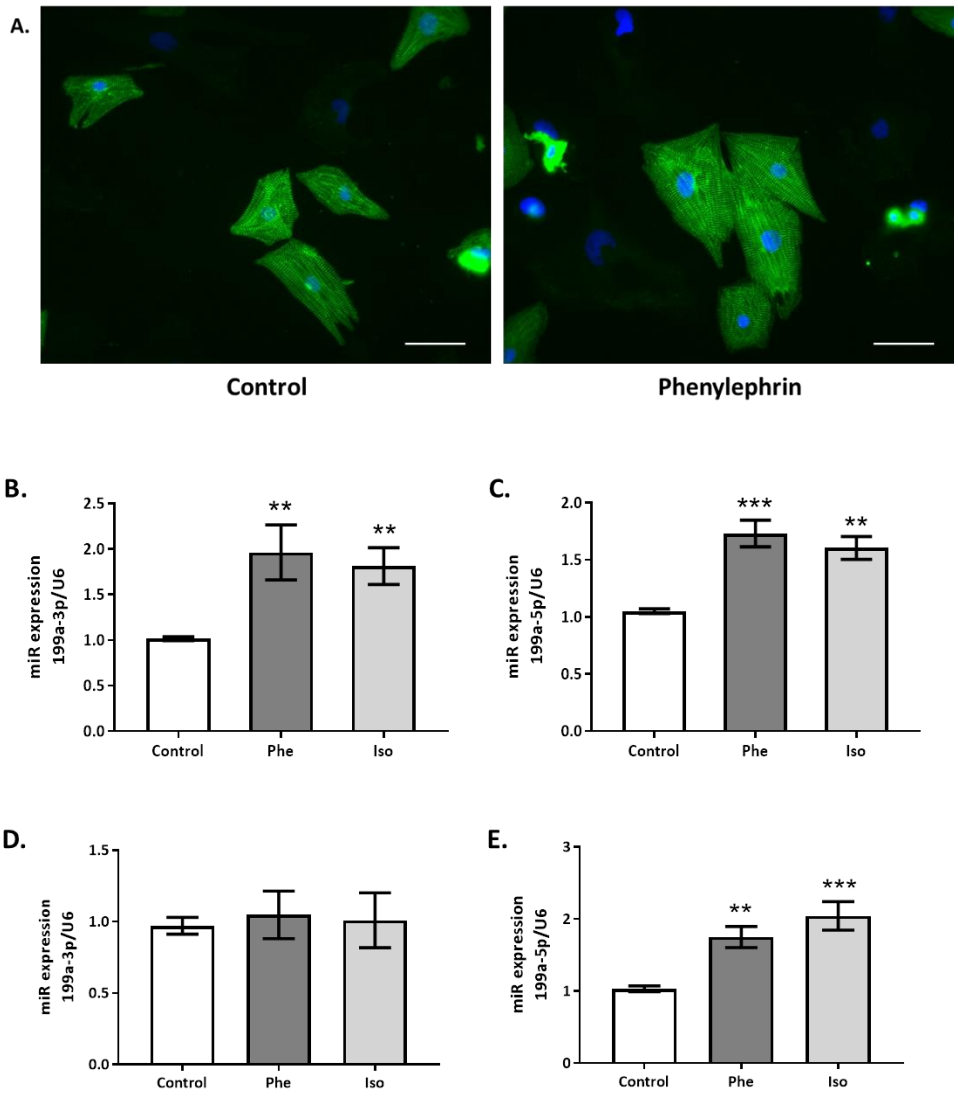

Figure 43: Cells treated with hypertrophic treatments present an increase of miR-199a family members. Cardiomyocytes were isolated from neonatal rats aged from 1 to 3 days. Phenylephrin (Phe, 50µM) and isoproterenol (Iso, 1µM) treatments were added for 24h. Morphologic changes in cardiomyocytes were assessed by immunofluorescence (A). MiR-199a-3p and miR-199a-5p levels were measured in cardiomyocytes (B-C) and culture medium (D-E) using RT-qPCR. Results are expressed as mean ± SEM of 5 individual experiments realised in duplicate. **, P.<0.01 and ***, P.<0.001 vs. Control.

Similar results were obtained when cardiomyocytes were stimulated with isoproterenol (1µM). Quantification of miR in the culture medium revealed an increase of miR-199a-5p after phenylephrine treatment but no modulation of miR-199a-3p expression.

AMPKα1 repression prevents the upregulation of miR199a-5p evoked by hypertrophic treatment *in vivo* and *in vitro*

As described above, TAC promotes the development of a LV cardiac hypertrophy of similar amplitude in both wild-type (WT) and AMPKα1 knockout (KO) mice (Figure 44A). In parallel TAC induces an upregulation of miR199a-5p expression in the heart and plasma of WT mice, which is blunted in AMPKα1 KO mice (Figure 44B). Interestingly, deficiency for AMPKα1 did not impact miR199a-3p upregulation as illustrated in Figure 44C. Plasmas of hypertrophic mice present an up-regulation of miR-199a-5p which is abrogated by AMPKα1 KO (Figure 44D). Plasmatic expression of miR-199a-3p was similar in all conditions (Figure 44E).

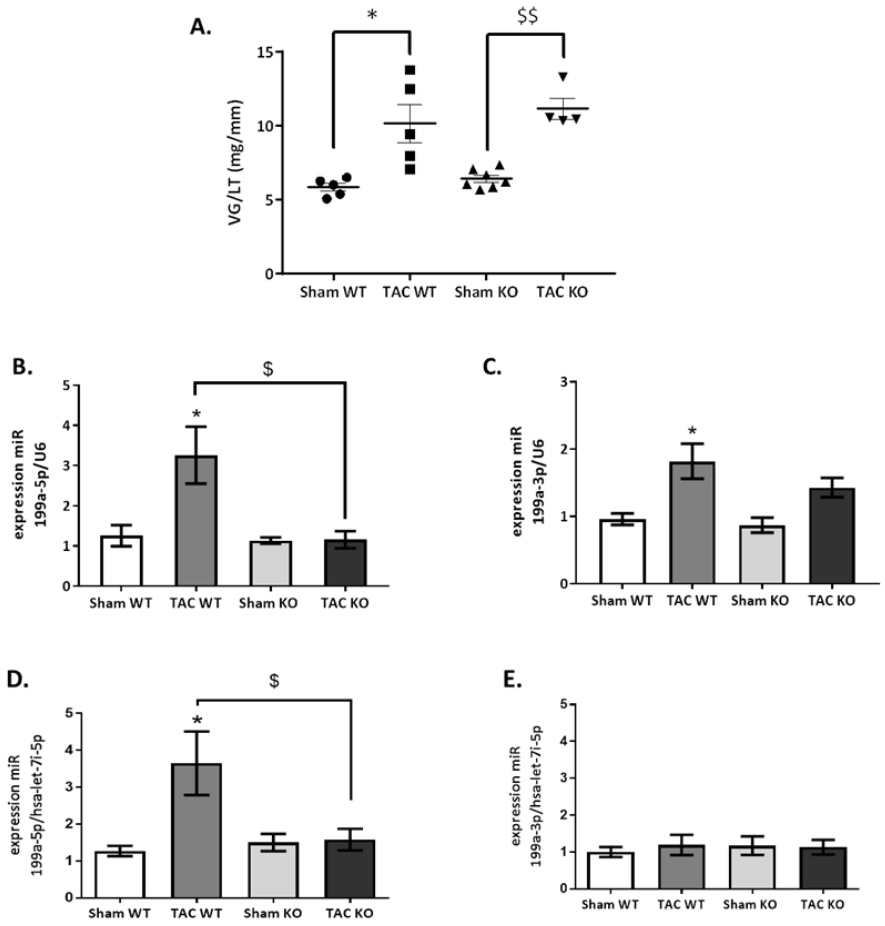

Figure 44: Hearts isolated of AMPKα1 KO mice undergoing TAC presented a reduced miR-199a-5p expression compared to WT TAC mice. TAC were performed on C57bl6J wild type (WT) male mice or genetically deficient for the α1 subunit of AMPK (KO) at 4 weeks of age. After 8 weeks, mice were sacrificed, blood and organs removed LV were weighted and normalized on tibial length (A). MiR-199a-3p and miR-199a-5p levels were measured in hearts (B-C) and plasmas (D-E) using RT-qPCR. Results are expressed as mean ± SEM of at least 4 animals. *, P.<0.05 vs. Sham and $, P.<0.05 and $$, P.<0.01 vs. WT.

Repression of AMPKα1 (figure 45C) was performed in neonatal rat cardiomyocytes. Pro-hypertrophic treatment induced an up-regulation of miR-199a-5p scramble treated cardiomyocytes and cultured medium, the upregulation was prevented in both cells and medium when expression of AMPKα1 was inhibited (Figures 45A and 45B).

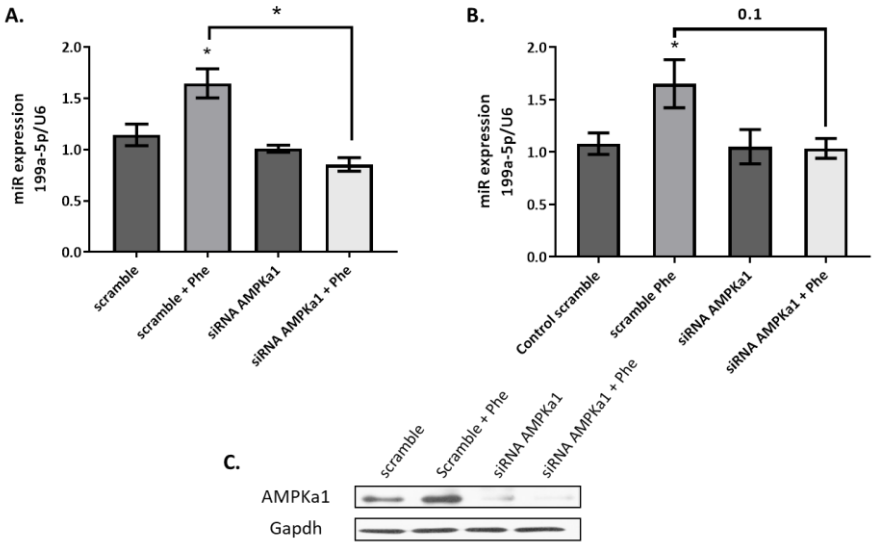

Figure 45: Phenylephrine-treated cardiomyocytes transfected with AMPKa1 siRNA presented a reduced miR-199a-5p expression compared to cells transfected with scramble. AMPKα1 siRNA or a scramble sequence was transfected at the beginning of the culture and after 5 days cells were exposed or not with phenyleprhine (Phe, 50µM) during 24h. MiR-199a-5p levels were measured in cardiomyocytes (A) and culture medium (B) using RT-qPCR. AMPKα1 expression was measured by Western Blot analysis (C). Results are expressed as mean ± SEM of at 3 individual experiments realised in duplicate. *, P.<0.05 vs. scramble.

AMPK activation induces an increase of miR199a family members *in vitro*

To study the implication of AMPK on miR-199a family members expression, primary culture of neonatal rat cardiomyocytes were treated with the well-known AMPK activator, metformin. Activation of AMPK *in vitro* induced the up-regulation of miR-199a-3p and miR-199a-5p expression (Figures 46A and 46B). As for hypertrophic treatment, no modulation of miR-199a-3p expression was highlighted in medium of these cells while extracellular miR-199a-5p was upregulated (Figure 46C and 46D). Cardiomyocytes treated with AICAR, another AMPK activator, presented the same expression profile (data not shown).

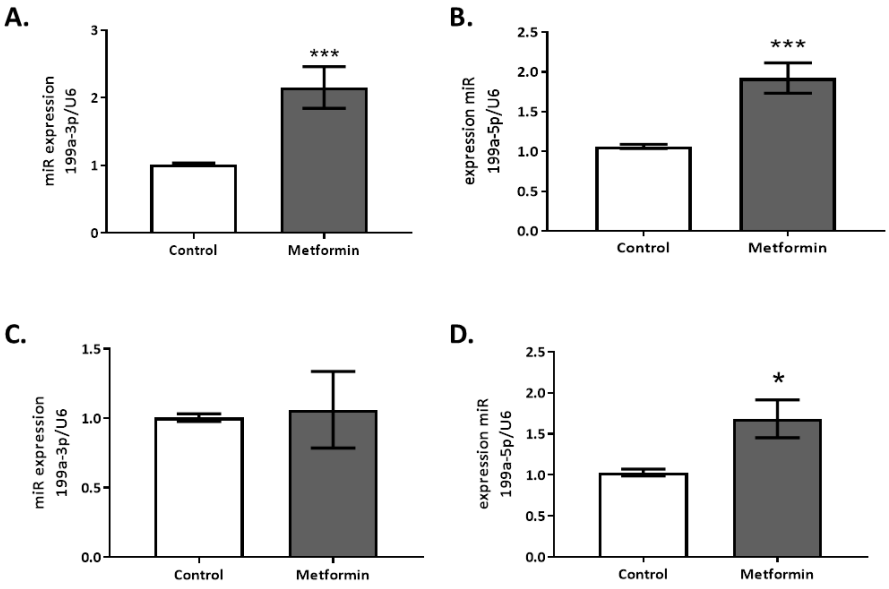

Figure 46: AMPK activation in cardiomyocytes induced an increase of miR-199a expression. After 5 days of culture, cardiomyoctyes were treated with metformin (1mM) during 24h. MiR-199a-3p and miR-199a-5p levels were measured in cardiomyocytes (A-B) and culture medium (C-D) using RT-qPCR. Results are expressed as mean ± SEM of 5 individual experiments realised in duplicate. *, P.<0.05 and ***, P.<0.001 vs. Control.

AMPKα1 KO do not impact pre-miR expression *in vivo*

In order to decipher between a transcription of post transcription regulation, pre-miR, 199a-1 and 199a-2 expression were assessed in the heart of WT and AMPKα1 KO mice. An up-regulation of the miR precursor was measured despite the AMPKα1 deficiency in mice hearts, suggesting that AMPKα1 regulates the stabilization of miR-199a-5p more than its production (Figure 47).

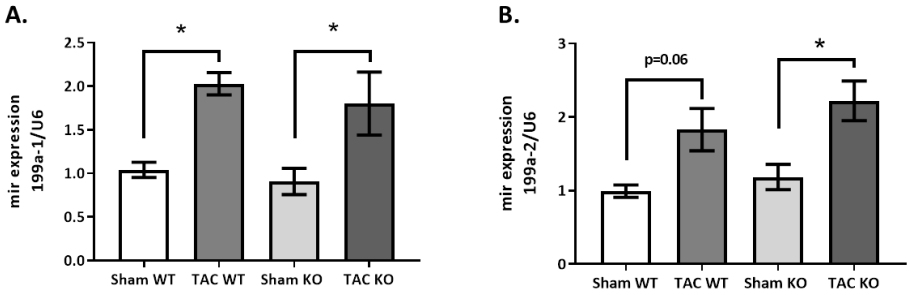

Figure 47: Hearts isolated from WT or AMPKα1 KO mice present an increase of pre-miR 199a expression after TAC. After 8 weeks of TAC, mir-199a-1 (A) and mir-199a-2 (B) levels were measured in hearts from wild type (WT) or AMPK α1 KO (KO) mice, using RT-qPCR. Results are expressed as mean ± SEM of at least 3 animals. *, P.<0.05 vs. Sham.

Hypertrophic treatments and AMPK activation induce an increase of PKA activity *in vitro*

To understand the pathway implicated in miR production during pharmacological treatments, we investigated the implication of PKA, a protein already described as a modulator of miR-199a expression. Stimulation of the adrenergic pathways or pharmacological activation of AMPK led to an upregulation of PKA activity measured by the phosphorylation state of its substrates. Moreover, direct activation of PKA by dBcAMP induces an increase of miR199a-5p expression (Figure 48A and 48B).

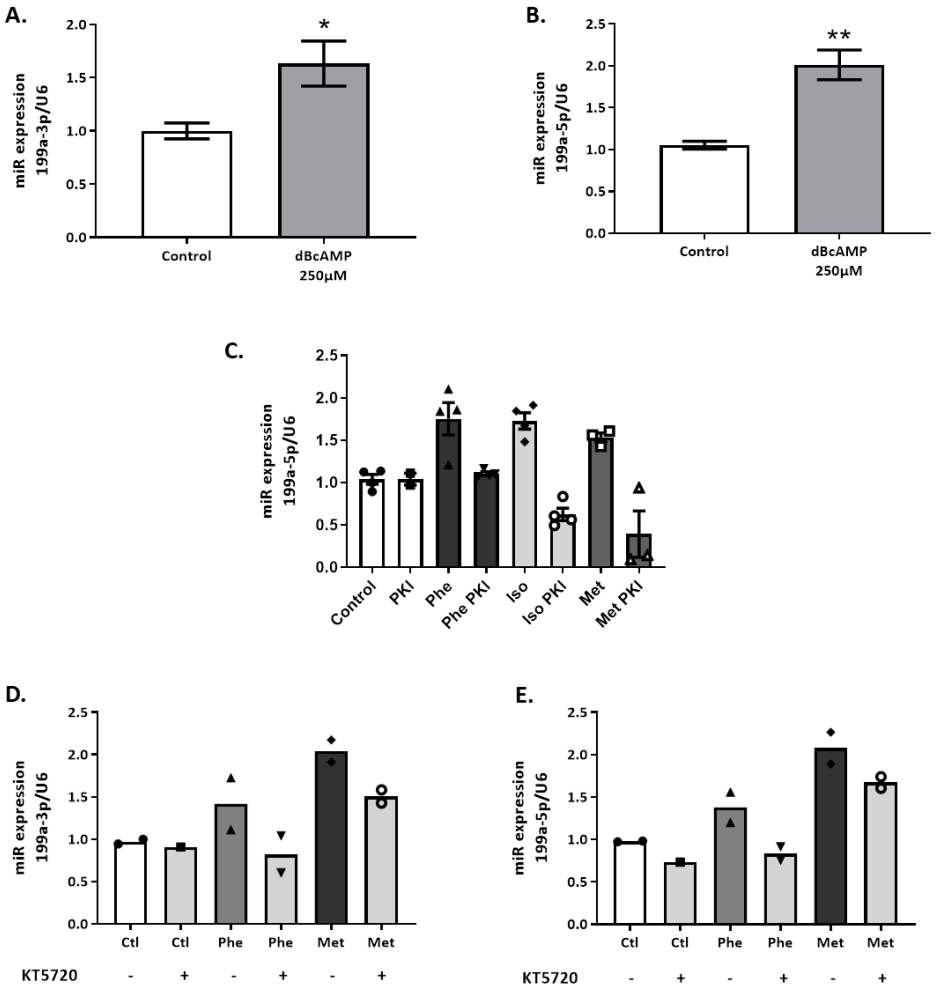

Figure 48: PKA modulate miR-199a expression in isolated cardiomyocytes. After 5 days of culture, cardiomyocytes from neonates were treated with dBcAMP (250µM), phenylephrin (Phe, 50µM), metformine (Met (1mM), PKI (2,5µM) and/or KT5720 (2µM). MiR-199a-3p and miR-199a-5p levels were measured in cardiomyocytes after dBcAMP treatment (A-B) or hypertrophic treatments coupled or not with PKA inhibitors (C-E) using RT-qPCR. Results are expressed as mean ± SEM of at least 2 individual experiments realised in duplicate. *, P.<0.05 and ***, P.<0.001 vs. Control.

Finally, the use of pharmacological PKA inhibitors (PKI or KT5720) counteracted the upregulation of miR199a-5p expression during hypertrophic treatment or metformin treatment (Figure 48C-E).

General discussion, conclusions and perspectives

The endothelium is obviously a (the) critical player to guarantee cardiovascular homeostasis due to its ability to regulate a wide range of functions as vascular tone, inflammation, thrombosis, vascular permeability or angiogenesis (13;395). Regulation of the NOS/NO pathway is multimodal and virtually all levels of regulation and mechanisms involved have been associated with cardiovascular risk factors or cardiovascular pathologies. With this study, we propose another mode of regulation for the NOS pathway. Despite the already rich therapeutic armamentarium known to promote a healthier endothelial function, the remaining burden of cardiovascular diseases urge the scientific world to seek for other pathways to explore. In this context, more and more attention is being paid to miR as their capacity to silence gene and regulate protein expression makes them potential modulators of the cardiovascular function (265). Hence, miR-199a family members, well conserved in different species, are already described as interesting players in the maintenance of cardiac homeostasis (265;308). Our findings have broadened the activity spectrum of miR-199a family members by showing that: (i) the two arms derived from miR-199a are significantly expressed in endothelial cells, (ii) they are two functional players and (iii) they participate to the switch between cardiovascular health and disease.

At the beginning of this work, it was been established that miR-199a is expressed in cardiomyocytes and is able to impact indirectly endothelial function (304), also, miR-199a-5p was proposed to regulated proliferation in pulmonary microvascular endothelial cell. Our work extends these findings by showing a functional expression of both miR-199a-3p and -5p in the endothelium. The significant expression that we reported in this work in different endothelial cell types (from bovine aortic endothelial cells, human aortic endothelial cells and human umbilical vein endothelial cells) and vessels (mice mesenteric and aorta)

argues in favor of a ubiquitous expression in the endothelium all along the vascular tree.

Both members of the miR-199a family have been described as mature miRs repressing specific targets in the context of cancer (269;274;289;290) which is not surprising considering that often both arms of premiRs could be functional, although their ratio varies according to the pathophysiological state (170;173). Here, we show that both strands are expressed and functional at the same time in a unique cell type, sharing some (but not all) targets within a common signaling cascade (the NOS/NO pathway). It is quite accepted that the range of action of microRNAs is limited to around 20% of expression of their targets, which should *de facto* limit their « clinical » impact (396). We can infer that the redundancy that we observed with two miR modulating the same cascade, with both targeting several players (activation of NOS by modulation of Calcineurin and Akt activation, and NO bioavailability through the control of SOD and PRDX1 for instance) would more profoundly affect endothelial function. This is indeed what we observed with the prominent improvement of NO-dependent relaxation that occurs upon repression of the miRs.

We should note that several proteins repressed by miR-199a that we highlighted in this work are also described as major targets in endothelial or other cell types. PI3K was already described as a direct target of miR-199a-5p in the hippocampus of rat (292) and regulation of Akt activity by both miR-199a family members was described in glioma (273;285) as well as in cardiovascular system (314;345;347). More interestingly, Wang et al. highlighted that the overexpression of miR-199a-3p in HUVECs promoted autophagy, migration as well as cell proliferation through activation of PI3K/Akt/NFκB pathway (397). This apparently contradictory information is not completely irreconcilable with our findings as

differences in vascular bed or quiescence could account for the discrepancies. miR-199a family members are also widely known in the field of cancers for their ability to modulate angiogenesis through the direct targeting of VEGF (272;287;288). Zhang and colleagues already demonstrated that repression of SIRT1/eNOS pathway by miR-199a-5p promotes tube formation in endothelial cells infected by cytomegalovirus (398). In agreement, we established that repression of miR-199a-5p induces a strong formation of tube in bovine aortic endothelial cells cultured in 2D-matrigel support in a more physiological context. MiR-199a-3p repression does not impact angiogenesis as much in our hands. This correlates with luciferase assays showing that miR-199a-5p is able to directly target bovine VEGF while miR-199a-3p is not. Interestingly, in human hepatocellular carcinoma, miR-199a-3p is described as directly repressing VEGF (272). *In silico* studies and other works proposed Cav1, the allosteric repressor of eNOS, as a direct target of miR-199a-5p (319;348). In our *in vitro* model, we failed to show a modulation of Cav1 expression after repression of each miR-199a family members. As well, our unpublished data showed no differences in Sirt1 expression in endothelial cells after miR-199a-5p repression even though *in silico* investigations and several works described it as a direct target (284;292;368). Incidentally, we demonstrated that Sirt1 expression, which is linked to improved cardiac function, is modulated in heart of running mice which presented a deregulation of miR-199a expression. This observation confirms the notion that a miR might target different pathways depending on the cell type or the biological context. This hypothesis is reinforced by the modified miR/miR* ratio in some pathological states compared to normal conditions (172;173). Indeed, the change in the balance between both miR-199a-3p and miR-199a-5p could re-dispatch the targets priority of each miR.

Oxidative stress has a profound impact on endothelial function, thus, studying the relation between miR-199a family members and ROS metabolism seems relevant. Some works have highlighted a direct link between ROS production and miR-199a expression. For instance, He et al. described ROS as able to increase miR-199a-5p expression in human lung epithelial cells following arsenic treatment (399). On the opposite, in ovarian cancers, ROS were highlighted as negative regulators of miR-199a expression via an up-regulation of miR promoter methylation (400). However, except a study performed in β-pancreatic cells and high glycose treatment (368), little is known on the ability of miR-199a family members to regulate ROS production or metabolism. Our study demonstrated that both miR-199a-3p and miR-199a-5p modify NO bioavailability through modulation of its degradation as repression of both miRs induces an increase in SOD1 expression *in vitro*, as well as *in vivo.* To our knowledge it is the first time that miR-199a family members are described as regulator of anti-oxidant enzymes. This ability to regulate ROS production and metabolism is important not only in vascular injuries but also in cardiac events as hypertrophy.

NO-independent modulators of endothelial function: direct targets of miR-199a?

Although prominent, NO is not the sole guardian of endothelial function. Interestingly, COX2 which regulates PGI2 production is described as a direct target of miR-199a family members in human bronchial epithelial cells (399). We did not investigate the expression of COX2 in our transfected endothelial cells. However, the blunted expression of miR-199a family members observed in running mice is correlated with an enhanced PGI2-dependent relaxation measured in mesenteric arteries. This observation is in agreement with COX2 as a direct target of miR. Hence, studying the impact of miR-199a family members' repression on this

protein could be interesting particularly in resistance arteries where the PGI2-mediated relaxation is more important than in conductance arteries.

miR-199a, a player in cardiac function and disease?

Our observation that miR-199a is regulated in models presenting modified endothelial function reinforce the significance of our work as it places the miR-199a family at the crossroad between physiology and pathology. It is well described that exercise is accompanied with positive cardiovascular modulation (126) with increased NO bioavailability and improved endothelial function. Now, we show that both miR-199a-3p and miR-199a-5p are down-regulated in vessels of running mice compared to sedentary and this independently of the vascular bed type. This argues in favor of a participation of miR-199a in this beneficial process. On the opposite, mice developing a pathological cardiac hypertrophy due to pressure-overload presented an impaired endothelial function (139;401;402) and we correlated this with an up-regulation of miR-199a family members. Obviously, regulation of miR-199a expression is one of the many factors altered by exercise or cardiac hypertrophy and we could not attribute all the positive or negative effects of exercise or pathology to their sole modulation. The term « redundancy » is again in application, bringing efficiency to the system.

More than ten years ago, van Rooij et al. highlighted a dysregulated level of miR-199a in plasma from patients presenting a cardiac hypertrophy. Hence, this miR was added to the list of already identified biomarkers of adverse cardiac remodeling (265;336).

We have observed that miR-199a-3p and miR-199a-5p were up-regulated in the hearts in different models of pathological hypertrophic mice and isolated cardiomyocytes stimulated with catecholamines or angiotensin II. This finding is in accordance with previous works describing an up-regulation of miR-199a-5p after

aortic banding or stimulation of adrenergic pathway (308;309). In their study, Song et al. proposed that miR-199a helps to maintain cardiomyocyte size during hypertrophy (308) while Li et al. demonstrated that miR-199a-5p induces cardiac hypertrophy by impairing autophagy (312). Yet, in our work, we did not decipher whether the miR is responsible of cardiac hypertrophy or if it is the hypertrophy which promotes miR expression. However our finding that despite a normal hypertrophic response, the heart of mice genetically deficient for AMPKα1 did not display any alteration of miR-199a-5p expression suggest that the miR is not absolutely required for the hypertrophic process itself. The cardiac down-regulation of miR-199a3p/5p in a context of chronic exercise and associated cardiac hypertrophy is also an argument against an obligatory role in the modulation of cardiomyocyte size. We should however keep in mind that the amplitude of hypertrophy was very different and the entire process might relate on a completely different signaling cascade. el Azzouzi et al. described the ability of miR-199a/214 cluster to regulate PPARδ and facilitate the metabolic shift from fatty acid oxidation in healthy myocardium towards increased reliance of glucose metabolism at the onset of heart failure (41). We did not specifically address this aspect but the upregulation of PGC1 alpha and Sirt-1 in our model of physiologic hypertrophy points to mIR-199a as a potential regulator of the metabolic shift. Confirmation requires further investigation. This might take part in the general fetal gene reprogramming process as miRNA-199e expression profile in adult remodeling heart tends to return to the original fetal levels (403). A limit of our study is that while we have ample proof of a regulation of miR-199a in endothelial cells and cardiomyocytes in a context of pathological hypertrophy, at this point we have no evidence for a dysregulation of miR-199a in cardiomyocytes in a physiologic hypertrophy (304).

In our model of chronic exercise, we emphasized a down-regulation of both miR-199a-3p and miR-199a-5p. Little is known about the impact of exercise on miR-199a expression but the ability of exercise to modulate global miR expression is well documented (194;259;359;404). Interestingly, reports often demonstrated a beneficial impact of exercise on miR described as dysregulated in pathological hypertrophy as for example miR-29 or miR-210 (338). Consequently, the study of miR-199a in context of physiological hypertrophy seems suitable. This is reinforced by a recent publication of Li et al. supporting that specific cardiac deletion of miR-199 induces the development of a physiological hypertrophy. In this work, the use of miR-199 sponge significantly down-regulates miR expression leading to an improved cardiac function through increased PGC-1α and Akt expression (314). Similar alterations in miR-199a profile observed in remodeling fetal heart (evaluating towards the lower level of expression observed in adult heart) has been interpreted as an endogenous protective strategy against cardiac dysfunction (403). This correlates with our results demonstrating an up-regulation of PGC1α as well as Sirt1 and mTOR in cardiac tissues of our running mice translating an improvement of cardiac metabolism in these mice. However, further work is necessary to prove the direct link between miR-199a regulation and modulation of proteins implicated in cardiac metabolism.

In our work and as observed in others, miR-199a acts as a deleterious regulator of cardiovascular functions. However, Lesizza and colleagues revealed that intra-cardiac injection of miR-199a-3p rescue cardiac function after MI (321). The same group highlighted the pro-proliferative effect of miR-199a-3p through activation of Yes-associating protein (YAP) by inhibition of YAP degradation. They demonstrated that miR-199a-3p also inhibits filamentous actin depolymerisation through targeting Cofilin 2 (405). Their last work on infarcted hearts of pigs showed that injection of miR-199a stimulates cardiac repair, improved

contractility, increases muscle mass and reduces scar size. Interestingly, this work also highlighted that the subsequent uncontrolled and persistent expression of miR-199a in heart leads to an arrhythmic death emphasizing the importance to use highly controlled dose (406). This last observation could suggest a positive impact of miR-199a at short-term which evolves in deleterious effect at long term.

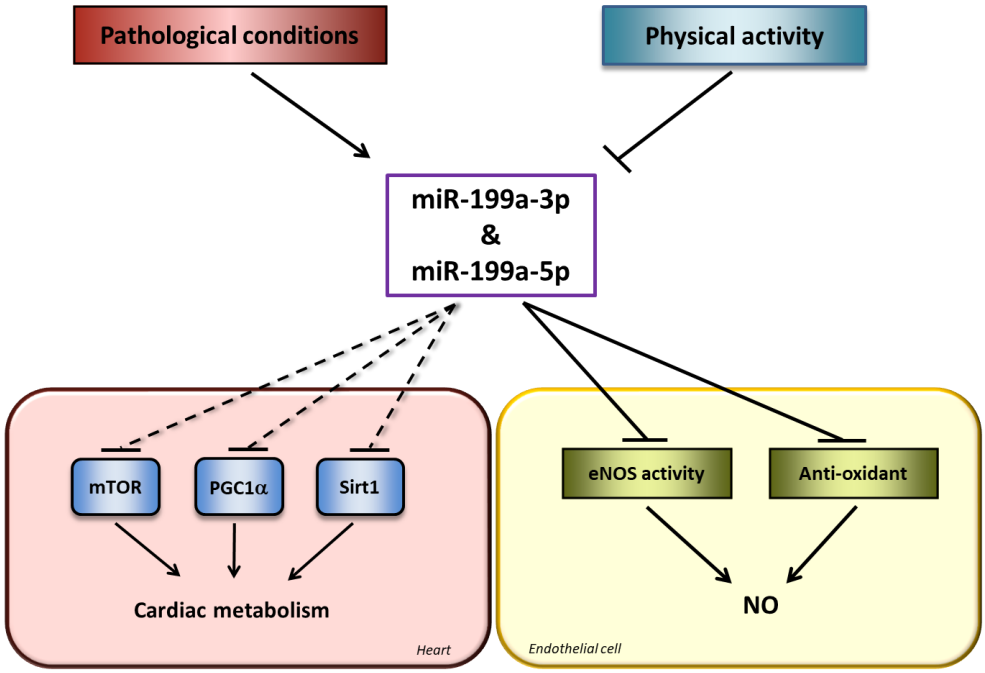

Figure 49: Implication of miR-199a-3p and miR-199a-5p in pathological and physiological mechanism of hypertrophy and vascular function. Indicated proteins are direct and indirect targets of miRs 199a-3p or -5p. In endothelial cells, eNOS activity and NO bioavailability are indirectly modulated by miR-199a products. Physical activity downregulates miR-199a expression in heart and vessels leading to a global improvement of cardiac and endothelial functions while pathological conditions have opposed effect. Straight lines indicate that we have verify the causal link between miR and protein expression; dotted lines that we have observed a correlation.

As mentioned earlier, our work places miR-199a family members as a switch between physiology and pathology. In this line, it could be implicated in other diseases associated with cardiovascular events or vascular alterations. For instance, miR-199a expression is enhanced in hepatic tissues of nonalcoholic fatty liver disease (NAFLD) and positively correlated with the fibrosis grade (407) as it regulates the TGFβ pathway. Moreover, plasmatic levels of miR-199a are increased in patients with NAFLD in parallel with cholesterol levels (408). It is interesting to remember that NASH patients die more from CV diseases that from an altered hepatic function and that when considering populations with equal CV risk factors, NASH patients are at an increased risk of CV events/death. We could hypothesize that through its blood circulation, miR-199a could impact other systems and particularly the cardiovascular tissues. In this line, preliminary results obtained in the lab demonstrated that hearts extracts from of $ApoE^{-/-}$ mice nourished with n-3-PUFA deficient diet that mimics most characteristics of the liver disease (59) present an increase of both miR-199a-3p and miR-199a-5p without cardiac hypertrophy, this was prevented by adding prebiotics in diet for 2weeks. Interestingly, an amelioration of hepatic steatosis by modulation of gut microbiota is already correlated with a decrease of miR-199a-3p expression (409). As a second example, thyroid samples from Basedow patients are characterized by increased angiogenesis and oxidative stress. Our preliminary data showed also a dysregulation of miR-199a-5p in these samples. More interestingly, the down-regulation is also patent in the blood and periorbital fat from Basedow patients exhibiting orbitopathy. In silico analyses have revealed several potential targets for both miR-199-3p and -5p in link with thyroid function. Additionally, we have observed that inhibition of miR-199a-3p in endothelial cells induced an up-regulation of deiodinase 2 (Dio2) expression for instance, DiO2 is the enzyme responsible for the conversion of triiodothyronine into thyroxine. Thyroid

hormones increase Akt and eNOS activation in endothelial cells, an inhibition of miR-199a-3p still upregulates this effect. Our preliminary data therefore suggest a potential implication of miR-199a in the response of endothelial cells to thyroid hormones.

miR-199a-5p capable of information transfer through its secretion?

The secretion and transfer of information via miR from one cell to another is highly studied. A remaining debate consists to clarify if a specific regulation exists for miRs secretion or if they are produced as a by-product during cell death or secretion (410). Indeed, some studies have highlighted that miR concentration in culture medium or blood correlate with cell death or organ damage (177;411;412). Concerning miR-199a, excretion of the miR in exosomes is well documented and correlates with our data describing the detection of miR-199a in both plasma and culture medium. However, the low concentration of miR detected in exosomes (molecule for 100 exosomes) suggest the existence of a sorting mechanism allowing the selection of miR-enriched exosomes (413). Post-transcriptional modifications of miR favor cell retention or exosomes inclusion (184). Furthermore, some proteins as heterogeneous nuclear ribonucleoprotein A2B1 (hnRNPA2B1B) are able to recognize specific miR sequences and promote their exosomal secretion (414). As mentioned earlier, more and more investigations suggest that circulating miRs are able to transfer information from one cell to another placing them as crucial players. Our data join this conclusion as endothelial cells treated with cardiomyocytes culture medium containing miR, react by an impairment of their function (not shown).

Regulation of miR-199a family members in CV system

The biogenesis of miRs is particularly complex as multiple transcription factors as well as post-transcriptional mechanisms can influence it (415). Our findings demonstrated that BAECs exposed to laminar shear stress and vessels from running mice*, in vivo*, present a decreased expression of miR-199a family members and a reduced expression of the transcriptional factor TWIST-1. This is interesting as it points to a link between shear laminar forces and miR-199a.

TWIST1 is a well-known positive regulator of miR-199a family members in different cell types and physio-pathological context as for instance in embryologic development or dilated cardiomyopathy (266;267). Our finding is also supported by other works describing the up-regulation of TWIST1 in site of turbulent flow and demonstrating a positive correlation between TWIST1 levels and appearance of atherosclerotic plaques (318). *In vivo*, the associated down-regulation of pre-miR-199a-2, is another argument pointing to transcriptional process evoked by shear stress to modulate miR production via a TWIST1/pre-miR/miR regulation.

Our data (although more preliminary) proposed AMPKα1 as a new modulator of miR-199a levels in the heart. This correlated with previous work demonstrating an implication of AMPK in miR synthesis. Actually, in pancreatic islets, AMPK deletion is already known to deregulate the expression of about twenty miRs (416). Moreover, in endothelial cells, the phosphorylation of p53 by AMPK induces miR143/145 cluster production (417). Yet, in our work, the absence of miR-199a-3p modulation by AMPKα1 KO suggests that miR regulation by AMPK occurs at post-transcriptional levels and impacts the stability of miR-199a-5p more than its production. *In silico* studies demonstrated that both Ago2 and exportin-5 could be potential targets of AMPK kinase activity, thereby modulating their function in miR biogenesis. Indeed, Sun et al. already described that

exportin-5 phosphorylation by ERK regulate the exportation of pre-miR from the nucleus to the cytoplasm (159;418). In this work, we also demonstrated that metformin, a pharmaceutical AMPK activator, up-regulates expression of miR-199a family members. Our observation that AMPKα1 stabilizes miR-199a-5p or that AMPK activation promotes the production of miR-199a-3p/5p is counter-intuitive if we have in mind the well-known cardio-protective effects of AMPK (419;420) and the fact that miR-199a is described as harmful for the heart. Before interpreting our data, we should however take into accounts several limits to our work. First, our experiments were performed on neonatal cardiomyocytes instead of adults and AMPKα1 is not the predominant catalytic isoform in the adult cardiomyocytes. Although a higher expression of the α1 subunit might be in link with the relatively higher expression of miR-199-5p in fetal heart in comparison to adult heart (403), additional investigations on miR-199a expression with AMPKα2 or AMPKα1/2 deletion in cardiomyocytes from neonates as well as adult animals must be performed. Second, we have used metformin to activate AMPK in neonatal cardiomyocytes, this anti-diabetic drug is known to reduce left ventricular dimension during heart failure with an improvement of fractional shortening and ejection fraction (421). Yin and colleagues also demonstrated that rats treated with metformin during MI present a smaller infarct size compared to vehicule-treated rats (422). Some beneficial aspects of metformin are also suspected to be related to due AMPK-dependent eNOS activation. This seems particularly at odds with our results. Metformin indiscriminately activates AMPKα1 and α2, the impact of the latter on miR-199a expression is still unknown. Also, we should consider that the effect of AMPK activation in endothelial cells might be sufficient to counteract any AMPK/miR-199a deleterious effect.

Therapeutic approach

In clinic, the use of miR as therapeutic is not yet a reality but the proof of concept is already available with the Miravirsen trials. The implication of miR-199a family members in cardiovascular events through the regulation of endothelial and cardiac function makes them a potential target for therapeutics approaches (265;303). Yet its inference in cancer metabolism makes its targeting unrealistic as the beneficial effect on cardiovascular function could be counterbalanced by adverse effect on pre-cancerous cells. Even if modulation of either miR-199a-3p or miR-199a-5p by intravenous injection of antagomiR did not lead to cancer development in mice, the long-term aspect of human therapy must be considered as a limiting factor. Tissue specific targeting of miR as already described in heart via the use of miR-sponge or specific aptamers (314) might be an option. miR-sponges relate to endogenous circular-RNA or long non-coding RNA which contain miR specific target sites and repress miR expression (423;424). However, a miR sponge can also consist of an exogenous transcript presenting 4 to 10 binding sites for mature miR. These sponges are usually not specific to a mature miR but block a whole family of miR, their tissue delivery can be obtained through viral vector as performed by Carè and colleagues. These authors successfully inhibited miR-133 expression using a decoy delivered by adenoviral way; in this setting, inhibition of miR-133 family induced cardiac hypertrophy (425). Instead of using a viral delivery, antisense or mimic materials may be delivered packaged in nanoparticles. This technique allows a protection against degradation or diffusion. Ideal nanocarriers should be biocompatible and biodegradable, they should have appropriate encapsulation efficiency, be stable in storage but allow a timely release in the bloodstream. Recently, Di Mauro and colleagues had brought the proof of concept that negatively charged calcium phosphate nanocarriers are safe and efficient to deliver miR sequences in

polarized cells such cardiomyocytes (426). Interestingly, inhalation of calcium-phosphate nanoparticules had shown an efficient translocation of the particles from the pulmonary tree to the bloodstream and to the myocardium, where the carriage content was delivered (427). Such a non-invasive approach would be a lot more attractive for patient then injection, especially when we consider the need of repetitive treatments.

The use of targeting devices to cell-specifically deliver either nude oligo sequences, liposomes or nanocarriers might also be required to reach therapeutical efficiency. In this context, aptamer might be helpful. Indeed, the oligonucleotidic molecule attached to the therapeutic sequence or its carrier, presents a designed conformation to recognize, in a non-Watson Crick pattern, a specific target at the cell surface. This was already used to target cancer cells through the oncogenic tyrosine kinase receptor, Axl, which is expressed by various types of solid tumors (428) or in gastric cancer cells through biding of nucleolin protein (429).

miRs are commonly used as biomarkers for many diseases. If the use of one miR as biomarker is not relevant due to their lack of tissue/organ specificity, (this is again the case for miR-199a), the use of a miRs panel (containing a few tissue-specific miRs) is recognized as powerful as validated clinical biomarkers (191). A dysregulated miR-199a plasma level is part of a specific signature pattern of cardiac hypertrophy (265;308;309). In cardiac diseases, central aspect is the prevention, meaning that the identification of a panel of miRs which can be used as biomarkers and allow an early diagnosis of cardiovascular events is more important than identification of new miR biomarkers for diseases easily diagnosable with another well-established biomarker (430). Cancer patients too often die from CV events, it should be evaluated whether the up-regulation of

circulating miR-199a that is observed in some gastric or ovarian cancers should not be considered also as a signal of an increased CV risk. In this line, miR-199a-3p has already been shown to be part of a signature associated with chemotherapy-related cardiac dysfunction in breast cancer patient treated with anthracyclines (431). Further studies are clearly needed in this context.

In summary, our work has identified the miR-199a family as key players of cardiac and endothelial functions at the crossroad of health and disease. At this stage, it quite unrealistic to imagine miR-199a's as therapeutic targets, as the tissue specific delivery still requires adjustments; the observation that circulating levels of the -5p arm reflect cardiac and endothelial levels (and therefore cardiac and vascular health) gives them however a high prognostic value.

Annexes

mTOR	199a-3p	3' a u u g g U U A C A C G U C - U G A U G A C a 5' 114 5' a u g u a A A U G A A A A G A A C U A C U G u 3'
	199a-5p	3' c u u g u c c a u c a g a c u u G U G A C C c 5' 480 5' a c c u a u c c c a a g a c c u C A C U G G u 3'
eNOS	199a-3p	/
	199a-5p	/
Akt1	199a-3p	/
	199a-5p	/
Calcineurin	199-3p	3' a u u g g u u a c a c g u c u G A U G A C a 5' 303 5' a a u g a a c a u g u u u u c C U A C U G c 3'
	199-5p	/
SOD1	199-3p	/
	199-5p	3' c u u g u c c a u c a G A C U U G U G A C c c 5' 68 5' c c u g a u a a a c a U U A A A C A C U G u a 3'
VEGF	199-3p	3' a u U G G U U A C A C G U C U G A U G A C a 5' 1734 5' u u A U U U A U - U G - G U G C U A C U G u 3'
	199-5p	3' c u U G U C C A U C A G A C U U G U G A C C c 5' 454 5' u u A U U G G U - G U C U - - U C A C U G G a 3'
CAV1	199-3p	/
	199-5p	3' c u u g u c c a u c a g a c U U G U G A C C c 5' 1558 5' u u g c a u u u a a a a c a G A C A C U G G c 3'
HSP90	199-3p	/
	199-5p	/
DDAH1	199-3p	3' a u u g g u u a c a c g u c u G A U G A C a 5' 72 5' g u u u u c c u u g a c a a u C U A C U G u 3'
	199-5p	/
PRMT1	199-3p	/
	199-5p	/
PDK1	199-3p	/
	199-5p	/
PRDX1	199-3p	3' a u u g g u U A C A C G U C U G A U G A C a 5' 191 5' g g c g u u G U G G G C A G G C U A C U G g 3'
	199-5p	/

Table A1: Alignment between miR-199a family members and mRNA of interest in human

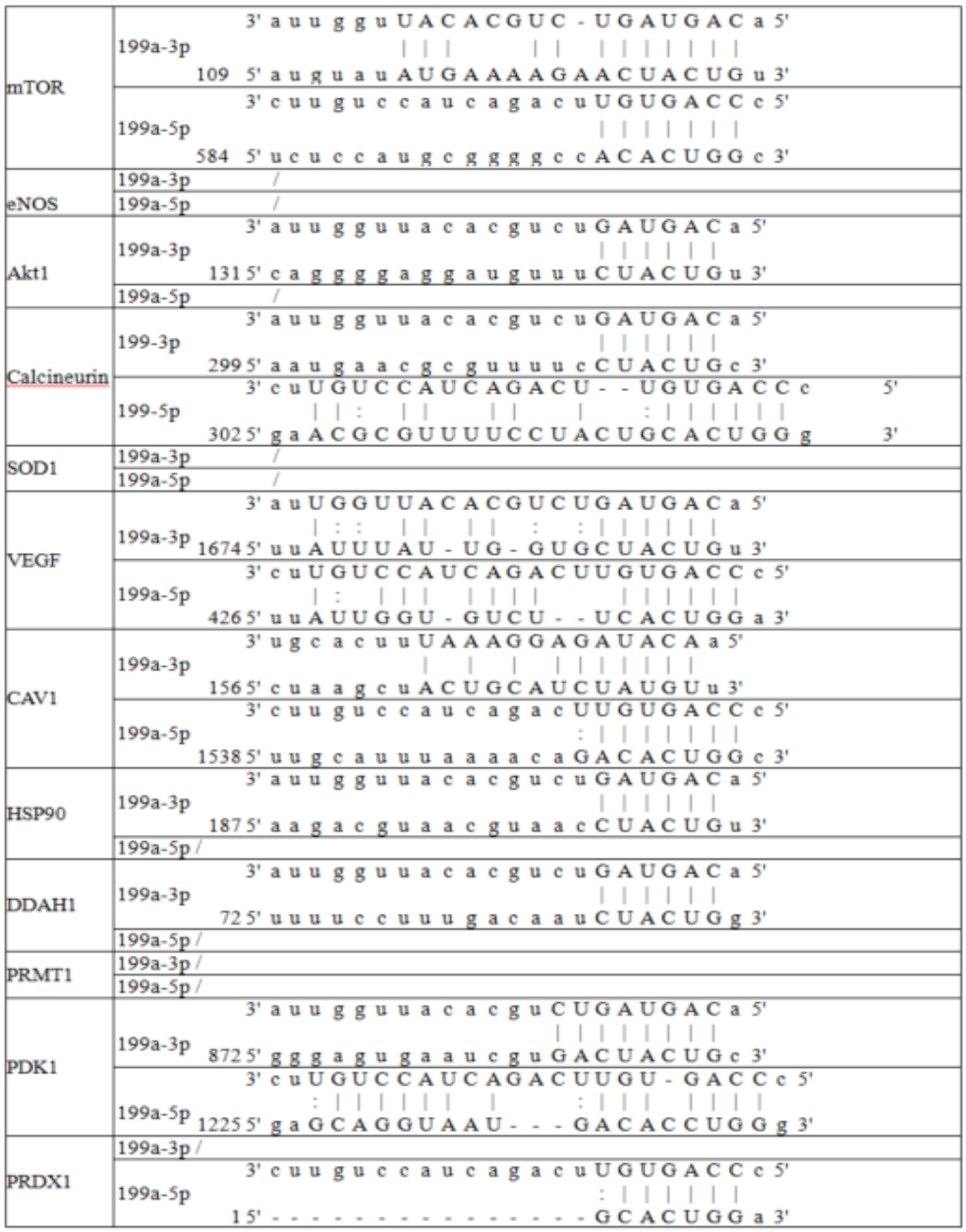

Table A2: Alignment between miR-199a family members and mRNA of interest in mouse

References

Reference List

(1) Lerman A, Zeiher AM. Endothelial function: cardiac events. Circulation 2005;111(3):363-368.
(2) Ozkor MA, Quyyumi AA. Endothelium-derived hyperpolarizing factor and vascular function. Cardiol Res Pract 2011;2011:156146.
(3) Dusting GJ, MacDonald PS. Prostacyclin and vascular function: implications for hypertension and atherosclerosis. Pharmacol Ther 1990;48(3):323-344.
(4) Altaany Z, Moccia F, Munaron L, Mancardi D, Wang R. Hydrogen sulfide and endothelial dysfunction: relationship with nitric oxide. Curr Med Chem 2014;21(32):3646-3661.
(5) Gomperts E, Belcher JD, Otterbein LE, Coates TD, Wood J, Skolnick BE et al. The role of carbon monoxide and heme oxygenase in the prevention of sickle cell disease vaso-occlusive crises. Am J Hematol 2017;92(6):569-582.
(6) Bohm F, Pernow J. The importance of endothelin-1 for vascular dysfunction in cardiovascular disease. Cardiovasc Res 2007;76(1):8-18.
(7) Watanabe T, Barker TA, Berk BC. Angiotensin II and the endothelium: diverse signals and effects. Hypertension 2005;45(2):163-169.
(8) Spijkers LJ, van den Akker RF, Janssen BJ, Debets JJ, De Mey JG, Stroes ES et al. Hypertension is associated with marked alterations in sphingolipid biology: a potential role for ceramide. PLoS One 2011;6(7):e21817.
(9) Rajagopalan S, Kurz S, Munzel T, Tarpey M, Freeman BA, Griendling KK et al. Angiotensin II-mediated hypertension in the rat increases vascular superoxide production via membrane NADH/NADPH oxidase activation. Contribution to alterations of vasomotor tone. J Clin Invest 1996;97(8):1916-1923.
(10) Lobysheva I, Rath G, Sekkali B, Bouzin C, Feron O, Gallez B et al. Moderate caveolin-1 downregulation prevents NADPH oxidase-dependent endothelial nitric oxide synthase uncoupling by angiotensin II in endothelial cells. Arterioscler Thromb Vasc Biol 2011;31(9):2098-2105.
(11) Arnal JF, el Amrani AI, Chatellier G, Menard J, Michel JB. Cardiac weight in hypertension induced by nitric oxide synthase blockade. Hypertension 1993;22(3):380-387.
(12) Haynes WG, Noon JP, Walker BR, Webb DJ. Inhibition of nitric oxide synthesis increases blood pressure in healthy humans. J Hypertens 1993;11(12):1375-1380.
(13) Vanhoutte PM, Zhao Y, Xu A, Leung SW. Thirty Years of Saying NO: Sources, Fate, Actions, and Misfortunes of the Endothelium-Derived Vasodilator Mediator. Circ Res 2016;119(2):375-396.
(14) Wadham C, Parker A, Wang L, Xia P. High glucose attenuates protein S-nitrosylation in endothelial cells: role of oxidative stress. Diabetes 2007;56(11):2715-2721.
(15) Bartesaghi S, Radi R. Fundamentals on the biochemistry of peroxynitrite and protein tyrosine nitration. Redox Biol 2018;14:618-625.

(16) Shiva S. Nitrite: A Physiological Store of Nitric Oxide and Modulator of Mitochondrial Function. Redox Biol 2013;1(1):40-44.
(17) Frerart F, Sonveaux P, Rath G, Smoos A, Meqor A, Charlier N et al. The acidic tumor microenvironment promotes the reconversion of nitrite into nitric oxide: towards a new and safe radiosensitizing strategy. Clin Cancer Res 2008;14(9):2768-2774.
(18) Greenacre SA, Ischiropoulos H. Tyrosine nitration: localisation, quantification, consequences for protein function and signal transduction. Free Radic Res 2001;34(6):541-581.
(19) Abdelmegeed MA, Song BJ. Functional roles of protein nitration in acute and chronic liver diseases. Oxid Med Cell Longev 2014;2014:149627.
(20) Forstermann U, Sessa WC. Nitric oxide synthases: regulation and function. Eur Heart J 2012;33(7):829-837d.
(21) Zhou L, Zhu DY. Neuronal nitric oxide synthase: structure, subcellular localization, regulation, and clinical implications. Nitric Oxide 2009;20(4):223-230.
(22) Forstermann U, Closs EI, Pollock JS, Nakane M, Schwarz P, Gath I et al. Nitric oxide synthase isozymes. Characterization, purification, molecular cloning, and functions. Hypertension 1994;23(6 Pt 2):1121-1131.
(23) Fehsel K, Jalowy A, Qi S, Burkart V, Hartmann B, Kolb H. Islet cell DNA is a target of inflammatory attack by nitric oxide. Diabetes 1993;42(3):496-500.
(24) Green DJ, Hopman MT, Padilla J, Laughlin MH, Thijssen DH. Vascular Adaptation to Exercise in Humans: Role of Hemodynamic Stimuli. Physiol Rev 2017;97(2):495-528.
(25) MacMicking JD, Nathan C, Hom G, Chartrain N, Fletcher DS, Trumbauer M et al. Altered responses to bacterial infection and endotoxic shock in mice lacking inducible nitric oxide synthase. Cell 1995;81(4):641-650.
(26) Lange M, Enkhbaatar P, Nakano Y, Traber DL. Role of nitric oxide in shock: the large animal perspective. Front Biosci (Landmark Ed) 2009;14:1979-1989.
(27) Marsden PA, Heng HH, Scherer SW, Stewart RJ, Hall AV, Shi XM et al. Structure and chromosomal localization of the human constitutive endothelial nitric oxide synthase gene. J Biol Chem 1993;268(23):17478-17488.
(28) Chan Y, Fish JE, D'Abreo C, Lin S, Robb GB, Teichert AM et al. The cell-specific expression of endothelial nitric-oxide synthase: a role for DNA methylation. J Biol Chem 2004;279(33):35087-35100.
(29) Krause BJ, Costello PM, Munoz-Urrutia E, Lillycrop KA, Hanson MA, Casanello P. Role of DNA methyltransferase 1 on the altered eNOS expression in human umbilical endothelium from intrauterine growth restricted fetuses. Epigenetics 2013;8(9):944-952.
(30) Searles CD. Transcriptional and posttranscriptional regulation of endothelial nitric oxide synthase expression. Am J Physiol Cell Physiol 2006;291(5):C803-C816.
(31) Laumonnier Y, Nadaud S, Agrapart M, Soubrier F. Characterization of an upstream enhancer region in the promoter of the human endothelial nitric-oxide synthase gene. J Biol Chem 2000;275(52):40732-40741.
(32) Jaenisch R, Bird A. Epigenetic regulation of gene expression: how the genome integrates intrinsic and environmental signals. Nat Genet 2003;33 Suppl:245-254.

(33) Venema RC, Nishida K, Alexander RW, Harrison DG, Murphy TJ. Organization of the bovine gene encoding the endothelial nitric oxide synthase. Biochim Biophys Acta 1994;1218(3):413-420.
(34) Anderson HD, Rahmutula D, Gardner DG. Tumor necrosis factor-alpha inhibits endothelial nitric-oxide synthase gene promoter activity in bovine aortic endothelial cells. J Biol Chem 2004;279(2):963-969.
(35) Cai H, Davis ME, Drummond GR, Harrison DG. Induction of endothelial NO synthase by hydrogen peroxide via a Ca(2+)/calmodulin-dependent protein kinase II/janus kinase 2-dependent pathway. Arterioscler Thromb Vasc Biol 2001;21(10):1571-1576.
(36) Hoffmann A, Gloe T, Pohl U. Hypoxia-induced upregulation of eNOS gene expression is redox-sensitive: a comparison between hypoxia and inhibitors of cell metabolism. J Cell Physiol 2001;188(1):33-44.
(37) Toporsian M, Govindaraju K, Nagi M, Eidelman D, Thibault G, Ward ME. Downregulation of endothelial nitric oxide synthase in rat aorta after prolonged hypoxia in vivo. Circ Res 2000;86(6):671-675.
(38) Moudgil R, Michelakis ED, Archer SL. Hypoxic pulmonary vasoconstriction. J Appl Physiol (1985) 2005;98(1):390-403.
(39) Zhang W, Yan L, Li Y, Chen W, Hu N, Wang H et al. Roles of miRNA-24 in regulating endothelial nitric oxide synthase expression and vascular endothelial cell proliferation. Mol Cell Biochem 2015;405(1-2):281-289.
(40) Sun HX, Zeng DY, Li RT, Pang RP, Yang H, Hu YL et al. Essential role of microRNA-155 in regulating endothelium-dependent vasorelaxation by targeting endothelial nitric oxide synthase. Hypertension 2012;60(6):1407-1414.
(41) el Azzouzi H., Leptidis S, Dirkx E, Hoeks J, van BB, Brand K et al. The hypoxia-inducible microRNA cluster miR-199a approximately 214 targets myocardial PPARdelta and impairs mitochondrial fatty acid oxidation. Cell Metab 2013;18(3):341-354.
(42) Ho JJ, Robb GB, Tai SC, Turgeon PJ, Mawji IA, Man HS et al. Active stabilization of human endothelial nitric oxide synthase mRNA by hnRNP E1 protects against antisense RNA and microRNAs. Mol Cell Biol 2013;33(10):2029-2046.
(43) Landmesser U, Dikalov S, Price SR, McCann L, Fukai T, Holland SM et al. Oxidation of tetrahydrobiopterin leads to uncoupling of endothelial cell nitric oxide synthase in hypertension. J Clin Invest 2003;111(8):1201-1209.
(44) Abdelghany TM, Ismail RS, Mansoor FA, Zweier JR, Lowe F, Zweier JL. Cigarette smoke constituents cause endothelial nitric oxide synthase dysfunction and uncoupling due to depletion of tetrahydrobiopterin with degradation of GTP cyclohydrolase. Nitric Oxide 2018;76:113-121.
(45) Daiber A, Xia N, Steven S, Oelze M, Hanf A, Kroller-Schon S et al. New Therapeutic Implications of Endothelial Nitric Oxide Synthase (eNOS) Function/Dysfunction in Cardiovascular Disease. Int J Mol Sci 2019;20(1).
(46) Chang F, Flavahan S, Flavahan NA. Potential pitfalls in analyzing structural uncoupling of eNOS: aging is not associated with increased enzyme monomerization. Am J Physiol Heart Circ Physiol 2019;316(1):H80-H88.

(47) Desjardins F, Lobysheva I, Pelat M, Gallez B, Feron O, Dessy C et al. Control of blood pressure variability in caveolin-1-deficient mice: role of nitric oxide identified in vivo through spectral analysis. Cardiovasc Res 2008;79:527-536.
(48) Balligand JL, Feron O, Dessy C. eNOS activation by physical forces: from short-term regulation of contraction to chronic remodeling of cardiovascular tissues. Physiol Rev 2009;89:481-534.
(49) Yang N, Ying C, Xu M, Zuo X, Ye X, Liu L et al. High-fat diet up-regulates caveolin-1 expression in aorta of diet-induced obese but not in diet-resistant rats. Cardiovasc Res 2007;76(1):167-174.
(50) Chen Z, Oliveira DS, Zimnicka AM, Jiang Y, Sharma T, Chen S et al. Reciprocal regulation of eNOS and caveolin-1 functions in endothelial cells. Mol Biol Cell 2018;29(10):1190-1202.
(51) Feron O, Dessy C, Moniotte S, Desager JP, Balligand JL. Hypercholesterolemia decreases nitric oxide production by promoting the interaction of caveolin and endothelial nitric oxide synthase. J Clin Invest 1999;103(6):897-905.
(52) Haque MM, Ray SS, Stuehr DJ. Phosphorylation Controls Endothelial Nitric-oxide Synthase by Regulating Its Conformational Dynamics. J Biol Chem 2016;291(44):23047-23057.
(53) Chen Y, Jiang B, Zhuang Y, Peng H, Chen W. Differential effects of heat shock protein 90 and serine 1179 phosphorylation on endothelial nitric oxide synthase activity and on its cofactors. PLoS One 2017;12(6):e0179978.
(54) Dimmeler S, Fleming I, Fisslthaler B, Hermann C, Busse R, Zeiher AM. Activation of nitric oxide synthase in endothelial cells by Akt-dependent phosphorylation. Nature 1999;399(6736):601-605.
(55) Brouet A, Sonveaux P, Dessy C, Balligand JL, Feron O. Hsp90 ensures the transition from the early Ca2+-dependent to the late phosphorylation-dependent activation of the endothelial nitric-oxide synthase in vascular endothelial growth factor-exposed endothelial cells. J Biol Chem 2001;276:32663-32669.
(56) Gao F, Gao E, Yue TL, Ohlstein EH, Lopez BL, Christopher TA et al. Nitric oxide mediates the antiapoptotic effect of insulin in myocardial ischemia-reperfusion: the roles of PI3-kinase, Akt, and endothelial nitric oxide synthase phosphorylation. Circulation 2002;105(12):1497-1502.
(57) Wang Y, Tian Z, Zang W, Jiang H, Li Y, Wang S et al. Exercise training reduces insulin resistance in postmyocardial infarction rats. Physiol Rep 2015;3(4).
(58) Kim F, Pham M, Maloney E, Rizzo NO, Morton GJ, Wisse BE et al. Vascular inflammation, insulin resistance, and reduced nitric oxide production precede the onset of peripheral insulin resistance. Arterioscler Thromb Vasc Biol 2008;28(11):1982-1988.
(59) Catry E, Neyrinck AM, Lobysheva I, Pachikian BD, Van HM, Cani PD et al. Nutritional depletion in n-3 PUFA in apoE knock-out mice: A new model of endothelial dysfunction associated with fatty liver disease. Mol Nutr Food Res 2016;60(10):2198-2207.
(60) Romero M, Leon-Gomez E, Lobysheva I, Rath G, Dogne JM, Feron O et al. Effects of BM-573 on Endothelial Dependent Relaxation and Increased Blood Pressure at Early Stages of Atherosclerosis. PLoS One 2016;11(3):e0152579.

(61) Kupatt C, Hinkel R, Vachenauer R, Horstkotte J, Raake P, Sandner T et al. VEGF165 transfection decreases postischemic NF-kappa B-dependent myocardial reperfusion injury in vivo: role of eNOS phosphorylation. FASEB J 2003;17(6):705-707.

(62) Somanath PR, Razorenova OV, Chen J, Byzova TV. Akt1 in endothelial cell and angiogenesis. Cell Cycle 2006;5:512-518.

(63) Garcia-Morales V, Luaces-Regueira M, Campos-Toimil M. The cAMP effectors PKA and Epac activate endothelial NO synthase through PI3K/Akt pathway in human endothelial cells. Biochem Pharmacol 2017;145:94-101.

(64) Erdogdu O, Nathanson D, Sjoholm A, Nystrom T, Zhang Q. Exendin-4 stimulates proliferation of human coronary artery endothelial cells through eNOS-, PKA- and PI3K/Akt-dependent pathways and requires GLP-1 receptor. Mol Cell Endocrinol 2010;325(1-2):26-35.

(65) Yang C, Talukder MA, Varadharaj S, Velayutham M, Zweier JL. Early ischaemic preconditioning requires Akt- and PKA-mediated activation of eNOS via serine1176 phosphorylation. Cardiovasc Res 2013;97(1):33-43.

(66) Morrow VA, Foufelle F, Connell JM, Petrie JR, Gould GW, Salt IP. Direct activation of AMP-activated protein kinase stimulates nitric-oxide synthesis in human aortic endothelial cells. J Biol Chem 2003;278(34):31629-31639.

(67) Murakami H, Murakami R, Kambe F, Cao X, Takahashi R, Asai T et al. Fenofibrate activates AMPK and increases eNOS phosphorylation in HUVEC. Biochem Biophys Res Commun 2006;341(4):973-978.

(68) Zippel N, Loot AE, Stingl H, Randriamboavonjy V, Fleming I, Fisslthaler B. Endothelial AMP-Activated Kinase alpha1 Phosphorylates eNOS on Thr495 and Decreases Endothelial NO Formation. Int J Mol Sci 2018;19(9).

(69) Schmitt CA, Heiss EH, Aristei Y, Severin T, Dirsch VM. Norfuraneol dephosphorylates eNOS at threonine 495 and enhances eNOS activity in human endothelial cells. Cardiovasc Res 2009;81(4):750-757.

(70) Kupatt C, Dessy C, Hinkel R, Raake P, Daneau G, Bouzin C et al. Heat shock protein 90 transfection reduces ischemia-reperfusion-induced myocardial dysfunction via reciprocal endothelial NO synthase serine 1177 phosphorylation and threonine 495 dephosphorylation. Arterioscler Thromb Vasc Biol 2004;24(8):1435-1441.

(71) Desjardins F, Delisle C, Gratton JP. Modulation of the cochaperone AHA1 regulates heat-shock protein 90 and endothelial NO synthase activation by vascular endothelial growth factor. Arterioscler Thromb Vasc Biol 2012;32(10):2484-2492.

(72) Guzik TJ, Mussa S, Gastaldi D, Sadowski J, Ratnatunga C, Pillai R et al. Mechanisms of increased vascular superoxide production in human diabetes mellitus: role of NAD(P)H oxidase and endothelial nitric oxide synthase. Circulation 2002;105(14):1656-1662.

(73) Cheang WS, Wong WT, Tian XY, Yang Q, Lee HK, He GW et al. Endothelial nitric oxide synthase enhancer reduces oxidative stress and restores endothelial function in db/db mice. Cardiovasc Res 2011;92(2):267-275.

(74) Oelze M, Daiber A, Brandes RP, Hortmann M, Wenzel P, Hink U et al. Nebivolol inhibits superoxide formation by NADPH oxidase and endothelial dysfunction in angiotensin II-treated rats. Hypertension 2006;48(4):677-684.
(75) Cai X, She M, Xu M, Chen H, Li J, Chen X et al. GLP-1 treatment protects endothelial cells from oxidative stress-induced autophagy and endothelial dysfunction. Int J Biol Sci 2018;14(12):1696-1708.
(76) Rahadian A, Fukuda D, Salim HM, Yagi S, Kusunose K, Yamada H et al. Canagliflozin Prevents Diabetes-Induced Vascular Dysfunction in ApoE-Deficient Mice. J Atheroscler Thromb 2020.
(77) Karbach S, Wenzel P, Waisman A, Munzel T, Daiber A. eNOS uncoupling in cardiovascular diseases--the role of oxidative stress and inflammation. Curr Pharm Des 2014;20(22):3579-3594.
(78) Zou MH, Hou XY, Shi CM, Nagata D, Walsh K, Cohen RA. Modulation by peroxynitrite of Akt- and AMP-activated kinase-dependent Ser1179 phosphorylation of endothelial nitric oxide synthase. J Biol Chem 2002;277(36):32552-32557.
(79) Hu C, Lu KT, Mukohda M, Davis DR, Faraci FM, Sigmund CD. Interference with PPARgamma in endothelium accelerates angiotensin II-induced endothelial dysfunction. Physiol Genomics 2016;48(2):124-134.
(80) Soliman E, Behairy SF, El-Maraghy NN, Elshazly SM. PPAR-gamma agonist, pioglitazone, reduced oxidative and endoplasmic reticulum stress associated with L-NAME-induced hypertension in rats. Life Sci 2019;239:117047.
(81) Mattagajasingh I, Kim CS, Naqvi A, Yamamori T, Hoffman TA, Jung SB et al. SIRT1 promotes endothelium-dependent vascular relaxation by activating endothelial nitric oxide synthase. Proc Natl Acad Sci U S A 2007;104(37):14855-14860.
(82) Zhang QJ, Wang Z, Chen HZ, Zhou S, Zheng W, Liu G et al. Endothelium-specific overexpression of class III deacetylase SIRT1 decreases atherosclerosis in apolipoprotein E-deficient mice. Cardiovasc Res 2008;80(2):191-199.
(83) Xia N, Strand S, Schlufter F, Siuda D, Reifenberg G, Kleinert H et al. Role of SIRT1 and FOXO factors in eNOS transcriptional activation by resveratrol. Nitric Oxide 2013;32:29-35.
(84) Ding M, Lei J, Han H, Li W, Qu Y, Fu E et al. SIRT1 protects against myocardial ischemia-reperfusion injury via activating eNOS in diabetic rats. Cardiovasc Diabetol 2015;14:143.
(85) Tarnow L, Hovind P, Teerlink T, Stehouwer CD, Parving HH. Elevated plasma asymmetric dimethylarginine as a marker of cardiovascular morbidity in early diabetic nephropathy in type 1 diabetes. Diabetes Care 2004;27(3):765-769.
(86) Achan V, Broadhead M, Malaki M, Whitley G, Leiper J, MacAllister R et al. Asymmetric dimethylarginine causes hypertension and cardiac dysfunction in humans and is actively metabolized by dimethylarginine dimethylaminohydrolase. Arterioscler Thromb Vasc Biol 2003;23(8):1455-1459.
(87) Chen Y, Xu X, Sheng M, Zhang X, Gu Q, Zheng Z. PRMT-1 and DDAHs-induced ADMA upregulation is involved in ROS- and RAS-mediated diabetic retinopathy. Exp Eye Res 2009;89(6):1028-1034.

(88) Pope AJ, Karuppiah K, Cardounel AJ. Role of the PRMT-DDAH-ADMA axis in the regulation of endothelial nitric oxide production. Pharmacol Res 2009;60(6):461-465.
(89) Leiper J, Nandi M. The therapeutic potential of targeting endogenous inhibitors of nitric oxide synthesis. Nat Rev Drug Discov 2011;10(4):277-291.
(90) Cooke JP. Does ADMA cause endothelial dysfunction? Arterioscler Thromb Vasc Biol 2000;20(9):2032-2037.
(91) Bae SW, Stuhlinger MC, Yoo HS, Yu KH, Park HK, Choi BY et al. Plasma asymmetric dimethylarginine concentrations in newly diagnosed patients with acute myocardial infarction or unstable angina pectoris during two weeks of medical treatment. Am J Cardiol 2005;95(6):729-733.
(92) Trittmann JK, Almazroue H, Jin Y, Nelin LD. DDAH1 regulates apoptosis and angiogenesis in human fetal pulmonary microvascular endothelial cells. Physiol Rep 2019;7(12):e14150.
(93) Kingwell BA. Nitric oxide-mediated metabolic regulation during exercise: effects of training in health and cardiovascular disease. FASEB J 2000;14(12):1685-1696.
(94) Davies PF. Hemodynamic shear stress and the endothelium in cardiovascular pathophysiology. Nat Clin Pract Cardiovasc Med 2009;6(1):16-26.
(95) Dumont O, Loufrani L, Henrion D. Key role of the NO-pathway and matrix metalloprotease-9 in high blood flow-induced remodeling of rat resistance arteries. Arterioscler Thromb Vasc Biol 2007;27(2):317-324.
(96) Parmar KM, Larman HB, Dai G, Zhang Y, Wang ET, Moorthy SN et al. Integration of flow-dependent endothelial phenotypes by Kruppel-like factor 2. J Clin Invest 2006;116(1):49-58.
(97) Young A, Wu W, Sun W, Benjamin LH, Wang N, Li YS et al. Flow activation of AMP-activated protein kinase in vascular endothelium leads to Kruppel-like factor 2 expression. Arterioscler Thromb Vasc Biol 2009;29(11):1902-1908.
(98) Topper JN, Gimbrone MA, Jr. Blood flow and vascular gene expression: fluid shear stress as a modulator of endothelial phenotype. Mol Med Today 1999;5(1):40-46.
(99) Dai G, Vaughn S, Zhang Y, Wang ET, Garcia-Cardena G, Gimbrone MA, Jr. Biomechanical forces in atherosclerosis-resistant vascular regions regulate endothelial redox balance via phosphoinositol 3-kinase/Akt-dependent activation of Nrf2. Circ Res 2007;101(7):723-733.
(100) Davies PF, Civelek M, Fang Y, Guerraty MA, Passerini AG. Endothelial heterogeneity associated with regional athero-susceptibility and adaptation to disturbed blood flow in vivo. Semin Thromb Hemost 2010;36(3):265-275.
(101) Hajra L, Evans AI, Chen M, Hyduk SJ, Collins T, Cybulsky MI. The NF-kappa B signal transduction pathway in aortic endothelial cells is primed for activation in regions predisposed to atherosclerotic lesion formation. Proc Natl Acad Sci U S A 2000;97(16):9052-9057.
(102) Glass CK, Witztum JL. Atherosclerosis. the road ahead. Cell 2001;104(4):503-516.
(103) Traub O, Berk BC. Laminar shear stress: mechanisms by which endothelial cells transduce an atheroprotective force. Arterioscler Thromb Vasc Biol 1998;18(5):677-685.

(104) Tardy Y, Resnick N, Nagel T, Gimbrone MA, Jr., Dewey CF, Jr. Shear stress gradients remodel endothelial monolayers in vitro via a cell proliferation-migration-loss cycle. Arterioscler Thromb Vasc Biol 1997;17(11):3102-3106.
(105) Givens C, Tzima E. Endothelial Mechanosignaling: Does One Sensor Fit All? Antioxid Redox Signal 2016;25(7):373-388.
(106) Ando J, Ohtsuka A, Korenaga R, Kawamura T, Kamiya A. Wall shear stress rather than shear rate regulates cytoplasmic Ca++ responses to flow in vascular endothelial cells. Biochem Biophys Res Commun 1993;190(3):716-723.
(107) Yamamoto K, Korenaga R, Kamiya A, Ando J. Fluid shear stress activates Ca(2+) influx into human endothelial cells via P2X4 purinoceptors. Circ Res 2000;87(5):385-391.
(108) Rodriguez I, Gonzalez M. Physiological mechanisms of vascular response induced by shear stress and effect of exercise in systemic and placental circulation. Front Pharmacol 2014;5:209.
(109) Cabral PD, Garvin JL. TRPV4 activation mediates flow-induced nitric oxide production in the rat thick ascending limb. Am J Physiol Renal Physiol 2014;307(6):F666-F672.
(110) Mendoza SA, Fang J, Gutterman DD, Wilcox DA, Bubolz AH, Li R et al. TRPV4-mediated endothelial Ca2+ influx and vasodilation in response to shear stress. Am J Physiol Heart Circ Physiol 2010;298(2):H466-H476.
(111) Iring A, Jin YJ, Albarran-Juarez J, Siragusa M, Wang S, Dancs PT et al. Shear stress-induced endothelial adrenomedullin signaling regulates vascular tone and blood pressure. J Clin Invest 2019;129(7):2775-2791.
(112) Albarran-Juarez J, Iring A, Wang S, Joseph S, Grimm M, Strilic B et al. Piezo1 and Gq/G11 promote endothelial inflammation depending on flow pattern and integrin activation. J Exp Med 2018;215(10):2655-2672.
(113) Zhang Y, Lee TS, Kolb EM, Sun K, Lu X, Sladek FM et al. AMP-activated protein kinase is involved in endothelial NO synthase activation in response to shear stress. Arterioscler Thromb Vasc Biol 2006;26(6):1281-1287.
(114) Florian JA, Kosky JR, Ainslie K, Pang Z, Dull RO, Tarbell JM. Heparan sulfate proteoglycan is a mechanosensor on endothelial cells. Circ Res 2003;93(10):e136-e142.
(115) Loufrani L, Henrion D. Role of the cytoskeleton in flow (shear stress)-induced dilation and remodeling in resistance arteries. Med Biol Eng Comput 2008;46(5):451-460.
(116) Chatzizisis YS, Coskun AU, Jonas M, Edelman ER, Feldman CL, Stone PH. Role of endothelial shear stress in the natural history of coronary atherosclerosis and vascular remodeling: molecular, cellular, and vascular behavior. J Am Coll Cardiol 2007;49(25):2379-2393.
(117) Mazumder B, Seshadri V, Fox PL. Translational control by the 3'-UTR: the ends specify the means. Trends Biochem Sci 2003;28(2):91-98.
(118) Weber M, Hagedorn CH, Harrison DG, Searles CD. Laminar shear stress and 3' polyadenylation of eNOS mRNA. Circ Res 2005;96(11):1161-1168.
(119) Carvalheira-Dos-Santos R, Delgado RM, Ferreira-Dos-Santos G, Vaz-Carneiro A. [Analysis of the Cochrane Review: Exercise-Based Cardiac Rehabilitation for

Coronary Heart Disease. Cochrane Database Syst Rev. 2016;1:CD001800]. Acta Med Port 2019;32(7-8):483-487.

(120) Goto C, Higashi Y, Kimura M, Noma K, Hara K, Nakagawa K et al. Effect of different intensities of exercise on endothelium-dependent vasodilation in humans: role of endothelium-dependent nitric oxide and oxidative stress. Circulation 2003;108(5):530-535.

(121) Goto C, Nishioka K, Umemura T, Jitsuiki D, Sakagutchi A, Kawamura M et al. Acute moderate-intensity exercise induces vasodilation through an increase in nitric oxide bioavailiability in humans. Am J Hypertens 2007;20(8):825-830.

(122) Wang J, Wolin MS, Hintze TH. Chronic exercise enhances endothelium-mediated dilation of epicardial coronary artery in conscious dogs. Circ Res 1993;73(5):829-838.

(123) Lee S, Park Y, Zhang C. Exercise Training Prevents Coronary Endothelial Dysfunction in Type 2 Diabetic Mice. Am J Biomed Sci 2011;3(4):241-252.

(124) Hambrecht R, Adams V, Erbs S, Linke A, Krankel N, Shu Y et al. Regular physical activity improves endothelial function in patients with coronary artery disease by increasing phosphorylation of endothelial nitric oxide synthase. Circulation 2003;107(25):3152-3158.

(125) Kingwell BA, Sherrard B, Jennings GL, Dart AM. Four weeks of cycle training increases basal production of nitric oxide from the forearm. Am J Physiol 1997;272(3 Pt 2):H1070-H1077.

(126) Clarkson P, Montgomery HE, Mullen MJ, Donald AE, Powe AJ, Bull T et al. Exercise training enhances endothelial function in young men. J Am Coll Cardiol 1999;33(5):1379-1385.

(127) Tinken TM, Thijssen DH, Hopkins N, Dawson EA, Cable NT, Green DJ. Shear stress mediates endothelial adaptations to exercise training in humans. Hypertension 2010;55(2):312-318.

(128) Tinken TM, Thijssen DH, Black MA, Cable NT, Green DJ. Time course of change in vasodilator function and capacity in response to exercise training in humans. J Physiol 2008;586(20):5003-5012.

(129) Nakamura M, Sadoshima J. Mechanisms of physiological and pathological cardiac hypertrophy. Nat Rev Cardiol 2018;15(7):387-407.

(130) Shimizu I, Minamino T. Physiological and pathological cardiac hypertrophy. J Mol Cell Cardiol 2016;97:245-262.

(131) Zhang S, Lu Y, Jiang C. Inhibition of histone demethylase JMJD1C attenuates cardiac hypertrophy and fibrosis induced by angiotensin II. J Recept Signal Transduct Res 2020;1-9.

(132) Sato PY, Chuprun JK, Schwartz M, Koch WJ. The evolving impact of g protein-coupled receptor kinases in cardiac health and disease. Physiol Rev 2015;95(2):377-404.

(133) Pantos C, Mourouzis I, Tsagoulis N, Markakis K, Galanopoulos G, Roukounakis N et al. Thyroid hormone at supra-physiological dose optimizes cardiac geometry and improves cardiac function in rats with old myocardial infarction. J Physiol Pharmacol 2009;60(3):49-56.

(134) Calvert JW, Condit ME, Aragon JP, Nicholson CK, Moody BF, Hood RL et al. Exercise protects against myocardial ischemia-reperfusion injury via stimulation of beta(3)-adrenergic receptors and increased nitric oxide signaling: role of nitrite and nitrosothiols. Circ Res 2011;108(12):1448-1458.
(135) Schiattarella GG, Hill JA. Inhibition of hypertrophy is a good therapeutic strategy in ventricular pressure overload. Circulation 2015;131(16):1435-1447.
(136) Anversa P, Levicky V, Beghi C, McDonald SL, Kikkawa Y. Morphometry of exercise-induced right ventricular hypertrophy in the rat. Circ Res 1983;52(1):57-64.
(137) Sano M, Minamino T, Toko H, Miyauchi H, Orimo M, Qin Y et al. p53-induced inhibition of Hif-1 causes cardiac dysfunction during pressure overload. Nature 2007;446(7134):444-448.
(138) Marcus ML, Koyanagi S, Harrison DG, Doty DB, Hiratzka LF, Eastham CL. Abnormalities in the coronary circulation that occur as a consequence of cardiac hypertrophy. Am J Med 1983;75(3A):62-66.
(139) Shimizu I, Minamino T, Toko H, Okada S, Ikeda H, Yasuda N et al. Excessive cardiac insulin signaling exacerbates systolic dysfunction induced by pressure overload in rodents. J Clin Invest 2010;120(5):1506-1514.
(140) Contard F, Koteliansky V, Marotte F, Dubus I, Rappaport L, Samuel JL. Specific alterations in the distribution of extracellular matrix components within rat myocardium during the development of pressure overload. Lab Invest 1991;64(1):65-75.
(141) Braunwald E. Heart failure. JACC Heart Fail 2013;1(1):1-20.
(142) Neppl RL, Wang DZ. The myriad essential roles of microRNAs in cardiovascular homeostasis and disease. Genes Dis 2014;1(1):18-39.
(143) Schwartz K, Boheler KR, de la Bastie D, Lompre AM, Mercadier JJ. Switches in cardiac muscle gene expression as a result of pressure and volume overload. Am J Physiol 1992;262(3 Pt 2):R364-R369.
(144) Taegtmeyer H, Sen S, Vela D. Return to the fetal gene program: a suggested metabolic link to gene expression in the heart. Ann N Y Acad Sci 2010;1188:191-198.
(145) Ke HY, Yang HY, Francis AJ, Collins TP, Surendran H, Alvarez-Laviada A et al. Changes in cellular Ca(2+) and Na(+) regulation during the progression towards heart failure in the guinea pig. J Physiol 2019.
(146) Carvalho BM, Bassani RA, Franchini KG, Bassani JW. Enhanced calcium mobilization in rat ventricular myocytes during the onset of pressure overload-induced hypertrophy. Am J Physiol Heart Circ Physiol 2006;291(4):H1803-H1813.
(147) de la Bastie D, Levitsky D, Rappaport L, Mercadier JJ, Marotte F, Wisnewsky C et al. Function of the sarcoplasmic reticulum and expression of its Ca2(+)-ATPase gene in pressure overload-induced cardiac hypertrophy in the rat. Circ Res 1990;66(2):554-564.
(148) Muller A, Simonides WS. Regulation of myocardial SERCA2a expression in ventricular hypertrophy and heart failure. Future Cardiol 2005;1(4):543-553.
(149) Lehman JJ, Barger PM, Kovacs A, Saffitz JE, Medeiros DM, Kelly DP. Peroxisome proliferator-activated receptor gamma coactivator-1 promotes cardiac mitochondrial biogenesis. J Clin Invest 2000;106(7):847-856.

(150) Matsui T, Li L, Wu JC, Cook SA, Nagoshi T, Picard MH et al. Phenotypic spectrum caused by transgenic overexpression of activated Akt in the heart. J Biol Chem 2002;277(25):22896-22901.
(151) Cong LN, Chen H, Li Y, Zhou L, McGibbon MA, Taylor SI et al. Physiological role of Akt in insulin-stimulated translocation of GLUT4 in transfected rat adipose cells. Mol Endocrinol 1997;11(13):1881-1890.
(152) Shiojima I, Sato K, Izumiya Y, Schiekofer S, Ito M, Liao R et al. Disruption of coordinated cardiac hypertrophy and angiogenesis contributes to the transition to heart failure. J Clin Invest 2005;115(8):2108-2118.
(153) Cross DA, Alessi DR, Cohen P, Andjelkovich M, Hemmings BA. Inhibition of glycogen synthase kinase-3 by insulin mediated by protein kinase B. Nature 1995;378(6559):785-789.
(154) Manning BD, Tee AR, Logsdon MN, Blenis J, Cantley LC. Identification of the tuberous sclerosis complex-2 tumor suppressor gene product tuberin as a target of the phosphoinositide 3-kinase/akt pathway. Mol Cell 2002;10(1):151-162.
(155) DeBosch B, Treskov I, Lupu TS, Weinheimer C, Kovacs A, Courtois M et al. Akt1 is required for physiological cardiac growth. Circulation 2006;113(17):2097-2104.
(156) Barger PM, Brandt JM, Leone TC, Weinheimer CJ, Kelly DP. Deactivation of peroxisome proliferator-activated receptor-alpha during cardiac hypertrophic growth. J Clin Invest 2000;105(12):1723-1730.
(157) Narkar VA, Downes M, Yu RT, Embler E, Wang YX, Banayo E et al. AMPK and PPARdelta agonists are exercise mimetics. Cell 2008;134(3):405-415.
(158) Burelle Y, Wambolt RB, Grist M, Parsons HL, Chow JC, Antler C et al. Regular exercise is associated with a protective metabolic phenotype in the rat heart. Am J Physiol Heart Circ Physiol 2004;287(3):H1055-H1063.
(159) Wu K, He J, Pu W, Peng Y. The Role of Exportin-5 in MicroRNA Biogenesis and Cancer. Genomics Proteomics Bioinformatics 2018;16(2):120-126.
(160) Desvignes T, Batzel P, Berezikov E, Eilbeck K, Eppig JT, McAndrews MS et al. miRNA Nomenclature: A View Incorporating Genetic Origins, Biosynthetic Pathways, and Sequence Variants. Trends Genet 2015;31(11):613-626.
(161) Catalanotto C, Cogoni C, Zardo G. MicroRNA in Control of Gene Expression: An Overview of Nuclear Functions. Int J Mol Sci 2016;17(10).
(162) Pan X, Wenzel A, Jensen LJ, Gorodkin J. Genome-wide identification of clusters of predicted microRNA binding sites as microRNA sponge candidates. PLoS One 2018;13(8):e0202369.
(163) Hammond SM. An overview of microRNAs. Adv Drug Deliv Rev 2015;87:3-14.
(164) Kozomara A, Griffiths-Jones S. miRBase: integrating microRNA annotation and deep-sequencing data. Nucleic Acids Res 2011;39(Database issue):D152-D157.
(165) Kozomara A, Griffiths-Jones S. miRBase: annotating high confidence microRNAs using deep sequencing data. Nucleic Acids Res 2014;42(Database issue):D68-D73.
(166) Kozomara A, Birgaoanu M, Griffiths-Jones S. miRBase: from microRNA sequences to function. Nucleic Acids Res 2019;47(D1):D155-D162.
(167) Okamura K, Phillips MD, Tyler DM, Duan H, Chou YT, Lai EC. The regulatory activity of microRNA* species has substantial influence on microRNA and 3' UTR evolution. Nat Struct Mol Biol 2008;15(4):354-363.

(168) O'Toole AS, Miller S, Haines N, Zink MC, Serra MJ. Comprehensive thermodynamic analysis of 3' double-nucleotide overhangs neighboring Watson-Crick terminal base pairs. Nucleic Acids Res 2006;34(11):3338-3344.
(169) Hwang HW, Wentzel EA, Mendell JT. A hexanucleotide element directs microRNA nuclear import. Science 2007;315(5808):97-100.
(170) Guo L, Lu Z. The fate of miRNA* strand through evolutionary analysis: implication for degradation as merely carrier strand or potential regulatory molecule? PLoS One 2010;5:e11387.
(171) Ro S, Park C, Young D, Sanders KM, Yan W. Tissue-dependent paired expression of miRNAs. Nucleic Acids Res 2007;35(17):5944-5953.
(172) You W, Zhang X, Ji M, Yu Y, Chen C, Xiong Y et al. MiR-152-5p as a microRNA passenger strand special functions in human gastric cancer cells. Int J Biol Sci 2018;14(6):644-653.
(173) Pink RC, Samuel P, Massa D, Caley DP, Brooks SA, Carter DR. The passenger strand, miR-21-3p, plays a role in mediating cisplatin resistance in ovarian cancer cells. Gynecol Oncol 2015;137(1):143-151.
(174) Zhao Y, Samal E, Srivastava D. Serum response factor regulates a muscle-specific microRNA that targets Hand2 during cardiogenesis. Nature 2005;436(7048):214-220.
(175) Park CY, Choi YS, McManus MT. Analysis of microRNA knockouts in mice. Hum Mol Genet 2010;19(R2):R169-R175.
(176) Mitchell PS, Parkin RK, Kroh EM, Fritz BR, Wyman SK, Pogosova-Agadjanyan EL et al. Circulating microRNAs as stable blood-based markers for cancer detection. Proc Natl Acad Sci U S A 2008;105(30):10513-10518.
(177) Turchinovich A, Weiz L, Langheinz A, Burwinkel B. Characterization of extracellular circulating microRNA. Nucleic Acids Res 2011;39(16):7223-7233.
(178) Akers JC, Gonda D, Kim R, Carter BS, Chen CC. Biogenesis of extracellular vesicles (EV): exosomes, microvesicles, retrovirus-like vesicles, and apoptotic bodies. J Neurooncol 2013;113(1):1-11.
(179) Raposo G, Stoorvogel W. Extracellular vesicles: exosomes, microvesicles, and friends. J Cell Biol 2013;200(4):373-383.
(180) Gibbings DJ, Ciaudo C, Erhardt M, Voinnet O. Multivesicular bodies associate with components of miRNA effector complexes and modulate miRNA activity. Nat Cell Biol 2009;11(9):1143-1149.
(181) Wang K, Zhang S, Weber J, Baxter D, Galas DJ. Export of microRNAs and microRNA-protective protein by mammalian cells. Nucleic Acids Res 2010;38(20):7248-7259.
(182) Vickers KC, Palmisano BT, Shoucri BM, Shamburek RD, Remaley AT. MicroRNAs are transported in plasma and delivered to recipient cells by high-density lipoproteins. Nat Cell Biol 2011;13(4):423-433.
(183) Arroyo JD, Chevillet JR, Kroh EM, Ruf IK, Pritchard CC, Gibson DF et al. Argonaute2 complexes carry a population of circulating microRNAs independent of vesicles in human plasma. Proc Natl Acad Sci U S A 2011;108(12):5003-5008.

(184) Koppers-Lalic D, Hackenberg M, Bijnsdorp IV, van Eijndhoven MAJ, Sadek P, Sie D et al. Nontemplated nucleotide additions distinguish the small RNA composition in cells from exosomes. Cell Rep 2014;8(6):1649-1658.
(185) Hergenreider E, Heydt S, Treguer K, Boettger T, Horrevoets AJ, Zeiher AM et al. Atheroprotective communication between endothelial cells and smooth muscle cells through miRNAs. Nat Cell Biol 2012;14(3):249-256.
(186) Florijn BW, Duijs JMGJ, Levels JH, Dallinga-Thie GM, Wang Y, Boing AN et al. Diabetic Nephropathy Alters the Distribution of Circulating Angiogenic MicroRNAs Among Extracellular Vesicles, HDL, and Ago-2. Diabetes 2019;68(12):2287-2300.
(187) Peng Y, Wang X, Guo Y, Peng F, Zheng N, He B et al. Pattern of cell-to-cell transfer of microRNA by gap junction and its effect on the proliferation of glioma cells. Cancer Sci 2019;110(6):1947-1958.
(188) Thuringer D, Boucher J, Jego G, Pernet N, Cronier L, Hammann A et al. Transfer of functional microRNAs between glioblastoma and microvascular endothelial cells through gap junctions. Oncotarget 2016;7(45):73925-73934.
(189) Thuringer D, Jego G, Berthenet K, Hammann A, Solary E, Garrido C. Gap junction-mediated transfer of miR-145-5p from microvascular endothelial cells to colon cancer cells inhibits angiogenesis. Oncotarget 2016;7(19):28160-28168.
(190) Fan X, Teng Y, Ye Z, Zhou Y, Tan WS. The effect of gap junction-mediated transfer of miR-200b on osteogenesis and angiogenesis in a co-culture of MSCs and HUVECs. J Cell Sci 2018;131(13).
(191) Lin XJ, Chong Y, Guo ZW, Xie C, Yang XJ, Zhang Q et al. A serum microRNA classifier for early detection of hepatocellular carcinoma: a multicentre, retrospective, longitudinal biomarker identification study with a nested case-control study. Lancet Oncol 2015;16(7):804-815.
(192) Pirola CJ, Fernandez GT, Castano GO, Mallardi P, San MJ, Mora Gonzalez Lopez LM et al. Circulating microRNA signature in non-alcoholic fatty liver disease: from serum non-coding RNAs to liver histology and disease pathogenesis. Gut 2015;64(5):800-812.
(193) Wang H, Chen F, Tong J, Li Y, Cai J, Wang Y et al. Circulating microRNAs as novel biomarkers for dilated cardiomyopathy. Cardiol J 2017;24(1):65-73.
(194) Dimassi S, Karkeni E, Laurant P, Tabka Z, Landrier JF, Riva C. Microparticle miRNAs as Biomarkers of Vascular Function and Inflammation Response to Aerobic Exercise in Obesity? Obesity (Silver Spring) 2018;26(10):1584-1593.
(195) Zeisel MB, Baumert TF. Clinical development of hepatitis C virus host-targeting agents. Lancet 2017;389(10070):674-675.
(196) Rupaimoole R, Slack FJ. MicroRNA therapeutics: towards a new era for the management of cancer and other diseases. Nat Rev Drug Discov 2017;16(3):203-222.
(197) Thum T, Gross C, Fiedler J, Fischer T, Kissler S, Bussen M et al. MicroRNA-21 contributes to myocardial disease by stimulating MAP kinase signalling in fibroblasts. Nature 2008;456(7224):980-984.

(198) Montgomery RL, Hullinger TG, Semus HM, Dickinson BA, Seto AG, Lynch JM et al. Therapeutic inhibition of miR-208a improves cardiac function and survival during heart failure. Circulation 2011;124(14):1537-1547.
(199) Trajkovski M, Hausser J, Soutschek J, Bhat B, Akin A, Zavolan M et al. MicroRNAs 103 and 107 regulate insulin sensitivity. Nature 2011;474(7353):649-653.
(200) Ai P, Shen B, Pan H, Chen K, Zheng J, Liu F. MiR-411 suppressed vein wall fibrosis by downregulating MMP-2 via targeting HIF-1alpha. J Thromb Thrombolysis 2018;45(2):264-273.
(201) Belmont PJ, Chen WJ, Thuerauf DJ, Glembotski CC. Regulation of microRNA expression in the heart by the ATF6 branch of the ER stress response. J Mol Cell Cardiol 2012;52(5):1176-1182.
(202) Suarez Y, Fernandez-Hernando C, Pober JS, Sessa WC. Dicer dependent microRNAs regulate gene expression and functions in human endothelial cells. Circ Res 2007;100(8):1164-1173.
(203) Kuehbacher A, Urbich C, Zeiher AM, Dimmeler S. Role of Dicer and Drosha for endothelial microRNA expression and angiogenesis. Circ Res 2007;101(1):59-68.
(204) Cichon C, Sabharwal H, Ruter C, Schmidt MA. MicroRNAs regulate tight junction proteins and modulate epithelial/endothelial barrier functions. Tissue Barriers 2014;2(4):e944446.
(205) Chatterjee V, Beard RS, Jr., Reynolds JJ, Haines R, Guo M, Rubin M et al. MicroRNA-147b regulates vascular endothelial barrier function by targeting ADAM15 expression. PLoS One 2014;9(10):e110286.
(206) Zeng Z, Li Y, Pan Y, Lan X, Song F, Sun J et al. Cancer-derived exosomal miR-25-3p promotes pre-metastatic niche formation by inducing vascular permeability and angiogenesis. Nat Commun 2018;9(1):5395.
(207) Muramatsu F, Kidoya H, Naito H, Sakimoto S, Takakura N. microRNA-125b inhibits tube formation of blood vessels through translational suppression of VE-cadherin. Oncogene 2013;32(4):414-421.
(208) Liu P, Jia SB, Shi JM, Li WJ, Tang LS, Zhu XH et al. LncRNA-MALAT1 promotes neovascularization in diabetic retinopathy through regulating miR-125b/VE-cadherin axis. Biosci Rep 2019;39(5).
(209) Hu XQ, Dasgupta C, Xiao J, Yang S, Zhang L. Long-term high altitude hypoxia during gestation suppresses large conductance Ca(2+) -activated K(+) channel function in uterine arteries: a causal role for microRNA-210. J Physiol 2018;596(23):5891-5906.
(210) DuPont JJ, McCurley A, Davel AP, McCarthy J, Bender SB, Hong K et al. Vascular mineralocorticoid receptor regulates microRNA-155 to promote vasoconstriction and rising blood pressure with aging. JCI Insight 2016;1(14):e88942.
(211) Li L, Liu M, He L, Wang S, Cui S. Baicalin relieves TNF-alpha-evoked injury in human aortic endothelial cells by up-regulation of miR-145. Phytother Res 2019.
(212) Dews M, Homayouni A, Yu D, Murphy D, Sevignani C, Wentzel E et al. Augmentation of tumor angiogenesis by a Myc-activated microRNA cluster. Nat Genet 2006;38(9):1060-1065.

(213) Bonauer A, Carmona G, Iwasaki M, Mione M, Koyanagi M, Fischer A et al. MicroRNA-92a controls angiogenesis and functional recovery of ischemic tissues in mice. Science 2009;324(5935):1710-1713.
(214) Chen LY, Wang X, Qu XL, Pan LN, Wang ZY, Lu YH et al. Activation of the STAT3/microRNA-21 pathway participates in angiotensin II-induced angiogenesis. J Cell Physiol 2019;234(11):19640-19654.
(215) Lu JM, Zhang ZZ, Ma X, Fang SF, Qin XH. Repression of microRNA-21 inhibits retinal vascular endothelial cell growth and angiogenesis via PTEN dependent-PI3K/Akt/VEGF signaling pathway in diabetic retinopathy. Exp Eye Res 2020;190:107886.
(216) Fiedler J, Jazbutyte V, Kirchmaier BC, Gupta SK, Lorenzen J, Hartmann D et al. MicroRNA-24 regulates vascularity after myocardial infarction. Circulation 2011;124(6):720-730.
(217) Fiedler J, Thum T. MicroRNAs in myocardial infarction. Arterioscler Thromb Vasc Biol 2013;33(2):201-205.
(218) Wang S, Aurora AB, Johnson BA, Qi X, McAnally J, Hill JA et al. The endothelial-specific microRNA miR-126 governs vascular integrity and angiogenesis. Dev Cell 2008;15(2):261-271.
(219) Harris TA, Yamakuchi M, Ferlito M, Mendell JT, Lowenstein CJ. MicroRNA-126 regulates endothelial expression of vascular cell adhesion molecule 1. Proc Natl Acad Sci U S A 2008;105(5):1516-1521.
(220) Zernecke A, Bidzhekov K, Noels H, Shagdarsuren E, Gan L, Denecke B et al. Delivery of microRNA-126 by apoptotic bodies induces CXCL12-dependent vascular protection. Sci Signal 2009;2(100):ra81.
(221) Fasanaro P, D'Alessandra Y, Di S, V, Melchionna R, Romani S, Pompilio G et al. MicroRNA-210 modulates endothelial cell response to hypoxia and inhibits the receptor tyrosine kinase ligand Ephrin-A3. J Biol Chem 2008;283(23):15878-15883.
(222) Cicchillitti L, Di S, V, Isaia E, Crimaldi L, Fasanaro P, Ambrosino V et al. Hypoxia-inducible factor 1-alpha induces miR-210 in normoxic differentiating myoblasts. J Biol Chem 2012;287(53):44761-44771.
(223) Xiao F, Qiu H, Zhou L, Shen X, Yang L, Ding K. WSS25 inhibits Dicer, downregulating microRNA-210, which targets Ephrin-A3, to suppress human microvascular endothelial cell (HMEC-1) tube formation. Glycobiology 2013;23(5):524-535.
(224) Yi F, Shang Y, Li B, Dai S, Wu W, Cheng L et al. MicroRNA-193-5p modulates angiogenesis through IGF2 in type 2 diabetic cardiomyopathy. Biochem Biophys Res Commun 2017;491(4):876-882.
(225) Lee DY, Deng Z, Wang CH, Yang BB. MicroRNA-378 promotes cell survival, tumor growth, and angiogenesis by targeting SuFu and Fus-1 expression. Proc Natl Acad Sci U S A 2007;104(51):20350-20355.
(226) Hua Z, Lv Q, Ye W, Wong CK, Cai G, Gu D et al. MiRNA-directed regulation of VEGF and other angiogenic factors under hypoxia. PLoS One 2006;1:e116.
(227) Poliseno L, Tuccoli A, Mariani L, Evangelista M, Citti L, Woods K et al. MicroRNAs modulate the angiogenic properties of HUVECs. Blood 2006;108(9):3068-3071.

(228) Jeyapalan Z, Deng Z, Shatseva T, Fang L, He C, Yang BB. Expression of CD44 3'-untranslated region regulates endogenous microRNA functions in tumorigenesis and angiogenesis. Nucleic Acids Res 2011;39(8):3026-3041.
(229) Ho JJ, Metcalf JL, Yan MS, Turgeon PJ, Wang JJ, Chalsev M et al. Functional importance of Dicer protein in the adaptive cellular response to hypoxia. J Biol Chem 2012;287(34):29003-29020.
(230) Wu C, So J, Davis-Dusenbery BN, Qi HH, Bloch DB, Shi Y et al. Hypoxia potentiates microRNA-mediated gene silencing through posttranslational modification of Argonaute2. Mol Cell Biol 2011;31(23):4760-4774.
(231) Bruning U, Cerone L, Neufeld Z, Fitzpatrick SF, Cheong A, Scholz CC et al. MicroRNA-155 promotes resolution of hypoxia-inducible factor 1alpha activity during prolonged hypoxia. Mol Cell Biol 2011;31(19):4087-4096.
(232) Greco S, Gaetano C, Martelli F. HypoxamiR regulation and function in ischemic cardiovascular diseases. Antioxid Redox Signal 2014;21(8):1202-1219.
(233) Jiang X, Tsitsiou E, Herrick SE, Lindsay MA. MicroRNAs and the regulation of fibrosis. FEBS J 2010;277(9):2015-2021.
(234) Espinoza-Lewis RA, Wang DZ. MicroRNAs in heart development. Curr Top Dev Biol 2012;100:279-317.
(235) Fang Y, Shi C, Manduchi E, Civelek M, Davies PF. MicroRNA-10a regulation of proinflammatory phenotype in athero-susceptible endothelium in vivo and in vitro. Proc Natl Acad Sci U S A 2010;107(30):13450-13455.
(236) Demolli S, Doebele C, Doddaballapur A, Lang V, Fisslthaler B, Chavakis E et al. MicroRNA-30 mediates anti-inflammatory effects of shear stress and KLF2 via repression of angiopoietin 2. J Mol Cell Cardiol 2015;88:111-119.
(237) Wang KC, Garmire LX, Young A, Nguyen P, Trinh A, Subramaniam S et al. Role of microRNA-23b in flow-regulation of Rb phosphorylation and endothelial cell growth. Proc Natl Acad Sci U S A 2010;107(7):3234-3239.
(238) Qin X, Wang X, Wang Y, Tang Z, Cui Q, Xi J et al. MicroRNA-19a mediates the suppressive effect of laminar flow on cyclin D1 expression in human umbilical vein endothelial cells. Proc Natl Acad Sci U S A 2010;107(7):3240-3244.
(239) Schober A, Nazari-Jahantigh M, Wei Y, Bidzhekov K, Gremse F, Grommes J et al. MicroRNA-126-5p promotes endothelial proliferation and limits atherosclerosis by suppressing Dlk1. Nat Med 2014;20(4):368-376.
(240) Weber M, Baker MB, Moore JP, Searles CD. MiR-21 is induced in endothelial cells by shear stress and modulates apoptosis and eNOS activity. Biochem Biophys Res Commun 2010;393(4):643-648.
(241) Wu W, Xiao H, Laguna-Fernandez A, Villarreal G, Jr., Wang KC, Geary GG et al. Flow-Dependent Regulation of Kruppel-Like Factor 2 Is Mediated by MicroRNA-92a. Circulation 2011;124(5):633-641.
(242) Loyer X, Potteaux S, Vion AC, Guerin CL, Boulkroun S, Rautou PE et al. Inhibition of microRNA-92a prevents endothelial dysfunction and atherosclerosis in mice. Circ Res 2014;114(3):434-443.
(243) Son DJ, Kumar S, Takabe W, Kim CW, Ni CW, Alberts-Grill N et al. The atypical mechanosensitive microRNA-712 derived from pre-ribosomal RNA induces endothelial inflammation and atherosclerosis. Nat Commun 2013;4:3000.

(244) Ni CW, Qiu H, Jo H. MicroRNA-663 upregulated by oscillatory shear stress plays a role in inflammatory response of endothelial cells. Am J Physiol Heart Circ Physiol 2011;300(5):H1762-H1769.
(245) Bommer GT, Gerin I, Feng Y, Kaczorowski AJ, Kuick R, Love RE et al. p53-mediated activation of miRNA34 candidate tumor-suppressor genes. Curr Biol 2007;17(15):1298-1307.
(246) Fan W, Fang R, Wu X, Liu J, Feng M, Dai G et al. Shear-sensitive microRNA-34a modulates flow-dependent regulation of endothelial inflammation. J Cell Sci 2015;128(1):70-80.
(247) Hata A. Functions of microRNAs in cardiovascular biology and disease. Annu Rev Physiol 2013;75:69-93.
(248) Chen J, Wang DZ. microRNAs in cardiovascular development. J Mol Cell Cardiol 2012;52(5):949-957.
(249) Castaldi A, Zaglia T, Di M, V, Carullo P, Viggiani G, Borile G et al. MicroRNA-133 modulates the beta1-adrenergic receptor transduction cascade. Circ Res 2014;115(2):273-283.
(250) Di M, V, Crasto S, Colombo FS, Di PE, Catalucci D. Wnt signalling mediates miR-133a nuclear re-localization for the transcriptional control of Dnmt3b in cardiac cells. Sci Rep 2019;9(1):9320.
(251) van Rooij E., Sutherland LB, Thatcher JE, DiMaio JM, Naseem RH, Marshall WS et al. Dysregulation of microRNAs after myocardial infarction reveals a role of miR-29 in cardiac fibrosis. Proc Natl Acad Sci U S A 2008;105:13027-13032.
(252) Zhu ML, Yin YL, Ping S, Yu HY, Wan GR, Jian X et al. Berberine promotes ischemia-induced angiogenesis in mice heart via upregulation of microRNA-29b. Clin Exp Hypertens 2017;39(7):672-679.
(253) Arif M, Pandey R, Alam P, Jiang S, Sadayappan S, Paul A et al. MicroRNA-210-mediated proliferation, survival, and angiogenesis promote cardiac repair post myocardial infarction in rodents. J Mol Med (Berl) 2017;95(12):1369-1385.
(254) Watanabe K, Narumi T, Watanabe T, Otaki Y, Takahashi T, Aono T et al. The association between microRNA-21 and hypertension-induced cardiac remodeling. PLoS One 2020;15(2):e0226053.
(255) Nie X, Fan J, Li H, Yin Z, Zhao Y, Dai B et al. miR-217 Promotes Cardiac Hypertrophy and Dysfunction by Targeting PTEN. Mol Ther Nucleic Acids 2018;12:254-266.
(256) Soci UP, Fernandes T, Hashimoto NY, Mota GF, Amadeu MA, Rosa KT et al. MicroRNAs 29 are involved in the improvement of ventricular compliance promoted by aerobic exercise training in rats. Physiol Genomics 2011;43(11):665-673.
(257) Xiao L, He H, Ma L, Da M, Cheng S, Duan Y et al. Effects of miR-29a and miR-101a Expression on Myocardial Interstitial Collagen Generation After Aerobic Exercise in Myocardial-infarcted Rats. Arch Med Res 2017;48(1):27-34.
(258) Liu X, Xiao J, Zhu H, Wei X, Platt C, Damilano F et al. miR-222 is necessary for exercise-induced cardiac growth and protects against pathological cardiac remodeling. Cell Metab 2015;21(4):584-595.

(259) Ghorbanzadeh V, Mohammadi M, Dariushnejad H, Abhari A, Chodari L, Mohaddes G. Cardioprotective Effect of Crocin Combined with Voluntary Exercise in Rat: Role of Mir-126 and Mir-210 in Heart Angiogenesis. Arq Bras Cardiol 2017;109(1):54-62.

(260) Faccini J, Ruidavets JB, Cordelier P, Martins F, Maoret JJ, Bongard V et al. Circulating miR-155, miR-145 and let-7c as diagnostic biomarkers of the coronary artery disease. Sci Rep 2017;7:42916.

(261) Shi J, Liu H, Wang H, Kong X. MicroRNA Expression Signature in Degenerative Aortic Stenosis. Biomed Res Int 2016;2016:4682172.

(262) Gigante B, Papa L, Bye A, Kunderfranco P, Viviani C, Roncarati R et al. MicroRNA signatures predict early major coronary events in middle-aged men and women. Cell Death Dis 2020;11(1):74.

(263) Yi R, O'Carroll D, Pasolli HA, Zhang Z, Dietrich FS, Tarakhovsky A et al. Morphogenesis in skin is governed by discrete sets of differentially expressed microRNAs. Nat Genet 2006;38(3):356-362.

(264) Fischer L, Hummel M, Korfel A, Lenze D, Joehrens K, Thiel E. Differential micro-RNA expression in primary CNS and nodal diffuse large B-cell lymphomas. Neuro Oncol 2011;13(10):1090-1098.

(265) van Rooij E., Sutherland LB, Liu N, Williams AH, McAnally J, Gerard RD et al. A signature pattern of stress-responsive microRNAs that can evoke cardiac hypertrophy and heart failure. Proc Natl Acad Sci U S A 2006;103:18255-18260.

(266) Lee YB, Bantounas I, Lee DY, Phylactou L, Caldwell MA, Uney JB. Twist-1 regulates the miR-199a/214 cluster during development. Nucleic Acids Res 2009;37(1):123-128.

(267) Baumgarten A, Bang C, Tschirner A, Engelmann A, Adams V, von HS et al. TWIST1 regulates the activity of ubiquitin proteasome system via the miR-199/214 cluster in human end-stage dilated cardiomyopathy. Int J Cardiol 2013;168(2):1447-1452.

(268) Migliore C, Petrelli A, Ghiso E, Corso S, Capparuccia L, Eramo A et al. MicroRNAs impair MET-mediated invasive growth. Cancer Res 2008;68(24):10128-10136.

(269) Liu C, Xing M, Wang L, Zhang K. miR-199a-3p downregulation in thyroid tissues is associated with invasion and metastasis of papillary thyroid carcinoma. Br J Biomed Sci 2017;74(2):90-94.

(270) Kinose Y, Sawada K, Nakamura K, Sawada I, Toda A, Nakatsuka E et al. The hypoxia-related microRNA miR-199a-3p displays tumor suppressor functions in ovarian carcinoma. Oncotarget 2015;6(13):11342-11356.

(271) Callegari E, D'Abundo L, Guerriero P, Simioni C, Elamin BK, Russo M et al. miR-199a-3p Modulates MTOR and PAK4 Pathways and Inhibits Tumor Growth in a Hepatocellular Carcinoma Transgenic Mouse Model. Mol Ther Nucleic Acids 2018;11:485-493.

(272) Ghosh A, Dasgupta D, Ghosh A, Roychoudhury S, Kumar D, Gorain M et al. MiRNA199a-3p suppresses tumor growth, migration, invasion and angiogenesis in hepatocellular carcinoma by targeting VEGFA, VEGFR1, VEGFR2, HGF and MMP2. Cell Death Dis 2017;8(3):e2706.

(273) Shen L, Sun C, Li Y, Li X, Sun T, Liu C et al. MicroRNA-199a-3p suppresses glioma cell proliferation by regulating the AKT/mTOR signaling pathway. Tumour Biol 2015;36(9):6929-6938.
(274) Qu Y, Huang X, Li Z, Liu J, Wu J, Chen D et al. miR-199a-3p inhibits aurora kinase A and attenuates prostate cancer growth: new avenue for prostate cancer treatment. Am J Pathol 2014;184(5):1541-1549.
(275) Aravalli RN. Development of MicroRNA Therapeutics for Hepatocellular Carcinoma. Diagnostics (Basel) 2013;3(1):170-191.
(276) Shatseva T, Lee DY, Deng Z, Yang BB. MicroRNA miR-199a-3p regulates cell proliferation and survival by targeting caveolin-2. J Cell Sci 2011;124(Pt 16):2826-2836.
(277) Dolganiuc A, Petrasek J, Kodys K, Catalano D, Mandrekar P, Velayudham A et al. MicroRNA expression profile in Lieber-DeCarli diet-induced alcoholic and methionine choline deficient diet-induced nonalcoholic steatohepatitis models in mice. Alcohol Clin Exp Res 2009;33(10):1704-1710.
(278) Santhakumar D, Forster T, Laqtom NN, Fragkoudis R, Dickinson P, Abreu-Goodger C et al. Combined agonist-antagonist genome-wide functional screening identifies broadly active antiviral microRNAs. Proc Natl Acad Sci U S A 2010;107(31):13830-13835.
(279) Zhu H, Leung SW. Identification of microRNA biomarkers in type 2 diabetes: a meta-analysis of controlled profiling studies. Diabetologia 2015;58(5):900-911.
(280) Gu N, You L, Shi C, Yang L, Pang L, Cui X et al. Expression of miR-199a-3p in human adipocytes is regulated by free fatty acids and adipokines. Mol Med Rep 2016;14(2):1180-1186.
(281) Gao Y, Cao Y, Cui X, Wang X, Zhou Y, Huang F et al. miR-199a-3p regulates brown adipocyte differentiation through mTOR signaling pathway. Mol Cell Endocrinol 2018;476:155-164.
(282) Akhtar N, Haqqi TM. MicroRNA-199a* regulates the expression of cyclooxygenase-2 in human chondrocytes. Ann Rheum Dis 2012;71(6):1073-1080.
(283) Yang H, Kong W, He L, Zhao JJ, O'Donnell JD, Wang J et al. MicroRNA expression profiling in human ovarian cancer: miR-214 induces cell survival and cisplatin resistance by targeting PTEN. Cancer Res 2008;68(2):425-433.
(284) Lu RH, Xiao ZQ, Zhou JD, Yin CQ, Chen ZZ, Tang FJ et al. MiR-199a-5p represses the stemness of cutaneous squamous cell carcinoma stem cells by targeting Sirt1 and CD44ICD cleavage signaling. Cell Cycle 2020;19(1):1-14.
(285) Li W, Wang L, Ji XB, Wang LH, Ge X, Liu WT et al. MiR-199a Inhibits Tumor Growth and Attenuates Chemoresistance by Targeting K-RAS via AKT and ERK Signalings. Front Oncol 2019;9:1071.
(286) Gu S, Chan WY. Flexible and versatile as a chameleon-sophisticated functions of microRNA-199a. Int J Mol Sci 2012;13:8449-8466.
(287) Dai L, Lou W, Zhu J, Zhou X, Di W. MiR-199a inhibits the angiogenic potential of endometrial stromal cells under hypoxia by targeting HIF-1alpha/VEGF pathway. Int J Clin Exp Pathol 2015;8(5):4735-4744.

(288) Hsu CY, Hsieh TH, Tsai CF, Tsai HP, Chen HS, Chang Y et al. miRNA-199a-5p regulates VEGFA in endometrial mesenchymal stem cells and contributes to the pathogenesis of endometriosis. J Pathol 2014;232:330-343.
(289) Ding G, Huang G, Liu HD, Liang HX, Ni YF, Ding ZH et al. MiR-199a suppresses the hypoxia-induced proliferation of non-small cell lung cancer cells through targeting HIF1alpha. Mol Cell Biochem 2013;384(1-2):173-180.
(290) Wang LM, Zhang LL, Wang LW, Zhu L, Ma XX. Influence of miR-199a on rats with non-small cell lung cancer via regulating the HIF-1alpha/VEGF signaling pathway. Eur Rev Med Pharmacol Sci 2019;23(23):10363-10369.
(291) Liu X, Yao B, Wu Z. miRNA-199a-5p suppresses proliferation and invasion by directly targeting NF-kappaB1 in human ovarian cancer cells. Oncol Lett 2018;16(4):4543-4550.
(292) Chen J, Gong X, Huang L, Chen P, Wang T, Zhou W et al. MiR-199a-5p regulates sirtuin1 and PI3K in the rat hippocampus with intrauterine growth restriction. Sci Rep 2018;8(1):13813.
(293) Qi XB, Jia B, Wang W, Xu GH, Guo JC, Li X et al. Role of miR-199a-5p in osteoblast differentiation by targeting TET2. Gene 2020;726:144193.
(294) Zhang C, Ye B, Wei J, Wang Q, Xu C, Yu G. MiR-199a-5p regulates rat liver regeneration and hepatocyte proliferation by targeting TNF-alpha TNFR1/TRADD/CASPASE8/CASPASE3 signalling pathway. Artif Cells Nanomed Biotechnol 2019;47(1):4110-4118.
(295) He L, Tang M, Xiao T, Liu H, Liu W, Li G et al. Obesity-Associated miR-199a/214 Cluster Inhibits Adipose Browning via PRDM16-PGC-1alpha Transcriptional Network. Diabetes 2018;67(12):2585-2600.
(296) Murakami Y, Toyoda H, Tanaka M, Kuroda M, Harada Y, Matsuda F et al. The progression of liver fibrosis is related with overexpression of the miR-199 and 200 families. PLoS One 2011;6(1):e16081.
(297) Razani B, Zhang XL, Bitzer M, von GG, Bottinger EP, Lisanti MP. Caveolin-1 regulates transforming growth factor (TGF)-beta/SMAD signaling through an interaction with the TGF-beta type I receptor. J Biol Chem 2001;276(9):6727-6738.
(298) Lino Cardenas CL, Henaoui IS, Courcot E, Roderburg C, Cauffiez C, Aubert S et al. miR-199a-5p Is upregulated during fibrogenic response to tissue injury and mediates TGFbeta-induced lung fibroblast activation by targeting caveolin-1. PLoS Genet 2013;9(2):e1003291.
(299) Jansen F, Yang X, Proebsting S, Hoelscher M, Przybilla D, Baumann K et al. MicroRNA expression in circulating microvesicles predicts cardiovascular events in patients with coronary artery disease. J Am Heart Assoc 2014;3(6):e001249.
(300) Zanotti S, Gibertini S, Blasevich F, Bragato C, Ruggieri A, Saredi S et al. Exosomes and exosomal miRNAs from muscle-derived fibroblasts promote skeletal muscle fibrosis. Matrix Biol 2018;74:77-100.
(301) Wang C, Zhu G, He W, Yin H, Lin F, Gou X et al. BMSCs protect against renal ischemia-reperfusion injury by secreting exosomes loaded with miR-199a-5p that target BIP to inhibit endoplasmic reticulum stress at the very early reperfusion stages. FASEB J 2019;33(4):5440-5456.

(302) Yu Y, Zhou H, Xiong Y, Liu J. Exosomal miR-199a-5p derived from endothelial cells attenuates apoptosis and inflammation in neural cells by inhibiting endoplasmic reticulum stress. Brain Res 2020;1726:146515.

(303) Rane S, He M, Sayed D, Vashistha H, Malhotra A, Sadoshima J et al. Downregulation of miR-199a derepresses hypoxia-inducible factor-1alpha and Sirtuin 1 and recapitulates hypoxia preconditioning in cardiac myocytes. Circ Res 2009;104(7):879-886.

(304) Haghikia A, Missol-Kolka E, Tsikas D, Venturini L, Brundiers S, Castoldi M et al. Signal transducer and activator of transcription 3-mediated regulation of miR-199a-5p links cardiomyocyte and endothelial cell function in the heart: a key role for ubiquitin-conjugating enzymes. Eur Heart J 2011;32:1287-1297.

(305) Zhou Y, Pang B, Xiao Y, Zhou S, He B, Zhang F et al. The protective microRNA-199a-5p-mediated unfolded protein response in hypoxic cardiomyocytes is regulated by STAT3 pathway. J Physiol Biochem 2019;75(1):73-81.

(306) Tao Y, Zhang H, Huang S, Pei L, Feng M, Zhao X et al. miR-199a-3p promotes cardiomyocyte proliferation by inhibiting Cd151 expression. Biochem Biophys Res Commun 2019;516(1):28-36.

(307) Chen HP, Wen J, Tan SR, Kang LM, Zhu GC. MiR-199a-3p inhibition facilitates cardiomyocyte differentiation of embryonic stem cell through promotion of MEF2C. J Cell Physiol 2019;234(12):23315-23325.

(308) Song XW, Li Q, Lin L, Wang XC, Li DF, Wang GK et al. MicroRNAs are dynamically regulated in hypertrophic hearts, and miR-199a is essential for the maintenance of cell size in cardiomyocytes. J Cell Physiol 2010;225(2):437-443.

(309) Rane S, He M, Sayed D, Yan L, Vatner D, Abdellatif M. An antagonism between the AKT and beta-adrenergic signaling pathways mediated through their reciprocal effects on miR-199a-5p. Cell Signal 2010;22(7):1054-1062.

(310) Hou Y, Sun Y, Shan H, Li X, Zhang M, Zhou X et al. beta-adrenoceptor regulates miRNA expression in rat heart. Med Sci Monit 2012;18(8):BR309-BR314.

(311) Yang KC, Ku YC, Lovett M, Nerbonne JM. Combined deep microRNA and mRNA sequencing identifies protective transcriptomal signature of enhanced PI3Kalpha signaling in cardiac hypertrophy. J Mol Cell Cardiol 2012;53(1):101-112.

(312) Li Z, Song Y, Liu L, Hou N, An X, Zhan D et al. miR-199a impairs autophagy and induces cardiac hypertrophy through mTOR activation. Cell Death Differ 2017;24:1205-1213.

(313) Reddy S, Zhao M, Hu DQ, Fajardo G, Hu S, Ghosh Z et al. Dynamic microRNA expression during the transition from right ventricular hypertrophy to failure. Physiol Genomics 2012;44(10):562-575.

(314) Li Z, Liu L, Hou N, Song Y, An X, Zhang Y et al. miR-199-sponge transgenic mice develop physiological cardiac hypertrophy. Cardiovasc Res 2016;110(2):258-267.

(315) Chan YC, Roy S, Huang Y, Khanna S, Sen CK. The microRNA miR-199a-5p down-regulation switches on wound angiogenesis by derepressing the v-ets erythroblastosis virus E26 oncogene homolog 1-matrix metalloproteinase-1 pathway. J Biol Chem 2012;287(49):41032-41043.

(316) Sun Y, Xiong X, Wang X. HIF1alpha/miR-199a/ADM feedback loop modulates the proliferation of human dermal microvascular endothelial cells (HDMECs) under hypoxic condition. Cell Cycle 2019;18(21):2998-3009.
(317) Tian X, Yu C, Shi L, Li D, Chen X, Xia D et al. MicroRNA-199a-5p aggravates primary hypertension by damaging vascular endothelial cells through inhibition of autophagy and promotion of apoptosis. Exp Ther Med 2018;16(2):595-602.
(318) Mahmoud MM, Kim HR, Xing R, Hsiao S, Mammoto A, Chen J et al. TWIST1 Integrates Endothelial Responses to Flow in Vascular Dysfunction and Atherosclerosis. Circ Res 2016;119(3):450-462.
(319) Heuslein JL, Gorick CM, McDonnell SP, Song J, Annex BH, Price RJ. Exposure of Endothelium to Biomimetic Flow Waveforms Yields Identification of miR-199a-5p as a Potent Regulator of Arteriogenesis. Mol Ther Nucleic Acids 2018;12:829-844.
(320) Xue S, Zhu W, Liu D, Su Z, Zhang L, Chang Q et al. Circulating miR-26a-1, miR-146a and miR-199a-1 are potential candidate biomarkers for acute myocardial infarction. Mol Med 2019;25(1):18.
(321) Lesizza P, Prosdocimo G, Martinelli V, Sinagra G, Zacchigna S, Giacca M. Single-Dose Intracardiac Injection of Pro-Regenerative MicroRNAs Improves Cardiac Function After Myocardial Infarction. Circ Res 2017;120(8):1298-1304.
(322) Lundberg JO, Gladwin MT, Weitzberg E. Strategies to increase nitric oxide signalling in cardiovascular disease. Nat Rev Drug Discov 2015;14:623-641.
(323) Roviezzo F, Cuzzocrea S, Di LA, Brancaleone V, Mazzon E, Di PR et al. Protective role of PI3-kinase-Akt-eNOS signalling pathway in intestinal injury associated with splanchnic artery occlusion shock. Br J Pharmacol 2007;151:377-383.
(324) Brouet A, Sonveaux P, Dessy C, Moniotte S, Balligand JL, Feron O. Hsp90 and caveolin are key targets for the proangiogenic nitric oxide-mediated effects of statins. Circ Res 2001;89:866-873.
(325) Qian J, Fulton D. Post-translational regulation of endothelial nitric oxide synthase in vascular endothelium. Front Physiol 2013;4:347.
(326) Pacher P, Szabo C. Role of peroxynitrite in the pathogenesis of cardiovascular complications of diabetes. Curr Opin Pharmacol 2006;6:136-141.
(327) Pacher P, Szabo C. Role of the peroxynitrite-poly(ADP-ribose) polymerase pathway in human disease. Am J Pathol 2008;173:2-13.
(328) Williams IL, Wheatcroft SB, Shah AM, Kearney MT. Obesity, atherosclerosis and the vascular endothelium: mechanisms of reduced nitric oxide bioavailability in obese humans. Int J Obes Relat Metab Disord 2002;26:754-764.
(329) Agnoletti L, Curello S, Bachetti T, Malacarne F, Gaia G, Comini L et al. Serum from patients with severe heart failure downregulates eNOS and is proapoptotic: role of tumor necrosis factor-alpha. Circulation 1999;100:1983-1991.
(330) Oemar BS, Tschudi MR, Godoy N, Brovkovich V, Malinski T, Luscher TF. Reduced endothelial nitric oxide synthase expression and production in human atherosclerosis. Circulation 1998;97:2494-2498.
(331) Li H, Wallerath T, Munzel T, Forstermann U. Regulation of endothelial-type NO synthase expression in pathophysiology and in response to drugs. Nitric Oxide 2002;7:149-164.

(332) Sena CM, Pereira AM, Seica R. Endothelial dysfunction - a major mediator of diabetic vascular disease. Biochim Biophys Acta 2013;1832:2216-2231.
(333) Duan Z, Choy E, Harmon D, Liu X, Susa M, Mankin H et al. MicroRNA-199a-3p is downregulated in human osteosarcoma and regulates cell proliferation and migration. Mol Cancer Ther 2011;10:1337-1345.
(334) He J, Jing Y, Li W, Qian X, Xu Q, Li FS et al. Roles and mechanism of miR-199a and miR-125b in tumor angiogenesis. PLoS One 2013;8:e56647.
(335) van Rooij E., Marshall WS, Olson EN. Toward microRNA-based therapeutics for heart disease: the sense in antisense. Circ Res 2008;103:919-928.
(336) Catalucci D, Latronico MV, Condorelli G. MicroRNAs control gene expression: importance for cardiac development and pathophysiology. Ann N Y Acad Sci 2008;1123:20-29.
(337) Craps J, Wilvers C, Joris V, De Jongh B., Vanderstraeten J, Lobysheva I et al. Involvement of nitric oxide in iodine deficiency-induced microvascular remodeling in the thyroid gland: role of nitric oxide synthase 3 and ryanodine receptors. Endocrinology 2015;156:707-720.
(338) van RE, Sutherland LB, Thatcher JE, DiMaio JM, Naseem RH, Marshall WS et al. Dysregulation of microRNAs after myocardial infarction reveals a role of miR-29 in cardiac fibrosis. Proc Natl Acad Sci U S A 2008;105(35):13027-13032.
(339) Caballero-Garrido E, Pena-Philippides JC, Lordkipanidze T, Bragin D, Yang Y, Erhardt EB et al. In Vivo Inhibition of miR-155 Promotes Recovery after Experimental Mouse Stroke. J Neurosci 2015;35:12446-12464.
(340) Gelinas R, Mailleux F, Dontaine J, et al. AMPK activation counteracts cardiac hypertrophy by reducing O-GlcNAcylation. Nat Commun 2018;9:374.
(341) Rouaud F, Romero-Perez M, Wang H, Lobysheva I, Ramassamy B, Henry E et al. Regulation of NADPH-dependent Nitric Oxide and reactive oxygen species signalling in endothelial and melanoma cells by a photoactive NADPH analogue. Oncotarget 2014;5:10650-10664.
(342) Ghisdal P, Gomez JP, Morel N. Action of a NO donor on the excitation-contraction pathway activated by noradrenaline in rat superior mesenteric artery. J Physiol 2000;522 Pt 1:83-96.
(343) Saliez J, Bouzin C, Rath G, Ghisdal P, Desjardins F, Rezzani R et al. Role of caveolar compartmentation in endothelium-derived hyperpolarizing factor-mediated relaxation: Ca2+ signals and gap junction function are regulated by caveolin in endothelial cells. Circulation 2008;117:1065-1074.
(344) Yu H, Littlewood T, Bennett M. Akt isoforms in vascular disease. Vascul Pharmacol 2015;71:57-64.
(345) Jia L, Li YF, Wu GF, Song ZY, Lu HZ, Song CC et al. MiRNA-199a-3p regulates C2C12 myoblast differentiation through IGF-1/AKT/mTOR signal pathway. Int J Mol Sci 2014;15:296-308.
(346) Condorelli G, Latronico MV, Cavarretta E. microRNAs in cardiovascular diseases: current knowledge and the road ahead. J Am Coll Cardiol 2014;63:2177-2187.
(347) Park KM, Teoh JP, Wang Y, Broskova Z, Bayoumi AS, Tang Y et al. Carvedilol-responsive microRNAs, miR-199a-3p and -214 protect cardiomyocytes from

simulated ischemia-reperfusion injury. Am J Physiol Heart Circ Physiol 2016;311:H371-H383.

(348) Zeng J, Chen L, Chen B, Lu K, Belguise K, Wang X et al. MicroRNA-199a-5p Regulates the Proliferation of Pulmonary Microvascular Endothelial Cells in Hepatopulmonary Syndrome. Cell Physiol Biochem 2015;37(4):1289-1300.

(349) Nishiguchi T, Imanishi T, Akasaka T. MicroRNAs and cardiovascular diseases. Biomed Res Int 2015;2015:682857.

(350) Bracken CP, Scott HS, Goodall GJ. A network-biology perspective of microRNA function and dysfunction in cancer. Nat Rev Genet 2016;17:719-732.

(351) Mozaffarian D. Dietary and Policy Priorities for Cardiovascular Disease, Diabetes, and Obesity: A Comprehensive Review. Circulation 2016;133(2):187-225.

(352) Schuler G, Adams V, Goto Y. Role of exercise in the prevention of cardiovascular disease: results, mechanisms, and new perspectives. Eur Heart J 2013;34(24):1790-1799.

(353) Nocon M, Hiemann T, Muller-Riemenschneider F, Thalau F, Roll S, Willich SN. Association of physical activity with all-cause and cardiovascular mortality: a systematic review and meta-analysis. Eur J Cardiovasc Prev Rehabil 2008;15(3):239-246.

(354) Redberg RF, Benjamin EJ, Bittner V, Braun LT, Goff DC, Jr., Havas S et al. ACCF/AHA 2009 performance measures for primary prevention of cardiovascular disease in adults: a report of the American College of Cardiology Foundation/American Heart Association Task Force on Performance Measures (Writing Committee to Develop Performance Measures for Primary Prevention of Cardiovascular Disease) developed in collaboration with the American Academy of Family Physicians; American Association of Cardiovascular and Pulmonary Rehabilitation; and Preventive Cardiovascular Nurses Association: endorsed by the American College of Preventive Medicine, American College of Sports Medicine, and Society for Women's Health Research. J Am Coll Cardiol 2009;54(14):1364-1405.

(355) Adams V, Reich B, Uhlemann M, Niebauer J. Molecular effects of exercise training in patients with cardiovascular disease: focus on skeletal muscle, endothelium, and myocardium. Am J Physiol Heart Circ Physiol 2017;313(1):H72-H88.

(356) Kersten JR, Pagel PS, Chilian WM, Warltier DC. Multifactorial basis for coronary collateralization: a complex adaptive response to ischemia. Cardiovasc Res 1999;43(1):44-57.

(357) Wende AR, Schaeffer PJ, Parker GJ, Zechner C, Han DH, Chen MM et al. A role for the transcriptional coactivator PGC-1alpha in muscle refueling. J Biol Chem 2007;282(50):36642-36651.

(358) Kukreja RC, Yin C, Salloum FN. MicroRNAs: new players in cardiac injury and protection. Mol Pharmacol 2011;80(4):558-564.

(359) Improta Caria AC, Nonaka CKV, Pereira CS, Soares MBP, Macambira SG, Souza BSF. Exercise Training-Induced Changes in MicroRNAs: Beneficial Regulatory Effects in Hypertension, Type 2 Diabetes, and Obesity. Int J Mol Sci 2018;19(11).

(360) Ultimo S, Zauli G, Martelli AM, Vitale M, McCubrey JA, Capitani S et al. Cardiovascular disease-related miRNAs expression: potential role as biomarkers and effects of training exercise. Oncotarget 2018;9(24):17238-17254.
(361) Latronico MV, Condorelli G. microRNAs in hypertrophy and heart failure. Exp Biol Med (Maywood) 2011;236(2):125-131.
(362) Joris V, Gomez EL, Menchi L, Lobysheva I, Di Mauro V, Esfahani H et al. MicroRNA-199a-3p and MicroRNA-199a-5p Take Part to a Redundant Network of Regulation of the NOS (NO Synthase)/NO Pathway in the Endothelium. Arterioscler Thromb Vasc Biol 2018;38(10):2345-2357.
(363) Fu J, Hao L, Tian Y, Liu Y, Gu Y, Wu J. miR-199a-3p is involved in estrogen-mediated autophagy through the IGF-1/mTOR pathway in osteocyte-like MLO-Y4 cells. J Cell Physiol 2018;233(3):2292-2303.
(364) Manzanares G, Brito-da-Silva G, Gandra PG. Voluntary wheel running: patterns and physiological effects in mice. Braz J Med Biol Res 2018;52(1):e7830.
(365) Halpern W, Mulvany MJ, Warshaw DM. Mechanical properties of smooth muscle cells in the walls of arterial resistance vessels. J Physiol 1978;275:85-101.
(366) De Bono JP, Adlam D, Paterson DJ, Channon KM. Novel quantitative phenotypes of exercise training in mouse models. Am J Physiol Regul Integr Comp Physiol 2006;290(4):R926-R934.
(367) Ghosh P, Mora Solis FR, Dominguez JM, Spier SA, Donato AJ, Delp MD et al. Exercise training reverses aging-induced impairment of myogenic constriction in skeletal muscle arterioles. J Appl Physiol (1985) 2015;118(7):904-911.
(368) Lin N, Li XY, Zhang HM, Yang Z, Su Q. microRNA-199a-5p mediates high glucose-induced reactive oxygen species production and apoptosis in INS-1 pancreatic beta-cells by targeting SIRT1. Eur Rev Med Pharmacol Sci 2017;21(5):1091-1098.
(369) Soares DDS, Pinto GH, Lopes A, Caetano DSL, Nascimento TG, Andrades ME et al. Cardiac hypertrophy in mice submitted to a swimming protocol: Influence of training volume and intensity on myocardial renin angiotensin system. Am J Physiol Regul Integr Comp Physiol 2019.
(370) Fagard R. Athlete's heart. Heart 2003;89(12):1455-1461.
(371) Kemi OJ, Haram PM, Loennechen JP, Osnes JB, Skomedal T, Wisloff U et al. Moderate vs. high exercise intensity: differential effects on aerobic fitness, cardiomyocyte contractility, and endothelial function. Cardiovasc Res 2005;67(1):161-172.
(372) Derumeaux G, Ichinose F, Raher MJ, Morgan JG, Coman T, Lee C et al. Myocardial alterations in senescent mice and effect of exercise training: a strain rate imaging study. Circ Cardiovasc Imaging 2008;1(3):227-234.
(373) Wang Y, Wisloff U, Kemi OJ. Animal models in the study of exercise-induced cardiac hypertrophy. Physiol Res 2010;59(5):633-644.
(374) Lerman I, Harrison BC, Freeman K, Hewett TE, Allen DL, Robbins J et al. Genetic variability in forced and voluntary endurance exercise performance in seven inbred mouse strains. J Appl Physiol (1985) 2002;92(6):2245-2255.
(375) Bellafiore M, Sivverini G, Palumbo D, Macaluso F, Bianco A, Palma A et al. Increased cx43 and angiogenesis in exercised mouse hearts. Int J Sports Med 2007;28(9):749-755.

(376) Sturgeon K, Muthukumaran G, Ding D, Bajulaiye A, Ferrari V, Libonati JR. Moderate-intensity treadmill exercise training decreases murine cardiomyocyte cross-sectional area. Physiol Rep 2015;3(5).

(377) Bueno CR, Jr., Ferreira JC, Pereira MG, Bacurau AV, Brum PC. Aerobic exercise training improves skeletal muscle function and Ca2+ handling-related protein expression in sympathetic hyperactivity-induced heart failure. J Appl Physiol (1985) 2010;109(3):702-709.

(378) Moreira-Goncalves D, Henriques-Coelho T, Fonseca H, Ferreira R, Padrao AI, Santa C et al. Intermittent cardiac overload results in adaptive hypertrophy and provides protection against left ventricular acute pressure overload insult. J Physiol 2015;593(17):3885-3897.

(379) Stepien-Walek A, Wozakowska-Kaplon B. The effect of exercise on the secretion of B-type natriuretic peptide in the groups of patients with diabetes and myocardial infarction with preserved left ventricular systolic function. Przegl Lek 2016;73(2):72-77.

(380) Yin R, Yang Z, Peng J, Li B, Fu Y, Zheng Z. Predictive value of exercise-induced atrial natriuretic peptide secretion for the presence of left atrial low-voltage areas in patients with persistent atrial fibrillation. Acta Cardiol 2017;72(4):433-439.

(381) Caravia XM, Fanjul V, Oliver E, Roiz-Valle D, Moran-Alvarez A, Desdin-Mico G et al. The microRNA-29/PGC1alpha regulatory axis is critical for metabolic control of cardiac function. PLoS Biol 2018;16(10):e2006247.

(382) Bechara LR, Tanaka LY, Santos AM, Jordao CP, Sousa LG, Bartholomeu T et al. A single bout of moderate-intensity exercise increases vascular NO bioavailability and attenuates adrenergic receptor-dependent and -independent vasoconstrictor response in rat aorta. J Smooth Muscle Res 2008;44(3-4):101-111.

(383) Arany Z, Foo SY, Ma Y, Ruas JL, Bommi-Reddy A, Girnun G et al. HIF-independent regulation of VEGF and angiogenesis by the transcriptional coactivator PGC-1alpha. Nature 2008;451(7181):1008-1012.

(384) Mendzef SD, Slovinski JR. Neurohormones and heart failure. Nurs Clin North Am 2004;39(4):845-861.

(385) Conti S, Cassis P, Benigni A. Aging and the renin-angiotensin system. Hypertension 2012;60(4):878-883.

(386) Rokosh DG, Stewart AF, Chang KC, Bailey BA, Karliner JS, Camacho SA et al. Alpha1-adrenergic receptor subtype mRNAs are differentially regulated by alpha1-adrenergic and other hypertrophic stimuli in cardiac myocytes in culture and in vivo. Repression of alpha1B and alpha1D but induction of alpha1C. J Biol Chem 1996;271(10):5839-5843.

(387) Castellano M, Bohm M. The cardiac beta-adrenoceptor-mediated signaling pathway and its alterations in hypertensive heart disease. Hypertension 1997;29(3):715-722.

(388) Zhong J, Hume JR, Keef KD. beta-Adrenergic receptor stimulation of L-type Ca2+ channels in rabbit portal vein myocytes involves both alphas and betagamma G protein subunits. J Physiol 2001;531(Pt 1):105-115.

(389) Bisognano JD, Weinberger HD, Bohlmeyer TJ, Pende A, Raynolds MV, Sastravaha A et al. Myocardial-directed overexpression of the human beta(1)-adrenergic receptor in transgenic mice. J Mol Cell Cardiol 2000;32(5):817-830.

(390) Dahl EF, Wu SC, Healy CL, Harsch BA, Shearer GC, O'Connell TD. Subcellular compartmentalization of proximal Galphaq-receptor signaling produces unique hypertrophic phenotypes in adult cardiac myocytes. J Biol Chem 2018;293(23):8734-8749.

(391) Mhatre KN, Wakula P, Klein O, Bisping E, Volkl J, Pieske B et al. Crosstalk between FGF23- and angiotensin II-mediated Ca2+ signaling in pathological cardiac hypertrophy. Cell Mol Life Sci 2018;75(23):4403-4416.

(392) Horman S, Beauloye C, Vanoverschelde JL, Bertrand L. AMP-activated protein kinase in the control of cardiac metabolism and remodeling. Curr Heart Fail Rep 2012;9(3):164-173.

(393) Hernandez JS, Barreto-Torres G, Kuznetsov AV, Khuchua Z, Javadov S. Crosstalk between AMPK activation and angiotensin II-induced hypertrophy in cardiomyocytes: the role of mitochondria. J Cell Mol Med 2014;18(4):709-720.

(394) Li HL, Yin R, Chen D, Liu D, Wang D, Yang Q et al. Long-term activation of adenosine monophosphate-activated protein kinase attenuates pressure-overload-induced cardiac hypertrophy. J Cell Biochem 2007;100(5):1086-1099.

(395) Forstermann U, Munzel T. Endothelial nitric oxide synthase in vascular disease: from marvel to menace. Circulation 2006;113(13):1708-1714.

(396) Baumann V, Winkler J. miRNA-based therapies: strategies and delivery platforms for oligonucleotide and non-oligonucleotide agents. Future Med Chem 2014;6(17):1967-1984.

(397) Wang H, Wang Z, Tang Q. Reduced expression of microRNA-199a-3p is associated with vascular endothelial cell injury induced by type 2 diabetes mellitus. Exp Ther Med 2018;16(4):3639-3645.

(398) Zhang S, Liu L, Wang R, Tuo H, Guo Y, Yi L et al. MiR-199a-5p promotes migration and tube formation of human cytomegalovirus-infected endothelial cells through downregulation of SIRT1 and eNOS. Arch Virol 2013;158(12):2443-2452.

(399) He J, Wang M, Jiang Y, Chen Q, Xu S, Xu Q et al. Chronic arsenic exposure and angiogenesis in human bronchial epithelial cells via the ROS/miR-199a-5p/HIF-1alpha/COX-2 pathway. Environ Health Perspect 2014;122(3):255-261.

(400) He J, Xu Q, Jing Y, Agani F, Qian X, Carpenter R et al. Reactive oxygen species regulate ERBB2 and ERBB3 expression via miR-199a/125b and DNA methylation. EMBO Rep 2012;13(12):1116-1122.

(401) Segers VFM, Brutsaert DL, De Keulenaer GW. Cardiac Remodeling: Endothelial Cells Have More to Say Than Just NO. Front Physiol 2018;9:382.

(402) Poulikakos D, Ross L, Recio-Mayoral A, Cole D, Andoh J, Chitalia N et al. Left ventricular hypertrophy and endothelial dysfunction in chronic kidney disease. Eur Heart J Cardiovasc Imaging 2014;15(1):56-61.

(403) Yan H, Li Y, Wang C, Zhang Y, Liu C, Zhou K et al. Contrary microRNA Expression Pattern Between Fetal and Adult Cardiac Remodeling: Therapeutic Value for Heart Failure. Cardiovasc Toxicol 2017;17(3):267-276.

(404) Silveira AC, Fernandes T, Soci UPR, Gomes JLP, Barretti DL, Mota GGF et al. Exercise Training Restores Cardiac MicroRNA-1 and MicroRNA-29c to Nonpathological Levels in Obese Rats. Oxid Med Cell Longev 2017;2017:1549014.
(405) Torrini C, Cubero RJ, Dirkx E, Braga L, Ali H, Prosdocimo G et al. Common Regulatory Pathways Mediate Activity of MicroRNAs Inducing Cardiomyocyte Proliferation. Cell Rep 2019;27(9):2759-2771.
(406) Gabisonia K, Prosdocimo G, Aquaro GD, Carlucci L, Zentilin L, Secco I et al. MicroRNA therapy stimulates uncontrolled cardiac repair after myocardial infarction in pigs. Nature 2019;569(7756):418-422.
(407) Ceccarelli S, Panera N, Gnani D, Nobili V. Dual role of microRNAs in NAFLD. Int J Mol Sci 2013;14(4):8437-8455.
(408) Mehta R, Otgonsuren M, Younoszai Z, Allawi H, Raybuck B, Younossi Z. Circulating miRNA in patients with non-alcoholic fatty liver disease and coronary artery disease. BMJ Open Gastroenterol 2016;3(1):e000096.
(409) Jia N, Lin X, Ma S, Ge S, Mu S, Yang C et al. Amelioration of hepatic steatosis is associated with modulation of gut microbiota and suppression of hepatic miR-34a in Gynostemma pentaphylla (Thunb.) Makino treated mice. Nutr Metab (Lond) 2018;15:86.
(410) Turchinovich A, Cho WC. The origin, function and diagnostic potential of extracellular microRNA in human body fluids. Front Genet 2014;5:30.
(411) Laterza OF, Lim L, Garrett-Engele PW, Vlasakova K, Muniappa N, Tanaka WK et al. Plasma MicroRNAs as sensitive and specific biomarkers of tissue injury. Clin Chem 2009;55(11):1977-1983.
(412) Corsten MF, Dennert R, Jochems S, Kuznetsova T, Devaux Y, Hofstra L et al. Circulating MicroRNA-208b and MicroRNA-499 reflect myocardial damage in cardiovascular disease. Circ Cardiovasc Genet 2010;3(6):499-506.
(413) Chevillet JR, Kang Q, Ruf IK, Briggs HA, Vojtech LN, Hughes SM et al. Quantitative and stoichiometric analysis of the microRNA content of exosomes. Proc Natl Acad Sci U S A 2014;111(41):14888-14893.
(414) Villarroya-Beltri C, Gutierrez-Vazquez C, Sanchez-Cabo F, Perez-Hernandez D, Vazquez J, Martin-Cofreces N et al. Sumoylated hnRNPA2B1 controls the sorting of miRNAs into exosomes through binding to specific motifs. Nat Commun 2013;4:2980.
(415) Treiber T, Treiber N, Meister G. Regulation of microRNA biogenesis and its crosstalk with other cellular pathways. Nat Rev Mol Cell Biol 2019;20(1):5-20.
(416) Martinez-Sanchez A, Nguyen-Tu MS, Cebola I, Yavari A, Marchetti P, Piemonti L et al. MiR-184 expression is regulated by AMPK in pancreatic islets. FASEB J 2018;32(5):2587-2600.
(417) Kohlstedt K, Trouvain C, Boettger T, Shi L, Fisslthaler B, Fleming I. AMP-activated protein kinase regulates endothelial cell angiotensin-converting enzyme expression via p53 and the post-transcriptional regulation of microRNA-143/145. Circ Res 2013;112(8):1150-1158.
(418) Sun HL, Cui R, Zhou J, Teng KY, Hsiao YH, Nakanishi K et al. ERK Activation Globally Downregulates miRNAs through Phosphorylating Exportin-5. Cancer Cell 2016;30(5):723-736.

(419) Tian R, Musi N, D'Agostino J, Hirshman MF, Goodyear LJ. Increased adenosine monophosphate-activated protein kinase activity in rat hearts with pressure-overload hypertrophy. Circulation 2001;104(14):1664-1669.
(420) Sag D, Carling D, Stout RD, Suttles J. Adenosine 5'-monophosphate-activated protein kinase promotes macrophage polarization to an anti-inflammatory functional phenotype. J Immunol 2008;181(12):8633-8641.
(421) Sasaki H, Asanuma H, Fujita M, Takahama H, Wakeno M, Ito S et al. Metformin prevents progression of heart failure in dogs: role of AMP-activated protein kinase. Circulation 2009;119(19):2568-2577.
(422) Yin M, van der Horst IC, van Melle JP, Qian C, van Gilst WH, Sillje HH et al. Metformin improves cardiac function in a nondiabetic rat model of post-MI heart failure. Am J Physiol Heart Circ Physiol 2011;301(2):H459-H468.
(423) Hansen TB, Jensen TI, Clausen BH, Bramsen JB, Finsen B, Damgaard CK et al. Natural RNA circles function as efficient microRNA sponges. Nature 2013;495(7441):384-388.
(424) Jiang Z, Zhang Y, Chen X, Wu P, Chen D. Long noncoding RNA RBMS3-AS3 acts as a microRNA-4534 sponge to inhibit the progression of prostate cancer by upregulating VASH1. Gene Ther 2019.
(425) Care A, Catalucci D, Felicetti F, Bonci D, Addario A, Gallo P et al. MicroRNA-133 controls cardiac hypertrophy. Nat Med 2007;13(5):613-618.
(426) Di M, V, Iafisco M, Salvarani N, Vacchiano M, Carullo P, Ramirez-Rodriguez GB et al. Bioinspired negatively charged calcium phosphate nanocarriers for cardiac delivery of MicroRNAs. Nanomedicine (Lond) 2016;11(8):891-906.
(427) Miragoli M, Ceriotti P, Iafisco M, Vacchiano M, Salvarani N, Alogna A et al. Inhalation of peptide-loaded nanoparticles improves heart failure. Sci Transl Med 2018;10(424).
(428) Kortylewski M, Nechaev S. How to train your dragon: targeted delivery of microRNA to cancer cells in vivo. Mol Ther 2014;22(6):1070-1071.
(429) Daei P, Ramezanpour M, Khanaki K, Tabarzad M, Nikokar I, Hedayati CM et al. Aptamer-based Targeted Delivery of miRNA let-7d to Gastric Cancer Cells as a Novel Anti-Tumor Therapeutic Agent. Iran J Pharm Res 2018;17(4):1537-1549.
(430) Zampetaki A, Willeit P, Tilling L, Drozdov I, Prokopi M, Renard JM et al. Prospective study on circulating MicroRNAs and risk of myocardial infarction. J Am Coll Cardiol 2012;60(4):290-299.
(431) Freres P, Bouznad N, Servais L, Josse C, Wenric S, Poncin A et al. Variations of circulating cardiac biomarkers during and after anthracycline-containing chemotherapy in breast cancer patients. BMC Cancer 2018;18(1):102.